The role of reactive oxygen species in the stabilisation of hypoxia-inducible factor-1α (HIF-1α)

Leanne Stephanie Boorn

A thesis submitted in part fulfillment for the Degree of Doctor of Philosophy in the University College London

December 2010

Wolfson Institute for Biomedical Research
University College London
The Cruciform Building
Gower Street
London
WC1E 6BT

Declaration of ownership

I, Leanne Stephanie Boorn, declare that this thesis is the result of my own work. All help and advice has been acknowledged and primary and secondary sources of information have been properly attributed.

Abstract:

At physiological oxygen concentrations ([O_2]) hypoxia-inducible factor-1α (HIF-1α) is constantly hydroxylated and thus prepared for proteosomal degradation through the action of the prolyl hydroxylases (PHDs) (Jiang *et al.*, 1996). In hypoxia, however, the oxygen-sensitive PHDs are inhibited and HIF-1α is stabilised. Other agents, including cytokines and growth factors have been shown to stabilise HIF-1α at physiological [O_2] through different mechanisms such as activation of the phosphatidylinositol 3-kinase (PI3K) or mitogen-activated protein kinase pathways (Semenza, 2003). Increased production of reactive oxygen species (ROS) during hypoxia have also been claimed to stabilise HIF-1α (Chandel *et al.*, 1998) and we have now investigated the effect of endogenous ROS on HIF-1α stabilisation.

HIF-1α stabilisation and ROS production in human embryonic kidney (HEK 293T) cells were determined by immunoblotting and the use of fluorescent probes, respectively. γGlutamyl cysteine synthetase (γGCS) is the rate limiting enzyme of glutathione (GSH) biosynthesis and therefore a crucial antioxidant. We used small interfering RNA (siRNA) to silence this enzyme and thus impair the capacity of the cells to detoxify ROS.

In order to determine whether mitochondria are a major source of ROS we used cells depleted of mitochondrial DNA (*Rho*^{0}); these were characterised *in vitro* by monitoring oxygen consumption. RT-PCR was used to determine mitochondrial DNA content and immunoblotting to assess mitochondrial-encoded protein expression. The effects of a *Rho*^{0} phenotype were then assessed in relation to HIF-1α stabilisation and ROS production.

HIF-1α is stabilised in an oxygen-dependent manner. HIF-1α stabilisation at low [O_2] (3%), but not at 0.5% O_2 is prevented by treatment with antioxidants. Silencing γGCS augmented free radical production in HEK 293T cells. This was associated with HIF-1α stabilisation at ambient [O_2] (21%) and could be prevented by treatment with antioxidants. *Rho*^{0} cells produced less ROS than wild-type cells and did not stabilise HIF-1α either at low [O_2] (3%) in wild-type cells or at 21% O_2 in γGCS silenced cells.

The data suggest that HIF-1α can be stabilised by ROS generated by the mitochondria.

Acknowledgements:

In pursuing my ambition to become a research scientist I could not have hoped to gain a studentship under a more prestigious scientist than Professor Sir Salvador Moncada. It has been a real privilege to have your guidance and ideas to direct me on this project. Thank you.

I was also fortunate enough to have worked with the incredible people within Salvador's laboratory. Dr Sergio Colombo provided me with support, guidance, encouragement and patience. Thank you for teaching me so much, and for always being there for me. I would also like to thank Nanci Frakich and Dr Miriam Palacios-Callender, who have also offered me so much support and guidance throughout my PhD. I would also like to thank Dr Christoph Schmitt for his kindness and support whilst reading this thesis. A special thank you must also be given to Neale Foxwell for his technical support and advice. Not only have you all helped me during my studentship, I consider you all as friends, and for this I am most grateful.

I would also like to thank all the other people in wing 2.3. And also a special thank you goes to Rayomand Khambata for giving me continuous support and friendship.

I would also like to thank my parents, brother and friends for all their support throughout the duration of my PhD.

Last but not least, a big thank you to my husband Alan for being there for me during what is to date, the most challenging undertaking of my life. I love you.

Table of contents:

List of figures and tables:

Figures:

Tables:

Abbreviations:

2-OG	2-oxyglutarate
AcCoA	Acetyl coenzyme A
ADM	Adrenomedullin
ADP	Adenosine diphosphate
AMF	Autocrine motility factor
AngII	Angiotensin II
ANGPT1/2	Angiopoietin 1/2
AO	Antioxidant
AP-1	Activator protein-1
ARNT	Aryl hydrocarbon nuclear receptor translocator
Asn	Asparagine
ATP	Adenosine triphosphate
BCA	Bicinchoninic acid
Bcl2	B cell lymphoma 2
BH_4	Tetrahydrobiopterin
bHLH	Basic-helix-loop-helix
$[Ca^{2+}]_c$	Cytosolic calcium concentration
CAD	C-terminal activation domain
CaM	Calmodulin
camK	Calcium-calmodulin kinase
CBP	cAMP response element binding protein
C*c*O	Cytochrome *c* oxidase
cDNA	Complementary DNA
CDS	Coding domain sequence
CFP	Cyan fluorescent protein
CM-H_2DCFDA	5-(and-6)-chloromethyl-2',7'-dicholorodihydrofluorescien-diacetate acetyl ester
C-terminal	Carboxyl-terminal
Cu/ZnSOD	Copper/ zinc SOD
Ctl	Control
Cyt *c*	Cytochrome *c*
CXCR4	Chemokine receptor 4
dH_2O	Distilled water

DC	Doxycycline
DCF	Dicholorohydrofluorescien
DFX	Desferoxamine
DIC	Dicarboxylate carrier
DMEM	Dulbecco modified eagle medium
DMOG	Dimethyloxallyl gylcine
DMSO	Dimethylsulphoxide
DNA	Deoxyribonucleic acid
dNTP	Deoxynucleotidetriphosphate
DPI	Diphenyleneiodonium
dsRNA	Double stranded ribonucleic acid
DUOX	Dual oxidase
ECL	Enhanced chemiluminescence
EC	Effective concentration
E. *coli*	Escherichia *coli*
EDTA	Ethylendiaminetetraacetic acid
EGF	Epidermal growth factor
EG-VEGF	Endocrine gland derived VEGF
ENG	Endoglin
ENO	Enolase
eNOS	Endothelial NOS
EPO	Erythropoietin
EtBr	Ethidium bromide
ETC	Electron transport chain
$FADH_2$	Flavin adenine dinucleotide
FCCP	p-trifluoromethoxy carbonyl cyanide phenyl hydrazone
FCS	Foetal calf serum
Fe^{2+}	Ferrous iron
Fe^{3+}	Ferric iron
Fe-S	Iron-sulphur
FH	Fumerate hydratase
FIH	Factor inhibiting HIF
FMN	Flavinmononucleotide
g	Relative centrifugal force
GAPDH	Glyceraldehyde-3-P-dehydrogenase

GCL	Glutamylcysteine ligase
γGCS	γ- Glutamylcysteine synthetase
GFP	Green fluorescent protein
GGT	γ-glutamyltransferase
GLUT-1	Glucose transporter 1
GS	Glutathione synthetase
GSSG	Glutathione (oxidised form)
GSH	Glutathione (reduced form)
h	Hours
H_2O_2	Hydrogen peroxide
HCl	Hydrochloric acid
HEK	Human embryonic kidney
Hep3B	Human hepatoma
HIF-1	Hypoxia inducible factor- 1
HIV	Human immunodeficiency virus
HK 1	Hexokinase 1
HK 2	Hexokinase 2
HO	Heme oxygenase
HOCl	Hypochlorous acid
HRE	Hypoxic response element
HRP	Horse radish peroxidise
HSP	Heat shock protein
HUVEC	Human umbilical vein endothelial cells
IF	Immunofluorescence
IFNγ	Interferon-γ
IGF2	insulin-like growth-factor 2
IGF-BP1	IGF-factor-binding-protein 1
IGF-BP2	IGF-factor-binding-protein 2
IGF-BP3	IGF-factor-binding-protein 3
IH	Intermittent hypoxia
iNOS	Inducible NOS
IU	International unit
KGM	Keratinocyte growth medium
K_m	Michaelis constant
LB	Luria-Bertani

L-BSO	L-buthionine sulfoximine
LDHA	Lactate dehydrogenase A
LDL	Low density lipoprotein
LEP	Leptin
L-NMMA	N5-[imino(methylamino)methyl]-L-ornithine, citrate
LPS	Lipopolysaccharide
LRP1	LDL-receptor-related protein 1
LZIP	Leucine zipper
MΦ	Macrophage
MAPK	Mitogen- activated protein kinase
mDNA	Mitochondrial DNA
MEF	Murine embryonic fibroblasts
Met-GSH	Methylglutathione
MnSOD	Manganese SOD
mRNA	Messenger ribonucleic acid
MRP	Multi drug resistance protein
MOPS	3-(N-morpholino)propanesulfonic acid
MPA	Metaphosphoric acid
MtDNA	Mitochondrial DNA
mTOR	Mammalian target of rapamycin
NAC	N-acetyl-L-cysteine
NaCl	Sodium chloride
NAD	N-terminal activation domain
NADH	Nicotinamide adenine dinucleotide
NADPH	Nicotamide adenine dinucleotide phosphate
NADPH oxidase	Nicotamide adenine dinucleotide phosphate oxidase
NaOH	Sodium hydroxide
Neg. Ctl	Negative control
NF-κB	Nuclear factor kappa B
nNOS	Neuronal NOS
NO	Nitric oxide
NO^+	Nitrosonium cation
NO^-	Nitroxylanion
NO_2^-	Nitrate
NOHA	N^Ghydroxy-L-arginine

NOS	Nitric oxide synthase
NOS2	Nitric oxide synthase 2
NOX	NADPH oxidase
N-terminal	NH_2 -terminus
O_2^-	Superoxide
O_3	Ozone
ODD	Oxygen dependent degradation domain
OGC	Monocarboxylate carrier
OH^-	Hydroxyl
O/N	Overnight
$OONO^-$	Peroxynitrite
P13-kinase	Phosphoinositide 3' kinase
PAS	Per-arnt-sim
PBS	Phosphate buffered saline
PBST	Phosphate buffered saline tween
PCR	Polymerase chain reaction
PDGRβ	Platelet-derived growth factor β
PDH	Pyruvate dehydrogenase
PDK-1	Pyruvate dehydrogenase kinase 1
PFKFB3	6-phosphofructo-2-kinase/fructose-2,6-biphosphatase-3
PFKL	Phosphofructokinase L
PGF	Placental growth factor
PGK1	Phosphoglycerate kinase 1
PHD1	Prolyl hydroxylase domain 1
PHD2	Prolyl hydroxylase domain 2
PHD3	Prolyl hydroxylase domain 3
PKC	Protein kinase C
PKM	Pyruvate kinase M
POLγ	Polymerase γ
Pos. Ctl	Positve control
PPARs	Peroxisome proliferator-activated receptors),
Prx	Peroxiredoxin
PTK	Protein tyrosine kinase
PTP	Protein tyrosine phosphatase
pVHL	Von hippel-lindau protein

RAS	Rat sarcoma
RCC	Renal carcinoma cell
RD	Regulatory domain
RNA	Ribonucleic acid
RNAi	RNA interference
RNS	Reactive nitrogen species
ROS	Reactive oxygen species
RO·	Alkoxyl
RO_2·	Peroxyl
Rot	Rotenone
RT-PCR	Reverse rranscription polymerase chain reaction
s	Seconds
Scr	Scrambled (siRNA)
SDF1	Stromal derived factor 1
SDH	Succinate hydrogenase
SDS	Sodium dodecyl sulphate
SDS-PAGE	SDS polyacrylamide gel electrophoresis
SEITU	S-ethyl-isothiourea
SFM	Serum free medium
shRNA	Small hairpin ribonucleic acid
siRNA	Small interfering ribonucleic acid
SOD	Superoxide dismutase
Sp1	Specificity protein 1
sPBS	Sterile phosphate buffered saline
TAD	Transactivation domain
TAE	Tris acetic acid EDTA buffer
TCA cycle	Tricarboxylic acid cycle
TEMED	N'N'N'N' Tetramethyletheylenediamine
TGF-α	Transforming growth factor-α
TGF-β3	Transforming growth factor-β3
TMRM	Tetramethyl rhodamine methyl ester
TNF-α	Tumour necrosis factor-α
TPI	Triosephosphate isomerase
Tris	Tris(hydroxymethyl)methylamine
Trx	Thioredoxin

Q	coenzyme Q
Ub	Ubiquitin
VEGF	Vascular endothelial growth factor
VEGFR1	VEGF receptor 1
VLS	Visible light spectrophy
VO_2	Oxygen consumption
WB	Western blot
YFP	Yellow fluorescent protein

Chapter one:
Introduction

Chapter one: Introduction

1.1 General introduction

Oxygen accounts for approximately 21% of the earth's atmosphere. The evolutionary development of respiratory, cardiovascular and haematopoietic systems provides a means to capture oxygen from the environment and distribute it throughout the body. It is used as a substrate for oxidative phosphorylation amongst many other vital biochemical reactions. In 1938, Corneille Heymans was awarded the Nobel Prize in Physiology or Medicine for showing how blood pressure and oxygen content of the blood are sensed by the body and transmitted to the brain. It is the ability of cells to adapt to the changes in oxygen availability which provides one of the most essential mechanisms for survival.

Hypoxia is used to describe reduced oxygen concentrations or availability, characterised by low partial pressure of oxygen (pO_2). However, hypoxia is a relative term, for example the arterial pO_2 in mammalian adults is ~ 13 kPa, and in the foetus it is ~ 5 kPa (Ward, 2008). Hypoxia is better defined as a situation in which oxygen becomes the limiting step in physiological and biological reactions and occurs in tissues when the oxygen supply fails to meet the demand of oxygen consuming cells. This includes physiological settings such as embryonic development and exercising muscle, as well as in pathophysiological conditions such as myocardial infarction, inflammation and solid tumour growth (Simon, 2006).

Hypoxia is sensed and results in changes in the activity or expression of a large number of hypoxic-sensitive genes. However, only within the past few years have the molecular mechanisms underlying this fundamental response of cells to hypoxic stress started to be elucidated.

1.2 Hypoxia-inducible factor family

1.2.1 Introduction

Mammalian cells respond to hypoxia by activating the transcription factors named hypoxia-inducible factors (HIFs), which are expressed by virtually all cells of the body (Chandel and Budinger, 2007). The HIF protein is composed of a α- and a β-subunit (also known as aryl hydrocarbon nuclear receptor translocator, ARNT) and belongs to a large family of proteins termed basic-helix-loop-helix (bHLH). The HIF proteins also contain a Per-Arnt-Sim (PAS) domain (Figure 1) which has diverse functions, including a range of regulatory and sensory functions for oxygen tension and redox potential (Erbel *et al.*, 2003). HIFs bind to hypoxia-response elements (HRE), consensus sequences in the promotor region of over one hundred genes (Table 1), which are known to activate the transcription of genes that allow the cell to respond to and survive the hypoxic environment. Genes such as those associated with angiogenesis in cancer, exercise and ischemia, as well as erythropoiesis, iron metabolism, glucose metabolism, cell survival, proliferation, apoptosis and motility.

	HIF-1 gene targets
Angiogenesis	EG-VEGF, ENG, LEP, LRP1, TGF-β3, VEGF
Erythropoiesis	EPO
Iron metabolism	Transferrin, Transferrin receptor
Glucose metabolism	HK1, HK2, AMF, ENO1, GLUT1, GAPDH, LDHA, PFKFB3, PFKL, PGK1, PKM, TPI
Cell survival	ADM, EPO, IGF2, IGF-BP1, IGF-BP2, IGF-BP3, NOS2, TGF-α, VEGF
Cell proliferation	Cyclin G2, GF2, GF-BP1, GF-BP2, GF-BP3, TGF-α, TGF-β3
Apoptosis	NIP3, NIX
Motility	AMF/GP, LRP1, TGF-α

Table 1 – Genes that are transcriptionally activated by HIF-1

A selection of target genes that are transcriptionally activated by HIF-1, including genes involved in angiogenesis, erythropoieses, iron metabolism, glucose metabolism, cell survival, cell proliferation, apoptosis and motility (Semenza, 2003).

There are three members of the HIF α-subunit, coded by different genes, as well as a number of mRNA splice variants, which have been described (Pouyssegur and Mechta-Grigoriou, 2006). Primarily, research has focused on HIF-1α, however further research is now emerging on HIF-2α. HIF-1α and HIF-2α have 48% overall sequence homology, with the N-terminal region showing the highest similarity. HIF-3α is the least studied of the three isoforms, though it is known to be similar to HIF-1α and -2α in the bHLH-PAS region. Yet it lacks structures for trans-activation (Bardos and Ashcroft, 2005) found in the C-terminus of HIF-1α and HIF-2α and has been shown to repress oxygen-regulated gene expression (Makino *et al.*, 2001). Database analyses have revealed that multiple alternatively spliced variants of HIF-3α exist, some of which contain the von Hippel-Lindau (VHL)-targeted oxygen-dependent degradation (ODD) domain that is also found in HIF-1α and -2α (Figure 1).

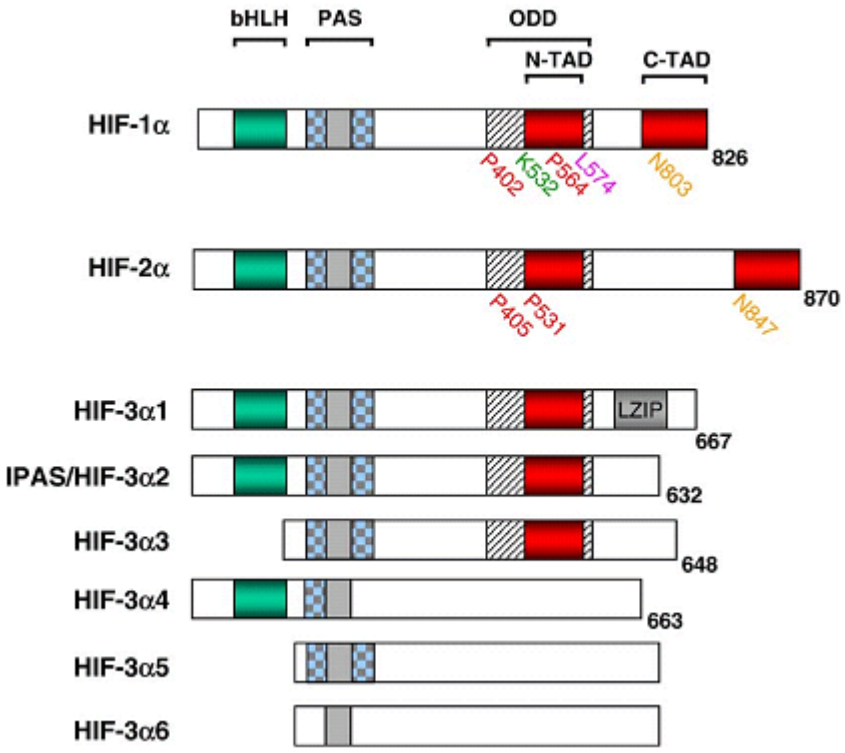

Figure 1 – Schematic representation of the different HIFα subunits

Functional domains are indicated by boxes and the locations of the amino acid residues relevant for HIF-1α and HIF-2α regulation are marked. bHLH, basic helix-loop-helix domain; PAS, Per/ARNT/Sim domains; ODD, oxygen-dependent degradation domain; N-TAD, N-terminal activation domain; C-TAD, C-terminal activation domain; LZIP, leucine zipper (Bardos and Ashcroft, 2005).

The α-subunits are highly unstable in the presence of oxygen, while the β-subunit is constitutively present in the nucleus, regardless of oxygen tension. The inherent instability of HIF-α subunits results from successive post-translational hydroxylation and ubiquitination, leading to proteasomal degradation (Brahimi-Horn and Pouyssegur, 2007).

1.2.2 Hypoxia-inducible factor-1

Hypoxia-inducible factor-1 (HIF-1) was first identified in human hepatoma (Hep3B) cells under reduced oxygen tension, and was found to be necessary for the activation of the erythropoietin gene enhancer, in hypoxic cells (Wang and Semenza, 1993). Since its discovery, HIF-1 has been identified as a heterodimeric transcription factor mediating responses to changes in tissue oxygenation, consisting of both α (100-120 kDa, dependent on hydroxylation status) and β subunits (~ 92 kDa) (Hellwig-Burgel *et al.*, 2005). HIF-1α expression and HIF-1 transcriptional activity increase exponentially as cellular oxygen concentrations decrease (Jiang *et al.*, 1996). *In vitro*, HIF-1α protein expression progressively accumulates as the pO_2 decreases to anoxia. The stability of HIF-1α in hypoxic conditions is caused by the inhibition of its proteasomal degradation (section 1.4). When HIF-1α has not been targeted for degradation, it translocates to the nucleus where it dimerises with HIF-1β partner and binds to site-specific HRE on target genes (Table 1). The binding of HIF-1 to HRE results in the induction or repression of over one hundred genes which are involved in a vast array of cellular functions (Table 1).

1.3 HIF-1 mediated adaptive responses to hypoxia

1.3.1 Metabolic regulation

Cells largely derive their metabolic energy for active processes from the hydrolysis of the high-energy phosphate bond of ATP. The most efficient metabolic pathway for the generation of ATP is through the oxidative metabolism of glucose. This process involves three distinct phases: glycolysis, the tricarboxylic acid (TCA) cycle (also known as the Krebs cycle or citric acid cycle) and oxidative phosphorylation.

1.3.1.1 Glycolysis

The first stage of respiration is glycolysis, which occurs in the cell cytoplasm and involves the co-ordinated activity of ten enzymes in the conversion of glucose into pyruvate. The net ATP gain of glycolysis is two molecules of ATP per molecule of glucose metabolised. As well as generating this yield of ATP, glycolysis also generates two electron-carrying NADH equivalents which facilitate oxidative phosphorylation.

During normoxic oxygen conditions (steady state), the primary metabolic function of glycolysis is to feed pyruvate into the TCA cycle. However, eukaryotic cells are able to shift the primary source of metabolic energy in situations of metabolic crisis, such as hypoxia. In such situations there is an increase in the rate of flux through the glycolytic pathway resulting in increased glycolytic ATP production, through HIF-dependent transcriptional up-regulation of the genes involves in glycolysis (Table 1).

1.3.1.2 TCA cycle

Each molecule of glucose that is metabolised through glycolysis results in the generation of two molecules of pyruvate. In the steady state, the majority of pyruvate generated is oxidised by pyruvate dehydrogenase (PDH) to form acetyl coenzyme A (AcCoA), which combines with oxaloacetic acid to form citric acid. This then enters the TCA cycle, located within the mitochondria where a series of enzymatic reactions result in the net generation of one molecule of ATP, three molecules of NADH and one molecule of $FADH_2$ per molecule of pyruvate metabolised.

The entry of pyruvate into the TCA cycle can be a regulated by the HIF pathway (Semenza, 2007). A fundamental adaptation during hypoxia is the shunting of pyruvate away from the mitochondria by the HIF-1-mediated activation of PDK1 (pyruvate dehydrogenase kinase 1) (Kim *et al.*, 2006;Papandreou *et al.*, 2006). PDK1 down regulates the activity of PDH (the enzyme responsible for converting pyruvate into AcCoA), causing a decrease in the pyruvate available for entry into the TCA cycle.

The reduced delivery of substrate to the mitochondria for oxidative phosphorylation results in reduced ATP synthesis. This is compensated for by increased glucose uptake via glucose transporters. Conversion of pyruvate to lactate by the activity of glycolytic enzymes and lactate dehydrogenase A (LDHA), which are encoded by HIF-1 target

genes also increase ATP synthesis (Semenza *et al.*, 1996;Ryan *et al.*, 1998;Seagroves *et al.*, 2001).

1.3.1.3 Oxidative phosphorylation

Oxidative phosphorylation is the process by which cells utilise over 20 electron-carrying proteins. These are located within the mitochondrial electron transport chain (ETC) and are arranged in four polypeptide Complexes which generate the cellular energy necessary to generate ATP. This process utilises the NADH and $FADH_2$ generated during glycolysis and the TCA cycle as electron donor molecules. The mechanism underlying oxidative phosphorylation involves the transport of electrons from high energentic molecules such as NADH and $FADH_2$ through a series of carrier molecules (i.e. cytochrome *c* and coenzyme Q) which donate the electrons to gradually lower energy levels.

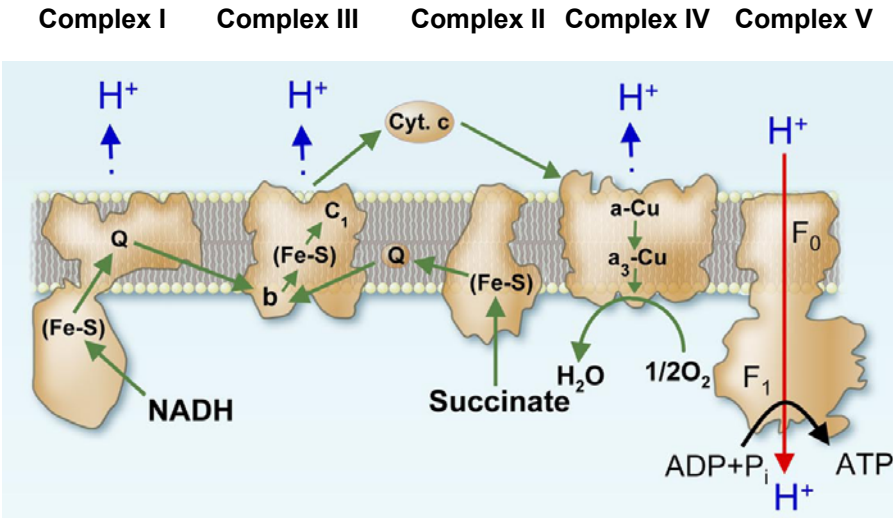

Figure 2 – Summary of protein subunits of the five respiratory chain complexes

Depicted is a schematic of the five respiratory Complexes (I–V) embedded in the lipid bilayer of the inner mitochondrial membrane. Dissociable electron carriers cytochrome *c* (Cyt c) and coenzyme Q (Q) are also shown. Arrows (green) show the pathway of electrons from the various electron donors. Broken arrows (blue) show the sites of proton pumping from the matrix side to the cytosolic side by Complexes I, III, and IV. The red arrow shows the flow of protons through Complex V from the cytosolic side to the matrix coupled to the synthesis of ATP (Scarpulla, 2008).

As a consenquence of this process, energy is released from the different redox reactions, part as heat and also as coupled to the generation of a proton gradient across the inner mitochondrial membrane which finally fuels the activity of ATP synthase (Complex V), promoting the phosphorylation of ADP to form ATP. Molecular oxygen acts as the final electron acceptor at Complex IV of the ETC (cytochrome *c* oxidase). This enzyme has a high affinity for molecular oxygen (K_m < 1 μM) and is responsible for over 90% of the body's oxygen consumption (Rolfe and Brown, 1997).

As in the case of glycolysis and the TCA cycle, oxidative phosphorylation through the ETC can be regulated by gene products of the HIF pathway in conditions of hypoxia. This involves a subunit switch within the cytochrome *c* oxidase (C*c*O) (the oxygen-binding subunit), in which the C*c*O4-1 regulatory subunit is replaced by the C*c*O4-2 isoform. This is a result of HIF-1-mediated transcriptional activation of genes encoding C*c*O4-2 and LON, a mitochondrial protease that degrades C*c*O4-1 (Fukuda *et al.*, 2007). This subunit switch optimises the energy consumption in conditions of low oxygen (Fukuda *et al.*, 2007) due to the higher affinity of C*c*O4-2 isoform towards oxygen.

From the above hypoxic metabolic adaptations, the following conclusions can be drawn. The increase in glycolysis and decrease in respiration that occur in response to hypoxia do not represent a passive effect of substrate (O_2) deprivation but instead represent an active response of the cell to counteract the reduced efficiency of energy generation by oxidative phosphorylation under hypoxic conditions.

1.3.2 HIF-dependent regulation of erythropoiesis

Acute blood loss, ascent to high altitudes and pneumonia each results in a reduction in blood oxygen content. The ensuing tissue hypoxia induces HIF-1 activity in cells throughout the body, including specialised cells in the kidney that produce erythropoietin (EPO), a glycoprotein hormone that is secreted into the blood and binds to its cognate receptor on erythroid progenitor cells, thereby stimulating their survival and differentiation (Gerber *et al.*, 1997). HIF-1 has been shown to orchestrate erythropoiesis by co-ordinately regulating the expression of multiple genes, including transferrin (Rolfs *et al.*, 1997), transferrin receptor (Tacchini *et al.*, 1999), ceruloplasmin (Mukhopadhyay *et al.*, 2000) and hepadin (Peyssonnaux *et al.*, 2007).

These proteins are responsible for the intestinal uptake, tissue recycling and delivery of iron to the bone marrow for its use in the synthesis of haemoglobin. Erythropoiesis is impaired in *Hif1a*$^{-/-}$ (homozygous HIF-1α-null) embryos and erythropoietic defects in HIF-1α-deficient erythroid colonies could not be restored by cytokines, such as vascular endothelial growth factor (VEGF) or EPO (Yoon *et al.*, 2006).

1.3.3 HIF-dependent regulation of angiogenesis

Erythropoiesis represents an adaptive response to systemic hypoxia, whereas angiogenesis describes the local tissue response to decreased oxygenation. As cells grow and proliferate, their oxygen consumption increases and HIF-1 activity is induced either as a result of growth factor mediated induction via phosphatidylinositol 3-kinase, (P13K) or mitogen-activated protein kinase (MAPK) pathways (Figure 6), or as a result of tissue hypoxia (Figure 4). HIF-1 activates the transcription of multiple factors encoding angiogenic growth factors and cytokines (Figure 3), including VEGF, stromal-derived factor-1 (SDF1), placental growth factor (PGF), angiopoietin 1 and 2 and platelet-derived growth factor β (PDGRβ) (Forsythe *et al.*, 1996;Kelly *et al.*, 2003;Ceradini *et al.*, 2004;Bosch-Marce *et al.*, 2007;Simon *et al.*, 2008). These bind to cognate receptors on vascular endothelial and smooth muscle cells as well as on endothelial progenitor cells, mesenchymal stem cells and other bone marrow-derived angiogenic cells (Figure 3) leading to increased tissue vascularisation.

Hypoxia-induced expression of HIF-1 provides a mechanism to ensure that every cell receives adequate perfusion in young and healthy animals. Ageing and diabetes impair angiogenesis (Figure 3) by inhibiting the induction of HIF-1 (Bosch-Marce *et al.*, 2007;Chang *et al.*, 2007). However, this impairment in angiogenesis can be restored by HIF-1α gene therapy in ischemic muscle (Bosch-Marce *et al.*, 2007) and wound tissue (Liu *et al.*, 2008b) or by local administration of an iron chelator (desferrioxamine) that inhibits HIF-1α hydroxylases, into ischemic skin (Chang *et al.*, 2007).

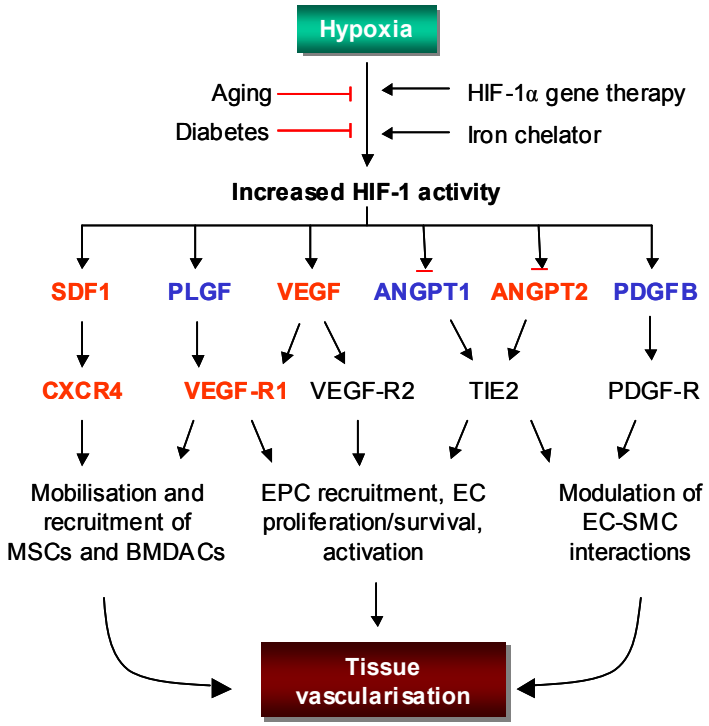

Figure 3 – Regulation of angiogenesis by HIF-1α

Direct HIF-1 target genes are indicated in red, whereas genes that may be either direct or indirect (secondary) targets of HIF-1 are indicated in blue. The combination arrows/ blocked arrows indicate that the genes encoding angiopoietin (ANGPT) 1 and 2 may be activated or repressed by HIF-1 in response to hypoxia depending on the cell type.

1.4 Oxygen-dependent regulation of HIF-1α stability

HIF-1α mRNA is ubiquitously expressed, regardless of the level of oxygen tension. The regulation of HIF-1α protein levels in cells occurs at the level of protein stability. HIF-1α protein accumulates under hypoxic conditions. At physiological oxygen concentrations, the HIF-1α protein is unstable with a half-life of less than 5 minutes. This rapid turnover is mediated via hydroxylation of prolyl and asparaginyl residues.

1.4.1 Prolyl hydroxylation

The HIF-1α prolyl hydroxylases are crucial for the intricate and finely tuned cellular oxygen-sensing system. Three mammalian prolyl hydroxylase enzymes have so far been

identified, termed PHD1, 2 and 3. Their activity relies absolutely on the availability of oxygen (in the form of dioxygen O_2) and 2-oxoglutarate as substrates; ferrous iron (Fe^{2+}) is also an important co-factor. Ascorbate is also required to reduce ferric iron (Fe^{3+}) back to Fe^{2+}, after oxidation reactions, in order for the PHD enzyme to be recycled (Counts *et al.*, 1978). Hydroxylation of proline residues 402 and 564 of human HIF-1α (Hellwig-Burgel *et al.*, 2005) in the ODD domain of HIF-1α mediates the binding of von Hippel-Lindau (VHL) complex; the substrate recognition component of an E3 ligase complex that targets HIF-1α for ubiquitination and proteasomal degradation (Pan *et al.*, 2007). The leucine residue 574 mediates the recognition of HIF-1α by VHL by recruiting a prolyl hydroxylase for the hydroxylation of Pro 564, but both Pro 402 and 564 can interact independently with VHL.

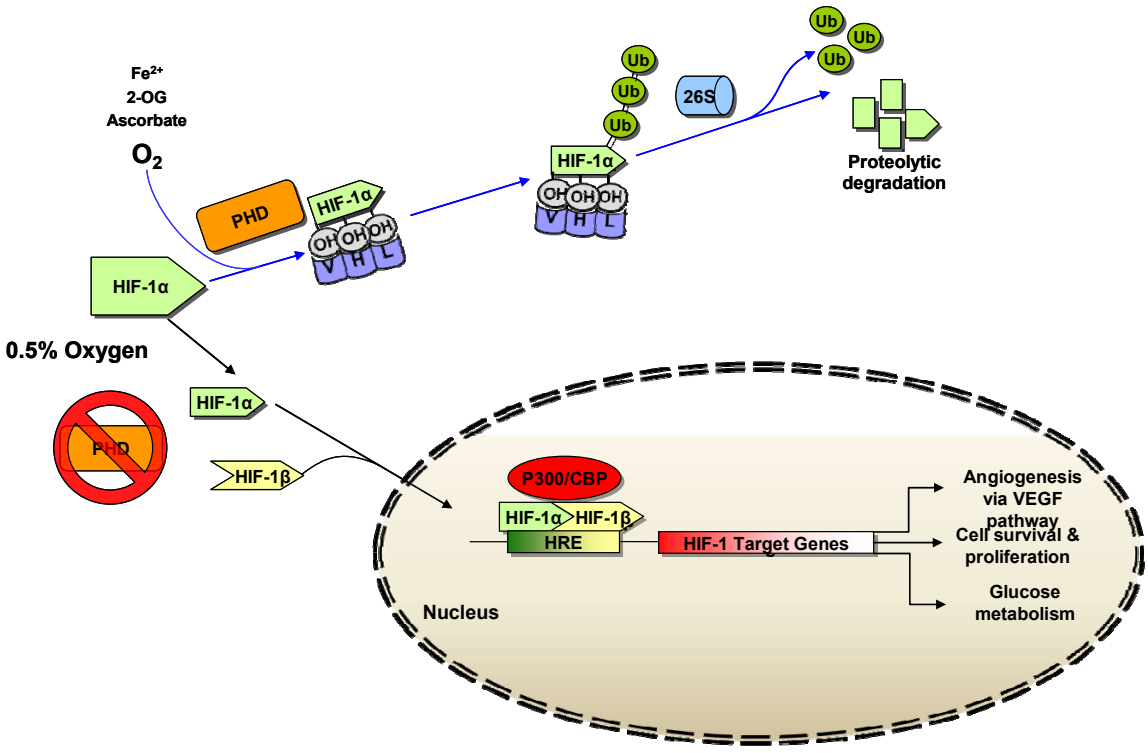

Figure 4 – Schematic of HIF-1α destabilisation and stabilisation

Schematic illustration of HIF-1α degradation at 21% oxygen, and stabilisation at 0.5% oxygen. In the presence of oxygen, PHD targets the α-subunit for proteasomal degradation. In the absence of sufficient substrate, the α-subunit binds to its β-subunit, translocating to the nucleus where a myriad of genes are either activated or suppressed. (Abbreviations: Fe^{2+}, ferrous iron; 2-OG, 2-oxoglutarate; O_2, oxygen; PHD, prolyl hydroxylases; VHL, von Hippel-Lindau; OH, hydroxylation; Ub, Ubiquitinated, HRE, hypoxic response element).

1.4.2 Asparaginyl hydroxylation

Asparaginyl hydroxylation of HIF-1α occurs in the HIF-1α C-TAD, preventing trans-activation. A yeast two-hybrid screen led to the identification of factor inhibiting HIF-1 (FIH-1). FIH-1 is the asparaginyl hydroxylase that hydroxylates human HIF-1α at asparagine (Asn) 803. Hydroxylation of this specific asparagine residue prevents transcriptional activity through inhibiting the interaction with the transcriptional coactivator CBP/p300 [where CBP is CREB (cAMP-response-element-binding protein)- binding protein] (Brahimi-Horn *et al.*, 2007) thus rendering the HIF-1α protein incapable of mediating transcriptional activation. Thus, hydroxylases confer a two-pronged oxygen-dependent repression of the HIF pathway. In hypoxia, the repression imposed by PHDs and FIH is removed and the HIF pathway is activated.

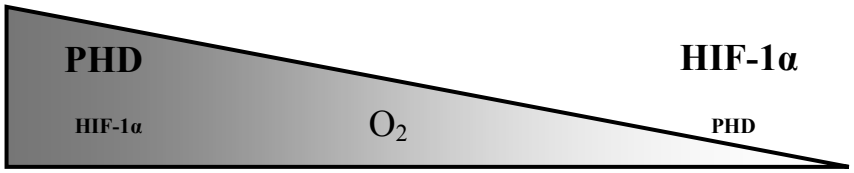

High pO_2

- Active HIF hydroxylases
- Unstable HIF-1α
- pVHL mediated proteolysis
- Inactivation of HIF-1 transcriptional activity

Low pO_2

- Inactive HIF hydroxylases
- Stable α-subunit
- Co-activator recruitment
- Activation of HIF-1 transcriptional activity

Figure 5 – Summary of the regulation of HIF-1α stability

A gradient of pO_2 from normoxic (left) to hypoxic/ anoxic conditions (right), highlighting the crucial events which occur at high pO_2 verses events occurring at low pO_2 (adapted from Pouyssegur *et al.,* 2007).

1.5 Oxygen-independent regulation of HIF-1α stability/ activity

Though HIF-1α stability is most frequently associated with hypoxia, non-hypoxic regulation has been demonstrated.

1.5.1 Pharmacological

Iron chelators such as desferoxamine (DFX) bind free iron, such as the iron found in the reactive centre of the PHDs, thus are able to mimic hypoxia (Schofield and Ratcliffe, 2005) by the reducing the availability of iron as a co-factor. Cobalt chloride ($CoCl_2$) is another agent which has been used to stabilise HIF-1α in normoxic oxygen conditions (Chandel *et al.*, 2001) and this may be due to competition from $CoCl_2$ with iron. However, it has been claimed to 'mimic hypoxia' by inhibiting the interaction between HIF-1α and the VHL protein by direct binding to HIF-1α (Yuan *et al.*, 2003). It has also been reported that transcriptional activity of erythropoitin, glycolytic enzymes and vascular endothelial growth factor occurs in response to $CoCl_2$ in human heptoma cells. The mechanism of which was attributed to the production of reactive species generation via mitochondrial-independent means (Chandel *et al.*, 1998).

1.5.2 Genetic mutations

The von Hippel–Lindau tumor suppressor protein (pVHL) is encoded by the VHL gene and when inactivated is associated with von Hippel–Lindau disease. Maxwell *et al*., 1999 demonstrated that renal carcinoma cells (RCC) lacking VHL constitutively express both HIF-1α and HIF-2α as well as multiple HIF target genes. This effect is observed because VHL-dependent ubiquitination and proteasomal degradation of HIF-1α and HIF-2α can no longer occur. Hypoxic regulation of HIF could be restored upon reintroduction of plasmids encoding the VHL polypeptide (Maxwell *et al.*, 1999).

1.5.3 Growth factors

HIF-1α concentration can also increase in response to growth factor stimulation. However, HIF-dependent growth factor stimulation differs in two important respects from the increase in HIF-1α concentration in response to hypoxia. First, growth factor stimulation induces HIF-1α expression in a cell type-specific manner and secondly, growth factors stimulate the synthesis of HIF-1α via activation of the P13K or MAPK

pathways (Fukuda *et al*., 2002) (Figure 6) and this regulation is not at the level of protein stability.

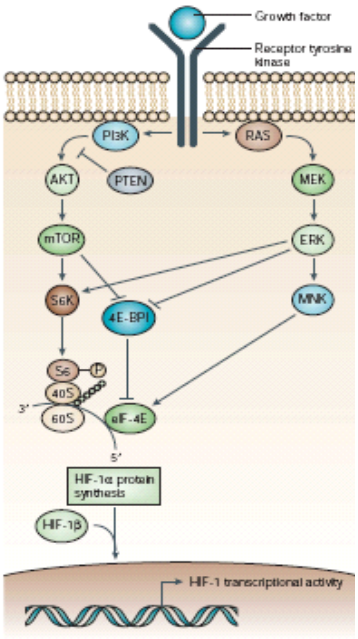

Figure 6 – Growth factor stimulation of HIF-1α protein synthesis

Growth factor binding to a cognate receptor tyrosine kinase activates the phosphatidylinositol 3-kinase (PI3K) and mitogen-activated protein kinase (MAPK) pathways. The effect of growth factor signalling is an increase in the rate at which a subset of mRNAs within the cell (including HIF-1α mRNA) are translated into protein (Semenza, 2003).

1.5.4 Metabolic intermediates

Hydroxylation of HIF-1α is required for degradation of HIF-1α by VHL. PHDs catalyse HIF-1α hydroxylation using 2-oxoglutarate as a cofactor and generate succinate as an end product (Schofield and Ratcliffe, 2004). This mechanism indicates that increased levels of succinate could antagonise HIF-1α hydroxylation, leading to HIF activation. Indeed, this has been confirmed in cells lacking fumarate hydratase (FH) and succinate hydrogenase (SDH) (Pollard *et al.*, 2005), enzymes of the TCA cycle. Loss of function mutations in FH and SDH lead to inherited cancer syndromes. Mutations lead to increased levels of both succinate and fumarate, sequential metabolites of the mitochondrial TCA cycle, which have been shown to inhibit PHD and to increase HIF-1α protein levels.

1.5.5 S-nitrosylation

In murine tumours, exposure to ionising radiation stimulated the generation of NO in tumour associated macrophages. As a result, the HIF-1α protein is S-nitrosylated at Cys533 in the ODD domain, which prevents its destruction. Importantly, this mechanism appears to be independent of the prolyl hydroxylase-based pathway that is involved in oxygen-dependent regulation of HIF-1α. Selective disruption of this S-

nitrosylation significantly attenuated both radiation-induced and macrophage-induced activation of HIF-1α (Li *et al.*, 2007).

1.5.6 Free radicals

Recent data has shown that free radicals play a role in the regulation of HIF-1α stabilisation (Klimova and Chandel, 2008). Some authors have proposed a model in which ROS (section 1.6) generation increases under hypoxia. As early as 1998, Chandel *et al*., reported ROS generation from the mitochondria were sufficient to trigger HIF-1α DNA binding activity and mRNA expression of EPO and VEGF (downstream HIF-1α targets) in human hepatoma cells. They later reported that during hypoxia, superoxide was generated at Complex III of the mitochondrial electron transport chain. This superoxide passes into the cytosol via anion channels where is converted to hydrogen peroxide (H_2O_2) which induces PI3K and protein phosphatase activity leading to HIF-1α stabilisation and transcription of downstream target genes in hypoxic cells (Chandel *et al.*, 2000a). Data obtained by Agani *et al*., 2000 demonstrated that inhibitors of the electron transport chain, specifically at Complex I, blocked HIF-1α expression in mice exposed to a hypoxic environment. These data are also supported by evidence from human ape xenomitochondrial cybrids (HAXC) (the introduction of mtDNA from non-human apes into a human cells lacking mtDNA), where a decrease in HIF-1α expression was observed. Mitochondrial Complexes II, III, IV and V had activities indistinguishable from parental human or non-human primate cells. However, there was a 40% reduction in the activity (V_{Max}) of the electron transport chain at Complex I (Agani *et al.*, 2000), consequently there would be no ROS generated from the mitochondria as Complex I lies upstream of Complex III (section 1.6.2.5).

Although several groups have confirmed the above data (Guzy *et al.*, 2005;Brunelle *et al.*, 2005), the generation of free radicals in hypoxia and their effect of stabilising HIF-1α remains controversial since there is evidence to the contrary. For example, Genius and Fandrey, demonstrate decreased NADPH oxidase (section 1.6.2.2) ROS production in hypoxia (Genius and Fandrey, 2000). Another group, in 2001, demonstrated that HIF-1 activation does not require an active mitochondrial respiratory chain. Their data shows that cells without functional mitochondria (*Rho*^{0}), generated by prolonged exposure to ethidium bromide have a normal response to hypoxia, measured at the level of HIF-1α stabilisation, translocation and its transcriptional activation activity. Furthermore, over expression of catalase (section 1.7.3), which degrades hydrogen

peroxide, either in the mitochondria or cytosol, fails to modify the hypoxic response, indicating hydrogen peroxide is not a signalling molecule in the hypoxic signalling cascade (Srinivas *et al.*, 2001).

Vaux *et al*., 2001 studied HIF-1α stabilisation and the HIF target gene, glucose-transporter-1, in a variety of Rho^0 cells or in cells which had other genetic defects in mitochondrial respiration. HIF induction by hypoxia was essentially normal in all cells tested. Hydrogen peroxide production was measured and found to be reduced in Rho^0 versus wild-type cells and further reduced by hypoxia. Furthermore, concentrations of rotenone that maximally inhibited respiration did not affect HIF activation by hypoxia (Vaux *et al.*, 2001). These data do not support the model of ROS-induced HIF-1α stabilisation and indicate that a functional respiratory chain may not be necessary for the regulation of HIF by ROS.

The demonstration of free radical generation in hypoxia, and more specifically from the mitochondria remains contentious, largely due to methodologies used to measure free radicals. The formation of ROS and RNS may be monitored using a variety of procedures including fluorometric and spectrophotometric methods, chemiluminescence and electron paramagnetic resonance (Chance *et al.*, 1979;Pou *et al.*, 1989;Tarpey and Fridovich, 2001). These methods rely on the redox properties of specific ROS and RNS, and therefore are prone to artefacts (or false positive results) caused by species of similar reactivity or by reactive intermediates produced by the probe itself (Picker and Fridovich, 1984;Faulkner and Fridovich, 1993;Liochev and Fridovich, 1995;Liochev and Fridovich, 1998). Specific inhibitory enzymes may be added to unequivocally identify the species (such as superoxide dismutase or catalase to eliminate superoxide or hydrogen peroxide, respectively) but these enzymes do not determine whether ROS are the primary species or rather intermediates formed in the detection reaction. For example, it has been reported that superoxide was produced by the enzyme glucose oxidase since superoxide dismutase inhibited the reduction of nitroblue tetrazolium in the presence of glucose, when in fact the probe was reacting with the enzymes prosthetic group and superoxide was formed after this reaction (al-Bekairi *et al.*, 1994;Liochev and Fridovich, 1995). Similar results have been demonstrated with luminol and lucigenin (Liochev and Fridovich, 1998).

Studies using visible light spectroscopy (VLS) have shown that generation of ROS occurs at low oxygen concentration ($[O_2]$) (3% O_2) in the murine monocytic cell line, RAW246.7 and that it is dependent on the redox state of the electron transport chain (Palacios-Callender *et al.*, 2004), which is regulated by the interaction of NO on cytochrome c oxidase (Cooper and Giulivi, 2007). This has led to the suggestion that free-radical dependent stabilisation of HIF-1α is indeed a possible mechanism of HIF-1α stabilisation, particularly in pathological conditions such as cancer which are known to be associated with particularly high free-radical generation (Quintero *et al.*, 2006a). It also opens up the possibility of NO taking part in this regulation in situations in which the redox status of the oxidative-phosphorylation chain is reduced in the presence of enough oxygen to favour the generation of ROS. This might occur as a result of the relative ratio between $[O_2]$ and [NO] but not in hypoxia, where although the oxidative-phosphorylation chain is reduced there might not be enough oxygen to allow free-radical generation (Palacios-Callender *et al.*, 2004).

1.6 Free radicals

1.6.1 Introduction

Reactive oxygen species (ROS) are oxygen-derived small molecules, including oxygen radicals (superoxide ($O_2^{-\cdot}$), hydroxyl ($\cdot OH$), peroxyl ($RO_2\cdot$), and alkoxyl ($RO\cdot$)) and certain non-radicals that are either oxidising agents and/or easily converted into radicals, such as hypochlorous acid (HOCl), ozone (O_3), singlet oxygen ($^1O_2$) and hydrogen peroxide (H_2O_2). Nitrogen-containing oxidants, such as nitric oxide (NO), are called reactive nitrogen species (RNS).

The presence of free radicals in biological systems was discovered more than 50 years ago (Commoner *et al.*, 1954). Shortly thereafter, it was hypothesised that oxygen radicals could be by-products formed through enzymatic reactions *in vivo* (Harman, 1956). Denham Harman described free radicals as a Pandora's box of evils that may account for cellular damage, mutagenesis, and cancer and could play a role in biological ageing. However, one beneficial function of ROS production was also realised, namely, the importance of ROS in host defence, highlighted by deficiency in ROS generation and reduced killing ability of leukocytes. Over the last few decades, however, ROS have been shown to play an important role as regulatory mediators in signalling processes (Forman and Torres, 2002;Quintero *et al.*, 2006b;Colombo and Moncada, 2009).

1.6.2 Physiological sources of ROS

1.6.2.1 Introduction

In mammalian cells, ROS can be formed in response to toxic reagents or as products of O_2-utilising enzymes such as those in NADPH oxidases, xanthine oxidase, NO synthases (NOS) and the mitochondrial respiratory chain.

1.6.2.2 Nicotamide adenine dinucleotide phosphate (NADPH)-oxidases

1.6.2.2.1 Introduction

The NADPH oxidase (NOX) family are proteins that transfer electrons across biological membranes and have emerged as a major source of ROS in signal transduction (Brown and Griendling, 2009). NADPH oxidase proteins are membrane-associated, multiunit enzymes that catalyse the reduction of oxygen using NADPH as an electron donor, producing superoxide via a single electron reduction. The electron travels from NADPH down an electrochemical gradient first to flavin adenine dinucleotide (FAD), then through the NOX heme groups, and finally across the membrane to oxygen, forming superoxide (Figure 7). Historically, the NADPH oxidase was known as the source of phagocyte respiratory burst; however, in the past 15 years NOX family members and the ROS they produce have been identified as important contributors to many signalling pathways (Brown and Griendling, 2009).

1.6.2.2.2 Discovery

The first body of research to be undertaken into NOX proteins was carried out in neutrophils, whilst studying the respiratory burst NADPH oxidase complex (Babior *et al.*, 1973). The catalytic subunit of this protein is now known as NOX2, or $gp91^{phox}$. This phagocytic NADPH oxidase (NOX2) enzyme actively generates superoxide, and plays a key role in host defence. This enzyme consists of the integral membrane subunits $gp91^{phox}$ and $p22^{phox}$, which form the heme-containing catalytic core of the enzyme termed flavocytochrome b_{558} (Bedard and Krause, 2007) which are dispersed between the cytosol and the membranes whilst inactive. The other components of the NADPH complex ($p47^{phox}$, $p67^{phox}$, $p40^{phox}$ and small G-protein Rac1/2) are cytosol proteins. The activation of phagocytes by various stimuli triggers the phosphorylation of the $p47^{phox}$, $p67^{phox}$ and $p40^{phox}$ cytosolic components and their translocation to the

plasma membrane, where they interact with flavocytochrome b_{558}. Concomitantly, Rac2 dissociates from its RhoGDP dissociation inhibitor, which allows it to interact with flavocytochrome b_{558} to form a binding partner for $p67^{phox}$. This allows transfer of electrons from NADPH to oxygen resulting in the rapid elevation of superoxide levels (Figure 7) (Kietzmann and Gorlach, 2005).

During the discovery of the phagocytic NADPH oxidase in the 1980's, a series of observations suggested that similar enzyme systems existed in many other cell types including fibroblasts, tumour cells, endothelial cells and vascular smooth muscle cells (Bedard and Krause, 2007). However, new NOX family members have only been cloned and studied in the past decade. The first homologue of NOX2 to be cloned was NOX1, originally described in 1999 as MOX1 (Suh *et al.*, 1999), and by a separate group as NOH-1 (Banfi *et al.*, 2000). Dual oxidase (DUOX) enzymes (longer homologues of NOX2) were cloned shortly after NOX1. In 2000, NOX3 was described as a $gp91^{phox}$ homologue expressed in foetal kidney and a cancer cell line (Kikuchi *et al.*, 2000). NOX3 was later determined to be primarily expressed in the inner ear in adults (Banfi *et al.*, 2004a) NOX4, was discovered in the kidney (Geiszt *et al.*, 2000;Shiose *et al.*, 2001), and soon afterwards was described in osteoclasts (Yang *et al.*, 2001). NOX5 was discovered in 2001 by two different groups (Cheng *et al.*, 2001;Banfi *et al.*, 2004b).

1.6.2.2.3 Structure and activation

Structurally, all members of the NOX family contain at least six transmembrane domains and cytosolic FAD and NADPH binding domains. NOX1-4 lack extra functional domains that NOX5 and DUOX1 /2 contain (Figure 7). A number of regulatory subunits have been identified for the NOX isoforms. Activation can occur as a result of various stimuli such as angiopoietin-1, angiotensin II (AngII), insulin, thrombin and VEGF. These stimuli alter the activity and/or expression of the NOX proteins and subunits, and ultimately the amount of ROS produced. Activation mechanisms for NOX1-3 are similar, and involve complex formation with regulatory cytosolic subunits. Regulation of NOX4 is poorly understood, but may be primarily at the expression level (Krause, 2004). In contrast, NOX5 and the DUOXs appears to be activated by calcium (Ca^{2+}) (Banfi *et al.*, 2001;Meziane-El-Hassani *et al.*, 2005).

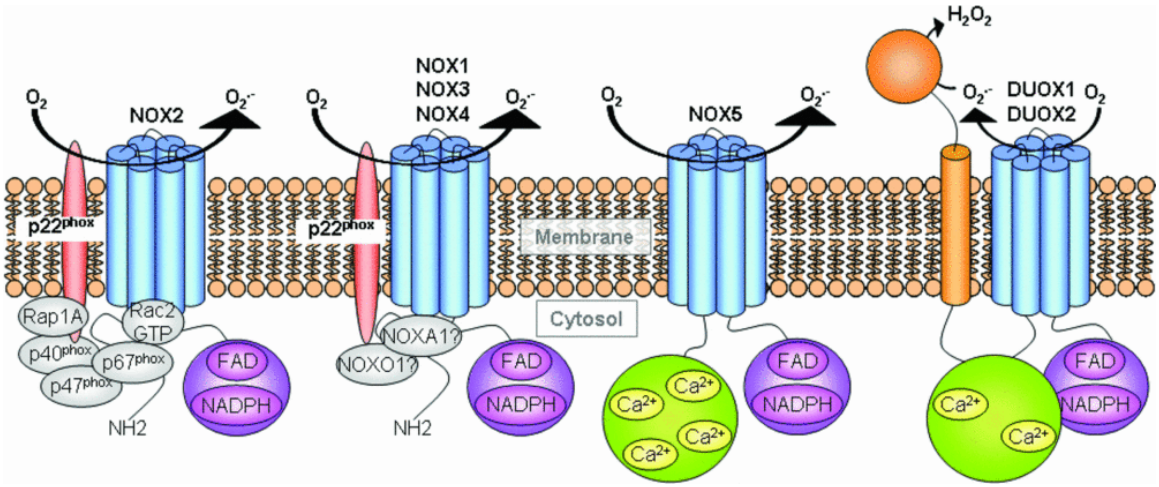

Figure 7 – NADPH oxidase family

NADPH oxidase (NOX2) is a multiunit enzyme system that catalyses the NADPH-dependent reduction of oxygen to $O_2^{\bullet-}$. NOX2 comprises a membrane-bound $gp91^{phox}/p22^{phox}$ heterodimer and other subunits (p67phox, p47phox, p40phox and Rac), which associate with this complex in the activated enzyme. Six homologues (NOX1, NOX3, NOX4, NOX5, DUOX1 and DUOX2) with levels of identity with NOX2 have been identified. NOXO1 and NOXA1, which may interact with NOX1 and NOX4, are two homologues of $p67^{phox}$ and $p47^{phox}$ respectively. NOX family homologues have putative NADPH- and flavin-binding sites, as well as functional oxidase activity that produces $O_2^{\bullet-}$. NOX5, DUOX1, and DUOX2 also have a Ca^{2+}-binding site, whereas DUOX1 and DUOX2 have an additional transmembrane and a peroxidase-like domain.

1.6.2.2.4 NOX derived ROS and the relationship of NOX to other sources of ROS

Superoxide is the primary product of NOX enzymes. Superoxide can dismutate to a secondary signalling molecule intermediate; hydrogen peroxide, either spontaneously or enzymatically via superoxide dismutase (SOD) (section 1.7.2). As a consequence, superoxide must be produced in very close proximity to its target to be effective as a signalling molecule. Superoxide is also capable of reacting with nitric oxide, forming highly reactive peroxynitrite. This inactivates nitric oxide, resulting in pathological consequences particularly in vascular endothelial cells (1.6.4.1). Superoxide also reacts with iron-sulphur (FeS_4) clusters within proteins, which may release ferric ions (Panov *et al.*, 2005). In the case of aconitase, superoxide inactivates the enzymes, leading to reduced mitochondrial function (Gardner *et al.*, 1995). Superoxide is also known to react with protein thiols such as cysteine residues, but it has also been demonstrated that the reaction rate of SOD converting superoxide to hydrogen peroxide is much faster than the reaction rate of biothiols (Forman *et al.*, 2004).

Hydrogen peroxide is more stable than superoxide and is also capable of crossing biological membranes. Hydrogen peroxide formation is tightly regulated by catalase, glutathione and peroxiredoxins (section 1.7), which convert hydrogen peroxide to water and other metabolites.

NADPH oxidases are not the only source of ROS-producing molecules expressed physiologically (see below) and there appears to be a reciprocal relationship between many of these sources of ROS. For example, exposure of endothelial cells to oscillatory shear stress leads to NOX-dependent activation of xanthine oxidase (McNally *et al.*, 2003), while Ang II stimulation results in mitochondrial ROS production downstream of NOX activation (Dikalov *et al.*, 2008). Endothelial NOS (eNOS) uncoupling has also been shown to be a direct result of NOX activation (Landmesser *et al.*, 2003). It therefore seems that NOX enzymes play roles as initiators and integrators of redox signalling via cross talk with other ROS-producing enzymes (Brown and Griendling, 2009).

1.6.2.3 Xanthine oxidoreductase

Xanthine oxidoreductase (XOR) is a meloflavoprotein enzyme that exists in two interconvertible, although functionally distinct forms, namely, xanthine dehydrogenase (XD) and xanthine oxidase (XO). Of them, only the latter generates superoxide by the oxidation of hypoxanthine to uric acid using molecular oxygen as the electron acceptor (Puddu *et al.*, 2008). Usually levels of XO activity are un-measurable in most cell types, although XO may play an important role in vascular superoxide generation in experimental models of type I diabetes (Forbes *et al.*, 2008). Xanthine oxidase is also activated by pro-inflammatory mediators and is up-regulated by NADPH oxidase activation. *In vitro* experiments with endothelial cells have shown that incubation with apocynin (a NAPDH oxidase inhibitor) or disruption of $gp47^{phox}$ gene markedly decreases XO expression and activity (McNally *et al.*, 2003).

1.6.2.4 Nitric oxide synthases (NOS)

Nitric oxide (NO) is a stable, hydrophobic, diatomic radical gas, which is both lipid and water-soluble. It is produced by the catalytic conversion of L-arginine to L-citrulline by one of three nitric oxide synthase (NOS) isoforms (Palmer *et al.*, 1987;Bredt and

Snyder, 1990;Pollock *et al.*, 1991;Stuehr *et al.*, 1991a). Each isoform requires several co-factors for the reaction, including nicotinamide adenine dinucleotide phosphate (NADPH), tetrahydrobiopterin (BH_4), flavin adenine dinucleotide (FAD), flavinmononucleotide (FMN), calmodulin (CaM) and O_2 (Knowles and Moncada, 1994). The catalytic reaction involves two steps. L-arginine is initially hydroxylated to N^Ghydroxy-L-arginine (NOHA; (Stuehr *et al.*, 1991b)) followed by NOHA oxidation to equimolar quantities of NO and L-citrulline (Lirk *et al.*, 2002).

There are three major isoforms of NOS: neuronal NOS (nNOS), endothelial NOS (eNOS) and inducible NOS (iNOS). They all exist as homodimers in their active form, share 50–60% sequence homology and show 80–90% conservation among species (Forstermann and Kleinert, 1995).

Endothelial-derived NO is a paracrine factor that controls vascular tone, inhibits platelet function, prevents adhesion of leukocytes and reduces proliferation of the intima. An enhanced inactivation and/or reduced synthesis of NO is seen in conjunction with risk factors for cardiovascular disease (section 1.6.4.1). This condition, referred to as endothelial dysfunction, can promote vasospasm, thrombosis, vascular inflammation and proliferation of vascular smooth muscle cells. Vascular oxidative stress with an increase in ROS contributes to mechanisms of vascular dysfunction. Oxidative stress is mainly caused by an imbalance between the activity of pro-oxidative enzymes and anti-oxidative enzymes, in favor of the former. Increased ROS concentrations reduce the amount of bioactive NO by chemical inactivation to form toxic peroxynitrite. Peroxynitrite in turn can uncouple eNOS to become a dysfunctional superoxide-generating enzyme that contributes to vascular oxidative stress. Oxidative stress and endothelial dysfunction can promote atherogenesis (section 1.6.4.1) (Forstermann, 2010).

Inducible NO provides a primary defense mechanism against tumour cells and intracellular and extracellular microorganisms in macrophages (Moncada and Higgs, 1993). The ‘high output’ NO from iNOS is cytotoxic and cytostatic and is thus important in combating bacterial infections. During the course of an inflammatory response, stimulated macrophages produce high levels of NO that surpass physiological concentrations and this diffuses to target cells (e.g. bacteria, fungi or tumour cells) where it causes DNA damage, low density lipoprotein (LDL) oxidation, isoprostane

formation, tyrosine nitration and inhibits mitochondrial respiration (Guzik *et al.*, 2003). NO binds with iron-sulphur centres in key enzymes involved in the target's respiratory chain and DNA synthesis pathway. NO target enzymes include aconitase, which is part of the TCA cycle, reduced nicotinamide adenine dinucleotide (NADH) dehydrogenase, which belongs to Complex I of the mitochondrial respiratory pathway, succinate dehydrogenase part of mitochondrial Complex II and ribonucleoside-diphosphate reductase, which is essential in DNA synthesis (Moncada and Higgs, 1993). The high NO levels are usually paralleled with the production of superoxide anion. Nitric oxide and oxygen combine forming peroxynitrite, which complements the cytotoxic effects of NO (Linares *et al.*, 2001). Animal models and human clinical data have demonstrated the importance of iNOS and 'high output' NO in the development of septic shock, a heightened inflammatory response (Ochoa *et al.*, 1991;Liu *et al.*, 1993).

1.6.2.5 Mitochondrial

1.6.2.5.1 Introduction

The mitochondria are the largest consumers of oxygen and the electron transport chain (ETC) is responsible for most of the ROS produced in human tissues (Chance *et al.*, 1979). Mitochondrial respiration accounts for approximately 90% of cellular oxygen uptake, and as much as 3% of the oxygen consumed is converted to ROS (Turrens, 2003). This ROS production contributes to a range of pathologies and is also involved in redox signalling from the organelle to the rest of the cell (Droge, 2002;Balaban *et al.*, 2005).

1.6.2.5.2 Sites of superoxide formation in the respiratory chain

There are a variety of respiratory components, including flavoproteins, iron-sulphur clusters and ubisemiquinone that are thermodynamically capable of transferring one electron to oxygen. Moreover, most steps in the respiratory chain involve single-electron reactions, which favours the reduction of oxygen. However, only a small proportion of mitochondrial electron carriers with the thermodynamic potential to reduce oxygen to superoxide do so (Murphy, 2009).

Superoxide formation occurs on the outer mitochondrial membrane, in the matrix and on both sides of the inner mitochondrial membrane (Figure 8). Whilst the superoxide generated in the matrix is eliminated in that compartment by superoxide dismutase

(section 1.7.2), part of the superoxide produced in the intermembrane space may be carried to the cytoplasm via voltage-dependent anion channels (Han *et al.*, 2003). The relative contribution of every site to the overall superoxide production varies from organ to organ and also depends on whether the mitochondria are actively respiring (State 3) or the respiratory chain is highly reduced (State 4) (Barja, 1999).

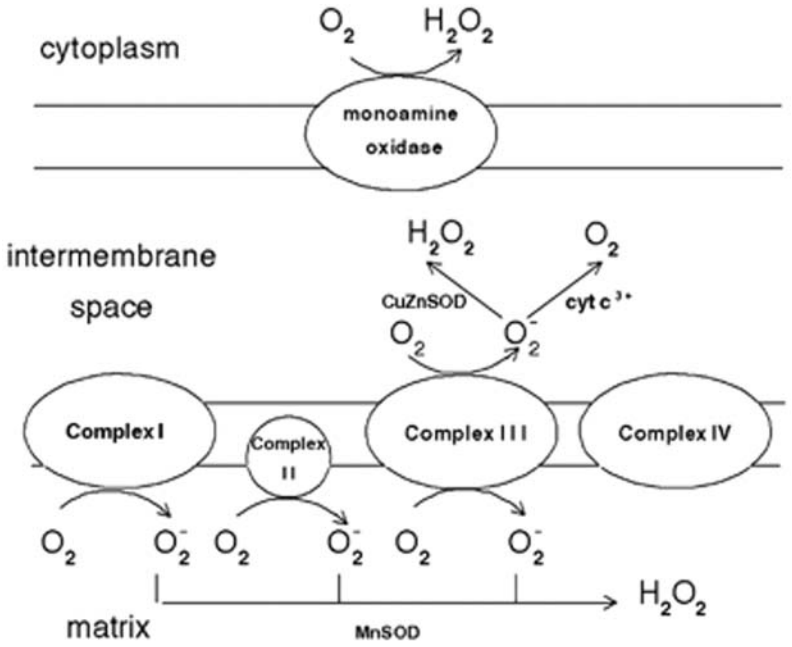

Figure 8 – Sites of superoxide formation in the respiratory chain

Various respiratory Complexes leak electrons to oxygen producing primarily superoxide anion (O_2^-•). This species may reduce cytochrome *c* (in the intermembrane space), or may be converted to hydrogen peroxide (H_2O_2) and oxygen (in both the matrix and the intermembrane space). Increased steady state concentrations of O_2^-• may reduce transition metals (which in turn react with H_2O_2 producing hydroxyl radicals (OH•)) or may react with nitric oxide to form peroxynitrite. Both OH• and peroxynitrite are strong oxidants which indiscriminately react with nucleic acids lipids and proteins (Turrens, 2003).

The rate of superoxide formation by the respiratory chain is controlled primarily by mass action, increasing both when electron flow slows down (increasing the concentration of electron donors) and when the concentration of oxygen increases (Turrens *et al.*, 1982). The energy released as electrons flow through the respiratory chain is converted to a proton (H^+) gradient through the inner mitochondrial membrane (Mitchell, 1977). This gradient in turn, dissipates through the ATP synthase (Complex V) and is responsible for the turning of a rotor-like protein Complex required for ATP synthesis (Noji and Yoshida, 2001). In the absence of ADP, the movement of protons

through ATP synthase ceases and the proton gradient builds up causing electron flow to slow down and the respiratory chain to become more reduced (State 4 respiration). As a result, the physiological steady state concentration of superoxide formation increases (Boveris *et al.*, 1972).

1.6.2.5.3 Sites of nitric oxide formation in the respiratory chain

Two separate laboratories have discovered that the mitochondrial matrix contains a unique form of NOS (Ghafourifar and Richter, 1997;Giulivi *et al.*, 1998;Alvarez *et al.*, 2003). It appears this formation of NO in the mitochondria may have important consequences, as this NO binds to haem groups from cytochromes (in particular cytochrome *c* oxidase) and inhibits respiration (Poderoso *et al.*, 1996). In turn, this may stimulate superoxide formation, which in turn may react with NO forming peroxynitrite, a strong oxidant capable of inhibiting enzymes and affecting mitochondrial integrity (Cassina and Radi, 1996;Radi *et al.*, 2002).

1.6.2.5.4 Mitochondrial ROS formation during hyperoxia

Mitochondrial production of superoxide increases with oxygen concentration. The proportion of oxygen converted into superoxide *in vitro* ($[O_2]$ = 220 μM) accounts for approximately 1-3% of the overall oxygen consumption. *In vivo*, particularly in tissues not exposed to atmospheric oxygen, the proportion of oxygen converted to superoxide is likely to be smaller since the intramitochondrial oxygen concentration is between 3 and 30 μM (Wittenberg and Wittenberg, 1989). As oxygen concentrations increase, the rate of mitochondrial superoxide production increases linearly (Turrens *et al.*, 1982). However, the release of hydrogen peroxide from mitochondria is biphasic, increasing at a faster rate above 60% oxygen (Turrens *et al.*, 1985). The slower release of hydrogen peroxide at lower pO_2 suggests that the mitochondrial antioxidant defences (section 1.7.2) can compensate for sudden increases in the concentration hydrogen peroxide. These defences become overwhelmed at higher pO_2, which explains the mitochondrial alterations observed in the lungs of animals exposed to oxygen concentrations above 60% (Crapo *et al.*, 1983).

Under normobaric hyperoxic conditions, the lungs are the only organs affected by ROS, since they are in direct contact with atmospheric oxygen. Under hyperbaric conditions, however, more oxygen is dissolved in the plasma, and therefore other tissues become exposed to a hyperoxic environment. Under these conditions, the brain is the first organ

to show the effects of an increased ROS formation, resulting in convulsions (Turrens, 2003).

1.6.2.5.5 Mitochondrial ROS formation during hypoxia

The formation of ROS should decrease with hypoxia, since mitochondrial activity is proportional to ROS. However the paradoxical increase in oxidative stress under moderately hypoxic conditions (1.5% oxygen, equivalent to an oxygen concentration of around 16 μM) has been reported (Schumacker, 2002;Waypa and Schumacker, 2002). These studies show that when cells are incubated with dichlorofluorescin, a fluorescent probe for ROS, hypoxia increases fluorescence in cells with functioning mitochondria (Chandel *et al.*, 1998). Mutants without a functioning respiratory chain do not show this increase in fluorescence (Chandel *et al.*, 1998;Schroedl *et al.*, 2002). This response is eliminated when cells are made severely hypoxic (Schumacker, 2002). The proposed increase in ROS formation during hypoxia is paradoxical, given the high affinity of cytochrome *c* oxidase for oxygen; at low pO_2 any remaining oxygen should be reduced to water by the terminal oxidase. However, two factors may contribute to an increase in mitochondrial superoxide formation. Firstly, under hypoxic conditions, low concentrations of NO radical may still be produced since the K_m for oxygen of mitochondrial NOS is around 30-40 μM (Alvarez *et al.*, 2003). Secondly, NO may bind and inhibit cytochrome *c* oxidase, resulting in an increase in its K_m for oxygen and an increased reduction of electron carriers located upstream from the terminal oxidase (Cooper and Davies, 2000), favouring superoxide formation at low oxygen concentrations (Palacios-Callender *et al.*, 2004).

In summary, it has long been recognised that ROS such as superoxide and hydrogen peroxide are produced in cells either as by-products during mitochondrial electron transport or by several oxidoreductases. Stimulated production of ROS was first described in phagocytic cells such as neutrophils and macrophages and was named the 'respiratory burst' due to the transient consumption of oxygen (Arnold *et al.*, 2001). The production of ROS has been demonstrated in a variety of cells other than phagocytes and several studies have implicated ROS in physiological signalling (Bejarano *et al.*, 2007).

1.6.3 Physiological function of ROS

1.6.3.1 Introduction

The balance between oxidants and antioxidants is reflected in the redox state within cells, and is important in the regulation of gene expression. Indeed, changes in cellular redox state may be integrally associated with cell differentiation, progression through the cell cycle and ageing processes. In some instances, ROS may act as bona fide second messengers. Extracellular ROS can initiate cellular signalling by activation of growth factor and cytokine receptors in a manner that does not require the presence of the receptor ligands (Hayes and Lockwood, 1987;Kadota *et al.*, 1987;Koshio *et al.*, 1988;Huang *et al.*, 1996) or via generation of lipid peroxides within cell membranes (Suzuki *et al.*, 1997). A variety of stimuli lead to intracellular ROS production. Tumour necrosis factor-α (TNF-α) provokes a rise in hydrogen peroxide production from mitochondria, and other ROS, via induction of NADPH oxidase (Lo and Cruz, 1995;Garcia-Ruiz *et al.*, 1997). Interaction of platelet-derived growth factor (PDGF) and epidermal growth factor (EGF) with their receptors causes a transient increase in hydrogen peroxide. In the case of PDGF, this increase in hydrogen peroxide has been shown to be essential for growth induction.

The effects of NO and RNS have been shown to parallel the effects of ROS. It is widely recognised that nitric oxide has beneficial physiological effects such as enhancing vasodilatation and inhibiting formation of platelet thrombi and, therefore, is protective against cardiovascular disease (Li and Forstermann, 2000).

1.6.3.2 NOX derived ROS

The NOX family of proteins has been demonstrated to be essential in normal physiology. Expression of NADPH oxidases is ubiquitous in mammals, though the individual NOX isoforms have different distributions between tissues (section 1.6.2.2). NOX proteins have been shown to regulate many fundamental physiological processes including cell growth, differentiation, apoptosis, and cytoskeleton remodelling. In addition, they have specialised functions, such as host defence (NOX2) (Rada *et al.*, 2008), otoconium formation in the inner ear (NOX3) (Krause, 2004), iodination of

thyroid hormone (DUOX2) (Milenkovic *et al.*, 2007), and control of vascular tone (NOX2) (Cave *et al.*, 2006).

More recently, NOX proteins have been implicated in oxygen sensing. During the discovery of the different NOX isoforms, *in vitro* studies showed that NOX enzymes were less active in hypoxia than normoxia (Gabig *et al.*, 1979). *In vivo* data has demonstrated the production of mitochondrial ROS in low oxygen, which activates HIF-1α (section 1.5.6). There is also evidence to suggest NADPH oxidase-derived ROS (He *et al.*, 2002) are involved in oxygen sensing, but the mechanism is unclear.

1.6.3.3 Cellular signalling

Reactive oxygen species act through different pathways of signal transduction, making use of signalling molecules such as calcium, protein tryrosine phosphatases (PTPs), protein tyrosine kinases (PTKs) and transcription factors.

1.6.3.3.1 Intracellular calcium signalling

The cytosolic free Ca^{2+} concentration ($[Ca^{2+}]_c$) is an important intracellular messenger system. Usually, this concentration is kept low (100 nM) by Ca^{2+} pumps. In response to various stimuli, $[Ca^{2+}]_c$ rises to micromolar levels, which leads to the activation of Ca^{2+}-dependent cellular processes. The rise in $[Ca^{2+}]_c$ occurs through Ca^{2+} influx across the plasma membrane and/or through Ca^{2+} release from intracellular stores. Oxidant induced inositol 1,4,5-triphosphate (IP3) release represents one component of the signal transduction pathway for Ca^{2+} release. IP3 promotes the release of Ca^{2+} ions from stores in the endoplasmic reticulum, thus activating protein kinase C (PKC), promoting its translocation to the plasma membrane. PKC phospholipase A2 (PLA2) is also activated and translocated to the plasma membrane in response to increased ($[Ca^{2+}]_c$. The products of PLA2 activity are arachidonic acid and its metabolites, which are primary mediators of immune and inflammatory responses.

1.6.3.3.2 Protein phosphatases

Despite its toxicity, hydrogen peroxide is produced as a signalling molecule that oxidises critical cysteine residues of effectors such as protein tyrosine phosphatases (PTPs) in response to activation of cell surface receptors.

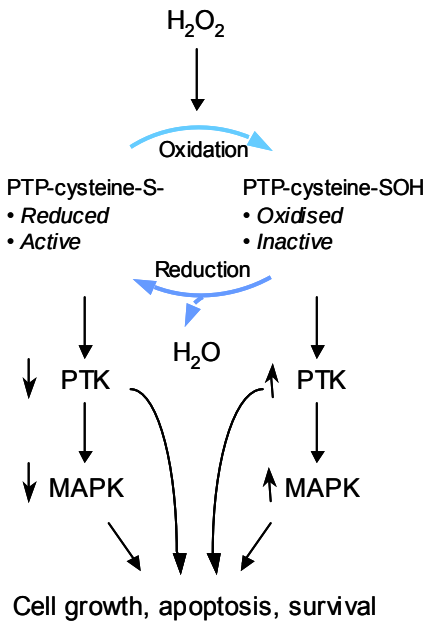

Figure 9 – Oxidative inactivation of protein tyrosine phosphatases by ROS

All PTPs possess a redox-regulated cysteine, which catalyses the hydrolysis of protein phosphotyrosine residues by the formation of a cysteinyl-phosphate intermediate. Oxidation of this cysteine residue to sulfenic acid (RSOH) by H_2O_2 renders PTP completely inactive. Since the oxidation of PTP is reversible, PTPs exist in two forms; an active state with a reduced cysteine or an inactive state with an oxidised cysteine. Inactivation of PTP is associated with increased activation of protein tyrosine kinases (PTK) and mitogen-activated protein kinases (MAPK).

PTPs are involved in the regulation of cell proliferation, differentiation, survival, metabolism, and motility by controlling the phosphorylation state of numerous signal-transducing proteins. The catalytic domain of PTPs contains a conserved region with a single cysteine residue, which are susceptible to oxidative inactivation. Mutation or oxidation of this cysteine renders the enzymes inactive (Chiarugi and Cirri, 2003). Inactivation of PTP is associated with increased activation of protein tyrosine kinases (PTK) and mitogen-activated protein kinases (MAPK).

Until recently, it had remained unclear how, even in the presence of the abundant detoxification enzymes peroxiredoxin (Prx) I and II (section 1.7.6), hydrogen peroxide can accumulate in the cytosol to a concentration sufficient for it to modify target

proteins. Woo *et al*., 2010 show that PrxI associated with membranes is transiently phosphorylated on tyrosine-194 and thereby inactivated both in cells stimulated via growth factor or immune receptors *in vitro* and those at the margin of healing cutaneous wounds in mice. The localised inactivation of PrxI allows for transient accumulation of hydrogen peroxide around membranes, where signalling components are concentrated, while preventing the toxic accumulation of hydrogen peroxide elsewhere. In contrast, PrxII was inactivated not by phosphorylation but rather by hyper-oxidation of its catalytic cysteine during sustained oxidative stress (Woo *et al.*, 2010).

1.6.3.3.3 Protein kinases

Numerous studies (Bauskin *et al.*, 1991;Devary *et al.*, 1992;Abe *et al.*, 1997;Kurata, 2000) have found that oxidant treatment of cells produces elevations in protein phosphorylation and various protein kinases. The p38 mitogen-activated protein kinases (MAPK) are one of the most extensively studied families of protein kinases. There is evidence for activation of the MAPK system by NADPH oxidases, specifically NOX4 (Brown and Griendling, 2009). This is thought to be due to the activation of signalling pathways upstream of ERK1/2 kinase, or it may be an indirect effect due to the inhibition of phosphatase activity by ROS (Figure 9) (Touyz, 2004).

Another important kinase signalling pathway involves protein kinase C (PKC). PKC is not a single enzyme, rather PKC arises from a family of at least 12 related enzymes. The mechanism of activation involves lipids, calcium and PKC phosphorylation (Newton, 1997). Reactive oxygen species have also been demonstrated to activate members of the PKC family (Newton, 1995;Nishizuka, 1995). Treatment of cells with hydrogen peroxide stimulates PKC activity (Larsson and Cerutti, 1989;Whisler *et al.*, 1995). Hydrogen peroxide can induce tyrosine phosphorylation of PKC, enhancing its activity (Konishi *et al.*, 1997). PKCs also contain structural motifs that are susceptible to redox modification. Selective oxidation within the amino-terminal domain, which contains a zinc-thiolate structure, can activate PKC (Gopalakrishna and Anderson, 1989). Conversely, oxidative modification within the carboxyl terminal domain inactivates PKC (Gopalakrishna and Anderson, 1989). Hence, PKC is subject to dual redox regulation, with lower levels of ROS stimulating its activity but higher levels inhibiting it (Gopalakrishna and Anderson, 1991;Jackson *et al.*, 2002).

1.6.3.3.4 Transcirption factor, NF-κ*B*

There is experimental evidence that links NF-κB activity to cellular redox status (Li and Karin, 1999). NF-κB regulates the transcription of a host of genes including acute phase genes, cytokines and cell surface receptors (Baeuerle and Baltimore, 1996;Baeuerle and Henkel, 2003;Epstein *et al.*, 2009). Hydrogen peroxide treatment of many cell types activates NF-κB (Schreck *et al.*, 1991;Meyer *et al.*, 1993;Manna *et al.*, 1998;Wang *et al.*, 1998) and in some systems antioxidants have been demonstrated to reduce or block NF-κB activation (Schreck *et al.*, 1991;Meyer *et al.*, 1993;Manna *et al.*, 1998). However, hydrogen peroxide does not stimulate NF-κB activation in all cells suggesting that it is not a general mediator of NF-κB activation process (Anderson *et al.*, 1994). Various other stimuli including pro-inflammatory cytokines and bacterial endotoxins have been shown to activate NF-κB (Li and Karin, 1999). It has been suggested that intracellular ROS levels may be involved in the stimulatory mechanism since treatment with these agents increases intracellular ROS levels, and antioxidant treatment can prevent NF-κB activation by these agents (Beg *et al.*, 1993;Manna *et al.*, 1998).

Cells may respond to changes in environmental exposure to oxidative stress and to endogenous free radical production by increasing or decreasing cell proliferation, changing immune response or by induction of apoptotic cell death. In contrast, extreme levels of oxidative stress may give rise to necrotic cell death.

1.6.4 Pathophysiological function of ROS

1.6.4.1 Cardiovascular disease

Oxidative stress in vascular disease (specifically a relative overproduction of ROS), contributes markedly to endothelial dysfunction. In the state of oxidative stress, the production of ROS exceeds the available antioxidant defence systems. In the case of NO, as a consequence, its bioavailability is reduced. A dominant mechanism reducing bioavailability of vascular NO related to it rapid oxidative inactivation by the ROS superoxide. In addition, there is evidence that persisting oxidative stress will render eNOS dysfunctional such that it no longer produces NO, but superoxide (Forstermann, 2010). Risk factors for cardiovascular disease include hypertension (Li *et al.*, 2006), diabetes mellitus (Hink *et al.*, 2001), hyperchloesterlemia (Warnholtz *et al.*, 1999) and atherosclerosis (Sorescu *et al.*, 2002). These risk factors lead to a dramatic increase in

ROS in the vascular wall, a situation that culminates into oxidative stress. There are several enzymes that can potentially produce ROS in the vessel wall. Four major sources include NOX, xanthine oxidase, dysfunctional eNOS and enzymes of the ETC (section 1.6.2).

Several isoforms of superoxide-producing NOX oxidases exist in vascular wall. Evidence for an inactivation of NOX in the vasculature has been provided in animal models of vascular disease such as angiotensin II-induced hypertension (Fukui *et al.*, 1997;Matsuno *et al.*, 2005), genetic hypertension (Li *et al.*, 2006), diabetes mellitus (Hink *et al.*, 2001) and hyperchloesterlemia (Warnholtz *et al.*, 1999). In atherosclerotic arteries, there is also evidence for increased expression of NADPH oxidase subunits $gp91^{phox}$ (NOX2) and NOX4 (Sorescu *et al.*, 2002); angiotensin II leads to an overexpression of NOX1 (Matsuno *et al.*, 2005). A confirmation of the role of NOX-derived ROS in hypertension and atherosclerosis came from studies with genetic disruption of subunits of the enzyme. Knockout of $p47^{phox}$ subunit reduced blood pressure responses to angiotensin II and diminished atherogenesis in apolipoprotein E (apoE) $^{-/-}$ mice (Barry-Lane *et al.*, 2001;Landmesser *et al.*, 2002).

Xanthine oxidase readily donates electrons to molecular oxygen, thereby producing superoxide. Oxypurinol, an inhibitor of XO, has been shown to reduce superoxide production and improve endothelium-dependent vascular relaxations to acetylcholine in blood vessels from hyperlipidemic animals (Ohara *et al.*, 1993). This suggests a contribution of XO to endothelial dysfunction in early hyperchloesterlemia. The source of XO is not entirely clear, but increased levels of cholesterol have been shown to stimulate the release of the enzyme from the liver into the circulation. The circulating XO can then associate with endothelial glycosaminoglycans (White *et al.*, 1996).

Superoxide production from the mitochondria is largely generated from two locations within the respiratory chain. However, the amount of superoxide released from the mitochondria also depends on the activity of Mn-containing superoxide dismutase-2 (SOD, section 1.7.2) located in the mitochondrial matrix. There is evidence to suggest that some cardiovascular diseases are associated with mitochondrial dysfunction (Ramachandran *et al.*, 2002) and that mitochondrial ROS production may be linked to the development of early atherosclerotic lesions (Ballinger *et al.*, 2002). Mitochondrial

dysfunction, arising from SOD2 deficiency, increases mitochondrial DNA (mtDNA) damage and accelerates atherosclerosis in apoE $^{-/-}$ mice (Ohashi *et al.*, 2006).

Nitric oxide synthase (NOS) enzymes contain four redox active prosthetic groups (FAD, FMN, heme and BH_4) that, in principle, could pass electrons to oxygen (Heinzel *et al.*, 1992;Masters *et al.*, 1996;Xia *et al.*, 1998;Pou *et al.*, 1999). Electron transfer to NOS enzymes needs to be tightly controlled to prevent uncoupling of oxygen reduction from nitric oxide synthesis that will turn a functional NOS into a dysfunctional superoxide generating enzyme (Stuehr *et al.*, 2001). Evidence for eNOS uncoupling has been obtained in peroxynitrite-treated rat aorta (Laursen *et al.*, 2001), in endothelial cells treated with low-density lipoprotein (Pritchard, Jr. *et al.*, 1995), and in isolated blood vessels from animals with pathphysiological conditions such as stroke prone spontaneously hypertensive rats (Kerr *et al.*, 1999), deoxycorticosterone acetate (DOCA)- salt hypertension (Mollnau *et al.*, 2002) or streptozotocin-induced diabetes (Hink *et al.*, 2001).

1.6.4.2 Cancer

A hallmark of solid cancer growth is hypoxia. Unregulated cellular proliferation leads to formation of cellular masses that extend beyond the resting vasculature, resulting in oxygen and nutrient deprivation. The resulting hypoxia triggers a number of critical adaptations that enable cancer cell survival, including apoptosis suppression, altered glucose metabolism, and an angiogenic phenotype. There is also evidence to suggest that oxygen depletion stimulates mitochondria to increase ROS production, with subsequent activation of signalling pathways, such as hypoxia inducible factor (HIF)-1α (section 1.5.6) that promote cancer cell survival and tumour growth.

Considerable interest has focused on cancers, where the involvement of ROS as regulators of cell proliferation and apoptosis is clearly an important factor. ROS-mediated DNA damage has long been thought to play a role in carcinogenesis initiation and malignant transformation (Valko *et al.*, 2006). Hydroxyl radicals, for example react with pyrimidines, purines and chromatin protein, resulting in base modifications, genomic instability, and alterations in gene expression. Mitochondrial DNA is a particularly vulnerable target because of its proximity to the ETC constituents, and is an important variable in carcinogenesis (Singh, 2006). Pathological sources of transforming ROS include chronic inflammation secondary to infections or chronic

chemical irritants such as tobacco smoke and asbestos (Knaapen *et al.*, 2004). Transformed cells commonly lack cell cycle checkpoints and over-express oncogene growth factors and their tyrosine kinase receptors that drive cell proliferation, ultimately leading to tumour formation and chronic hypoxia (Hanahan and Weinberg, 2000).

Several tyrosine kinase receptors have been shown to signal via ROS-dependent mechanisms (Bae *et al.*, 1997). Both the epidermal growth factor (EGF) receptor and platelet-derived growth factors (PDGF) receptor signal in part through hydrogen peroxide generation (Figure 10). Ligand-induced receptor dimerisation activates phosphatidylinositol 3-kinase (PI3K), resulting in inositol 1,4,5-triphosphate (IP3) activation of Rac, which, in turn, activates NADPH oxidase (NOX) complex to produce superoxide and downstream signalling through superoxide and hydrogen peroxide. Hydrogen peroxide modulates signal transduction through its oxidation of the catalytic cysteine of protein tyrosine phosphatases, such as PTEN, preventing inactivation of tyrosine kinase signalling through activator protein-1 and Akt (Wang *et al.*, 2000) (Figure 10). Hydrogen peroxide-mediated inhibition of protein phosphatases contributes to both cellular proliferation and apoptosis suppression and links oncogene over-expression, a hallmark of cancers, with ROS-mediated signalling (Benhar *et al.*, 2002). With a few as 300 malignant cells, this can drive cell proliferation beyond the carrying capacity of the resting vasculature, producing a hypoxic environment that switches on angiogenesis (Li *et al.*, 2000).

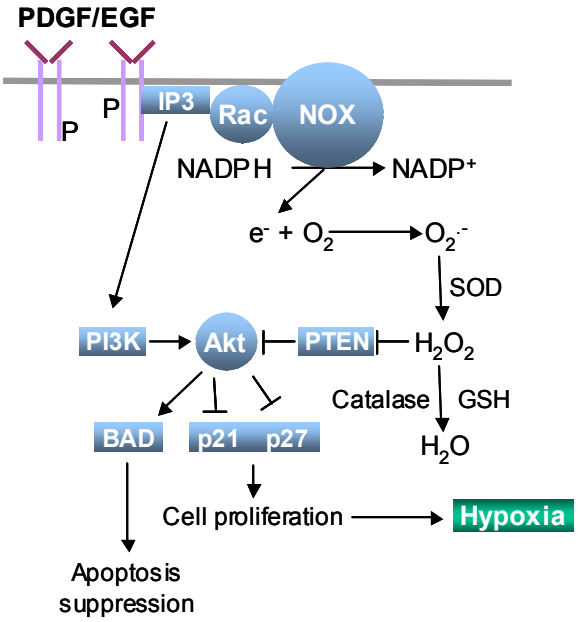

Figure 10 – Tyrosine kinase signalling (in part) through hydrogen peroxide

Tyrosine kinase receptor signalling is amplified by ROS via inhibition of PTEN, stimulating cell proliferation and suppressing apoptosis.

There is also experimental data from Vaquero *et al*, 2004 demonstrating that pancreatic cancer cells produce ROS, which is stimulated by growth factors (Vaquero *et al.*, 2004). The authors demonstrate that inhibition of ROS with antioxidants tiron and NAC or with the NADPH oxidase inhibitor, DPI, stimulated apoptosis. They also showed that inhibition of ROS with NOX4 antisense over-expression decreased ROS levels and stimulated apoptosis. They suggest ROS (most likely generated from NOX4), promote survival and act as anti-apoptotic factors in pancreatic cancer cells. Evidence from Quintero *et al*., 2006a has also demonstrated ROS generation in human head and neck carcinoma cells in normoxia (21% oxygen), and this was associated with the stabilisation of HIF-1α. Treatment with antioxidants prevented the accumulation of HIF-1α in these cells.

1.6.4.3 Diabetes

The hallmarks of type II diabetes include pancreatic β-cell dysfunction and insulin resistance. Under diabetic conditions, chronic hyperglycemia and subsequent augmentation of ROS deteriorate β-cell function and increase insulin resistance which leads to the aggravation of type II diabetes. There are several sources of ROS in cells (as previously described) including the ETC in mitochondria and membrane bound NADPH oxidase that during diabetic conditions augment ROS production. Acute exposure of β-cells to high glucose concentrations stimulates insulin gene expression, but chronic exposure has adverse effects on β-cell function. However, chronic hyperglycemia causes impairment of insulin biosynthesis and secretion. In the diabetic

state, hyperglycemia per se and subsequent ROS production decrease insulin gene expression and secretion and finally bring about apoptosis (Kaneto *et al.*, 2010). Pancreatic β-cells are also rather vulnerable to ROS as they have a low expression of antioxidant enzymes such as catalase and glutathione (Lenzen *et al.*, 1996;Tiedge *et al.*, 1997) thus the removal of deleterious β-cell ROS is inadequate in diabetic conditions. It has been shown that when β-cell-derived cell lines or rat-isolated islets were exposed to ROS, insulin gene promoter activity and mRNA expression were suppressed (Kaneto *et al.*, 1999;Kaneto *et al.*, 2001).

While the majority of research has concentrated on cardiovascular disease and cancer, ROS have been implicated in an array of disorders such as diabetes, degenerative neurological disorders including Alzheimer's and Parkinson's diseases, autoimmune disorders including rheumatoid arthritis and eye disorders including macular degeneration (Droge, 2002).

The effects of oxidative stress depend on the cell type, the level of oxidative stress experienced, and the protective mechanisms in place in that cell type. Modifications of redox-regulated processes may play a role in these conditions. Also the sensitivity of cells to oxidative stress depends largely on their intrinsic antioxidant systems, in particular the levels of glutathione (GSH) within the cell.

1.7 Antioxidant defence systems

1.7.1 Introduction

Antioxidants are substances that, at relatively low concentrations, compete with other oxidisable substrates and thus act to significantly delay or inhibit the oxidation of these substances (Halliwell and Gutteridge, 1989). In biological systems, these include free radical scavenging enzymes such as superoxide dismutase (SOD), and abundant radical scavenging chemicals such as glutathione (section 1.7.7). Living cells and tissues have a number of mechanisms for re-establishing redox homeostasis after exposure to increased free radicals (ROS or RNS) (Droge, 2002). A major mechanism of redox homeostasis is based on the ROS-mediated induction of redox sensitive signal cascades that lead to increased expression of antioxidant enzymes.

1.7.2 Superoxide dismutase

The formation of ROS is kept under tight control by various antioxidant systems. Within the mitochondria, superoxide is enzymatically converted to hydrogen peroxide by a family of metalloenzymes called superoxide dismutases (SOD) (Fridovich, 1995). Since superoxide may either reduce transition metals, which in turn can react with hydrogen peroxide producing hydroxyl radicals or spontaneously react with NO to produce peroxynitrite, it is important to maintain steady-state concentration of superoxide at the lowest possible level (Turrens, 2003).

There are three mammalian SOD isoforms which include the copper and zinc-containing SOD (CuZnSOD/ SOD1) (McCord and Fridovich, 1969a), the manganese-containing SOD (MnSOD/ SOD2) (Weisiger and Fridovich, 1973), and the secreted extracellular SOD (ECSOD/ SOD3) (Marklund, 1982). CuZnSOD is composed of two identical 16 kDa subunits, each containing one Cu and one Zn atom, and is located in the cytosol and nucleus of all cell types (McCord and Fridovich, 1969a). The steady-state concentration of superoxide in the mitochondrial intermembrane space is controlled by CuZnSOD (Okado-Matsumoto and Fridovich, 2001). MnSOD is composed of four identical 22 kDa Mn-containing subunits and is found in the mitochondrial matrix (Weisiger and Fridovich, 1973) and thus eliminates the superoxide formed in the matrix or on the inner side of the inner membrane. The expression of MnSOD is further induced by agents that cause oxidative stress, including radiation and hyperoxia, in a process mediated by the oxidative activation of NF-κB (Warner *et al.*, 1996;Tsan *et al.*, 2001;Murley *et al.*, 2001). ECSOD is, unlike the other isoforms, a glycoprotein and is composed of four 30 kDa subunits, each containing a Cu and a Zn atom. It is secreted by a few distinct cell types (Marklund, 1990) and is primarily located in the interstitial matrix of tissues and the glycocalyx of cell surfaces anchored to heparan sulfate proteoglycans (Marklund, 1984;Karlsson and Marklund, 1989). A small fraction of the ECSOD in the body is found in extracellular fluids such as plasma, lymph, synovial fluid, and cerebrospinal fluid (Marklund *et al.*, 1982;Karlsson and Marklund, 1988).

In acute and chronic inflammation, the production of superoxide is increased at a rate that overwhelms the capacity of the endogenous SOD enzyme defence system to detoxify them, resulting in superoxide-mediated cellular damage (McCord and Fridovich, 1969b).

1.7.3 Catalase

The enzyme catalase, catalyzes the decomposition of two molecules of hydrogen peroxide to water and oxygen ($2H_2O_2 \rightarrow 2H_2O + O_2$) and is exclusively localised in peroxisomes (Woo *et al.*, 2010). The overall biological importance of catalase is not completely clear. Homozygous catalase knockout mice develop normally and show no abnormalities, indicating that this enzyme is not essential for animal life (Liu *et al.*, 2008a). Over-expression of catalase, however, has protective effects in the cardiovascular system such as delayed development of atherosclerosis (Yang *et al.*, 2004) and inhibition of angiotensis II-induced aortic wall hypertrophy (Zhang *et al.*, 2005). Catalase gene expression in micro-organisms is generally controlled either by sensors of ROS or by growth phase control mechanisms (Chelikani *et al.*, 2004).

1.7.4 Heme oxygenase

Heme oxygenase (HO) catalyzes the first step in heme breakdown to generate equimolar quantities of carbon monoxide, biliverdin, and free ferrous iron. There is evidence to suggest that HO can protect against vascular remodelling and atherogenesis (Stocker and Perrella, 2006). HO is induced by oxidative stress. The proposed mechanisms by which HO may protect cells include its abilities to degrade the pro-oxidative heme to biliverdin. This gets subsequently converted to bilirubin, which has radical-scavenging properties. Moreover, bilirubin seems to directly inhibit functional NOX and can also interrupt assembly and activation of the enzyme (Jiang *et al.*, 2006). In addition, a decrease in heme content caused by HO limits heme availability for maturation of the NOX2 subunit of NADPH oxidase, preventing assembly of a functional enzyme and in turn reduces cellular ROS generation (Taille *et al.*, 2004).

1.7.5 Thioredoxin

Thioredoxin (Trx) is a multifunctional low-molecular weight protein containing an active thiol/disulfide site and possessing oxidoreductase activity. The major Trx isoforms are cytosolic TrxI and mitochondrial TrxII. Human TrxI is substantially localised in cytoplasm, but is also found in the cell nucleus and blood plasma. TrxII is primarily synthesised in the form of a precursor protein which has a N-terminal 60-amnio acid sequences eliminated in the course of post-translational proteolysis to form TrxII and its transported into the mitochondria (Kalinina *et al.*, 2008). Both TrxI and

TrxII can be localised not only within cells, but also in the intracellular space (Soderberg *et al.*, 2000). Different cell types including tumour cells secrete TrxI (Powis *et al.*, 2000), with secretion appearing not to be sensitive to oxidation (Tanudji *et al.*, 2003). However, the secretion process can change in the presence of various xenobiotics including alkylating agents (Kalinina *et al.*, 2008). Trx has been recognised as a critical protective system acting via direct (antioxidant) and indirect (regulation of signal transduction) effects (Yamawaki *et al.*, 2003). Trx is present in endothelial cells and vascular smooth muscle cells. It appears to exert most of its ROS-scavenging properties through Trx peroxidase, which uses endogenous thiol (SH) groups as reducing equivalents. Trx reduces the oxidised form of Trx peroxidase and the reduced Trx peroxidase scavenges ROS.

1.7.6 Peroxiredoxins

Peroxiredoxin (Prx) -I to IV belong to the 2-Cys (cysteine) Prx subfamily of Prx enzymes, which exist as homodimers and reduce hydrogen peroxide with the use of reducing equivalents provided by Trx (Rhee *et al.*, 2005). PrxI and PrxII are localised to the cytosol, whereas PrxIII and PrxIV are restricted to the mitochondria and the endoplasmic reticulum, respectively. PrxI and PrxII are also abundant, constituting a total of 0.2% to 1% of soluble protein in cultured mammalian cells (Chae *et al.*, 1999). Prx enzymes are efficient in eliminating low concentrations of hydrogen peroxide because of their low K_m values for the substrate (Chae *et al.*, 1999).

1.7.7 Glutathione

1.7.7.1 Introduction

Glutathione was discovered over a century ago as an abundant thiol containing compound present at millimolar (mM) concentrations in cells and tissues. The central function of GSH in detoxification and protection against oxidants was recognised about 50 years ago (Mills, 1957). It serves as a short-term storage form of the amino acid cysteine, as a nucleophile for efficient detoxification of reactive electrophiles, and as an antioxidant.

1.7.7.2 Biosynthesis, degradation and transport of GSH

Glutathione concentrations, rates of synthesis and rates of turnover vary greatly from one tissue to another. This impacts on how rapidly GSH is depleted from a cell and how rapidly a cell can recover after a chemical insult (Potter and Tran, 1993).

GSH is synthesised by two sequential, ATP-dependent reactions in the cytoplasm catalysed by γ-glutamylcysteine synthetase (γGCS) and glutathione synthetase (Krzywanski *et al.*, 2004) (Figure 11). The majority of the biosynthetic activity resides in the cytoplasm with little if any activity in other organelles, including the mitochondria (Griffith and Meister, 1985). The degradation of GSH is mediated by a separate pathway which, in contrast to the synthetic pathway exhibits a discrete tissue distribution (Hinchman and Ballatori, 1990). The initial step in the breakdown of GSH involves the cleavage of the γ-glutamylpeptide bond by γ-glutamyltransferase (GGT), which is distinctly localised to the luminal membranes of epithelial cells such as the renal proximal tubule and enterocytes (Lash, 2006).

Glutathione is transported out of cells by several multi-drug resistance proteins (MRP) (Ballatori *et al.*, 2005) and is transported into the mitochondria by dicarboxylate carrier (DIC) and a monocarboxylate carrier (OGCP) (Lash, 2006).

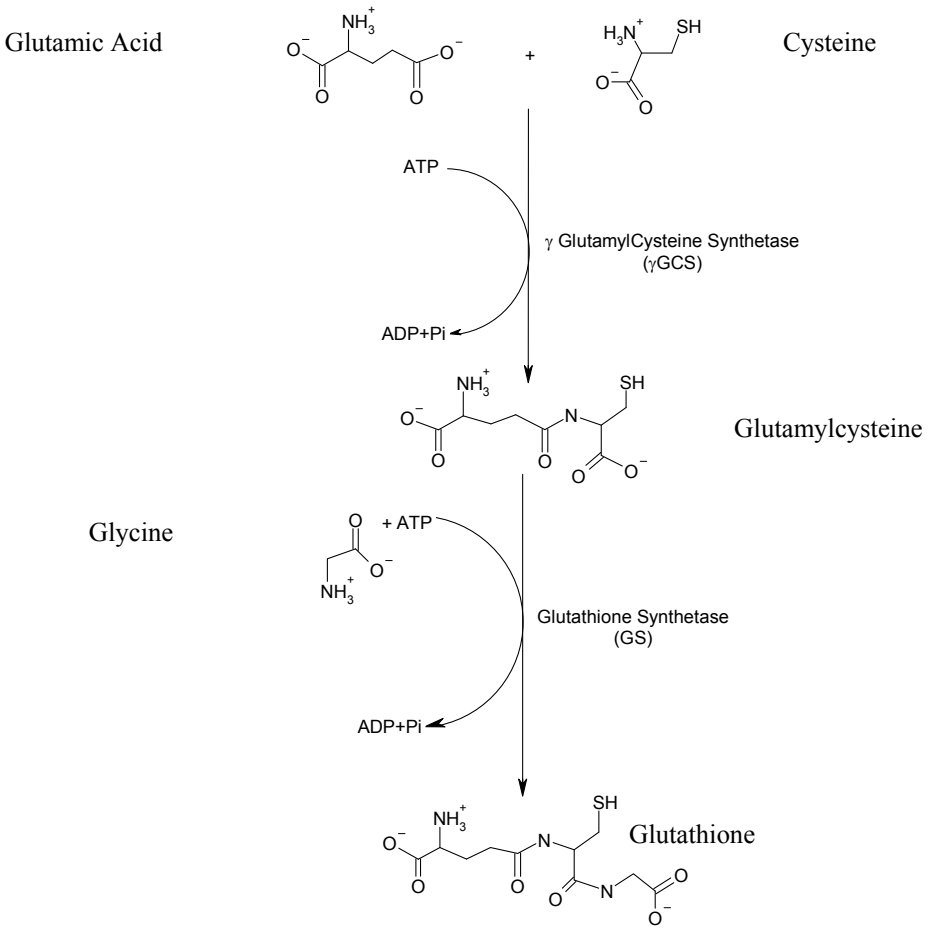

Figure 11 – Biosynthesis of glutathione

Glutathione is a powerful antioxidant defence system within mammalian cells. GSH is catalysed *de novo* in two ATP-dependent reactions. γGCS catalyses the first and rate limiting step in GSH biosynthesis. Reduced GSH donates electrons for the reduction of hydrogen peroxide.

1.7.7.3 Role of glutathione in detoxifying ROS

The main function of GSH is to protect cells from the toxic effects of reactive oxygen compounds, therefore acting as an endogenous antioxidant. Glutathione effectively scavenges free radicals and other reactive species such as hydroxyl radicals, peroxynitrite and H_2O_2 directly and indirectly through enzymatic reactions. In such reactions, GSH is oxidised to form GSSG, which is then reduced to GSH by NADPH-dependent glutathione reductase (Droge, 2002) (Figure 12). In addition, GSH maintains intracellular sulfhydryl-containing proteins in their reduced and active form by GSH-dependent reduction of H_2O_2 and other peroxides, mediated by glutathione peroxidases. Or by the action of thiol-disulfide exchange reactions which are mediated by thiol transferases to form oxidised glutathione (GSSG) (Lash, 2006).

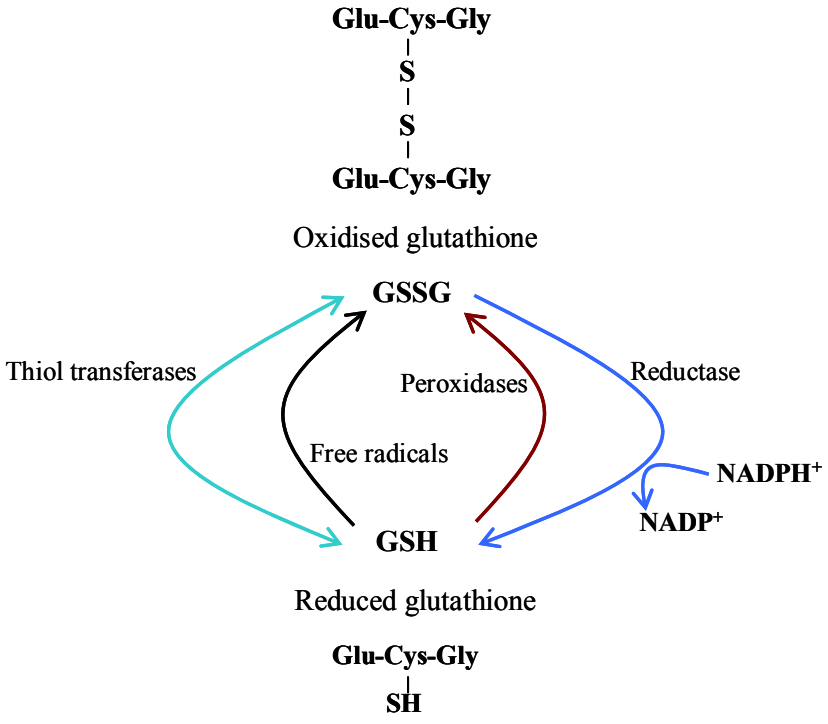

Figure 12 – Oxidation and reduction of glutathione

Schematic drawing showing the reactions of GSH thiol transferases, free radicals, GSH peroxidases and GSH reductase. The structures of both reduced and oxidised glutathione are also shown. (Adapted from (Meister, 1988).

1.7.7.4 Role of mitochondrial GSH in defence against oxidative damage

In mitochondria, GSH plays a key role in the protection against oxidative damage to mitochondrial components. Indeed, the oxidative damage to mitochondrial DNA that occurs upon ageing increases with age in mitochondria from liver, kidney and brain of rats (Vijg, 1999). Changes in [GSH]:[GSSG] redox status would indicate that mitochondrial antioxidant systems could not cope with the oxidant species being generated.

The GSH content found in the mitochondria is different, and is regulated in different ways, to that of cytosolic GSH, implying two separate GSH pools. As briefly mentioned previously, there is no synthesis of GSH in mitochondria. Rather, GSH is imported from the cytosol. The role of mitochondria in ageing attributed to free-radical damage of mitochondria function was first described in 1980 (Miquel *et al.*, 1980). Indeed, Miquel and colleagues highlighted that mitochondria are important sources of free radicals in ageing, and that mitochondrial components are essential targets of free radical damage. Changes of total cellular GSH upon ageing are only modest. Interestingly, changes in mitochondrial GSH are much more marked. Oxidised GSH levels in mitochondria from the brain of old animals have been observed to be at least four times higher than those in young animals (de la Asuncion *et al.*, 1996). Furthermore, changes in the redox state of GSH in mitochondria correlate with changes in oxidative damage of mitochondrial DNA. There is evidence to suggest, late onset administration of dietary antioxidants, such as thiol-containing compounds or vitamins C and E, prevents oxidation of GSH and oxidative damage to mitochondrial DNA (Pallardo *et al.*, 1998).

1.7.7.5 Disruption of the GSH system in disease

GSH/GSSG is the most important redox couple and plays crucial roles in antioxidant defence, nutrient metabolism and the regulation of pathways essential for whole body homeostasis. GSH deficiency contributes to oxidative stress in the pathogenesis of many diseases.

Glutamate plays a regulatory role in GSH synthesis through two mechanisms, firstly, in the uptake of cysteine and secondly, in the prevention of GSH inhibition of GCS. When extracellular glutamate concentrations are high, as in patients with advanced cancer, HIV infection and brain injury, cysteine uptake is competitively inhibited by glutamate,

resulting in a decrease in GSH synthesis (Tapiero *et al.*, 2002), leading to increased oxidative stress. Glycine availability can be reduced in response to protein malnutrition, sepsis and inflammatory stimuli (Grimble *et al.*, 1992). When hepatic glycine oxidation is enhanced in response to high levels of glycagon in diabetes (Mabrouk *et al.*, 1998), this amino acid may become a limiting factor for GSH synthesis, which in turn can lead to an increase in oxidative stress.

As well as conditions influenced by the availability of the key compounds involved in GSH synthesis, genetic mutations also exist which affect the metabolism of GSH. Humans with inborn deficiencies of γ-glutamylcysteine synthase, GSH synthetase, GSSG reductase or GSH peroxidases have been reported (Meister, 1988). Patients exhibiting such deficiencies often have defective brain function, and an increased sensitivity to oxidative stress leading to haemolysis (Meister, 1988).

Diaz-Hernandez *et al*., 2007 developed an endogenous model of oxidative stress in neurons from rats, using RNA interference (RNAi) to selectively knock down glutamate-cysteine ligase (GCL) (also known as γGCS). As described above, this is the rate-limiting enzyme of glutathione biosynthesis. Interference with glutathione biosynthesis in primary neurons by RNAi induced free radical production, and consequently triggered neuronal apoptotic death. The results from this paper provide *in vitro* data demonstrating the importance of GSH biosynthesis in protecting cells from the harmful effects of excessive free radical production.

In summary, glutathione plays an important role in antioxidant defence, nutrient metabolism and regulation of cellular events (including gene expression, DNA and protein synthesis, cell proliferation and apoptosis). GSH deficiency contributes to oxidative stress, which plays a key role in ageing and in the pathogenesis of many diseases (including Alzheimer disease, Parkinson's disease, HIV, brain injury, cancer and diabetes) (Droge, 2002).

1.8 Current study

1.8.1 Overview

In normoxia, the hypoxia-inducible factor-1α (HIF-1α) is constantly hydroxylated and thus prepared for proteosomal degradation through the action of the oxygen-sensitive prolyl hydroxylases (PHDs) (Jiang *et al.*, 1996). Hence, HIF-1α stabilisation is most frequently determined by the concentration of oxygen regulating the activity of the PHDs. As a consequence, in hypoxia, PHDs are inhibited and HIF-1α is stabilised. There is, however, as previously described in this chapter, numerous oxygen-independent mechanisms of HIF-1α regulation. There is compelling evidence in the literature to suggest a role for ROS in stabilising HIF-1α. It was originally suggested that ROS in hypoxia were responsible for this action (Chandel *et al.*, 2000a). However the data are conflicting, as both an increase and decrease in ROS in hypoxia have been reported in various cell types. It is therefore important to determine a definitive role for ROS in the stabilisation of HIF-1α.

1.8.2 Study aims

The aims of the current study were to:

1. Demonstrate oxygen-dependent stabilisation of HIF-1α in human embryonic kidney (HEK) 293T cells
2. Determine whether oxygen-independent mechanisms of HIF-1α stabilisation exist in HEK 293T cells or other cell types
3. Validate an *in vitro* model which generates free radicals in normoxia and study the effects of endogenously generated ROS on HIF-1α stabilisation
4. Investigate the cellular source of ROS involved in HIF-1α stabilisation

Chapter two:
Experimental procedures

Chapter two: Experimental procedures

2.1 Cells

2.1.1 Human embryonic kidney 293T cells

For part of this study human embryonic kidney (HEK 293T) cells were used. These cells were obtained from within the Wolfson Institute for Biomedical Research, University College London. HEK 293T is a cell line originally derived from human embryonic kidney, commonly used for both academic and industrial research (Graham *et al.*, 1977). The use of human embryonic kidney cells has become one of the most popular ways for expression/silencing of recombinant proteins. There are a variety of transfection protocols to deliver/reduce recombinant genes to these cells, and for the technique employed in this study, HEK 293T is recommended. Cells were cultured on tissue culture flasks and plates (Falcon, UK).

2.1.2 D890N HEK 293T cells

HEK 293T cells stably transfected with an inducible catalytically deficient isoform of mitochondrial DNA POLγ (D890N) were kindly provided by Johannes Spelbrink, Institute of Medical Technology and Tampere University Hospital, Tampere, Finland. Cells were cultured on tissue culture flasks and plates (Falcon, UK).

2.1.3 J774.A1 murine macrophages

A mouse macrophage (MΦ) carcinoma cell line was also used in this study. The murine MΦ cell line J774.A1 was chosen because they are known to represent a good model for experiments evaluating inflammatory responses. Cells were maintained in suspension in stirrer bottles (Techne) and were obtained from ATCC (TIB-67).

2.1.4 H157 human head and neck squamous cancer cells

Human head and neck squamous cell lines (H157) were also used in some experiments. These cells were generously provided by Professor E.K. Parkinson, Institute of Dentistry, Queen Mary's Medical and Dental School, London, UK. They were selected because of their high expression of nitric oxide synthases (NOS). Cells were grown in

standard keratinocyte growth medium (KGM) which comprised α-MEM (minimal essential media, containing Earls Salts, L-glutamine without ribonucleosides). Other cell culture reagents as specified were obtained from Sigma and Invitrogen, UK.

2.2 Cell culture

2.2.1 Culturing cells from liquid nitrogen

Cell culture medium was warmed in a water bath at 37˚C. Then an aliquot of cells were removed from liquid nitrogen and thawed quickly in a water bath (37˚C). The cells were then transferred to a 15 ml falcon tube and resuspended in 3-5 ml cell culture medium. For HEK (293T/ D890N) and H157, cells were then transferred to a sterile 75 cm^2 tissue culture plastic flask containing 10 ml cell culture medium; J774.A1 were transferred into a 250 ml stirrer bottle and placed on a magnetic platform. Cells were then cultured in a humidified incubator at 37˚C and 5% CO_2. Media was replaced after 24 h and cells were sub-cultured once 80-90% confluence was achieved.

2.2.2 HEK 293T, HEK D890N and H157 passaging

HEK 293T were grown and maintained in cell culture medium, DMEM (GIBCO) containing 10% (v/v) FCS (New Zealand origin, GIBCO) supplemented with 100 IU/L penicillin and 100 μg/L streptomycin (Invitrogen, UK). HEK D890N were grown and maintained in DMEM containing 10% (v/v) FCS (New Zealand Origin) supplemented with 200 μg/ml hygromycin (Invitrogen), 15 μg/ml blasticidin (Calbiochem), 50 μg/ml uridine (Sigma) and 1 mM pyruvate (Sigma). H157 were grown and maintained in α-MEM containing 10% (v/v) FCS (New Zealand origin) supplemented with 100 IU/L penicillin and 100 μg/L streptomycin, 8×10^4 mol/L adenine, 5 μg/ml insulin, 1×10^{-10} mol/L cholera toxin, 0.5 μg/ml hydrocortisone and 10 ng/ml epidermal growth factor. Typically, old medium was removed and cells rinsed with 10 ml sterile PBS (sPBS) then incubated with approximately 2 ml 1 × trypsin-EDTA, 37˚C for 5 min, followed by neutralisation using trypsin neutralising solution (TNS) purchased from Sigma, UK. Confirmation of cell detachment was obtained using an inverted light microscope (Axiovert25, Carl Zeiss, MicroImaging Inc., Hertfordshire, UK). Cells were then pelleted by centrifugation (800 × g, 10 min), the supernatant was removed carefully and the cell pellet resuspended in fresh medium. Cells were then seeded 1 in 10 into 75 cm^2 flasks in a final volume of 10 ml cell culture medium. Routinely, cell number and

viability were assessed using trypan blue exclusion. Equal volumes of cell suspension and trypan blue (Life Technologies) were mixed and a small volume (approximately 20 µl) was transferred to a haemocytometer. Cells were counted under an inverted microscope with unstained cells counted as viable and blue cells counted as dead. Cells were used experimentally if viability was above 95%.

2.2.3 Preparation of *Rho*^{0} media for H157 cells

Uridine (purchased from Sigma) was added to double-distilled water (ddH_2O) to make up a final concentration of 10 mg/mL, this was filtered though a 0.45 µm Nalgene syringe filter (purchased from Fisher Scientific UK Ltd) to make a sterile stock. Pyruvate (purchased from Sigma) was also added to ddH_2O to make a final concentration of 1M and then filtered though a 0.45 µm Nalgene syringe filter to make a sterile stock. Ethidium Bromide 10 mg/mL aqueous solution (Sigma) was filtered though a 0.45 µm Nalgene syringe filter and then added to ddH_2O to make a 10 µg/mL sterile stock solution, which was kept in a foil covered 15 mL Falcon tube to protect it from light. Uridine and pyruvate stock was added to the media to give a final concentration of 50 µg/mL and 1 mM respectively.

Rho^0 cells were generated by adding ethidium bromide stock to the *Rho*^{0} media (complete H157 media plus uridine and pyruvate) to reach a final concentration of 200 ng/mL. Ethidium bromide is a toxic mutagenic compound and all work with this reagent was carried out with appropriate protective clothing in a ventilated hood. The respective media was changed every 2–3 days.

2.2.4 J774.A1 passaging

J774.A1 murine macrophages were grown and maintained in cell culture medium, DMEM (GIBCO, UK) containing 10% (v/v) FCS (New Zealand origin, GIBCO) supplemented with 100 IU/L penicillin, 100 µg/L streptomycin, 25 mM D-glucose, 2 mM L-glutamine. J774.A1 cells are grown in suspension, and are simply removed from culture, pelleted by centrifugation (800 × g, 10 min) and the supernatant removed before resuspending the cell pellet in fresh medium. Cells were then either seeded and allowed to adhere onto 10 cm^2 tissue culture plates in a final volume of 10 ml cell culture medium or suspended back into an appropriate volume of media in a magnetic stirrer

bottle. Routinely cell number and viability were assessed using trypan blue exclusion (2.2.2).

2.2.5 Storing cells in liquid nitrogen

A flask of confluent cells was rinsed with 10 ml sPBS and incubated with 2 ml 1 × trypsin-EDTA (37˚C, 5 min). The cells were then removed with an additional 5-10 ml of cell culture medium to a 50 ml falcon tube and pelleted by centrifugation (800 × g, 5 min). The supernatant was removed and discarded without disturbing the pellet and cells resuspended in supplemented DMEM. 10% DMSO was added to the cell suspension just prior to freezing. Approximately 1 ml cell suspension was then transferred to a 1.5 ml cryogenic vial. Cryogenic cells were then kept on ice in the fridge (4˚C) for 10 min; transferred to –20˚C for 2 h; and then removed to –80˚C overnight. Following at least 24 h incubation under this condition, vials were transferred to liquid nitrogen for long-term preservation of the cells. Alternatively, cryogenic cells were placed in a cryogenic 1˚C freezing container (Nalgene), and stored at –80˚C, until transferred to liquid nitrogen.

2.2.6 Preparation of cell lysates

In order to use proteomic techniques, the proteins obtained from cell lysates need to be solubilised. To lyse cells the medium is removed and the cells were rinsed at least twice with copious ice cold PBS. Then between 100-500 µl (depending on tissue culture plastic being used) of Novagen cytobuster protein extraction reagent (Merck Chemicals Ltd) containing protease inhibitors (Roche Diagnostics), was added and the lysate was scraped and collected. The lysate was then left on ice for 10 min, followed by centrifugation (13,000 × g, 15 min, 4˚C). The supernatant was then collected, and stored at –20˚C.

2.3 Protein quantification

2.3.1 Bicinchoninic acid (BCA) kit

Protein concentrations were determined using the bicinchoninic acid based BCA protein assay kit (Pierce). Total protein was quantified by its reaction with Cu^{2+} reducing it to Cu^{1+} in an alkaline medium known as the biuret reaction. The colourimetric change is

brought about by the reaction of biocinchoninic acid with Cu^{1+} and the protein concentrations are determined based on a standard curve produced from a series of dilutions of known concentrations (0, 0.0625, 0.125, 0.25, 0.5, 1.0 and 2.0) using the purified protein bovine serum albumin.

20 µl sample or standard were mixed with 180 µl working reagent (made in a 50:1 ratio of reagents A:B) and loaded in triplicate into wells of a 96 well plate, and incubated for 30 min at 37˚C. Absorbance was measured at 562 nm (Molecular Devices, SpectraMax Plus) and was plotted of the absorbance of the standards against the protein concentration in µg/ml. From the equation of this standard curve the concentrations of the total protein of the samples was calculated.

2.4 Sodium dodecyl sulphate polyacrylamide gel electrophoresis (SDS-PAGE)

2.4.1 Sample preparation for SDS-PAGE

Following protein quantification by the BCA assay (2.3.1) samples were diluted accordingly with loading buffer (5 ×). The samples were then heated at 100˚C in a heating block (Grant Instruments, Cambridge, UK) for 10 min, and then centrifuged at 10,000 × g for 1 min at 4˚C. Samples were then loaded onto the gel for separation or stored at –20˚C for future analysis.

2.4.2 SDS-PAGE

Protein samples were routinely analysed by SDS-PAGE. This technique separates proteins according to their molecular mass. Total protein were analysed by electrophoresis in pre-cast SDS-PAGE 4-15% Tris.HCL gradient gels (BioRAD, Hertfordshire, UK). The gel was placed into the BioRAD mini trans-blot cell gel tank system, and the comb removed. The buffer reservoir was then filled with SDS running buffer (section 2.16.5). Samples were electrophoresed against 15 µl of a pre-stained protein marker, (New England Biolabs) towards the anode at a constant voltage of 120 V, usually for 65 min, or until the dye front reached the bottom of the gel.

2.5 Western blotting

2.5.1 Western blot transfer

Western blotting was performed using a standard transfer tank. Four pieces of Whatman paper (gel sized), 2 fibre pads and nitrocellulose membrane (GE Healthcare) were soaked in transfer buffer (section 2.16.5) (per gel). After electrophoresis, a sandwich of filter paper, nitrocellulose, SDS-PAGE gel and fibre pads was built up on the positive side of the gel holder cassette. The gel holder cassettes were placed into the electrode module and the tank was filled with transfer buffer. The transfer was carried out at 100 V for 75 min at 4˚C.

2.5.2 Immunoblotting (detection)

Following transfer, the nitrocellulose membrane (GE Healthcare) was usually stained with 1% ponceau S solution (Sigma) to visualise transferred proteins and then washed three times in distilled water and finally with TBS. Membranes were then incubated in 10% dried skimmed milk (Marvel, Premier International Food Ltd, Spalding, Lincolnshire, UK) in PBS/Tween 20 (20% 10 × PBS without calcium and magnesium (Life Technologies), 0.001% polyoxyethylenesorbitan monolaurate (Tween 20) from Sigma in distilled water) for 1 h at room temperature or overnight at 4˚C with constant shaking. The blot was then washed 5 times in PBS/Tween 20 for 5-10 min with shaking, followed by incubation with primary antibody at the appropriate concentration (table 2.16.6) diluted in 1% dried skimmed milk PBS/Tween 20 with constant agitation for the appropriate time (table 2.16.6). Following incubation with the primary antibody the blot was washed 5 times in PBS/Tween 20 for 5-10 min with shaking. After sufficient washing the blot was then incubated with secondary antibody diluted in 1% dried skimmed milk in PBS/Tween 20 conjugated to HRP at 1:2000 for 1 h at room temperature. The membrane was then rinsed in PBS/Tween 20 (5 times, 5-10 min each wash) and the proteins were visualised using enhanced chemiluminescence (ECL) (Amersham Pharmacia). ECL reagents were mixed immediately before use, applied evenly over the membrane and incubated for 3 min. Excess ECL was drained off the membrane, which was then wrapped in Saran wrap, ensuring air bubbles were removed. Blots were then exposed to hyperfilm ECL in an autradiography hypercassette (GE Healthcare) and developed using an automated developer (Compact X4, Xograph, Whiltshire, UK). The images were scanned and analysed quantitatively by densitometry

(AlphaImager Imaging System, AlphaEase FC software version 4; AlphaInnotech, San Leandro, California, USA).

2.6 Immunoprecipitation

γGCS was silenced in 293T cells using siRNA against γGCS (see section 2.9.3). Protein A Sepharose magnetic beads (Immunoprecipitation Kit – Dynabeads Protein A, Invitrogen) were prepared following the manufacturer's guidelines, and then incubated with anti-ubiquitin (10 μg Dako, raised in rabbit) for 10 min at room temperature. To immunoprecipitate HIF-1α, cell lysates (500 μg) were incubated with the bead/Ab complex for 2 h at room temperature on a rotating wheel. Beads were then washed four times in 200 μl washing buffer (provided in kit). Immunoprecipitated proteins were eluted by heating at 70°C for 10 min in 20 μl elution buffer (provided in kit) and 10 μl SDS loading buffer. Proteins were detected using antibodies raised in a different species to avoid cross reactivity with the immunoprecipitated complexes.

2.7 Cloning γGCS siRNA sequences into pFIV-H1/U6 vector

Molecular cloning is a technique which allows the isolation and multiplication of a specific DNA sequence (gene or cDNA). These DNA fragments can be amplified by using plasmids *in vivo* in bacterial cells. Plasmid vectors are bacterial extra-chromosomal elements that allow the replication and selection of a DNA of interest. The pFIV-H1/U6 vector (System Biosciences, USA) was used to over-express a siRNA sequence against the γGCS. This vector drives the generation of dsRNA by opposing promoters H1 and U6. The pFIV-H1/U6 cloning vector is provided in a ready-to-ligate linearised form that has been digested with the BbsI restriction enzyme. The pFIV-H1/U6 vector contains two unique 5' overhangs which facilitate directional cloning with minimal self-ligation background.

2.7.1 Selection of siRNA sequences

The selection of γGCS sequences was performed on the coding domain sequence (CDS) of the mRNA for γGCS (Accession number NM_001498) using the RNAi consortium (TRE) information available on sigma.com.

2.7.2 Annealing of siRNA oligonucleotides

Prior to DNA ligation, both forward and reverse γGCS primers require annealing. The siRNA oligonucleotides were dissolved in deionised water to reach a final concentration of 1 µg/µl. The annealing reaction is assembled on ice in a 50 µl total volume. Each reaction contained 2.5 µl sense and anti-sense siRNA oligonucleotides, 25 µl 2 × annealing buffer (20 mM tris, pH 7.8; 100 mM NaCl; 0.2 mM EDTA) and 20 µl deionised water. The reaction mixture was heated to 95˚C for 5 min in a PCR heating block, which was then left to cool until at room temperature. Once room temperature was reached, the annealed oligonucleotides were stored at –20˚C.

2.7.3 Phosphorylation of template siRNA

Each phosphorylation reaction (one per experimental siRNA template) was built on ice, in a 10 µl reaction volume. The reactions contained 1 µl annealed double stranded (ds) template oligonucleotide, 1 µl 10 × T4 polynueclotide kinase buffer, 1 µl 10 mM ATP, 6 µl deionised water and 1 µl T4 polynucleotide kinase 10 U/µl, (New England Biolabs). Reactions were incubated at 37˚C for 30 min. The reaction was stopped by heating the mixture at 70˚C for 10 min.

2.7.4 DNA ligation into pFIV-H1/U6 siRNA vector

Ligation reactions were incubated on ice in a final volume of 10 µl for each phosphorylated siRNA template. Ligation reactions contained 2.5 µl linearised pFIV-H1/U6 vector (20 ng/µl), 1 µl phosphorylated ds siRNA template DNA (product from 2.7.3), 1 µl 10 × T4 DNA ligase buffer, 4.5 µl deionised water and 1 µl T4 DNA ligase diluted to 5 U/µl with 1 × reaction buffer (New England Biolabs). The reaction mixture was incubated at 16˚C for 2-4 h in a PCR block. The ligations were tested using 10 µl of the reaction to transform TOP10 *E. coli*.

2.7.5 Bacterial transformation

Competent TOP10 *E. coli* (50 µl aliquot) were thawed on ice before 50-100 ng of plasmid DNA was added. The cells were incubated on ice for 30 minutes, heat shocked for 30 s at 42˚C (in a water bath) and then placed back on ice for 2 min. SOC broth (200 µl) was then added to the cells and then incubated at 37°C, 220 rpm for 1 h. Then 100 µl of the transformed cells were then spread onto Luria-Bertani (LB) agar plates containing 100 µg/ml ampicillin and plates were incubated overnight at 37°C.

2.7.6 Identification of positive clones

Following overnight incubation at 37˚C, well-separated colonies were selected from each plate and grown in 2 ml LB broth with 100 µg/ml ampicillin at 37˚C for 2 h on an orbital shaker. After this time, 1 µl of each bacterial culture was screened for insert using PCR, and the remaining bacterial culture was incubated overnight. Cells were then pelleted and mini-prepped (2.8.1).

2.7.7 Polymerase chain reaction (PCR)

Bacterial colonies were screened using PCR. For each PCR, a master mix was made in a 25 µl final volume. Each PCR contained dNTPs (10 mM), appropriate buffer (1 ×), Mg^{2+} (1.5 mM), PCR enzyme (2 IU) and U6 and H1 forward/ reverse primers (0.2 mM). Double distilled water (ddH_2O) was then added to make the reaction volume up to 25 µl and mixed thoroughly. Reactions were started by the addition by 1 µl template (bacterial culture). Samples were then subject to the following PCR protocol: 95˚C, 2 minutes; 25 cycles of: A) 95˚C, 20 seconds (denaturing), B) 58˚C, 20 seconds (annealing temperature), C) 68˚C, 30 seconds (extension) and finally 68˚C, 20 minutes. The PCR products were then resolved on a 1% agarose gel, as described below in 2.7.8.

2.7.8 Agarose gel electrophoresis

DNA samples were analysed by agarose gel electrophoresis to separate the DNA according to its size. A 0.8 to 1% agarose solution was made in 1 × TAE running buffer and dissolved by heating in the microwave. To visualise DNA, 1 × (from 10,000 × stock) syber safe DNA gel stain (Invitrogen) was added. Samples for electrophoresis were prepared in TAE loading buffer and run along with 0.5 µg/ml of a known molecular weight DNA ladder (New England Biolabs). Samples were then resolved at 50 mA for 40 min to 1 h. To image the DNA the gel was visualised and photographed using the AlphaImager imaging system as described in 2.5.2.

2.8 Plasmid purification

2.8.1 Mini-prep (Qiagen mini-prep kit)

Transformed TOP10 E. *coli* competent cells were inoculated into 2-5 ml LB broth, supplemented with 100 µg/ml ampicillin and incubated at 37°C overnight at 220 rpm.

Bacteria from 1 ml of the culture were harvested by centrifugation at 13,000 rpm in a Micro centrifuge (MSE) for 1 minute at 4˚C. The supernatant was then removed and discarded using precept disinfectant tablets. Following the manufacturers guide (Qiagen) the pellet was then resuspended in 250 µl Solution I (section 2.16.2) via vortex, lysed with 250 µl of Solution II (section 2.16.2), and incubated for 5 min at room temperature. 350 µl of ice cold Solution III (section 2.16.2) was then added and mixed by inversion to precipitate the DNA. Cell debris was pelleted by centrifugation at 13,000 rpm for 10 min and the supernatant removed to a mini column (Qiagen). DNA was absorbed to the column matrix, washed and eluted to a new tube as indicated in the manufacturer's handbook.

2.8.2 Maxi-prep (Qiagen fast-speed kit)

Transformed TOP10 E. *coli* were inoculated into 2 ml LB broth, supplemented with 100 µg/ml ampicillin and incubated at 37°C for 8 h at 220 rpm. Then 1 ml culture was inoculated into 200 ml LB broth with 100 µg/ml ampicillin and incubated at 37°C overnight in an orbital shaker at 220 rpm. The bacteria were harvested by centrifugation at 6000 × g, 4°C for 30 min. Following the manufacturers guide (Qiagen), the pellet was resuspended via vortex in 10 ml P1 buffer (section 2.16.2) and lysed with 10 ml P2 buffer (section 2.16.2), via gentle mixing by inversion 4-6 times and incubated for 5 min at room temperature. Genomic DNA and membranes were precipitated by the addition of 10 ml chilled P3 buffer (section 2.16.2), which was mixed by inversion 4-6 times and incubated for 10 min in a filtering column. Eluate was applied to a column and was then loaded onto an anionic exchange column (Qiagen tip 500) which had been equilibrated with 10 ml buffer QBT (section 2.16.2) before the sample was allowed to drip through. The column was then washed with 60 ml buffer QC (section 2.16.2) and the DNA eluted with 15 ml buffer QF (section 2.16.2). The DNA was then precipitated by the addition of 10.5 ml room temperature isopropanol, mixed and incubated at room temperature for 10 min. The DNA sample was then concentrated with a filter (Qiagen Kit), washed with 2 ml 70% (v/v) ethanol and eluted in a new tube using 1 ml elution buffer (QF buffer). DNA was quantified by Nanodrop ND-1000 spectrophotometer (NanoDrop Technologies, Inc, USA) and stored at -20˚C until required.

2.8.3 Sequencing

100 ng/µl of each γGCS pFIV plasmid were used per sequencing reaction, with 5 pmol/ µl of either H1 or U6 primer.

Primer	Sequence	T_m (°C)
H1	5' -CTG GGA AAT CAC CAT AAA CGT GAA - 3'	55
U6	5' -GCT TAC CGT AAC TTG AAA GTA TTT CG - 3'	55

Sequence data was generated with ABI3730XL sequencer. Samples were cycle-sequenced by Scientific Support Services (Wolfson Institute for Biomedical Research, UCL) using BigDye® 3.1 Chemistry, and standard thermal cycling conditions. Chromas Lite Version 2.01 sequence software was used to analyse and display each DNA sequence.

2.9 Eukaryotic cell transformation

2.9.1 Lipofectamine transformation

HEK 293T cells were seeded one day prior to transfection in 2 ml HEK 293T cell culture medium without antibiotics to achieve ~ 90% confluence overnight. For a 6 well tissue culture plate, 4 µg DNA (per well) was diluted with 1 ml OptiMEM (Gibco, UK) serum free media without antibiotics. An additional 1 ml OptiMEM serum free media without antibiotics was used to dilute 40 µl Lipofectamine and this was incubated for 5 min at room temperature. DNA and Lipofectamine solutions were then combined and incubated for 20-30 min at room temperature. After incubation the mixed solution was added to the plate containing HEK 293T cells and the culture medium, and this was incubated for 24 h at 37˚C. After this time the medium was then replaced with complete HEK T294 media. Approximately 48 h after transfection, cells are split using 1 ml 1 × trypsin-EDTA per well and re-seeded in a 75 cm^2 tissue culture flask containing 10 ml HEK 293T cell culture media with antibiotic selection at 0.5 µg/ml puromycin. HEK 293T cells were viewed for expression between 5-10 days after selection.

2.9.2 Preparation of synthetic small interfering RNA (siRNA)

For synthetic siRNA transformation experiments an RNA free environment must be obtained by careful washing of the working area and equipment with RNase zap (Sigma). Then the siRNA (AllStars Negative siRNA conjugated to Alexa Fluor 555

(Qiagen) and ON-TARGETplus SMARTpool siRNA against human γGCS or NADPH oxidase 2 (NOX2) purchased from Dharmacon RNA Technologies) requires reconstitution in siRNA resuspension buffer (Qiagen), at an appropriate stock concentration (20 μM). AllStars Negative siRNA is then heated for 1 minute at 90°C, followed by incubation at 37°C for 60 minutes. The γGCS/ NOX2 siRNA is simply mixed for 30 minutes on an orbital shaker at room temperature. After this, the experiment is initiated or siRNA is stored at – 80˚C in 25 μl aliquots.

2.9.3 Gene silencing in 293T HEK with synthetic siRNA

Gene specific siRNA was purchased in order to generate a knockdown of the target gene (either γGCS or NOX2) and non-targeting AllStars siRNA (scrambled siRNA) was used as a negative control (used in all experimental designs performed). At least 24 h prior to gene silencing, 293T HEK were grown in media without antibiotics. For all siRNA gene- silencing experiments reverse transformation was used. This involves preparing the complexes inside the cell culture plastic wells prior to the addition of the cells contained in media (antibiotic free). Transfection of 293T HEK was performed using Lipofectamine RNAiMAX Transfection Reagent (Invitrogen). 5 nmol siRNA (per well) was diluted with 250 μl OptiMEM (Gibco, UK) serum free media without antibiotics. An additional 250 μl OptiMEM serum free media without antibiotics was used to dilute 5 μl Lipofectamine RNAiMAX and this was incubated for 5 min at room temperature. siRNA and Lipofectamine RNAiMAX solutions were then combined and incubated for 20-30 min at room temperature. During this 20-30 minute incubation period, cell suspensions were obtained by proteolysis with 1 × trypsin-EDTA. Cells were rinsed with 10 ml sterile PBS (sPBS) then incubated with approximately 2 ml 1 × trypsin-EDTA, 37˚C for 5 min. Insurance of cell detachment was observed under an inverted light microscope (Axiovert25, Carl Zeiss, MicroImaging Inc., Hertfordshire, UK). Cells were then pelleted by centrifugation (800 × g, 10 min), the supernatant was removed carefully and the cell pellet resuspended in 10 ml fresh antibiotic free media. Cells were checked for cell number and viability using trypan blue exclusion (section 2.2.2). Cells were resuspended in media without antibiotics at 0.5×10^6 /ml. Once the 20-30 minute liposome formation has ended, 500 μl siRNA complexes are added to each well (of a 6 well plate) and the plate is then gently rocked to ensure equal distribution. Then 2 ml of cell suspension (to a 6 well plate) is added to each well, rocked gently and incubated at 37˚C for 12 h. After this time the medium was then

replaced with complete HEK T294 media. Cell lysates were obtained as described in section 2.2.6. Following transfection, the efficiency was determined by flow cytometry. Cell acquisition and analysis was carried out in the CyAN flow cytometer, (Dako Becton-Dickinson). A minimum of 10,000 cell events was counted for each sample and non-staining samples were used for control.

2.10 Reverse transcription polymerase chain reaction (RT-PCR)

2.10.1 RNA isolation

Total ribonucleic acid (RNA) was isolated from cells using TRIzol reagent (Invitrogen). Briefly, 4-5 × 10^6 cells were lysed with 1 ml TRIzol then scraped and the lysate removed into a 50 ml universal tube and incubated for 5 min at room temperature. Chloroform was then added (0.5 ml per 1 ml TRIzol) and the tube shaken for 15 s by hand and then incubated for 2-3 min at room temperature. The emulsion formed was then separated by centrifugation (5000 × g, 4˚C, 15 min). Using RNase free solutions and equipment (pipette tips and centrifuge tubes), the upper aqueous phase was removed in 0.5 ml aliquots to a 1.5 ml centrifuge tubes. To each tube 0.5 ml isopropyl alcohol was added and incubated for 10 min at room temperature before centrifugation (13,000 × g, 10 min). The RNA pellet was washed with 1 ml 70% (v/v) ethanol, by centrifugation at 13,000 × g, 2 min. The pellet was air-dried for approximately 5 min and resuspended in 500 µl dH_2O.

2.10.2 RNA integrity

RNA concentration and purity were determined using a NanoDrop ND-1000 Spectrophotometer (NanoDrop Technologies, Wilmington, USA). The concentration was determined by measuring absorbance at 260 nm (A260). The ratio between 260 nm and 280 nm, and 260 nm and 230 nm indicate the purity of the RNA. Values of A260/A280 ratio should be approximately 2.0 (Glasel, 1995; Manchester, 1995) and A260/A230 ratio should be in the range of 1.8 – 2.2 for pure RNA according to the manufacturer's instructions.

2.10.3 cDNA synthesis

For each sample of RNA to be analysed, 4 wells were prepared (3 positive and 1 negative) on a standard 96-well PCR plate. To each well, the following were added: 1 μg RNA, 1 μg $OligoDT_{12-18}$ primer (Invitrogen) and RNase-free PCR grade water to reach a final volume of 10 μL per well. The reaction was heated to 65˚C for 5 minutes in a Primus 96 *plus* thermocycler (MWG Biotech, Milton Keynes, UK). The reaction mix was then placed on ice for 2-3 minutes. The following were added to each well: 4 μL 5 × first strand buffer, 1 μL 0.1 M DL-Dithiotheitol (DTT), 2 μL 10 mM deoxynucleotide triphosphate (dNTP) mix and 1 μL 40 unites per μL Rnase-out (all from Invitrogen). 1 μL Superscript II reverse transcriptase (Invitrogen) was added to each of the positive control wells. 1 μL PCR grade water was added to each negative control well. The reaction mix plate was then incubated at 42˚C for 60 minutes, then 70˚C for 15 minutes in a Primus 96 *plus* thermocycler. After this, 80 μL PCR grade water was added to each well, giving a total volume of 100 μL per well. Using a mulitchannel pipette, 10 μL from each column (of 4 wells) was transferred to a new optical-grade 96-well PCR plate for each gene of interest to be analysed by PCR. The cDNA was either used immediately for qPCR or placed at – 80˚C for long-term storage.

2.10.4 Real-time quantitative PCR (qPCR)

To reach a final reaction volume of 25 μL the following were added to each well: 12.5 μL SYBR Green Jumpstart Taq ReadyMix (Sigma), 0.5 μL reference dye (supplied with SYBR Green Jumpstart Taq ReadyMix kit), 0.2 μM forward primer, 0.2 μM reverse primer and 1 μL PCR grade water. The Eppendorf Realplex^4 Mastercycler was used to perform the PCR reaction. SYBR was used as the internal control and after an initial step of 50˚C for 2 minutes followed by 96˚C for 2 minutes the programme ran for 45 cycles (90˚C for 15 seconds, followed by 60˚C for 20 seconds). The data was acquired with Eppendorf Realplex^4 Mastercycler software and exported to Excel for analysis. Gene copy number was calculated using serial dilutions of standard DNA. Each value was corrected for background by subtracting the negative control. Corrected values were then expressed as a percentage of the control gene (either β-actin or 18S).

2.11 Biochemical assays

2.11.1 Measurement of reactive oxygen species

2.11.1.1 Using 2'-7'dichlorofluorescin (DCFH)

To measure reactive oxygen species (ROS) the probe, 5-(and-6)-chloromethyl-2',7'-dicholorodihydrofluorescien diacetate, acetyl ester (CM-H_2DCFDA) (Molecular probes, Invitrogen) was used. CM-H_2DCFDA is a cell permeable indicator for reactive oxygen species which is retained inside the cells after cleavage of acetate moiety by esterases. This compound then reacts with intracellular ROS changing its fluorescent properties which can be quantified. Shortly before performing the experiment, the CM-H_2DCFDA is reconstituted in 100% ethanol to make a stock concentration of 20 μM. Cells were then washed twice in sPBS (37°C), and incubated with the ROS indicator in phenol free media for 30 minutes. Due to the dye's susceptibility to photo-oxidation, care was taken to avoid light exposure, and hence low light conditions were used where possible. After the 30 minute incubation, the media was removed and the cells washed twice in PBS. To measure ROS using flow cytometry, cells were collected in 1 × trypsin-EDTA, 37°C for 5 min and then neutralised using an equal volume of TNS. Cells were then pelleted by centrifugation (800 × g, 10 min), the supernatant was removed and the cell pellet was homogenised in approximately 1 ml PBS. Cell acquisition and analysis was carried out in the CyAN flow cytometer, (Dako Becton-Dickinson). A minimum of 10,000 cell events was counted for each sample and non-staining samples were used for control.

To measure ROS using a fluorometer cells were seeded in a black-edged 96 well plate at 10,000 cells per well. Cells were seeded in phenol free media, in quadruple wells and left overnight to adhere. The following day cells washed twice in sPBS (37°C), and incubated with the ROS indicator in phenol free media for 30 minutes (covered with foil to reduce excessive light exposure). The probe was then removed and the cells washed twice in sPBS (37°C) before adding media containing defined treatments. Cells without the probe were used as negative controls to correct for background fluorescence. The plate was then placed in a Victor 2, 1420 Multi label counter, in a pre-warmed reading chamber (37˚C). Excitation and emission was measured at 488 nm and 520 nm, respectively (Wallac Victor 2, 1420 Multi label counter, Perkin Elmer). Sequential readings were taken every 10 minutes for up to 1 hour. At the end of the experiment protein concentration (see section 2.3) was determined to ensure equal loading of cells.

2.11.1.2 Using HyPer

HyPer consists of yellow fluorescent protein (YFP) inserted into the regulatory domain of the prokaryotic H_2O_2-sensing protein, OxyR (Belousov *et al.*, 2006). Cells were transfected with the plasmid carrying HyPer using Lipofectamine transfection reagent following the protocol previously described in section 2.9.1. HyPer-transfected cells exhibiting yellow florescent protein (YFP) positive staining were then selected using fluorescence-activated cell sorting (FACS), as the plasmid has no antibiotic selection in mammalian cells. FACS analysis was performed by Scientific Support Services (Wolfson Institute for Biomedical Research, UCL) using a MoFlow high-speed cell sorter. HyPer was kindly provided by Dr A Galkin, Wolfson Institute for Biomedical Research, UCL, London, UK. Following sorting, HyPer transfected cells were incubated with defined treatments and cell acquisition and analysis was carried out in the CyAN flow cytometer, (Dako Becton-Dickinson). A minimum of 10,000 cell events was counted for each sample and non-staining samples were used for control.

2.11.2 Nitrite quantification

The amount of nitric oxide (NO) was estimated by measuring nitrite (NO_2^-) levels in the extracellular medium using the Griess reagent kit (Molecular Probes, Leiden, Netherlands). Total nitrite was quantified by the conversion of sulfanilic acid to a diazonium salt by the reaction with nitrite in acid solution. The diazonium salt is then coupled to *N*-(1-naphthyl)ethylenediamine, forming an azo dye that brings about a colourimetric change which is spectorophotometrically detected. Nitrite concentrations were determined based on a standard curve produced from a series of dilutions of known concentrations of NO_2^-. 50 µl of sample or standard were mixed with 50 µl Griess reagent. Assays were performed in triplicate in a 96-well plate, and incubated for 10 minutes in the dark at room temperature. Absorbance was measured at 540 nm and 620 nm (Molecular Devices, SpectraMax Plus).

2.11.3 Lactate quantification

Lactate concentration was determined using a lactate oxidase-based assay (Trinity Biotech Ltd). Total lactate was quantified by the conversion of lactic acid to pyruvate and hydrogen peroxide (H_2O_2) by lactate oxidase. In the presence of the H_2O_2 formed, peroxidase catalyzes the oxidative condensation of the chromogen precursors to produce

a coloured dye with an absorption maximum at 540 nm. The increase in absorbance at 540 nm is directly proportional to the lactate concentration in the sample. 5 µl sample was added to a 96 well plate in triplicate, followed by 100 µl lactate reagent. The plate is then shaken briefly on a shaker table and then incubated in the dark for 10 minutes. Absorbance was measured at 540 nm (Molecular Devices, SpectraMax Plus).

2.11.4 Measurement of total glutathione

Total cellular glutathione (GSH) was measured in HEK 293T cells using a colorimetric assay GSH-400 kit (Oxis Research, Portland, USA). Glutathione was measured via a two-step chemical reaction which first involves the formation of thioethers between 4-chloro-1 –methyl-7-trifluromethyl-quinolinium methylsulfate (R1) and all mercaptans (RSH) present in the samples. The second step involves a β-elimation reaction which takes places under alkaline conditions, allowing for the transformation of the thioethers obtained from GSH into a chromophoric thione which has a maximal absorbance wavelength at 400 nm. Samples were collected in approximately 2 ml 1 × trypsin-EDTA, 37°C for 5 min. Cells were then pelleted by centrifugation (800 × g, 10 min), the supernatant was removed and the cell pellet was homogenised in 500 µl Metaphosphoric acid (MPA). Cells were then centrifuged at 3000 × g for 10 minutes, and the clear upper aqueous layer was collected. Then both samples and standards were prepared in a 900 µl final volume. 50 µl solution R1 was added, mixed thoroughly, followed by the addition of 50 µl solution R2, and mixed thoroughly again. The samples were then incubated at 25°C for 10 minutes in the dark. Absorbance was measured at 400 nm (Varian, Cary 4000 UV-Vis Spectrophotometer).

2.12 Visible light spectroscopy (VLS)

2.12.1 Principle

The visible light spectroscopy system (VLS, Figure 13) was used to monitor continuously the oxygen consumption (VO_2) of respiring cell and changes in the redox state of cytochrome aa_3 in cytochrome *c* oxidase (C*c*O) during respiration towards anoxia (Hollis *et al.*, 2003). The VLS system measures light absorbed by cytochromes aa_3 in the C*c*O. Changes in the cytochrome redox state are determined by multi-wavelength least squares fitting of the oxidised minus reduced cytochrome absorption spectra (Hollis *et al.*, 2003).

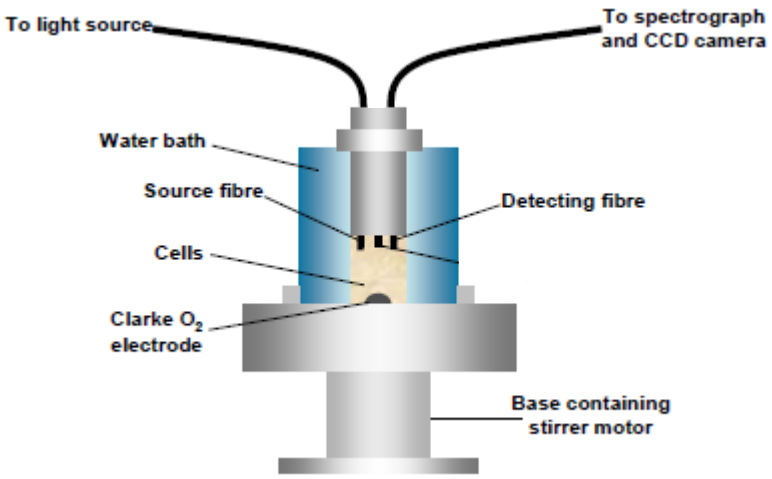

Figure 13 – Schematic of VLS instrumentation

The VLS system measures light absorbed by cytochromes aa_3 in the C*c*O. Changes in the cytochrome redox state are determined by multi-wavelength least squares fitting of the oxidised minus reduced cytochrome absorption spectra (Hollis *et al.*, 2003).

2.12.2 Oxygen calibration and measurement corrections

The Clark-type O_2 electrode is capable of measuring a current that is proportional to the partial pressure of O_2 (pO_2) in the sample. The current is converted to a voltage and input to the analogue-to-digital converter, which is sampled at a rate of 2 Hz by the acquisition software. The software converts the measured voltage to oxygen concentration [O_2] using values determined from the calibration procedure described fully by Hollis *et al.,* 2003. The rate of O_2 consumption (VO_2) in the chamber is also calculated on-line from the differential of [O_2] with respect to time, determined from a 20-data-point fourth order polynomial (i.e. fitting over a period of 10 s). The conversion of the O_2 electrode output to [O_2] involves a two-point calibration procedure, performed daily in 1 ml of the medium the cells are suspended in during their subsequent measurement in the chamber. For full details on VLS calibration and measurement corrections please refer to Hollis *et al.,* 2003. In this study, VLS calibration, measurement corrections, cell counting post VLS measurements and data analysis were performed by Miriam Palacios-Callender or/and Nanci Frakich.

2.12.3 VLS cell culture and protocol

Cells were cultured in sterile 175 cm^2 tissue culture plastic flasks containing 50 ml appropriate cell culture medium (section 2.2.2). Cell culture media was then removed and the cells were rinsed twice with copious sterile PBS (sPBS) containing 25 mM HEPES. Cells were then incubated with approximately 5 ml 1 × trypsin-EDTA, 37˚C for 5 min, followed by neutralisation using trypsin neutralising solution (TNS) purchased from Sigma, UK. Confirmation of cell detachment was obtained using an inverted light microscope (Axiovert25, Carl Zeiss, MicroImaging Inc., Hertfordshire, UK). Cells were then harvested by centrifugation (800 × g, 10 min), the supernatant was removed carefully and the cell pellet resuspended in medium without phenol red dye (to avoid interference with the optical technique) to a final concentration of 2-3 × 10^7 cells/ml. Cell counting and determination of viability at this point was carried out using Trypan blue exclusion method. After harvesting, cells were placed into a 50 ml Falcon tube and incubated at 37°C in a water bath for 40-60 minutes prior to measurement, gently resuspending every 15-20 minutes. At the time of measurement 1 ml of cells was placed into the respiration chamber and kept in suspension by stirring with a magnetic glass bar at 750 rpm, sealing the cells from the atmosphere with the plunger. At the end of each experiment, the cells were collected from the chamber and placed on ice for further determination of cell number.

2.13 Electron microscopy

Cells for electron microscopy (EM) were adhered for 1 hour to a 4 cm^2 glass cover slip. Cells were then gently washed with 2 ml PBS and fixed by incubation with 3% paraformaldehyde, 1.5% glutamine, 100 mM sodium cacodylate buffer, 5 mM $CaCl_2$ and 2.5% sucrose at room temperature for 10 minutes. Cells were then visualised and images taken using an electron microscope by M Turmaine, Division of Biosciences, University College London.

2.14 Immunofluorescence and confocal microscopy

D890N HEK 293T cells were seeded at a density of 0.1 × 10^6 cells/ 0.8 cm^2 growth area of a chamber cover glass (Lab-Tek, Nunc, Langenselbold, Germany) and incubated 12 h before confocal imagery. The medium was then removed, and the cells were rinsed twice with sPBS. Then 20 μg/ ml Hoechst 33342 plus 20 nM TMRM was added and

cells were incubated for 15 minutes in the dark. Confocal microscopic images were taken with Ultra *VIEW* ERS Live cell microscope (Perkin Elmer) with a × 63 oil immersion objective. The cells were kept at 37°C during the entire imaging period by a thermostatic chamber encasing the microscopic stage. Data acquisition and fluorescence analysis were carried out using Ultra *VIEW* software. Whole cell fluorescence was analysed by marking the individual cells in the field. Background fluorescence of a region without cells/ cell debris was subtracted from fluorescence values.

The mitochondrial membrane potential ($\Delta\Psi_m$) of control (untreated) and induced (doxycycline (DC) treated) D890N HEK cells was evaluated 10 days after DC induction by inhibiting the respiratory chain at Complex I using 1 μM rotenone. The kinetic action of rotenone on $\Delta\Psi_m$ was studied by recording the TMRM fluorescence in time-lapse experiments. Steady-state TMRM fluorescence was recorded for approximately 2 minutes to obtain a stable fluorescence signal. Subsequently, rotenone was added and the signal was recorded for approximately 30 s. The $\Delta\Psi_m$ was collapsed by the addition of 25 μM FCCP and TMRM fluorescence recorded for approximately a further 3 minutes.

2.15 Data analysis and statistics

Statistical analyses were performed using either Excel (Microsoft Office) or GraphPad Prism 5 software packages. Densitometric analyses were performed using AlphaEase FC software version 4 (AlphaInnotech). Exposed films were illuminated with transilluminating white light and an image was captured using a motorised lens camera (focal length: 8.0 ~ 48 mm, maximum aperture ratio: 1:1.2, 6x zoom) with flat field calibration to easily correct for non-uniformities in light gathering. The captured image was then analysed using FC software version 4 utilising 256 gray scale values. The software captures an integrated density value which is the sum of the gray levels of all the pixels within the boundaries of each band and then subtracts a background value computed as a mean of 16 lowest intensity points within the assigned boundaries. All data are plotted graphically as mean values, with vertical bars representing standard error of the mean (SEM). A Student's t-test was used to compare differences between two data groups. One-way ANOVA was used to assess differences between individual experimental conditions when multiple comparisons were being made to a control. For all statistical analyses a probability (P) value, *, of <0.05 was considered significant.

2.16 Materials and reagents

2.16.1 Eukaryotic cell culture

HEK 293T cell culture medium: DMEM (41965-039), 10% (v/v) FCS, 100 IU/L penicillin, 100 µg/L streptomycin

HEK 293T serum free medium (SFM): DMEM (41965-039), 100 IU/L penicillin, 100 µg/L streptomycin

HEK 293T phenol free medium (PFM): DMEM (21063-029), 10% (v/v) FCS, 100 IU/L penicillin, 100 µg/L streptomycin

D890N HEK 293T cell culture medium: DMEM (41965-039), 10% (v/v) FCS, 200 µg/ml hygromycin, 15 µg/ml blasticidin, 50 µg/ml uridine,1 mM pyruvate

D890N HEK 293T induction (*Rho*^{0}) cell culture medium: DMEM (41965-039), 10% (v/v) FCS, 200 µg/ml hygromycin, 15 µg/ml blasticidin, 50 µg/ml uridine, 1 mM pyruvate, 250 ng/ml doxycycline

H157 cell culture medium: α-MEM (22571-038), 10% FCS, 100 IU/L penicillin, 100 µg/L streptomycin, 1.8×10^{4} mol/L adenine, 5 µg/ml insulin, 1×10^{-10} mol/L cholera toxin, 0.5 µg/ml hydrocortisone and 10 ng/ml epidermal growth factor

H157 (*Rho*^{0}) cell culture medium: α-MEM (22571-038), 10% FCS, 100 IU/L penicillin, 100 µg/L streptomycin, 1.8×10^{4} mol/L adenine, 5 µg/ml insulin, 1×10^{-10} mol/L cholera toxin, 0.5 µg/ml hydrocortisone and 10 ng/ml epidermal growth factor, 50 µg/ml uridine, 50 µg/ml pyruvate, 200 ng/ml ethidium bromide

J774.A1 cell culture medium: DMEM (11960), 10% (v/v) FCS, 25 mM D-glucose, 2 mM L-glutamine, 100 IU/L penicillin, 100 µg/L streptomycin

Transfection medium: OpiMEM (31985047_464548114)

Trypsin EDTA: 0.05% EDTA

Cryo-buffer: 10% (v/v) dimethyl sulphoxide (DMSO), 90% (v/v) DMEM

Dulbecco's Modified Eagle Medium (DMEM) and other cell culture reagents, as specified, were obtained from Invitrogen, UK. Heat inactivated foetal calf serum (FCS) was of New Zealand Origin supplied by GIBCO (10691-145).

2.16.2 Bacterial cell culture and cloning

Luria bertani (LB) broth: 1% (w/v) bacto-peptone, 0.5% (w/v) yeast extract, 0.5% (w/v) NaCl

LB agar: LB broth, 1% (w/v) agar

Qiagen mini-prep solutions:

Solution I: 50 mM glucose, 10 mM EDTA, 25 mM Tris.HCL pH 8.0

Solution II: 1% (w/v) SDS, 0.2 M NaOH

Solution III: 3 M potassium acetate, 11.5% glacial acetic acid

Qiagen maxi-prep solutions:

Qiagen buffer P1 (resuspension buffer): 50mM Tris.HCL pH 8.0, 10mM EDTA, 100 µg/ml RNase

Qiagen buffer P2 (lysis buffer): 200 mM NaOH, 1% (w/v) SDS

Qiagen buffer P3 (neutralisation buffer): 3 M potassium acetate pH 5.5

Qiagen buffer QBT (equilibrium buffer): 750 mM NaCl, 50 mM MOPS pH 7.0, 15% (v/v) isopropanol, 0.15% (v/v) triton X-100

Qiagen buffer QC (wash buffer): 1 M NaCl, 50 mM MOPS pH 7.0, 15% (v/v) isopropanol

Qiagen buffer QF (elution buffer): 1.25 M NaCl, 50 mM Tris.HCL pH 8.5, 15% (v/v) isopropanol

2.16.3 Treatments

Table 2 – Treatments used, concentrations and suppliers

Treatment		Mode of action	Concentration	Supplier	Cat no.
Ascorbic acid	^	Antioxidant	1 mM	Sigma	A-5960
Cobalt chloride	*	HIF-1α stabiliser	300 μM	Sigma	C-2644
Doxycycline	*	Antibiotic	250 ng/ml	Sigma	D9891
Ethidium bromide	*	DNA replication inhibitor	200 ng/ml	Invitrogen	15585-011
FCCP	¬	Un coupler of OXPHOS	25 μM	Sigma	C2920
Hoeschst 33342	¬	Fluorescent nuclear stain	20 μg/ml	Invitrogen	H3570
Lipopolysaccharide	#	Bacterial endotoxin	10 ng/ml	Difco	0901
Menadione	*	Pro-oxidant	160 μM	Sigma	M2518
MG132	*	Proteasome inhibitor	10 μM	Sigma	C2211
Mouse IFNγ	#	Cytokine	10 IU/ml	Insight Biotech Ltd	IB-1092
N-acetyl-L-cysteine	^	Antioxidant	2.5 mM	Sigma	A8199
N^G-monomethy-L-arginine	^	NOS inhibitor	1 mM	Axxora Ltd	ALX-106-001-G001
S-ethyl isothiourea	#	iNOS inhibitor	500 μM	Caymen Chemical	1071-37-0
Rotenone	¬	Complex I inhibitor	1 μM	Sigma	R8875
TMRM	¬	Mitochondrial membrane potential fluorescent marker	20 nM	Invitrogen	T668

* Concentration detemined through dose response curves performed during thesis

Concentration from published literature: ^ (Quitero *et al.,* 2006a), # (Garedew and Moncada, 2008) and ¬ (Garedew *et al.*, 2010)

2.16.4 Hypoxic chamber

Some of the experiments described were carried out at different oxygen concentrations. Hypoxia was achieved by incubation of cells at 37°C in an oxygen-controlled hypoxic chamber (Coy Laboratory Products Inc, Ann Arbor, Michigan). Oxygen concentrations were maintained using a 5% CO_2/Nitrogen 200 BAR compressed gas cylinder (BOC Limited, Surrey).

2.16.5 Electrophoresis

SDS running buffer (1 ×): 50 mM Tris Base, 0.384 M glycine, 0.1% SDS in distilled water

SDS loading buffer (2 ×): 4 % SDS, 20% glycerol, 1.5 M Tris.HCL pH 6.8, 10% β-mercaptoethanol up to 10 ml dH_2O, bromophenol blue

Transfer buffer: 25 mM Tris Base, 192 mM glycine, 20% methanol, made up to 1 litre with distilled water

Tris acetate EDTA (TAE) buffer (50 ×): 2 M Tris, 25 mM sodium acetate, 50 mM EDTA pH 7.6

TAE loading buffer: 200 mM Tris, 25 mM sodium acetate, 5 mM EDTA pH 7.6, 80% glycerol, bromophenol blue

Western blot transfer membrane nitrocellulose was obtained from Amersham Biosciences, UK. Enhanced chemiluminescence (ECL) detection reagents were obtained from Pierce, UK and Hyperfilm ECL film was obtained from Amersham Biosciences, UK. Protein quantification was performed using bicinchoninic acid (BCA) kit, obtained from Sigma, UK.

2.16.6 Antibodies

Table 3 – Antibodies used, working dilutions, suppliers and targets

Antigen	Clone	Supplier	Cat no.	Dilution	Incubation time
α-tubulin	Monoclonal	Abcam	Ab7291	1:10,000	30 min
C*c*O	Monoclonal	BD Biosciences	556433	1:5000	O/N
γGCS	Polyclonal	Santa Cruz Biotechnolgy	Sc-28965	1:1000	O/N
HIF-1α	Monoclonal	BD Biosciences	610958	1:2000	O/N
Hydroxyated HIF-1α	Polyclonal	CoValab	P564	1:2000	O/N
Mouse IgG	Polyclonal	Dako	P0260	1: 2000	1 hour
NOX-2	Polyclonal	Millipore	07-024	1:2000	O/N
Ubiquitin	Polyclonal	Dako	Z0458	10 µg	2 hours
Rabbit IgG	Polyclonal	Vector Laboratories	P1-1000	1:2000	1 hour

2.16.7 Primers

Table 4 – Human primers used for real-time qPCR

Gene	Direction	Sequence 5' to 3'
18S	Forward	CGC CGC TAG AGG TGA AAT TC
	Reverse	TTG GCA AAT GCT TTC GCT C
Catalase	Forward	CAA AAT GCT TCA GGG CCG
	Reverse	TAA TTG GGT CCC AGG CGA
COX1	Forward	ATT TAG CTG ACT CGC CAC ACT CCA
	Reverse	TAG GCC GAG AAA GTG TTG TGG GAA
β-actin	Forward	TGT GCC ATC TAC GAG GGG TAT GC
	Reverse	GGT ACA TGG TGG TGC CGC CAG ACA
γGCS	Forward	GCA CAT CTA CCA CGC CGT C
	Reverse	CCA CCT CATCGC CCC AC
HIF-1α	Forward	CCA GTT ACG TTC CTT CGA TCA GT
	Reverse	TTT GAG GAC TTG CGC TTT CA
MnSOD	Forward	GGT GGT GGT CAT ATC AAT CAT AGC
	Reverse	GCT TCC AGC AAC TCC CCT TT
NfKB	Forward	CGA GCT CCG GAG CAG TGA CA
	Reverse	GTA AAG CTG AGT TTG CGG AAG G
NOX1	Forward	TTC ACC AAT TCC CAG GAT TGA AGT GGA TGG TC
	Reverse	GAC CTG TCA CGA TGT CAG TGG CCT TGT CAA
NOX2	Forward	GTC ACA CCC TTC GCA TCC ATT CTC AAG TCA GT
	Reverse	CTG AGA CTC ATC CCA GCC AGT GAG GTA G
NOX4	Forward	CTG GAG GAG CTG GCT CGC CAA CGA AG
	Reverse	GTG ATC ATG AGG AAT AGC ACC ACC ACC ATG CAG
NOX5	Forward	GTC GCT CTG CTG CTG CTG CTC CTC T
	Reverse	TGA TGG TGA AGG GGT GCC ACT CAT AGC
NrF2	Forward	AAA CCA GTG GAT CTG CCA AC
	Reverse	GAC CGG GAA TAT CAG GAA CA
Thioredoxin	Forward	TGG TGT GGG CCT TGC AA
	Reverse	TCA AGG AAT ATC ACG TTG GAA TAC TT

Chapter three:
Mechanisms of HIF-1α stabilisation

Chapter three: Mechanisms of HIF-1α stabilisation

3.1 Introduction

At physiological [O_2] hypoxia-inducible factor-1α (HIF-1α) is constantly hydroxylated and thus prepared for proteosomal degradation through the action of the prolyl hydroxylases (PHDs) (Jiang *et al.*, 1996). In hypoxia however, the oxygen-sensitive PHDs are inhibited and HIF-1α is stabilised. Other agents, including cytokines and growth factors have been shown to stabilise HIF-1α at physiological [O_2] through different mechanisms such as activation of the phosphatidylinositol 3-kinase (PI3K) or mitogen-activated protein kinase pathways (Semenza, 2003) (see introduction 1.5.3). Increased production of reactive oxygen species (ROS) at low [O_2] have also been claimed to stabilise HIF-1α (Chandel *et al.*, 1998).

Studies described in this chapter investigate the hypothesis that free radicals stabilise HIF-1α both in normoxia and low oxygen conditions. This was evaluated by examining the effect of pro-oxidant agents and antioxidants on HIF-1α protein expression.

3.2 Oxygen-dependent stabilisation of HIF-1α

3.2.1 Response of HIF-1α to decreasing oxygen

To verify that HIF-1α becomes stable when cells are exposed to decreasing oxygen concentrations, HEK 293T cells were incubated at 21%, 3% or 0.5% oxygen for 24 hours. Low [O_2] (3% oxygen) and hypoxic oxygen conditions (0.5% oxygen) were achieved in a humidified variable aerobic workstation. Cell lysates were prepared, separated by SDS-PAGE and analysed by Western blot. α-tubulin served as a loading control. Figure 14 shows that incubation of cells at decreasing oxygen concentrations for 24 hours results in oxygen-dependent stabilisation of HIF-1α. HIF-1α stabilisation increased significantly as the oxygen concentrations decreased from 21% to 3% and from 3% to 0.5%.

3.2.2 Effect of cobalt chloride on HIF-1α stabilisation

Cobalt chloride ($CoCl_2$) has been reported to result in HIF-1α stabilisation in normoxic oxygen conditions (Chandel *et al.*, 2001). Thus we decided to utilise this agent as a positive control for the detection of HIF-1α. To determine the optimal concentration of $CoCl_2$ in which to study HIF-1α stabilisation, cells were incubated with different concentrations of $CoCl_2$ for 4 hours at 21% oxygen. Figure 15 shows that the stabilisation of HIF-1α with $CoCl_2$ was dose-dependent, with the most significant stabilisation occurring at 160 μM $CoCl_2$.

3.2.3 Time course of HIF-1α stabilisation

The next objective was to study the kinetics of HIF-1α stabilisation. Cells were incubated at 3% or 0.5% oxygen for 1, 2, 4 and 24 hours and compared to cells incubated at 21% oxygen for 4 h in the presence of $CoCl_2$. Figure 16 shows that the most efficient stabilisation of HIF-1α was achieved after 4 h incubation with $CoCl_2$ at 21% O_2 (24 h incubation did not have a greater effect; data not shown). Stabilisation of HIF-1α in hypoxia (0.5% oxygen) was time-dependent with the maximum effect observed at 4 h, similar to $CoCl_2$. On the other hand a modest, time-dependent stabilisation could be observed at 3% [O_2]. This was time-dependent with the maximum effect achieved at 24 h.

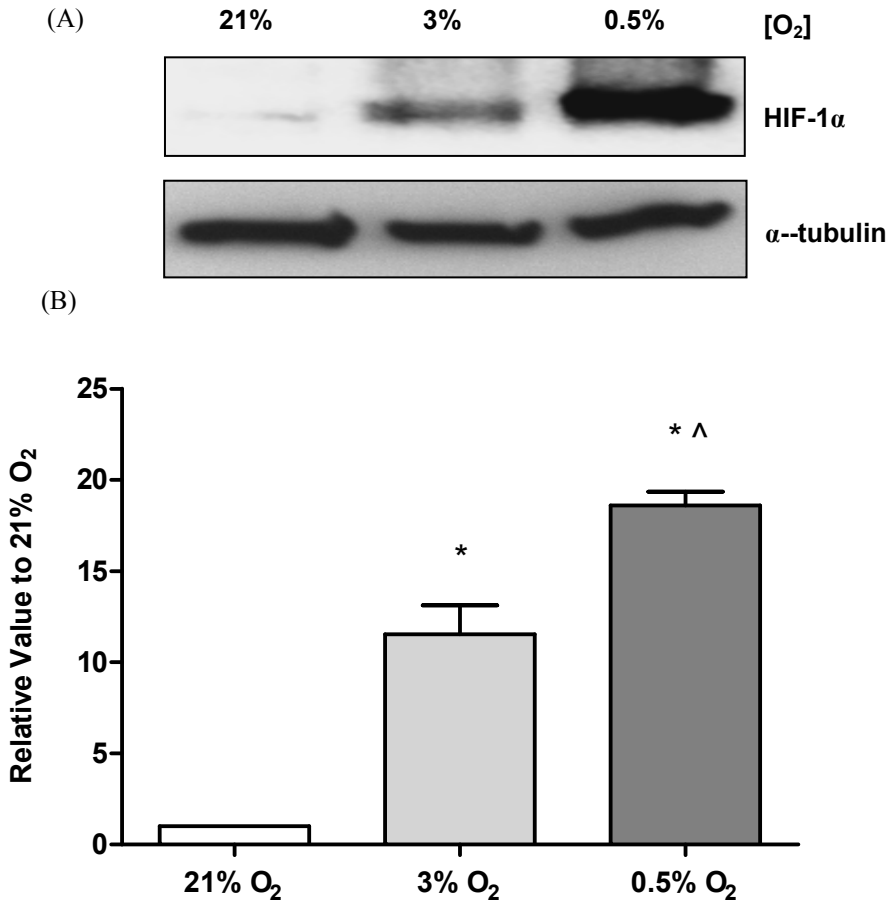

Figure 14 – HIF-1α stabilisation increases as the oxygen concentration decreases

HEK 293T cells were incubated at 21%, 3% or 0.5% oxygen (O_2) for 24 h. Cell lysates were subject to SDS-PAGE and analysed by Western blot with an anti-HIF-1α antibody (A) and quantified by densitometry (B). The corresponding densitometry values were normalised with α-tubulin and results are shown relative to 21% oxygen control. The values represent the mean $\pm$ SEM from 5 independent experiments; * represents a significant difference ($p < 0.05$) from 21% O_2 control values and ^ represents a significant difference ($p < 0.05$) from 3% O_2. One representative blot is shown.

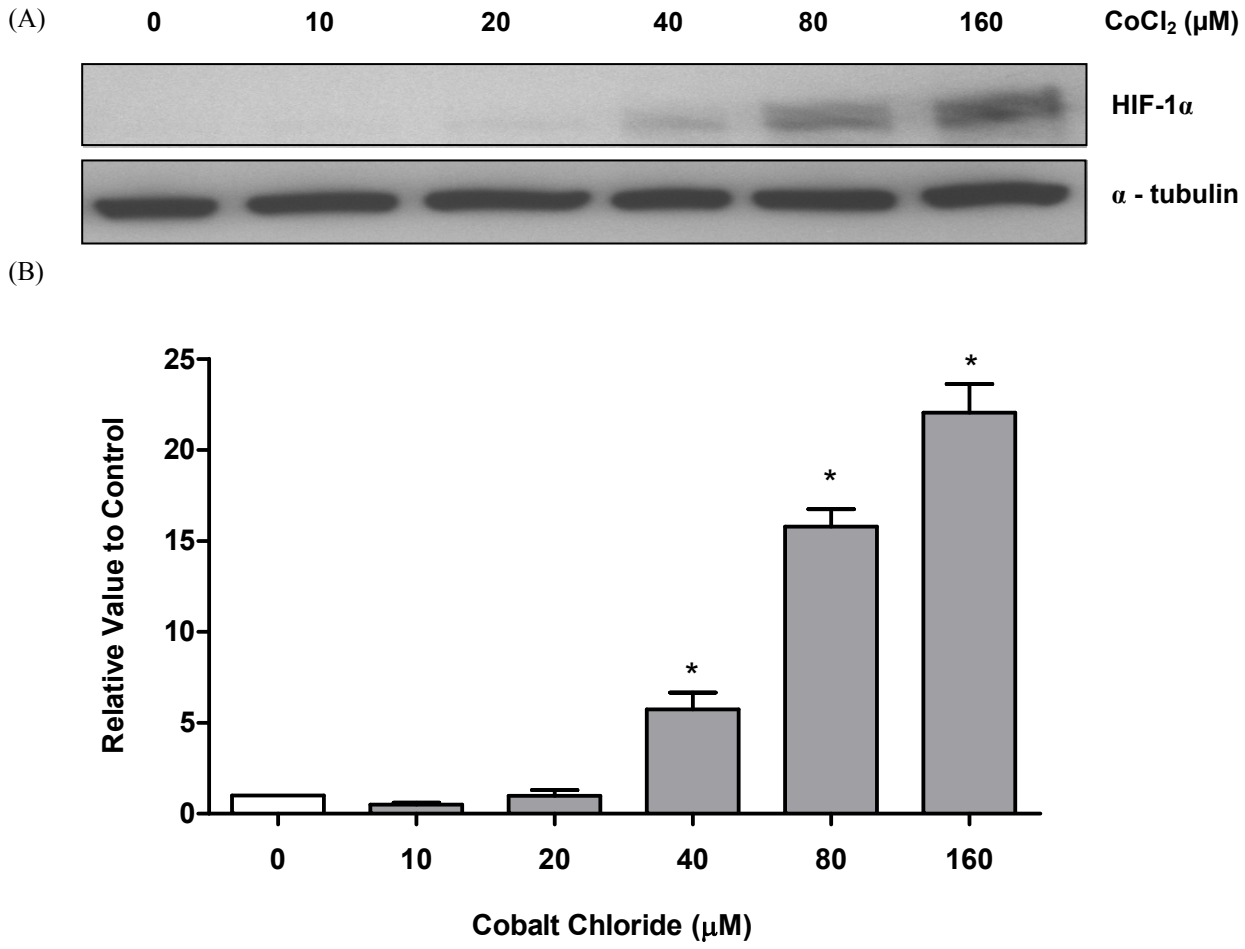

Figure 15 – HIF-1α stabilisation under increasing concentrations of $CoCl_2$

Cells were incubated at 21% oxygen for 4 h with different concentrations of cobalt chloride ($CoCl_2$, -160 μM). Protein expression was analysed by Western blot (A) and quantified by densitometry (B). The corresponding densitometry values were normalised with α-tubulin and are shown relative to control. The values represent the mean ± SEM from 3 independent experiments; * $p < 0.05$ versus control. One representative blot is shown.

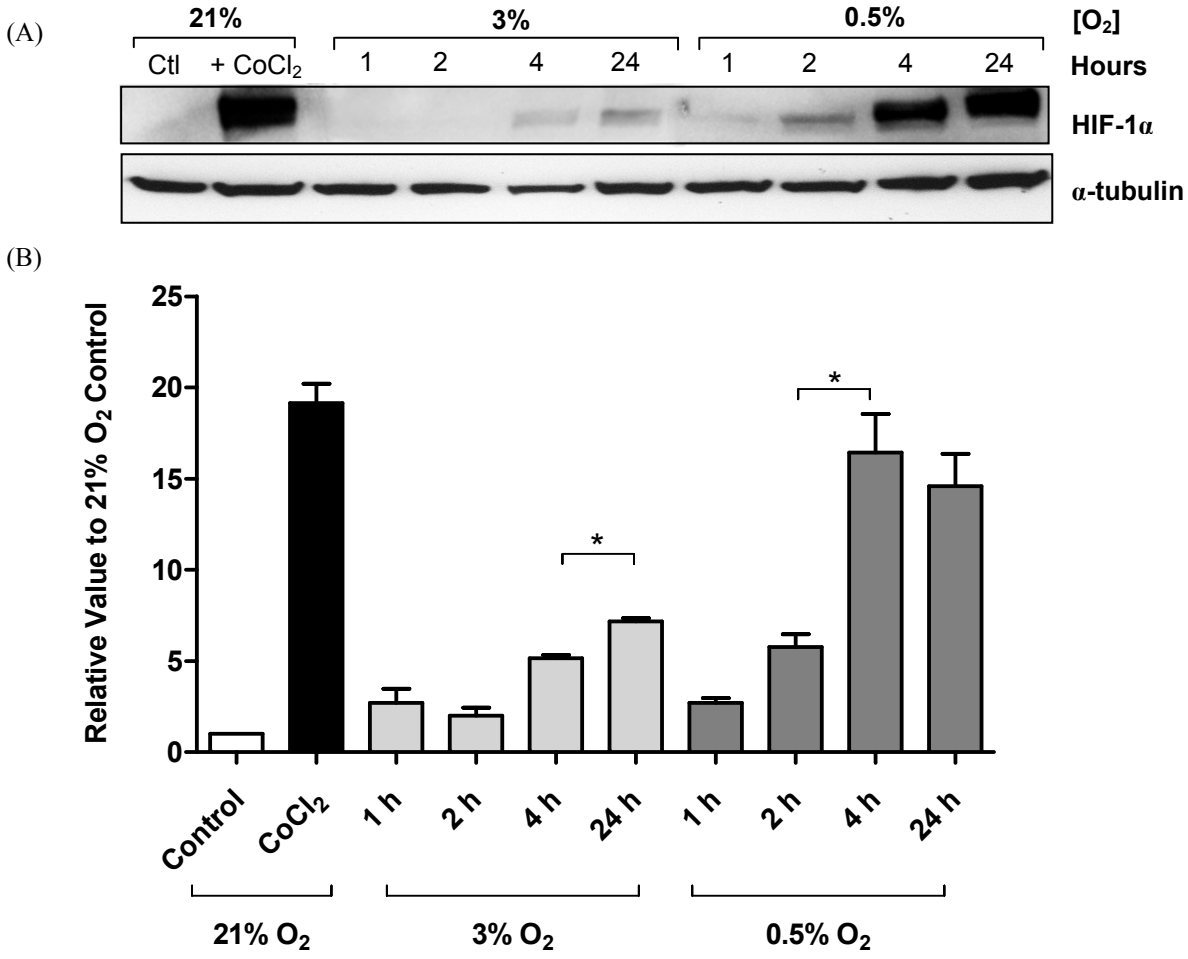

Figure 16 – Kinetics of HIF-1α stabilisation at 3% and 0.5% oxygen

Cells were incubated at 21%, 3% and 0.5% oxygen for 1-24 h. Cobalt chloride ($CoCl_2$, 160 μM) served as a positive control. Protein expression was analysed by Western blot (A) and quantified by densitometry (B). The corresponding densitometry values were normalised with α-tubulin and results are shown relative to 21% oxygen control. The values represent the mean ± SEM from 3 independent experiments; * $p < 0.05$. One representative blot is shown.

3.3 Oxygen-independent stabilisation of HIF-1α

3.3.1 Optimisation of 2'-7'-dicholorodihydrofluorescin (DCFH) to measure ROS in HEK 293T cells

In order to study the stabilisation of HIF-1α by pro-oxidant agents, first the ability of these compounds to produce ROS was evaluated. 2'-7'-dicholorodihydrofluorescin (DCFH) is widely used to measure oxidative stress in cells. However, artefacts caused by auto-oxidation of the probe can lead to false positive results (Picker and Fridovich, 1984;Faulkner and Fridovich, 1993;Liochev and Fridovich, 1995;Liochev and Fridovich, 1998). For this reason, experiments were initially performed to determine the fluorescence that can be attributed to ROS production. In order to distinguish between reactive intermediates produced by the probe and actual free radical formation, menadione (2-methyl-1,4-naphthoquinone; vitamin K3) was used as positive control due its association with the excessive generation of ROS such as superoxide, singlet oxygen, and hydrogen peroxide (Chung *et al.*, 1999). Cells were treated either with antioxidants to suppress ROS-derived fluorescence or with menadione to induce ROS. Two treatment groups were studied. Samples were either incubated with the treatments in the presence of DCFH (30 minutes) or the treatments were added immediately following the 30-minute DCFH incubation. To establish the level of background fluorescence originating from the probe, DCFH was also incubated in the absence or presence of cells.

There was no significant difference in DCF fluorescence when treatments are incubated with DCFH or post-DCFH incubation (Figure 17). There is also no significant difference between DCF fluorescence in cell negative treated groups and cell positive treated groups, suggesting in these cells, DCFH does not undergo auto-oxidation.

To determine the limit of detection of DCFH, cells were treated with menadione for 30 minutes (0-500 μM) and fluorescence was measured with excitation at 490 nm and emission at 520 nm. The results shown in Figure 18 demonstrate a clear dose-response effect of DCF fluorescence towards menadione-derived ROS. The lowest concentration of menadione required to detect DCF fluorescence is 40 μM. The first significant increase in DCF fluorescence is observed with 80 μM menadione.

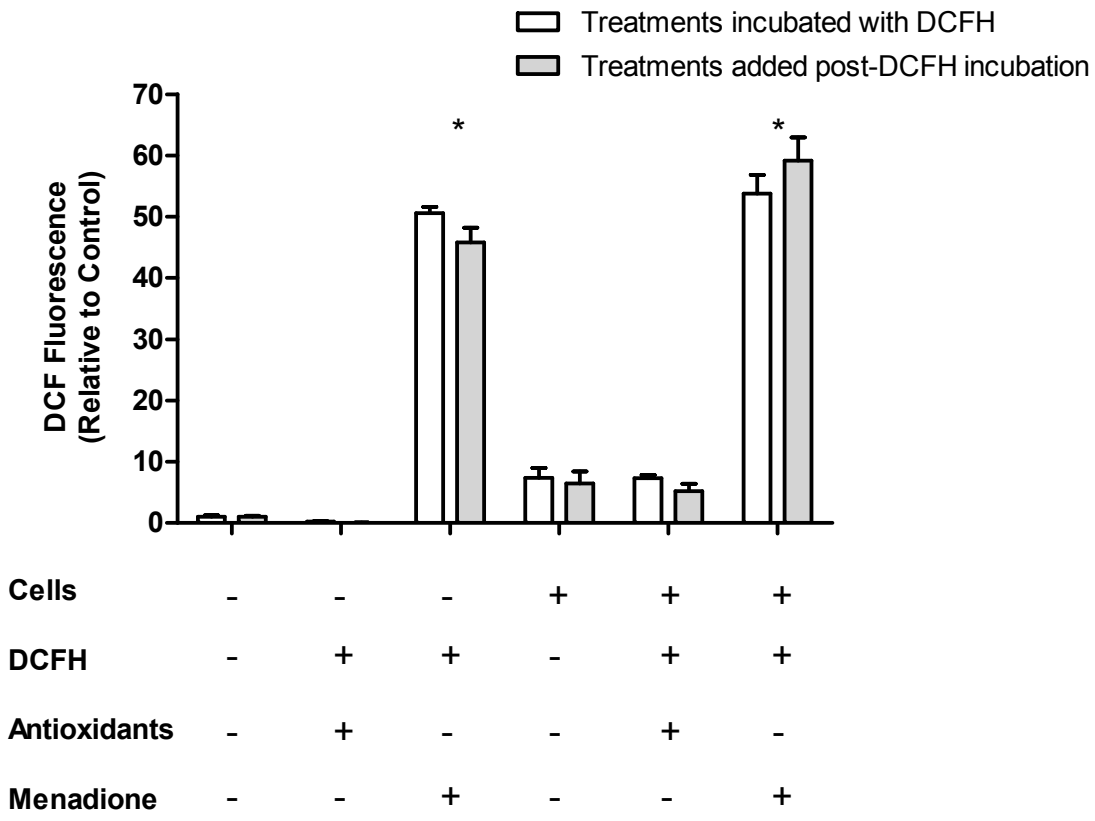

Figure 17 – DCF fluorescence in the absence and presence of cells

To establish the level of background fluorescence originating from auto-oxidation of the probe, 20 μM DCFH was incubated in the absence or presence of cells for 30 minutes. Cells were also treated with antioxidants (NAC 2.5 mM plus ascorbic acid 1 mM) or menadione 160 μM in the presence of DCFH or post-DCFH incubation. ROS was then measured using a fluorometer with excitation and emission measured at 490 nm and 520 nm, respectively. The values represent the mean $\pm$ SEM from 3 independent experiments; * represents a significant difference ($p < 0.05$) from all corresponding treatment groups.

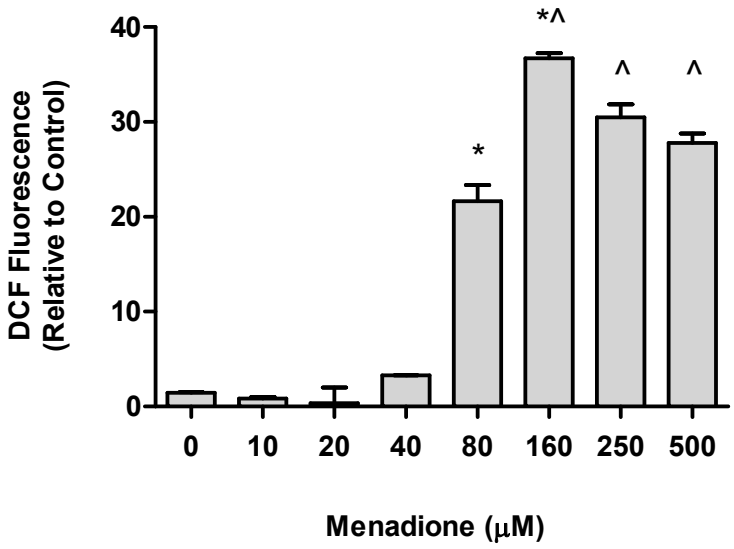

Figure 18 – DCF fluorescence dose response

Cells were treated with 0-500 μM menadione for 1 h and fluorescence analysed using a cytometer. Data represent the mean ± SEM from 3 independent experiments, * represents a significant difference ($p < 0.05$) from control, and ^ represents a significant difference from 80 μM menadione.

3.3.2 Effect of menadione on HIF-1α stabilisation

We next examined whether menadione, under the same conditions that induced ROS in cells (1 h, 0-160 μM, Figure 18) affects HIF-1α stabilisation. Menadione produced a concentration-dependent increase in HIF-1α stabilisation, with the most significant increase seen with 160 μM menadione (Figure 19), which corresponds to the highest ROS fluorescence in Figure 18. Cells were also treated with 160 μM menadione for shorter incubation periods (10-60 minutes) (incubation for longer than 1 h resulted in cell death). Stabilisation of HIF-1α was time-dependent, with the most significant increase observed at 60 minutes (Figure 20).

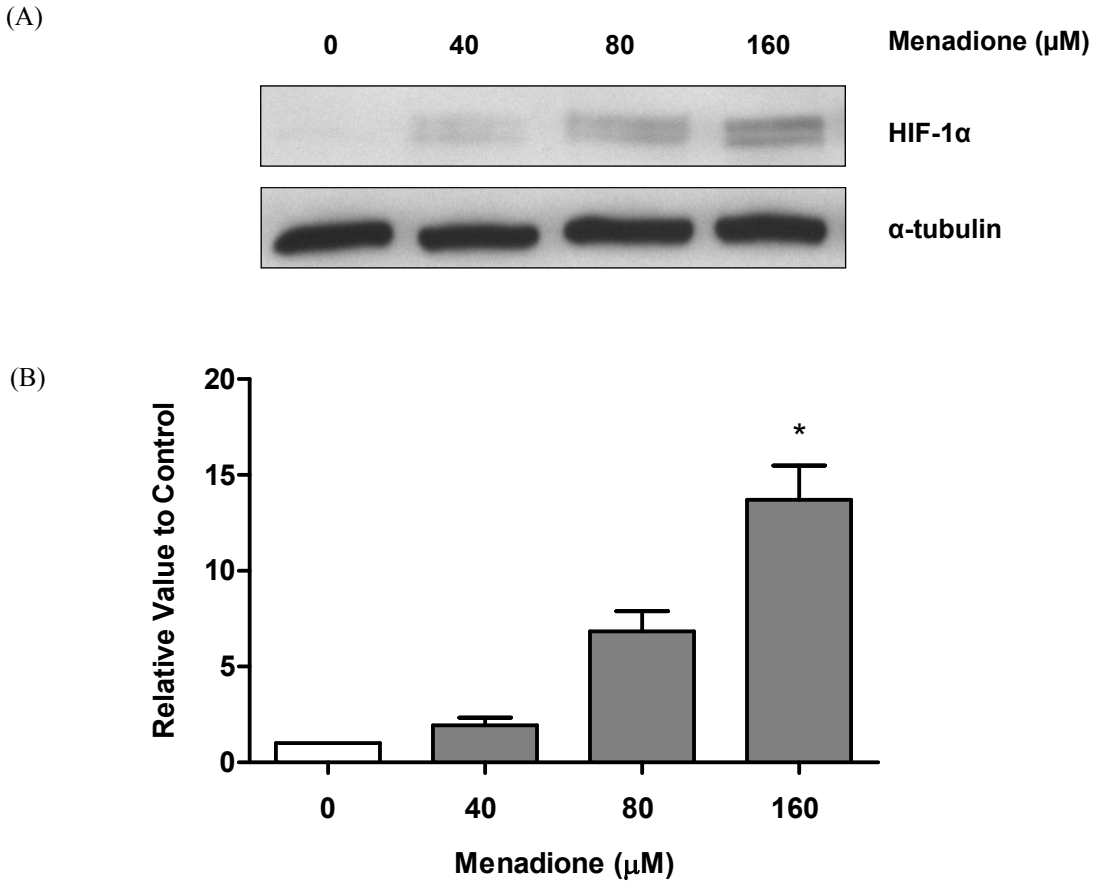

Figure 19 – Menadione induced HIF-1α expression in HEK 293T cells

Cells were incubated at 21% oxygen for 1 h with menadione (0-160 μM). Protein expression was analysed by Western blot (A) and quantified by densitometry (B). The corresponding densitometry values were normalised with α-tubulin and are shown relative to control. The values represent ± SEM from 3 independent experiments; * $p < 0.05$ versus control. One representative blot is shown.

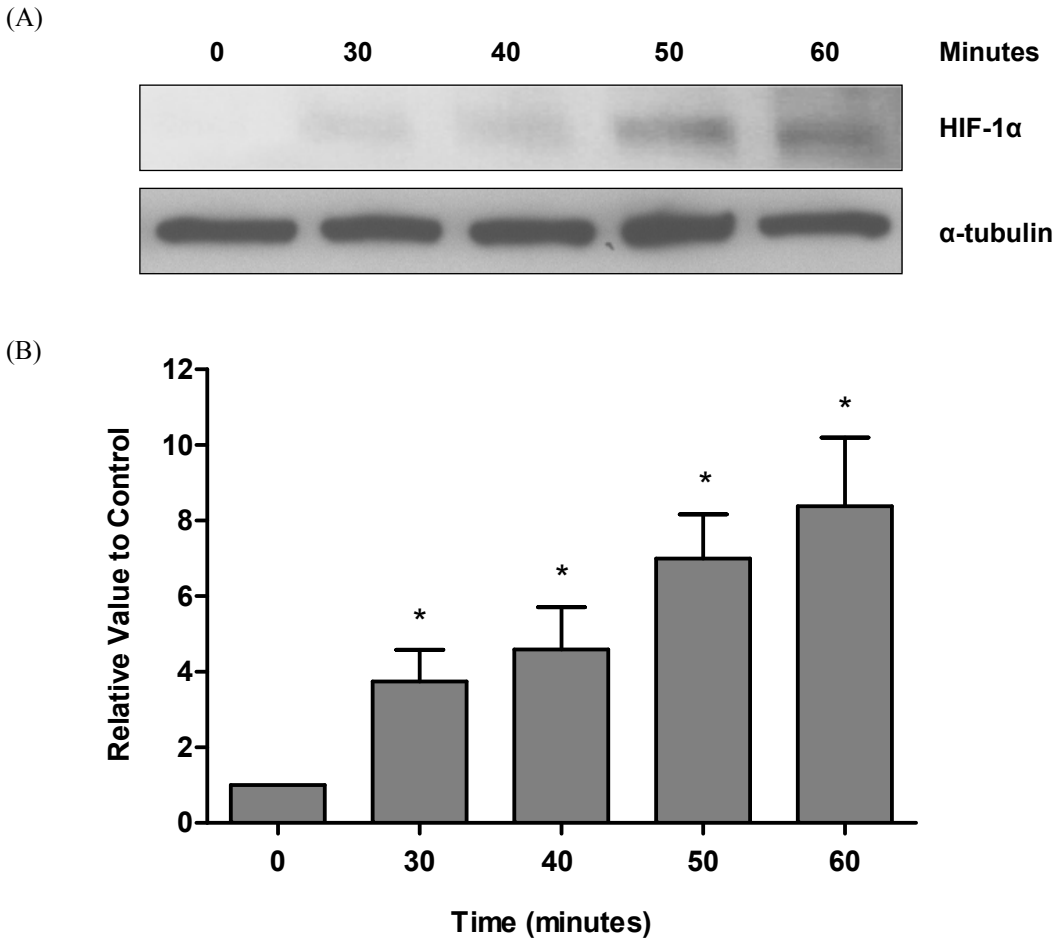

Figure 20 – Effect of menadione on HIF-1α stabilisation

Cells were incubated at 21% oxygen for up to 1 h with 160 μM menadione (0-60 minutes). Protein expression was analysed by Western blot (A) and quantified by densitometry (B). The corresponding densitometry values were normalised with α-tubulin and are shown relative to control. The values represent ± SEM from 3 independent experiments; * $p < 0.05$ versus control. One representative blot is shown.

3.3.3 Effect of antioxidants on HIF-1α stabilisation following treatment with menadione

Since treatment with menadione resulted in both ROS production and HIF-1α stabilisation, experiments were conducted using antioxidants to investigate the possible role of reactive oxygen species in menadione-induced HIF-1α stabilisation. Cells were treated with 160 μM menadione for 1 h in the presence or absence of an antioxidant (AO) mix, N-Acetyl-L-cysteine (NAC) at 2.5 mM plus ascorbic acid at 1 mM. Figure 21 shows menadione-induced HIF-1α stabilisation was reversed by treatment with antioxidants.

3.3.4 Synergism between menadione and hypoxia on HIF-1α stabilisation

Treatment with menadione (160 μM, 60 minutes) revealed an increase in ROS production and HIF-1α stabilisation which can be prevented by antioxidants. This result provides a connection between menadione and ROS production, and ROS production and HIF-1α stabilisation. Since the aim of my investigations was to establish, if any, a role of ROS in hypoxic HIF-1α stabilisation the effect of menadione in hypoxia (0.5% oxygen) was evaluated. Stabilisation of HIF-1α in hypoxia was significantly increased after 1 h incubation with menadione (Figure 22), and this effect was similar to that observed at 21% O_2 after $CoCl_2$ treatment (Figure 22).

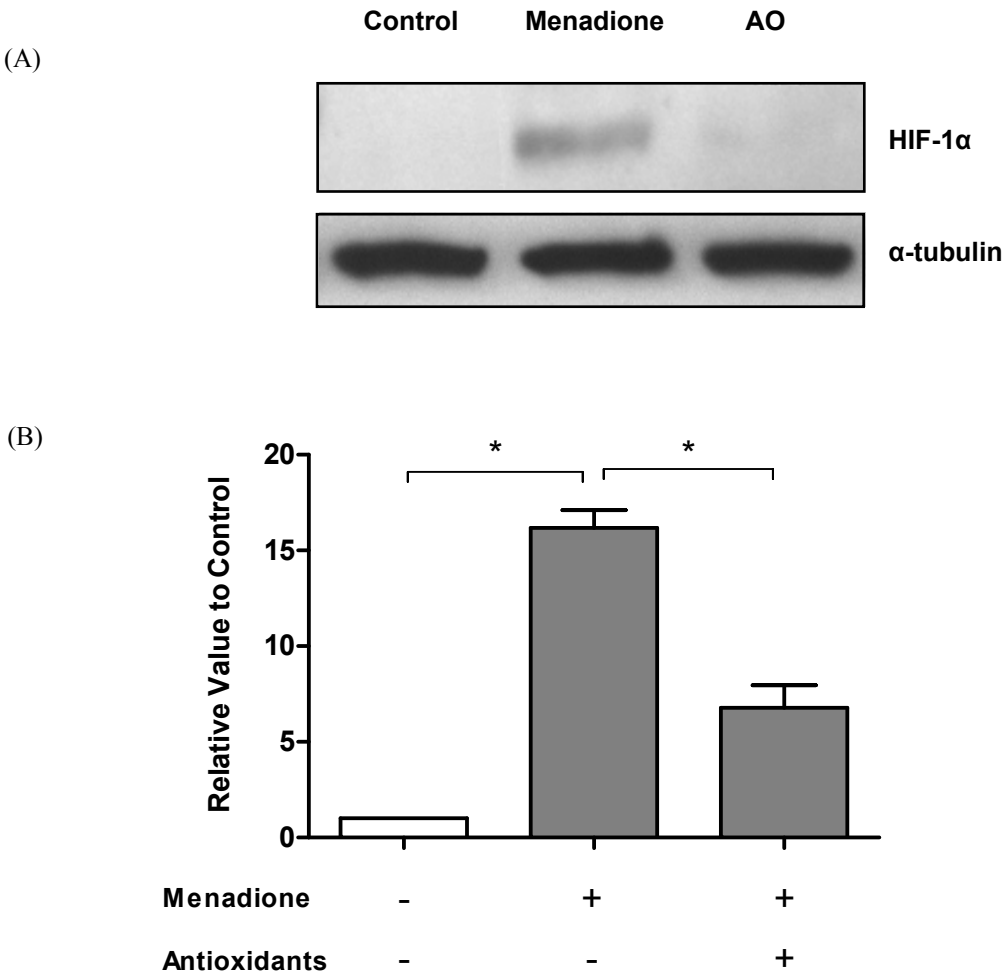

Figure 21 – Effect of antioxidants on menadione-induced HIF-1α stabilisation

Cells were incubated at 21% oxygen for 1 h with 160 μM menadione in the presence or absence of antioxidants (AO; NAC 2.5 mM plus ascorbic acid 1 mM). Protein expression was analysed by Western blot (A) and quantified by densitometry (B). The corresponding densitometry values were normalised with α-tubulin and are shown relative to control. The values represent ± SEM from 3 independent experiments; * $p < 0.05$ versus menadione alone treated cells. One representative blot is shown.

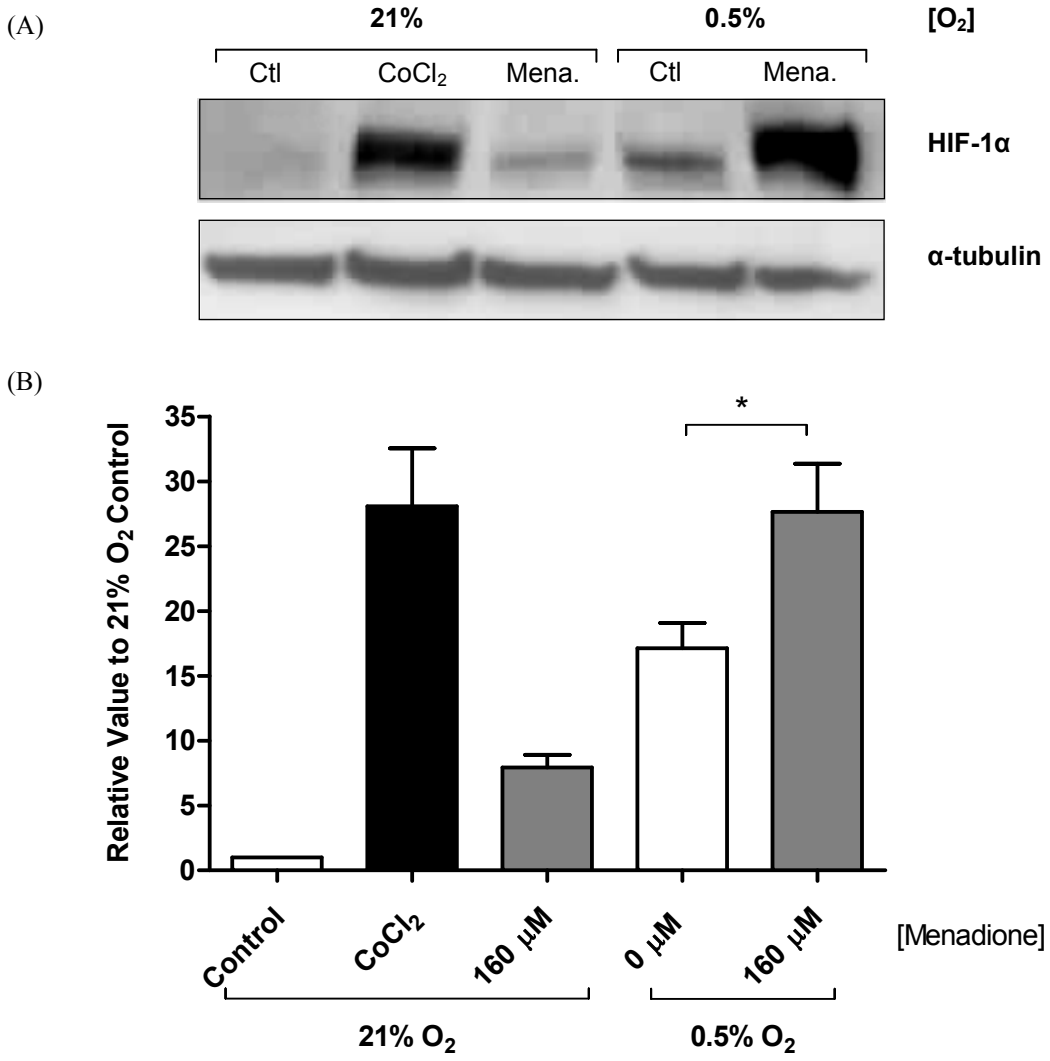

Figure 22 – Effect of menadione on HIF-1α stabilisation in hypoxia

Cells were incubated at 21% and 0.5% oxygen for 2 h in the presence or absence of 160 μM menadione (Mena) for 1 h. Cobalt chloride ($CoCl_2$, 160 μM) served as a positive control. Protein expression was analysed by Western blot (A) and quantified by densitometry (B). The corresponding densitometry values were normalised with α-tubulin and are shown relative to control. The values represent ± SEM from 3 independent experiments; * $p < 0.05$ versus control. One representative blot is shown.

3.3.5 Effect of antioxidants on HIF-1α stabilisation following treatment with cobalt chloride

Since treatment with $CoCl_2$ induces ROS (Chandel *et al.*, 1998) and our own data has shown $CoCl_2$-induced HIF-1α stabilisation, (Figure 15) experiments were conducted using antioxidants to investigate the possible role of reactive oxygen species. Cells were treated with 160 μM $CoCl_2$ for 4 h in the presence or absence of an AO mix. Figure 23 shows that $CoCl_2$-induced HIF-1α stabilisation was reversed by treatment with antioxidants.

3.3.6 Synergism between $CoCl_2$ and hypoxia on HIF-1α stabilisation

Treatment with $CoCl_2$ (160 μM, 4 h) demonstrated an increase in HIF-1α stabilisation at ambient [O_2], the effect of $CoCl_2$ in hypoxia (0.5% oxygen) was assessed, to further investigate the potential role for ROS-mediated HIF-1α stabilisation in hypoxia, as done in section 3.3.4. $CoCl_2$ increased HIF-1α stabilisation in a dose-dependent manner (Figure 24).

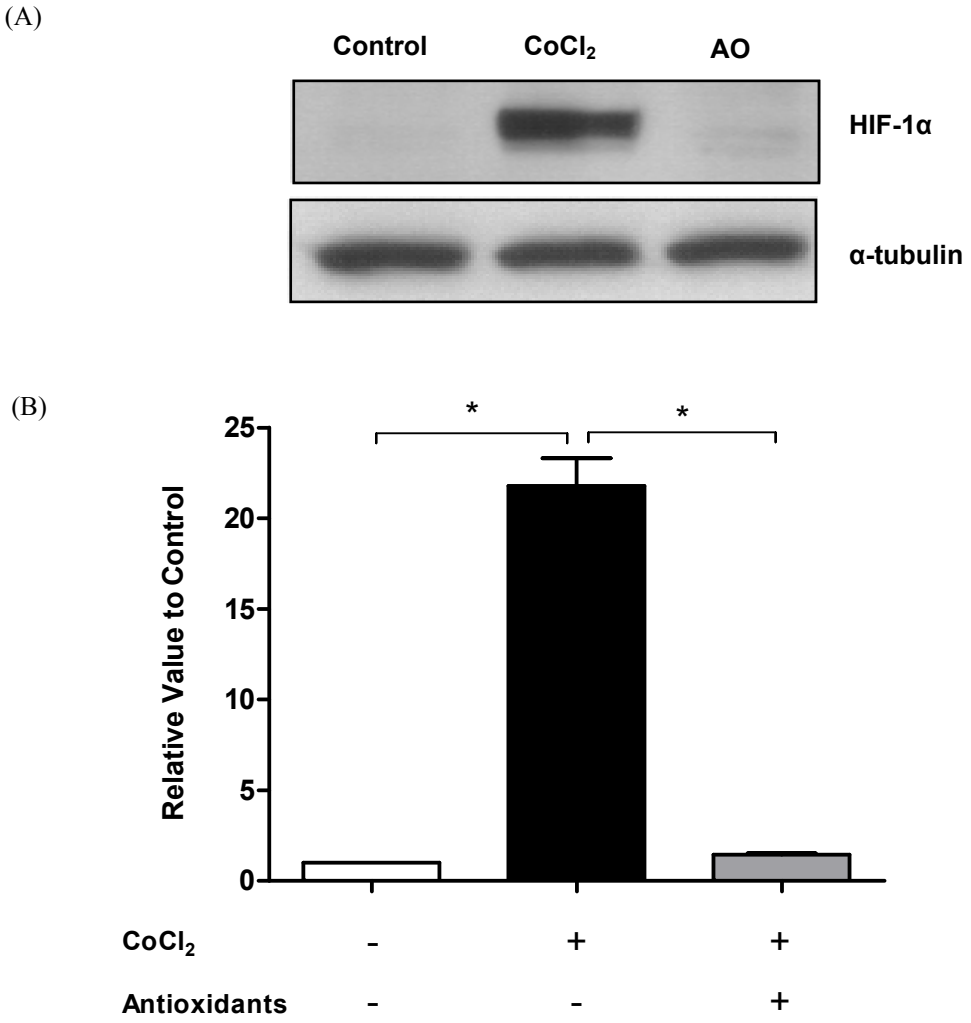

Figure 23 – Effect of antioxidants on $CoCl_2$-induced HIF-1α stabilisation

Cells were incubated at 21% oxygen for 4 h with cobalt chloride ($CoCl_2$, 160 µM) in the presence or absence of antioxidants (AO; NAC 2.5 mM plus ascorbic acid 1 mM). Protein expression was analysed by Western blot (A) and quantified by densitometry (B). The corresponding densitometry values were normalised with α-tubulin and are shown relative to control. The values represent the mean $\pm$ SEM from 3 independent experiments; * $p < 0.05$ versus $CoCl_2$ treatment. One representative blot is shown.

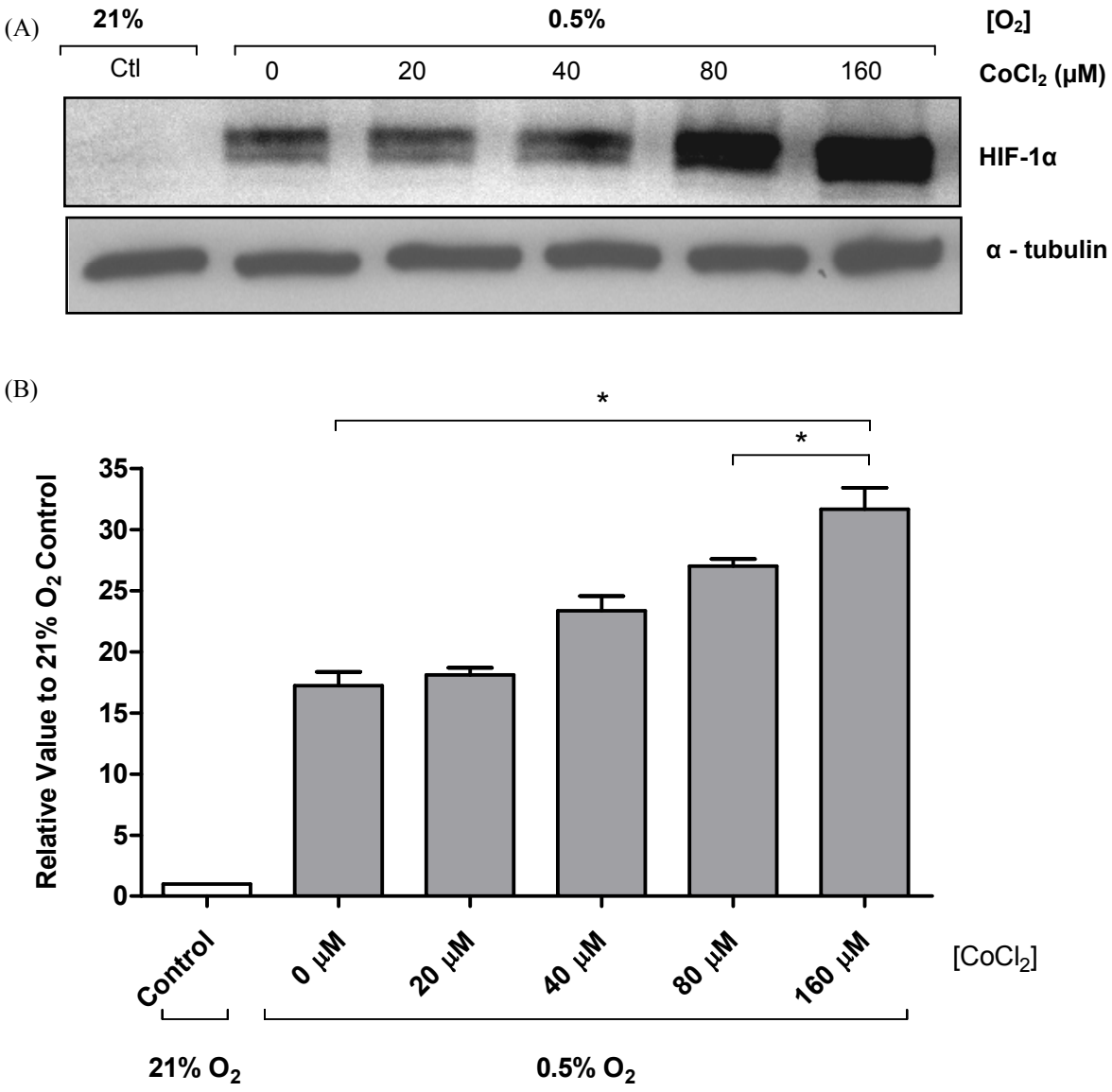

Figure 24 – Effect of $CoCl_2$ on HIF-1α stabilisation in hypoxia

Cells were incubated at 21% and 0.5% oxygen for 4 h. Cells at 0.5% oxygen were incubated with different concentrations of cobalt chloride ($CoCl_2$, 0-160 μM). Protein expression was analysed by Western blot (A) and quantified by densitometry (B). The corresponding densitometry values were normalised with α-tubulin and are shown relative to control. The values represent the mean ± SEM from 3 independent experiments; * $p < 0.05$. One representative blot is shown.

3.4 Antioxidants destabilise HIF-1α at 3% oxygen

3.4.1 Modulation of HIF-1α by antioxidants in HEK 293T cells

To investigate whether ROS are involved in the stabilisation of HIF-1α at low [O_2] we incubated cells at 3% and 0.5% oxygen for 24 h and 2 h respectively. This was done in the presence or absence of antioxidants (AO, NAC plus ascorbic acid) for 4 h and samples prepared. Figure 25 shows that HIF-1α stabilisation was reversed by antioxidant treatment at 3% O_2, with no effect at 0.5% O_2.

3.4.2 Effect of S-methylglutathione on HIF-1α stabilisation

Next we examined the effect of methylglutathione (a glutathione donor) on HIF-1α stabilisation at 3% oxygen only. As previous data (Figure 25) demonstrated that at this oxygen concentration, HIF-1α stabilisation could be prevented using antioxidants. A methylated form of glutathione was used as an alternative to NAC plus ascorbic acid as it enhances cell permeability. Cells were incubated at 3% oxygen for 24, treated with methylglutathione (0-100 μM) for the final 4 h and HIF-1α protein stabilisation was determined. Methylglutathione produced a dose-dependent decrease in HIF-1α stabilisation with the maximal effect observed at 50 μM (Figure 26).

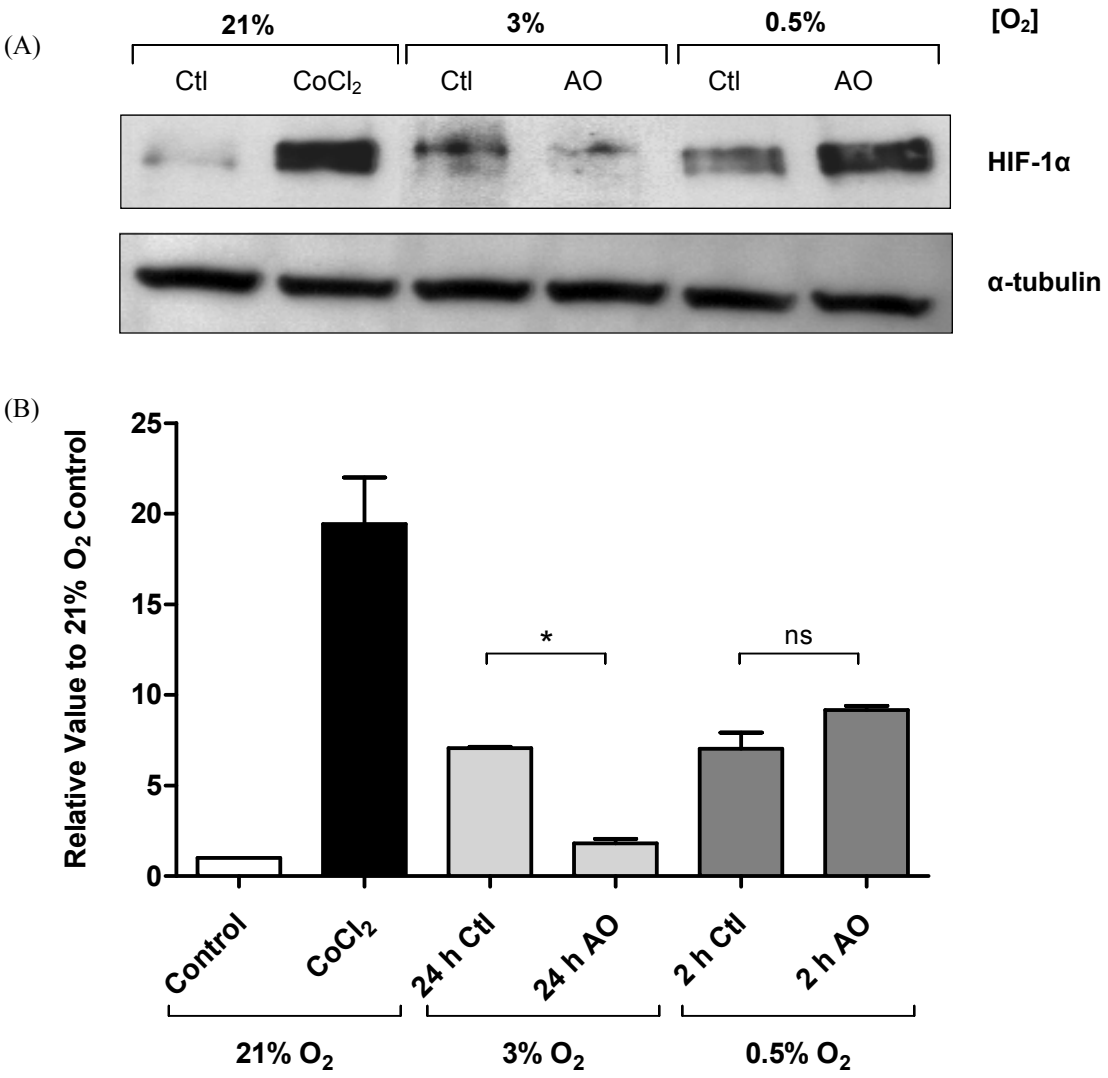

Figure 25 – Effect of antioxidants on HIF-1α stabilisation

Cells were incubated at 3% and 0.5% oxygen for 24 h or 2 h respectively, with or without antioxidants (AO; 2.5 mM NAC plus 1 mM ascorbic acid). Cobalt chloride ($CoCl_2$, 160 μM) severed as a positive control. Protein expression was analysed by Western blot (A) and quantified by densitometry (B). The corresponding densitometry values were normalised with α-tubulin and are shown relative to control. The values represent $\pm$ SEM from 3 independent experiments; * $p < 0.05$ versus 3% control. (ns, not significant). One representative blot is shown.

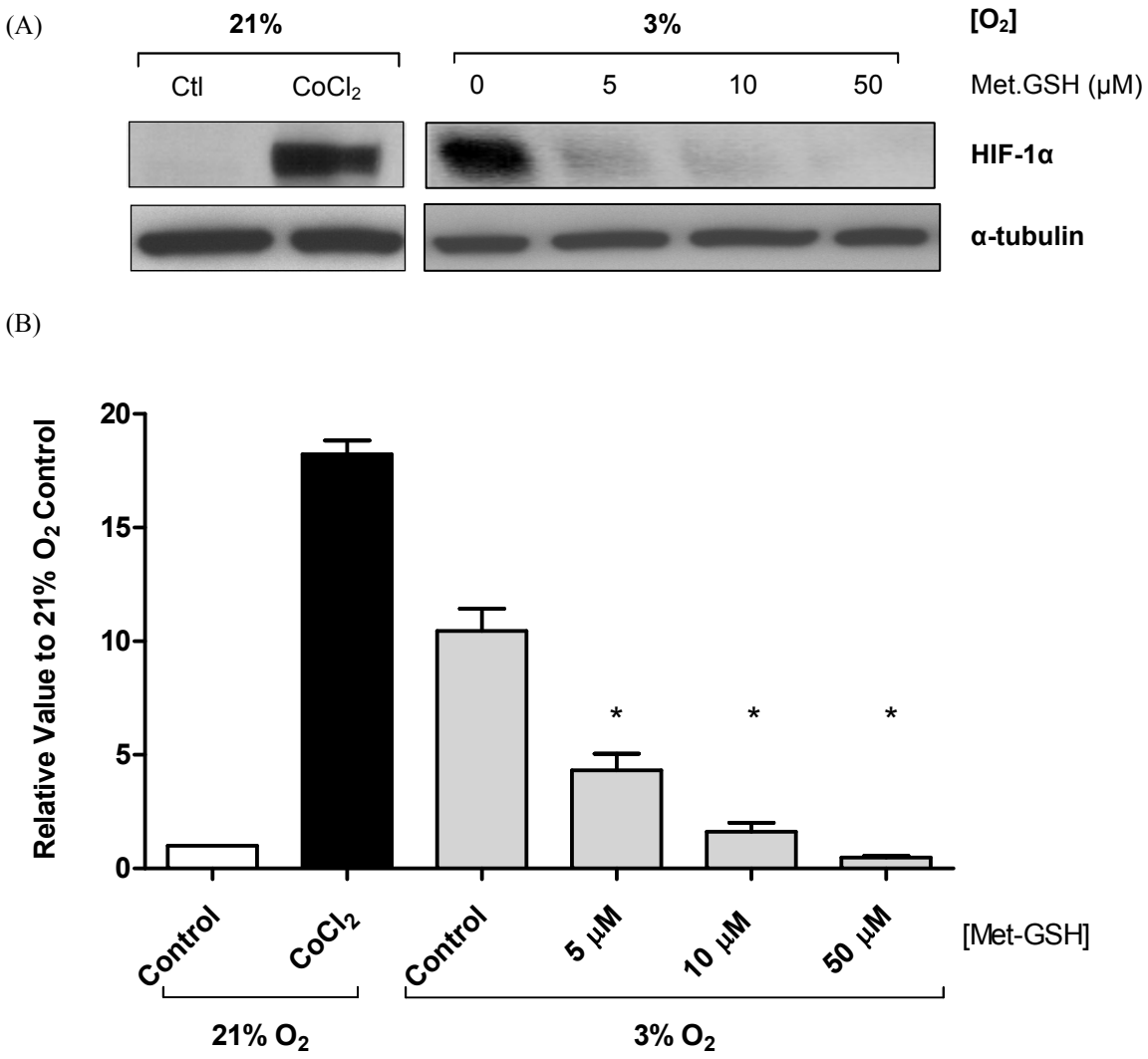

Figure 26 – Effect of S-methylgluathione on HIF-1α stabilisation

Cells were incubated at 21% and 3% oxygen for 4 h with or without methylgluathione (Met.GSH, -100 μM). Cobalt chloride ($CoCl_2$, 160 μM) served as a positive control. Protein expression was analysed by Western blot (A) and quantified by densitometry (B). The corresponding densitometry values were normalised with α-tubulin and are shown relative to control. The values represent $\pm$ SEM from 3 independent experiments; * $p < 0.05$ versus 3% control. One representative blot is shown.

3.5 Modulation of HIF-1α in human head and neck squamous carcinoma cells

HIF-1α activates the transcription of genes that are involved in crucial aspects of cancer biology including angiogenesis, cell survival, glucose metabolism and invasion (Semenza, 2003). The stabilisation of HIF-1α in cancer has a number of origins that allows it to engage in transcriptional activity at normoxic [O_2], including hypoxia (Wang and Semenza, 1993), genetic mutations (Maxwell *et al.*, 1999) and an increase in TCA cycle intermediates succinate and fumarate (Koivunen *et al.*, 2007). More recently it has also been suggested that the accumulation of ROS leads to the impairment of HIF-1α degradation (Gerald *et al.*, 2004). Experiments from our own group have previously demonstrated that NO was involved in the stabilisation of HIF-1α in head and neck squamous carcinoma (H157) cells and this was attributed to the high expression of NOS in these cells (Quintero *et al.*, 2006a).

3.5.1 NOS-dependent stabilisation of HIF-1α in cancer cells at 3% oxygen

In order to confirm this data, cells were incubated at 3% and 0.5% oxygen and treated with either L-NMMA (a non-specific nitric oxide synthase (NOS) inhibitor) or antioxidants. Cell lysates were prepared using the protocol described in 3.2 and samples prepared in the same way. Figure 27 shows that at 3% oxygen both L-NNMA and antioxidants significantly inhibit HIF-1α stabilisation. Stabilisation of HIF-1α at 0.5% oxygen is not affected by treatment with L-NNMA or antioxidants.

3.5.2 Effect of antioxidants on HIF-1α stabilisation in cancer cells at 21% oxygen

In non-cancerous cells, HIF-1α stabilisation is prevented in normoxic conditions by proteasomal degradation. However, H157 cancerous cells stabilise HIF-1α in normoxia (Quintero *et al.*, 2006a). Therefore, experiments using H157 carcinoma cells at 21% oxygen, treated with either L-NMMA or antioxidants were performed to decrease levels of ROS or NO and to investigate the effect on HIF-1α stabilisation. Figure 28 shows that whereas treatment with antioxidants significantly inhibited HIF-1α stabilisation, L-NMMA had no effect on HIF-1α stabilisation at 21% oxygen.

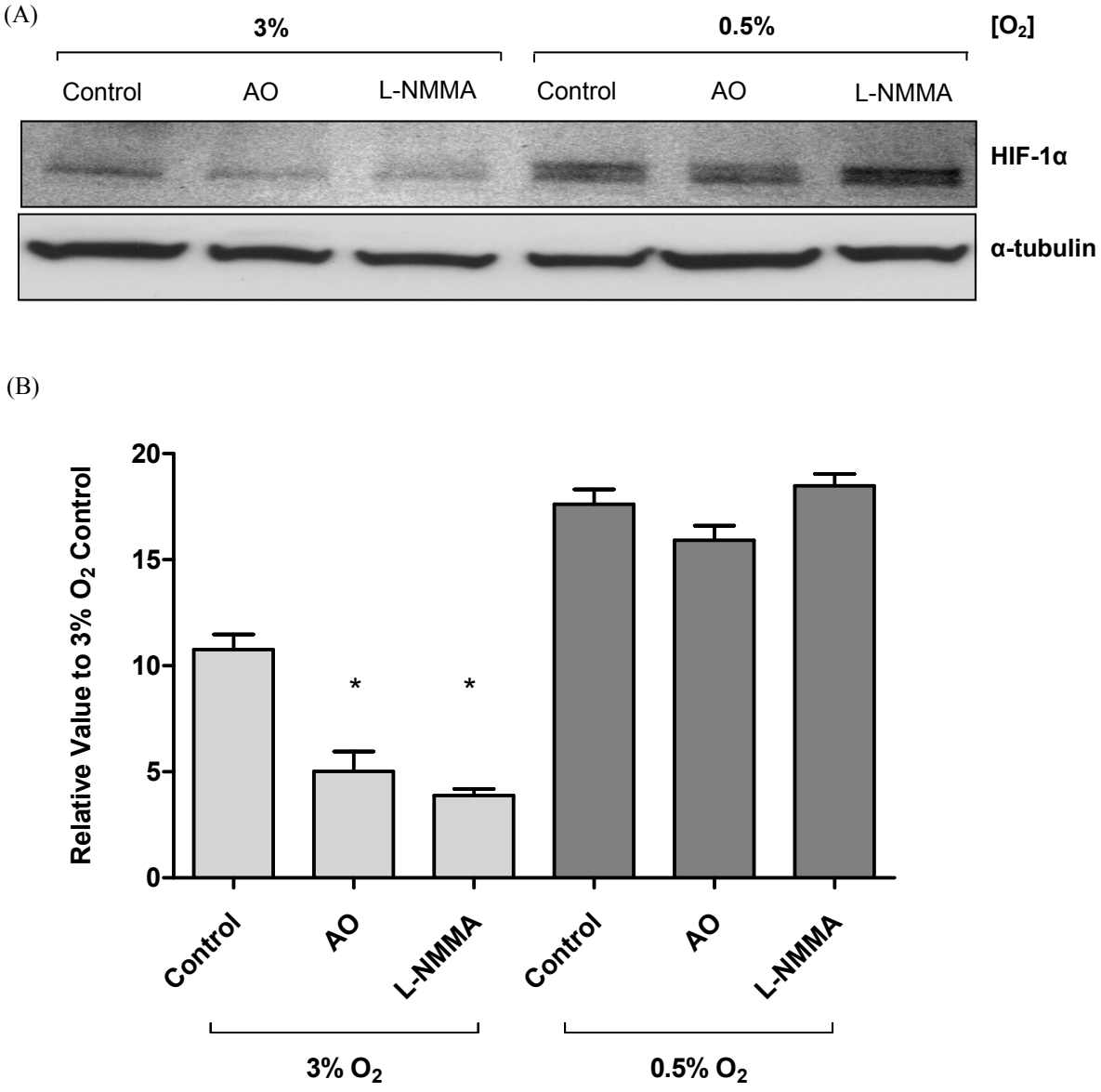

Figure 27 – Modulation of HIF-1α stabilisation in H157 cells at 3% oxygen

H157 carcinoma cells were incubated at 3% and 0.5% oxygen for 4 h with or without antioxidants (AO; 2.5 mM NAC plus 1 mM ascorbic acid) or 1 mM L-NMMA (non-specific NOS inhibitor). Protein expression was analysed by Western blot (A) and quantified by densitometry (B). The corresponding densitometry values were normalised with α-tubulin and are shown relative to 3% oxygen control. The values represent $\pm$ SEM from 3 independent experiments; * $p < 0.05$ versus 3% control. One representative blot is shown.

(A)

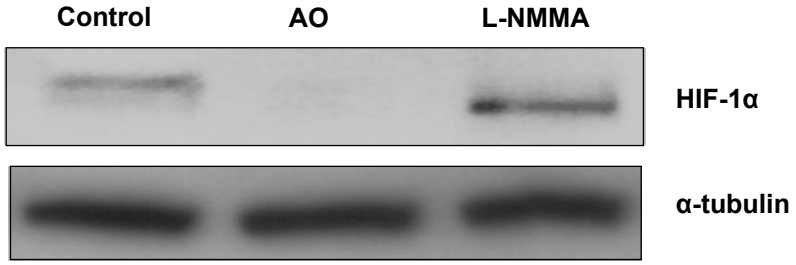

(B)

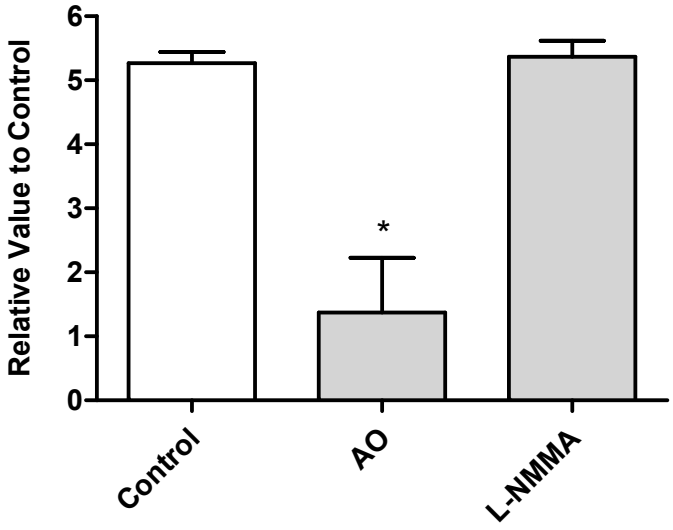

Figure 28 – Modulation of HIF-1α stabilisation in H157 cells at 21% oxygen

H157 carcinoma cells were incubated at 21% oxygen with or without antioxidants (AO; 2.5 mM NAC plus 1 mM ascorbic acid) or 1 mM L-NMMA (a non-specific NOS inhibitor). Protein expression was analysed by Western blot (A) and quantified by densitometry (B). The corresponding densitometry values were normalised with α-tubulin and are shown relative to control. The values represent $\pm$ SEM from 3 independent experiments; * $p < 0.05$ versus control. One representative blot is shown.

3.6 Stabilisation of HIF-1α in activated murine macrophages

Peyssonnaux *et al*, 2005 reported that bacterial infection and inflammation led to the stabilisation of HIF-1α in macrophages (MΦ) in a hypoxia-independent mechanism. As it is known that MΦ produce high concentrations of NO upon activation (Stuehr and Nathan, 1989;Garedew and Moncada, 2008) experiments were designed to study the effect of NO on HIF-1α stabilisation in normoxia.

3.6.1 NO-dependent stabilisation of HIF-1α in J774.A1 MΦ

J774.A1 macrophages (MΦ) were seeded on tissue culture plastic for 24 h prior to activation with interferon (IFN)γ (10 U/ml) and lipopolysaccharide (LPS, 10 ng/ml). One set of cells was co-treated with the NOS inhibitor S-ethyl isothiourea (SEITU, 500 μM). Non-activated cells were used as controls. At different time points (0, 1.5, 3, 6 and 12 h) cell lysates for activated and non-activated J774.A1 MΦ were prepared and HIF-1α protein expression was determined by Western blot. In parallel, lactate and nitrite accumulation were also determined, as markers for glycolytic and iNOS activity respectively.

Lactate accumulation increased in a time-dependent manner in both groups following activation (Figure 29, (A)). Figure 29 (B) shows there was a significant increase in nitrite accumulation 6 h after activation compared to control, with SEITU treated cells showing no increase in nitrite accumulation over the whole time course. Figure 30 shows that HIF-1α protein transiently stabilises within 1.5 h following activation. By 3 h, HIF-1α protein reverts back to the concentration of non-activated controls. However, after 6 h MΦ activation, HIF-1α protein concentrations increased, and continued to do so until the final 12 h time point (Figure 30) Co-treatment with SEITU had no effect on the early transient stabilisation of HIF-1α but prevented its accumulation at the latter time points (Figure 30).

(A)

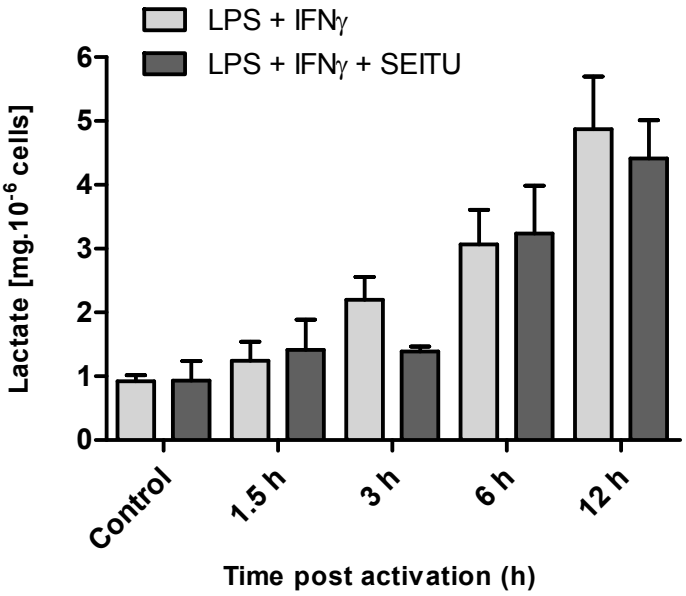

(B)

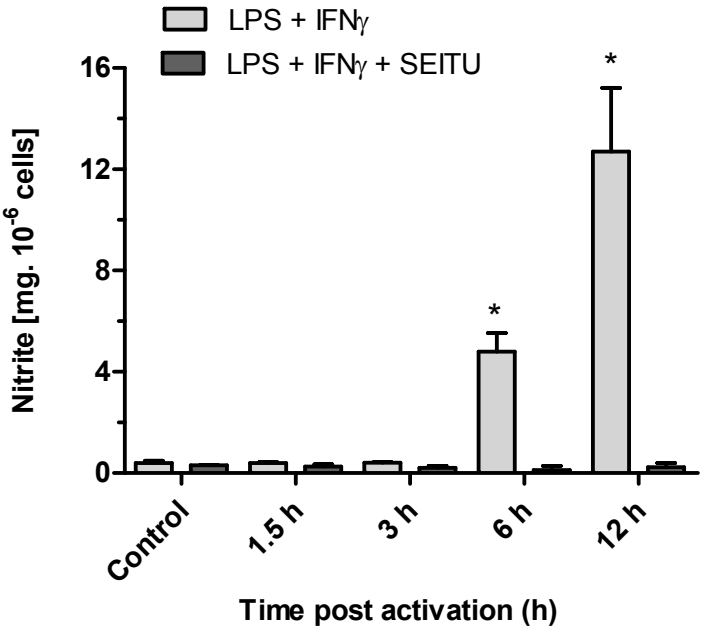

Figure 29 – Time course of lactate and nitrite accumulation in activated MΦ

MΦ were activated with LPS (10 ng/ml) and IFNγ (10 U/ml). A subset of cells was also co-treated with SEITU (500 μM). Lactate (A) and nitrite (B) accumulation in the cell culture medium was determined by chemiluminescence. The values represent ± SEM from 3 independent experiments, * $p < 0.05$ versus control.

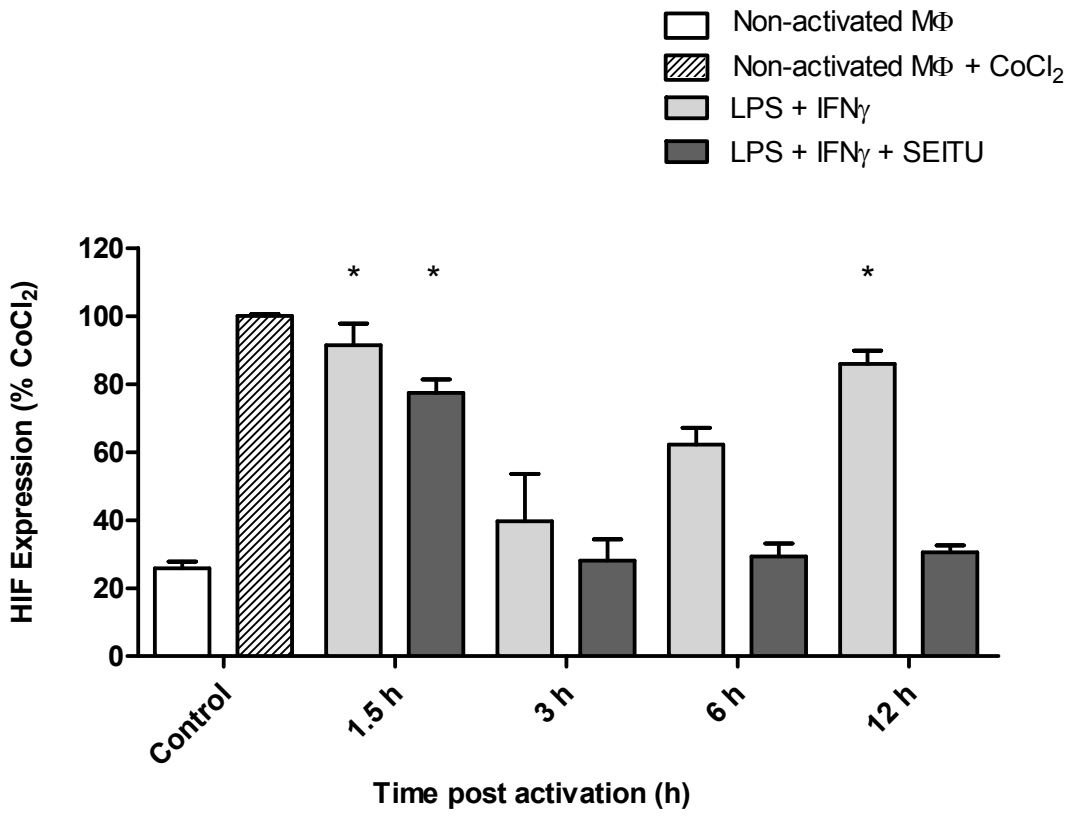

Figure 30 – Effect of MΦ activation on the stabilisation of HIF-1α

MΦ were plated and non-activated (control), activated with a positive control cobalt chloride ($CoCl_2$, 160 μM), or activated with LPS (10 ng/ml) and IFNγ (10 U/ml). A subset of the latter cells was also co-treated with SEITU (500 μM). Cells were incubated for 12 h at 21% oxygen, lysed and subject to SDS-PAGE. Protein expression was analysed by Western blot and quantified by densitometry. The corresponding densitometry values were normalised with α-tubulin and are shown relative to $CoCl_2$ treated non-activated MΦ control cells. The values represent $\pm$ SEM from 3 independent experiments, * $p < 0.05$ versus non-activated control MΦ cells.

3.6.2 The effect of antioxidants on HIF-1α stabilisation in J774.A1 MΦ

To investigate whether ROS were involved in the early (1.5 h) stabilisation of HIF1-α, MΦ were seeded and activated as described above, with a subset of cells treated with antioxidants. HIF-1α protein stabilisation, lactate and nitrate accumulation was determined.

Lactate accumulation increased in a time-dependent manner in both groups following activation (Figure 31, (A)). Figure 31 (B) shows there was an increase in nitrite accumulation 6 h after activation compared to control, with antioxidant treated cells showing a similar increase in nitrite accumulation over the whole time course. Figure 32 shows HIF-1α stabilisation was significantly inhibited by antioxidants at 1.5 h post-activation but there was no effect in the latter time points.

(A)

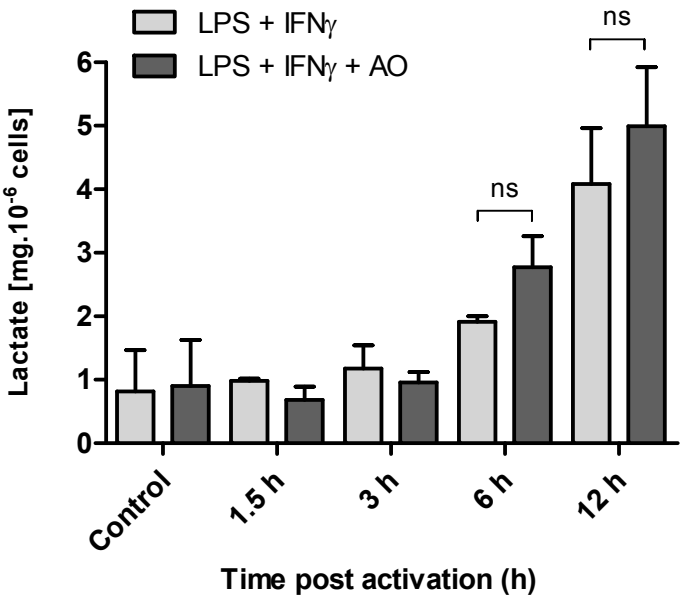

(B)

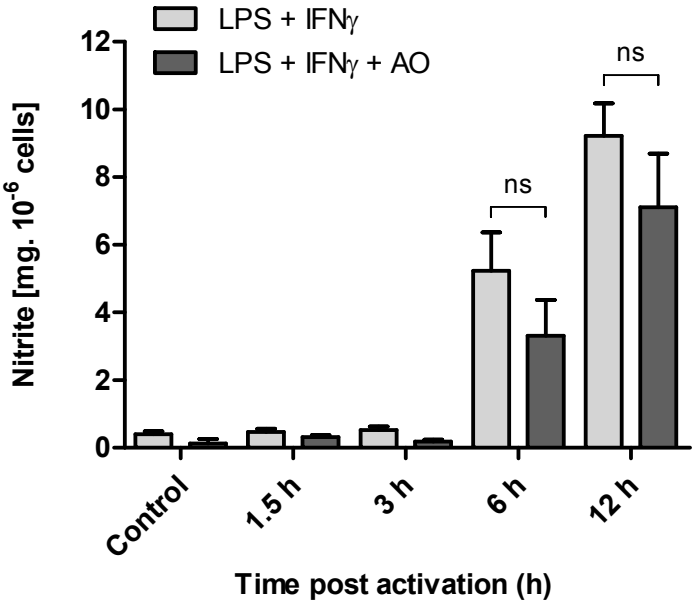

Figure 31 – Time course of lactate and nitrite accumulation in activated MΦ

MΦ were activated with LPS (10 ng/ml) and IFNγ (10 U/ml). A subset of cells was also co-treated with antioxidants (AO; 2.5 mM NAC plus 1 mM ascorbic acid). Lactate (A) and nitrite (B) accumulation in the cell culture medium was determined by chemiluminescence. The values represent ± SEM from 3 independent experiments, ns, not significant.

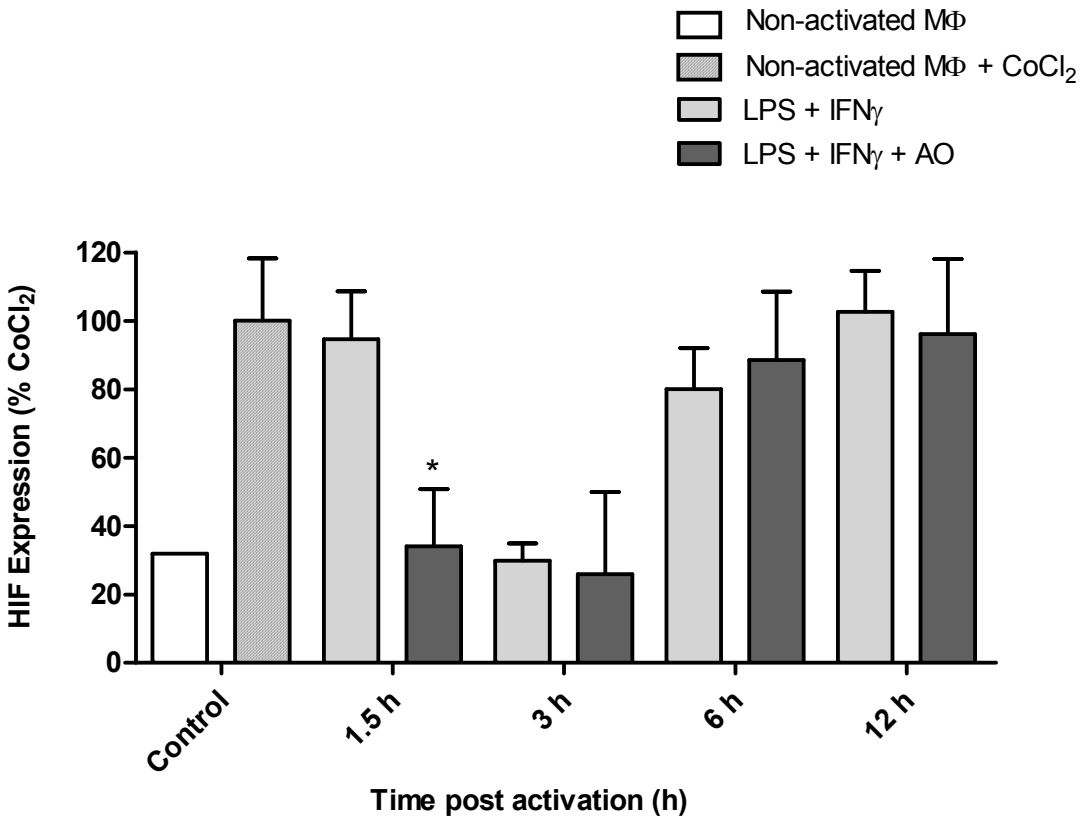

Figure 32 – Effect of antioxidants on HIF-1α stabilisation in activated MΦ

MΦ were plated and non-activated (control), activated with a positive control cobalt chloride ($CoCl_2$, 160 μM), or activated with LPS (10 ng/ml) and IFNγ (10 U/ml). A subset of cells were also co-treated with antioxidants (AO; 2.5 mM NAC plus 1 mM ascorbic acid). Cells were incubated for 12 h at 21% oxygen, lysed and subject to SDS-PAGE. Protein expression was analysed by Western blot and quantified by densitometry. The corresponding densitometry values were normalised with α-tubulin and are shown relative to $CoCl_2$ treated non-activated MΦ control cells. The values represent $\pm$ SEM from 3 independent experiments, * $p < 0.05$ versus activated MΦ at 1.5 h.

3.7 Summary of key results

Decreasing [O_2] causes HIF-1α stabilisation in HEK 293T cells. In these cells we also observed menadione- and $CoCl_2$-induced HIF-1α stabilisation at ambient [O_2] in a concentration-dependent manner. Accordingly, antioxidants and L-NMMA prevented HIF-1α stabilisation at 3% oxygen both in HEK 293T cells and head and neck carcinoma cells. Activation of MΦ led to HIF-1α stabilisation in a biphasic manner, with early stabilisation attributed to ROS and late stabilisation to NO.

Chapter four:
ROS-dependent HIF-1α stabilisation in normoxia

Chapter four: ROS-dependent HIF-1α stabilisation in normoxia

4.1 Introduction

Findings in chapter three indicate that HIF-1α stabilisation can be mediated by reactive oxygen species (ROS). We therefore set out to investigate the effect of endogenous ROS on HIF-1α stabilisation. Studies described in this chapter explore the hypothesis that endogenous ROS stabilise HIF-α at ambient oxygen concentrations (21%). Diaz-Hernandez *et al*., 2007 demonstrate that impairment in glutathione (GSH) biosynthesis induces free radical production in primary cortical neurons. γGlutamyl cysteine synthetase (γGCS) is the rate limiting enzyme of glutathione (GSH) biosynthesis and is therefore a crucial antioxidant. Silencing γGCS using small interfering RNA (siRNA) promoted hydroethidine (HE) fluorescence (a marker for ROS) which was prevented by tempol (100μM) and enhanced by H_2O_2 (500μM) (Diaz-Hernandez *et al.*, 2007). We therefore implemented the same strategy to further investigate the effect of endogenous ROS production on HIF-1α stabilisation in HEK 293T cells.

4.2 Expression vector pFIV and cloning of γGCS constructs

Short double-stranded RNAs can be used to silence genes in mammalian cells (Fire *et al.*, 1998). Template siRNAs can be cloned into a siRNA expression vector (such as pFIV), transfected and subsequently expressed in cells. This method of gene silencing by endogenous expression of siRNA effectors aims to provide long term silencing of the target gene, with a stable knockdown phenotype for functional evaluation studies. The expression vector pFIV (Figure 33) was obtained from System Biosciences, USA with the intention to silence γGCS in HEK 293T cells.

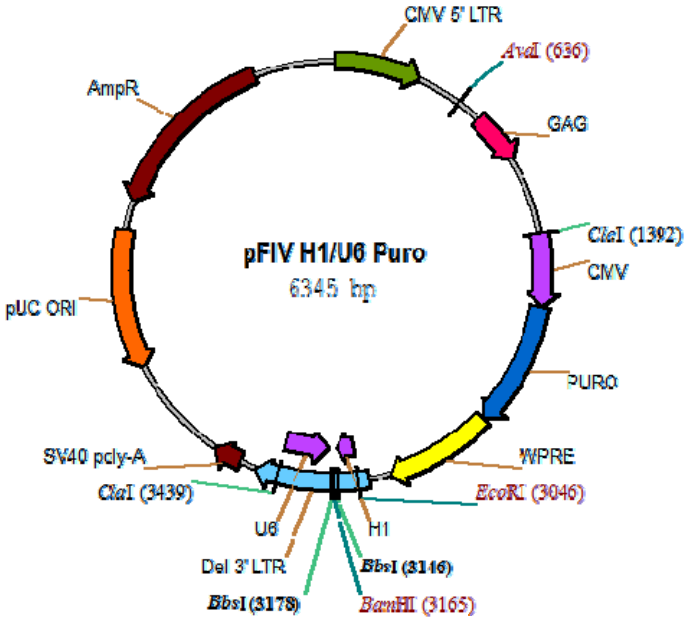

Figure 33 – Plasmid map of pFIV cloning and expression vector

Sequence features of pFIV: CMV-5' LTR 1-415, CMV promoter 1394-1745, puromycin-resistant marker 1753-2352, H1 RNA promoter 3051-3141, U6 RNA promotor 3194-3436, ampicillin resistant gene 5103-5963 (System Biosciences, USA).

Five different human γGCS sequences were selected using Sigma Aldrich predictor software (Figure 34). Confirmation of the cloning was done by sequencing (Figure 36) in house by Scientific Support Services, Wolfson Institute for Biomedical Research, UCL.

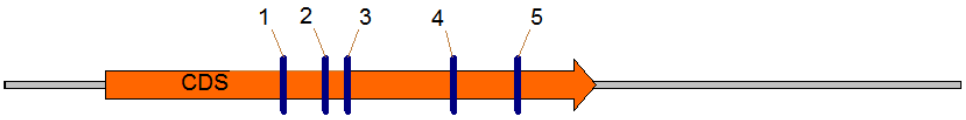

	Selected γGCS Sequences
1	5' ATCCATGTAAATATGATCCGG 3'
2	5' TAGTTATTGTTCTTCAATGGC 3'
3	5' AAATCCAATTTGTAGGAAAGG 3'
4	5' AAGGTAAGAGTTCAGAATTGG 3'
5	5' AATGTCTGACACATAGCCTCG 3'

Figure 34 – Diagram of CDS sequence of γGCS and table of individual sequences

CDS sequence of human γGCS (3717 bp) showing the sites of each sequence used to generate siRNA against human γGCS. Each of the five different sequences is shown in the table.

The plasmid was then transformed into bacterial cells and the ampicillin resistant colonies selected for screening by PCR. PCR, with primers flanking the plasmid location sites was used to confirm cloned fragment sizes. The result yielded from the screening of the γGCS products was successful, as it showed the expected fragment sizes (190 bp) (Figure 35). With the results obtained from the screening and sequencing, attempts were made to achieve a successful knock-down/silencing of γGCS in HEK 293T cells.

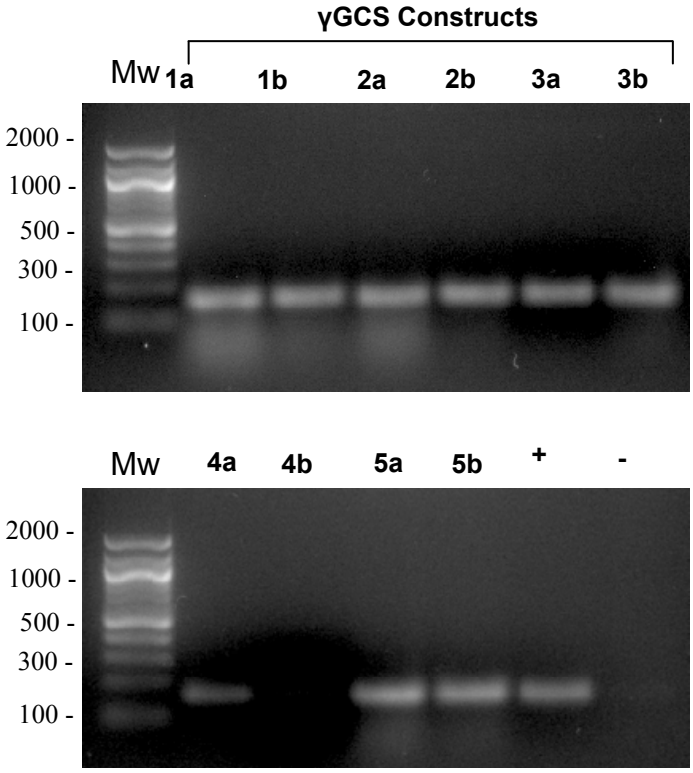

Figure 35 – Screening of γGCS cloning products

Expression of five γGCS constructs in duplicate (a and b). Products of expected size were obtained for all γGCS constructs (except 4b) of approximately 190 base pairs. Human cDNA was used for a positive control (lane +). Template DNA was omitted for negative control (lane -). PCR products were subjected to electrophoresis on a 1% agarose gel.

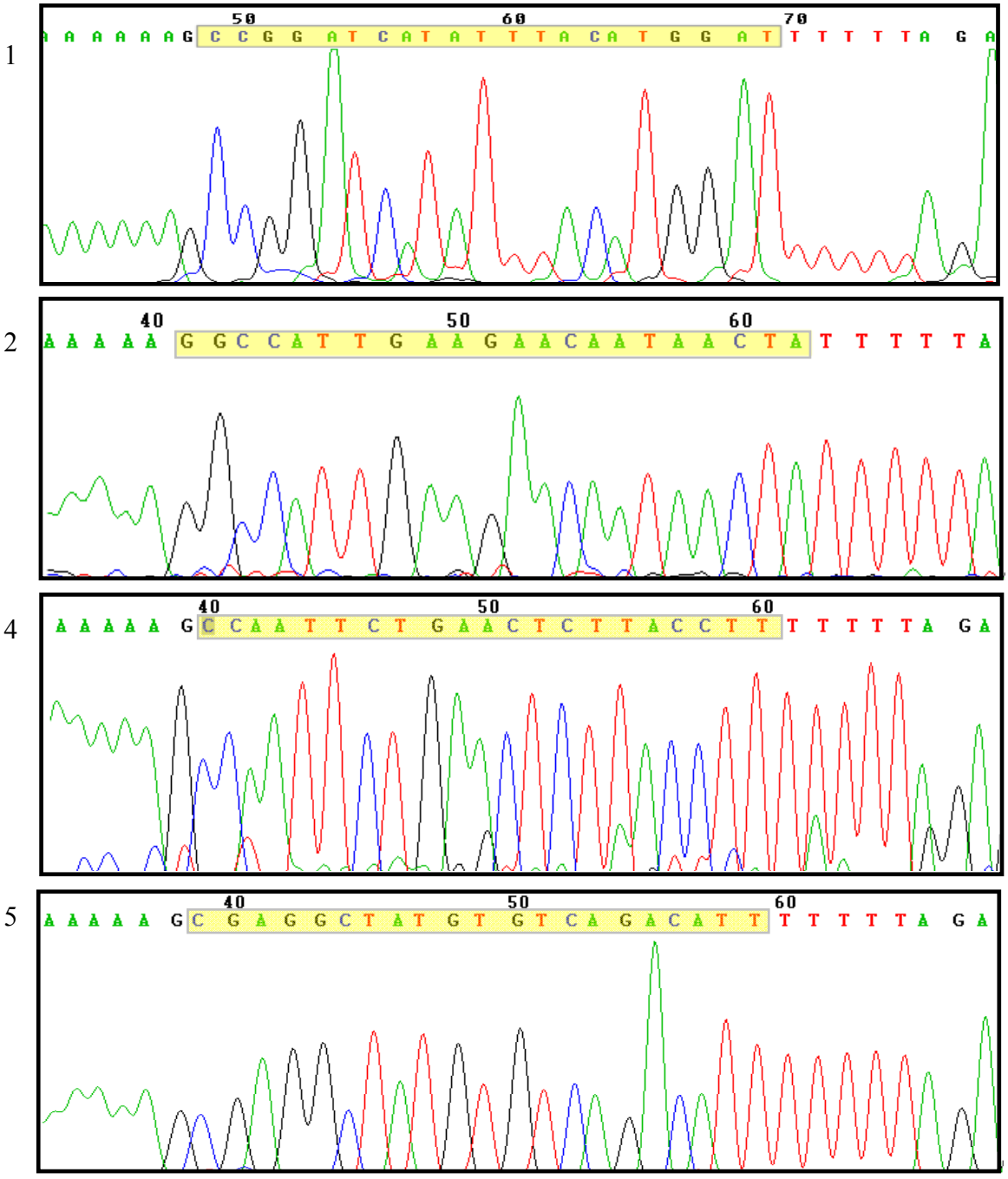

Figure 36 – Sequencing data for plasmid DNA containing γGCS cloning products

Sequence data generated with ABI3730XL sequencer. 100 ng/µl of each γGCS pFIV plasmid (1-5) was used per sequencing reaction. Samples were cycle-sequenced using BigDye® 3.1 Chemistry, and standard thermal cycling conditions. Chromas Lite Version 2.01 sequence scanner software was used to analyse and display each DNA sequence.

4.3 Silencing of γGCS in HEK 293T cells

To test the functionality of the γGCS siRNA, HEK 293T cells were transfected with the plasmid and efficiency of the knock-down was assessed by measuring protein levels as well as cellular GSH content.

4.3.1 Inhibition of γGCS protein in HEK 293T cells

Cells were transformed using Lipofectamine transfection reagent as described in experimental procedures section 2.9.1. A sub-set of cells was also co-transfected with a construct expressing the green fluorescent protein (GFP) marker, to ascertain a positive visual transfection in these cells (Figure 37).

Following transfection, cells were grown until confluence was reached. Since the pFIV plasmid carried a puromycin-resistant maker, transfected cells could be selected using media containing the appropriate antibiotic. Therefore to determine the optimal antibiotic concentration in which to maintain transfected cells, cells were grown in selection media containing 0-4 μg/ml puromycin. Cell viability was quantified using trypan blue exclusion. Figure 38 shows puromycin concentrations of less than 0.2 μg/ml resulted in 90-100% viable cells. At 0.5 μg/ml puromycin 50% of cells were viable, and concentrations above 1 μg/ml killed all cells. All further transfected cells were maintained in selection media containing 0.5 μg/ml puromycin. Once the optimal selection media had been ascertained and resistant cells begun to grow, cells were used experimentally for up to 4 weeks.

γGCS protein expression was determined via Western blot on cell lysates. Figure 39 shows γGCS protein to be reduced by 80% with construct 1 and 4, 95% with construct 2 and 60% with construct 5 when compared to control cells. Construct number two consistently showed the greatest reduction and was therefore used for all future silencing experiments with γGCS pFIV siRNA. However, cells for which γGCS had been silenced were inherently unstable thus puromycin resistance was no longer a valid tool for selection.

(A) Phase contrast

(B) GFP positive staining

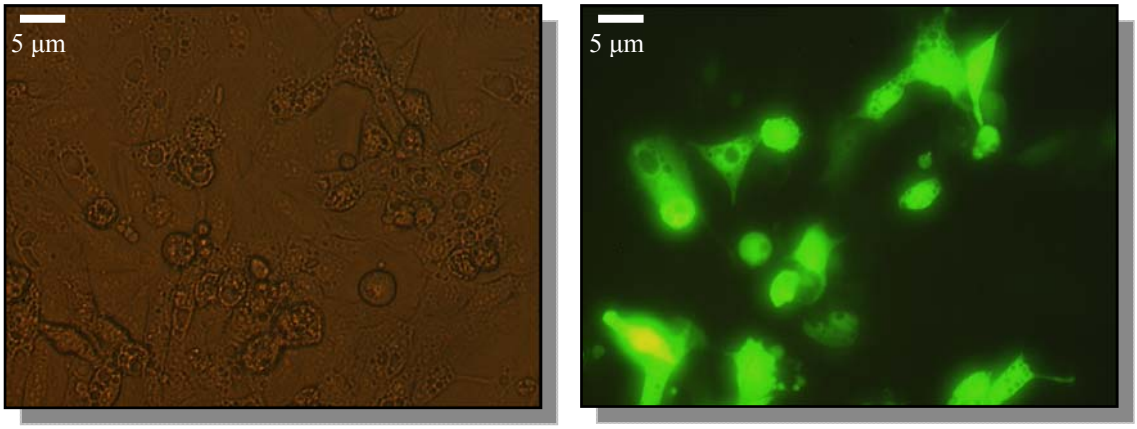

Figure 37 – Co-transfection of GFP with pFIV γGCS siRNA

Cells co-transfected with GFP and γGCS construct sequence #2 to obtain visual confirmation of positive cell transfection. Phase contrast image (A), cells transfected with GFP (B), as shown by visible green fluorescence.

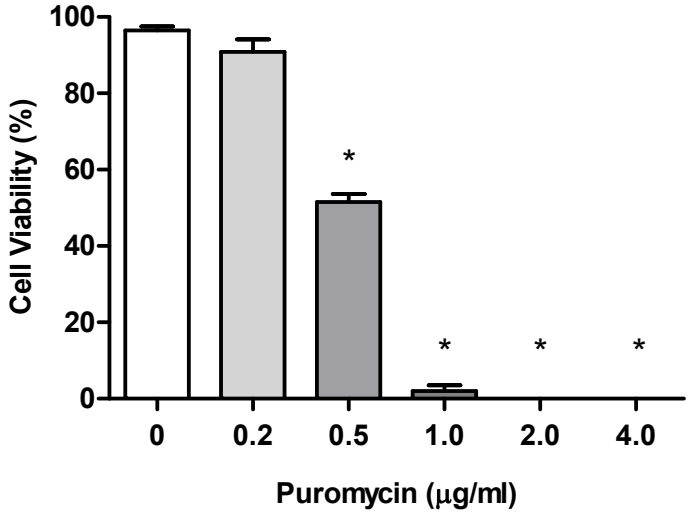

Figure 38 – Puromycin dose-response

Cells were grown in selection media containing 0-4 μg/ml puromycin. Cell viability was quantified using trypan blue exclusion. The values represent the mean ± SEM from 3 independent experiments; * represents a significant difference ($p < 0.05$) from control.

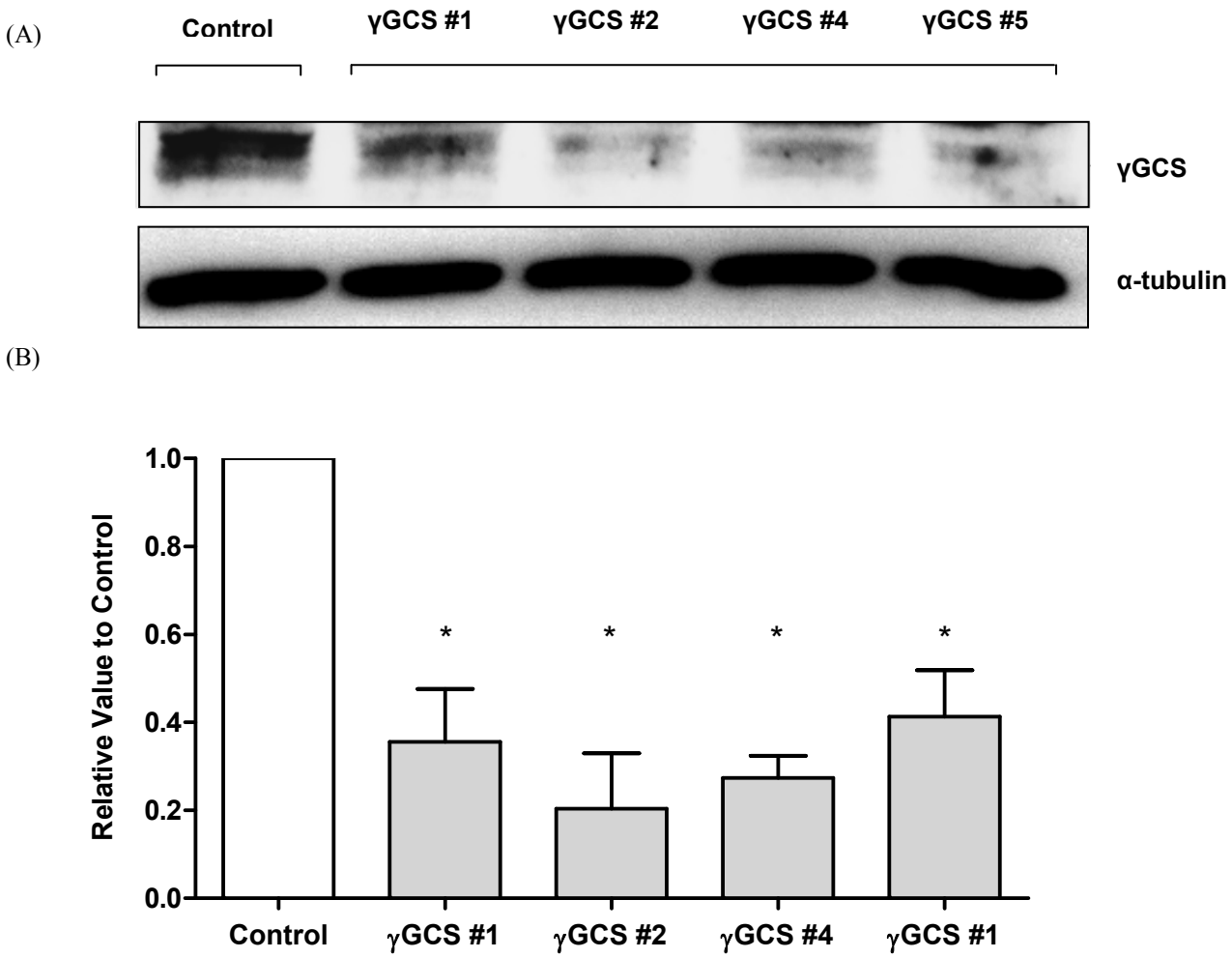

Figure 39 – Transfection with γGCS siRNA decreases γGCS protein levels

Cells were transfected with different γGCS siRNA constructs. Cell lysates were subject to SDS-PAGE and analysed by Western blot with an anti-γGCS antibody (A) and quantified by densitometry (B). The corresponding densitometry values were normalised with α-tubulin and results are shown relative to control. The values represent the mean $\pm$ SEM from 3 independent experiments; * represents a significant difference ($p < 0.05$) from control. One representative blot is shown.

4.3.2 Inhibiting γGCS protein expression decreases cellular glutathione

The next series of experiments were performed to investigate the functional consequence of γGCS protein knock-down. Firstly, measurements of GSH were made.

Cells were transfected using the protocol described in 4.3.1. Scrambled (non-specific) control plasmid was used as a control in all experiments. Total cellular GSH was measured using a colorimetric assay GSH-400 kit (Oxis Research, refer to experimental procedures, 2.11.4). Figure 40 shows approximately a 40% decrease of GSH in cells transfected with γGCS pFIV siRNA, compared to both control (untreated) and scrambled control cells.

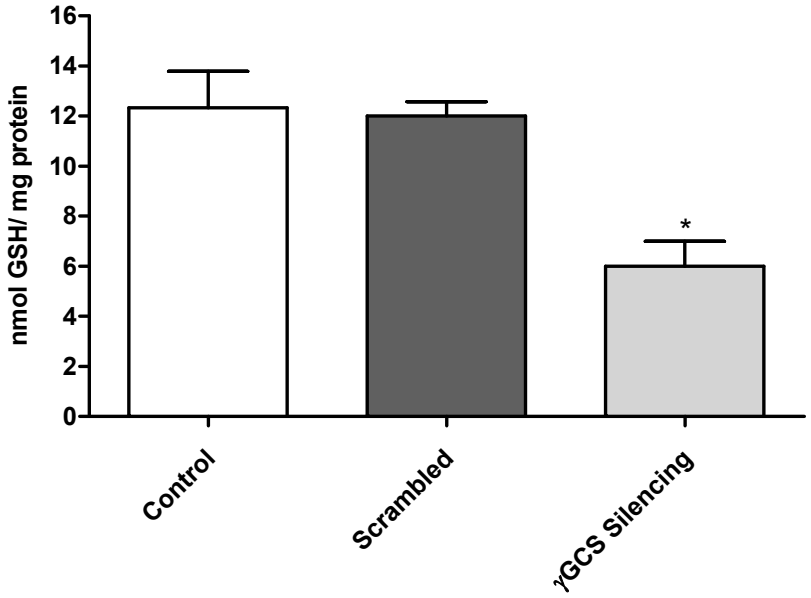

Figure 40 – Decreased glutathione in cells transfected with siRNA against γGCS

Cells were either transfected with siRNA against γGCS or treated with scrambled non-specific siRNA control sequence. Samples were analysed for GSH content using a GSH-400 kit (Oxis Research). Data was normalised to control. The values represent the mean $\pm$ SEM from 3 independent experiments; * represents a significant difference ($p < 0.05$) from control.

4.3.3 Silencing γGCS increases cellular reactive oxygen species generation

Experiments were then carried out to determine whether a decrease in GSH caused an effect on reactive oxygen species (ROS) generation in these cells.

To measure ROS, cells previously transfected with γGCS were seeded in a black-edged 96 well plate (Costa 3603) in phenol-free media, in quadruple wells and left overnight to adhere. Black plates were used to lower background fluorescence and to reduce cross talk between independent wells. γGCS silencing doubled DCF fluorescence (Figure 41).

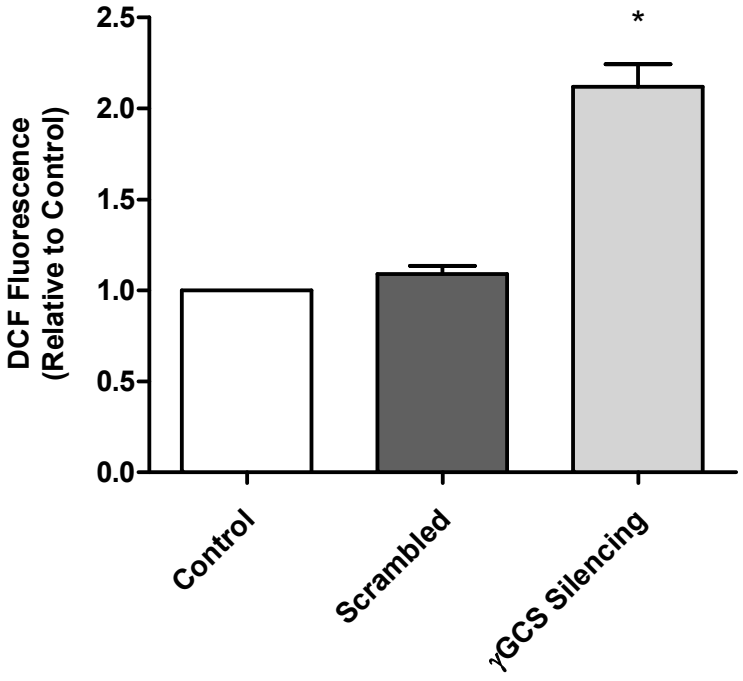

Figure 41 – Increased DCF fluorescence in cells transfected with γGCS siRNA

Cells were either transfected with siRNA against γGCS or treated with scrambled non-specific siRNA control sequence. Samples were analysed for ROS generation using 20 μM DCFH. Data was normalised to control. The values represent the mean $\pm$ SEM from 3 independent experiments; * represents a significant difference ($p < 0.05$) from control.

4.3.4 Effect of γGCS knock-down on HIF-1α stabilisation at 21% oxygen

Scrambled and γGCS transfected cells were treated with antioxidants (AO, NAC and ascorbic acid) for 4 h, sample lysates prepared and HIF-1α protein stabilisation was assessed by Western blot. Figure 42 shows cells transfected with a scrambled control do not stabilise HIF-1α. Silencing of γGCS stabilises HIF-1α in normoxia, yet this is prevented by treatment with AO.

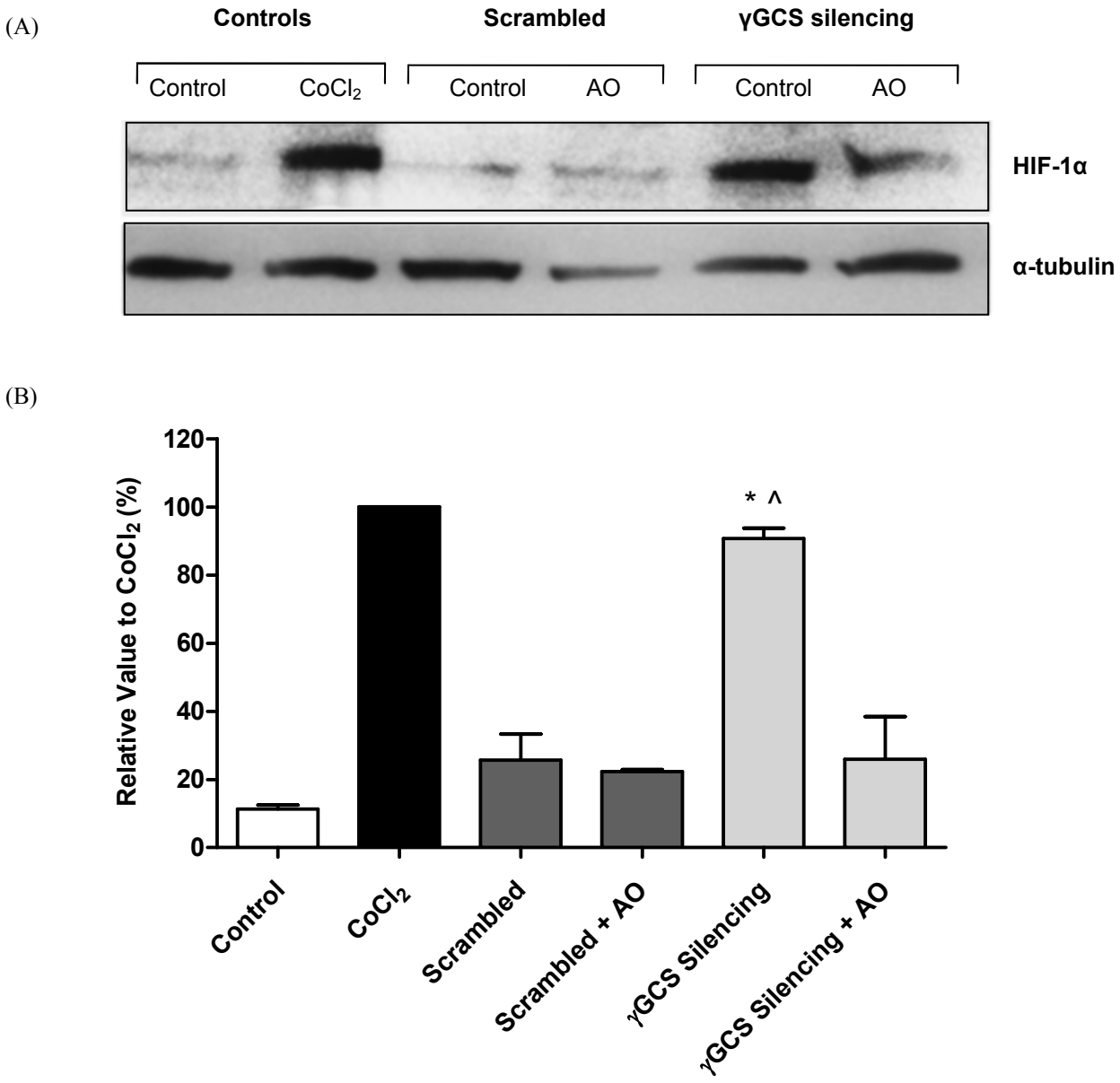

Figure 42 – HIF-1α stabilisation in cells transfected with siRNA against γGCS at 21% oxygen

Cells were either transfected with siRNA against γGCS or treated with scrambled non-specific siRNA control sequence. Cobalt chloride ($CoCl_2$, 160 μM) served as a positive control. Cell lysates were subject to SDS-PAGE and analysed by Western blot (A) and quantified by densitometry (B). The corresponding densitometry values were normalised with α-tubulin and expressed as a percentage to cells incubated with $CoCl_2$. The values represent the mean $\pm$ SEM from 3 independent experiments; * represents a significant difference ($p < 0.05$) from control, and ^ represents a significant difference from γGCS-transfected cells treated with AO.

4.4 Alternative strategy to promote a pro-oxidant environment

Due to the difficulties incurred in maintaining a stable knock-down of γGCS protein expression whilst using the pFIV expression vector, we decided to develop a method in which these restrictions could be controlled. This was achieved by employing synthetically generated siRNA with anti-sense homology against γGCS.

4.4.1 Validation of ON-TARGETplus SMARTpool siRNA against human γGCS

In order to determine the time point in which to study the highest efficiency of siRNA silencing, cells were transfected with a scrambled, negative control siRNA (conjugated to Alexa Fluor 555) over a 72 h time course, and transfection efficiency determined. Maximum fluorescence was observed between 12 and 24 h post silencing (Figure 43). Next we determined mRNA, protein and GSH levels in cells transfected with siRNA against γGCS. Silencing γGCS causes a temporary decrease in γGCS protein (Figure 44) and mRNA expression (Figure 45), which is associated with changes in GSH concentration (Figure 45). Transfection with scrambled siRNA had no effect (Figure 44), remaining undistinguishable from control. There was also no difference in mRNA and GSH concentration in scrambled transfected cells (data not shown).

(A)

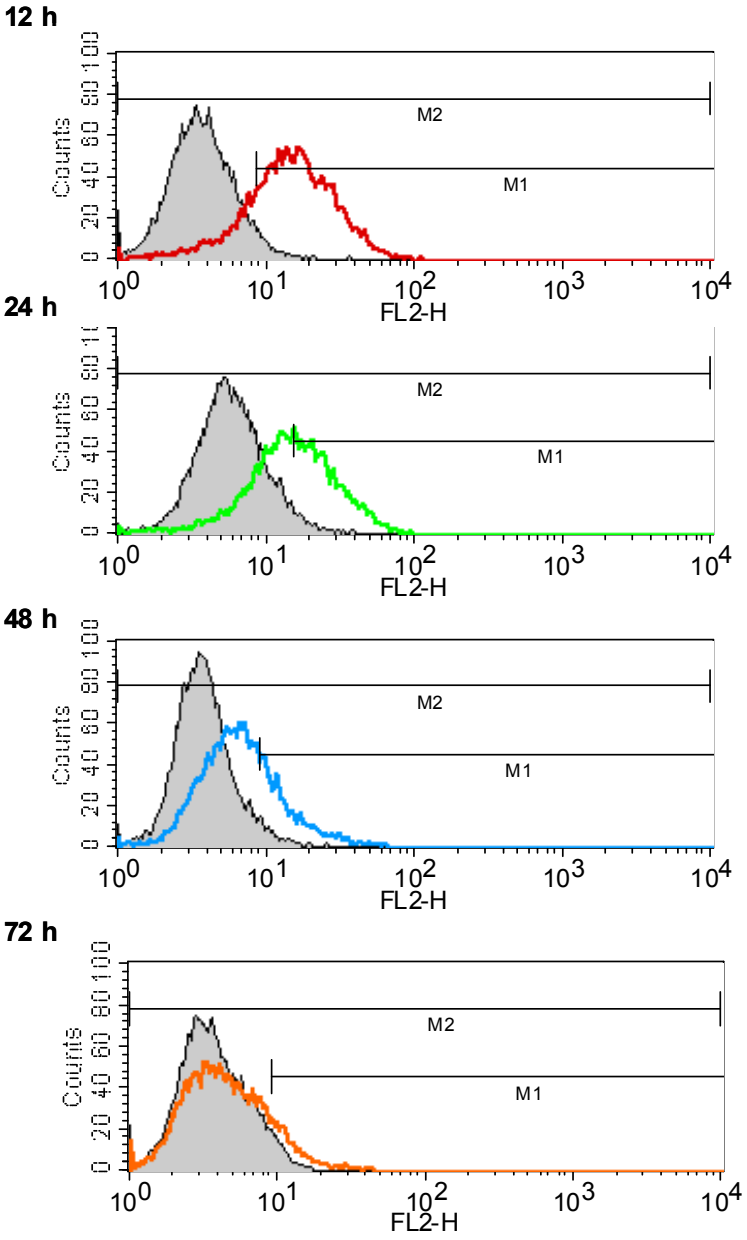

(B)

Time post silencing (h)	Transfection efficiency (Alexa positive cells, %)
0	0.00 ± 0.00
12	70.5± 0.93 *
24	70.2 ± 0.53 *
48	13.2 ± 3.6 ns
72	3.60 ± 1.60 ns

Figure 43 – Transfection efficiency of siRNA in HEK 293T cells

Cells were treated with a negative control siRNA conjugated to Alexa Fluor 555 over a 72 h time course. Cell suspensions were made and fluorescence analysed using a Flow Cytometer (A). The data represent the mean ± SEM from 3 independent experiments; * represents a significant difference ($p < 0.05$) from 0 h (B). ns represents no significant difference from 0 h (B). One representative experiment is shown.

(A)

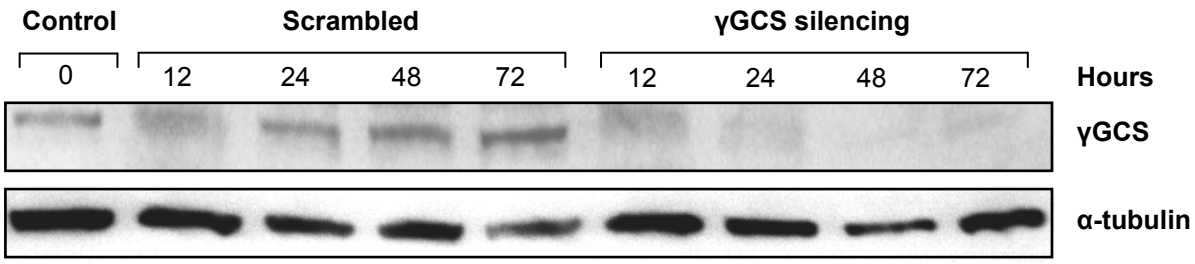

(B)

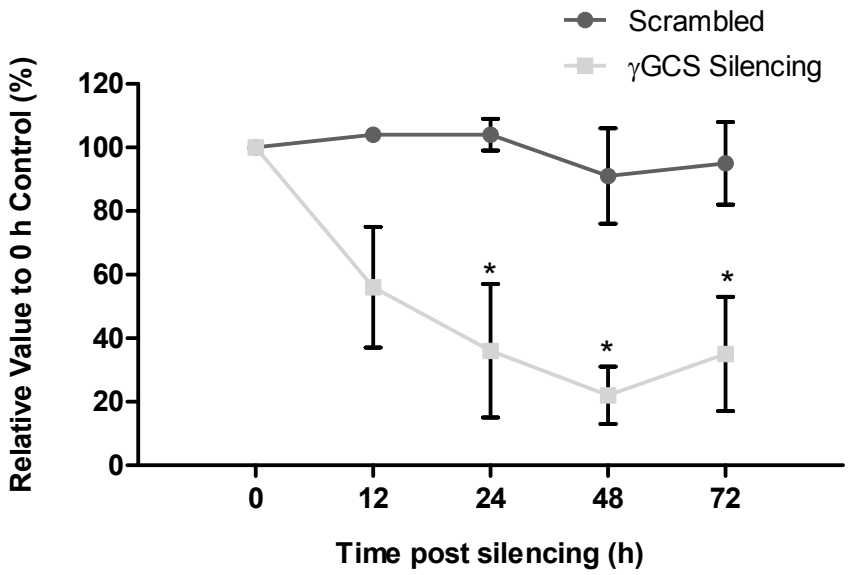

Figure 44 – Time course of γGCS protein expression in cells transfected with siRNA against γGCS

Cells were either transfected with siRNA against γGCS or treated with scrambled non-specific siRNA control sequence. Cell lysates were subjected to SDS-PAGE and analysed by Western blot (A) and quantified by densitometry (B). The corresponding densitometry values were normalised with α-tubulin and results are shown relative to control (0 h). Values are expressed as the mean $\pm$ SEM from 3 independent experiments; * represents a significant difference ($p < 0.05$) from the scrambled control.

(A)

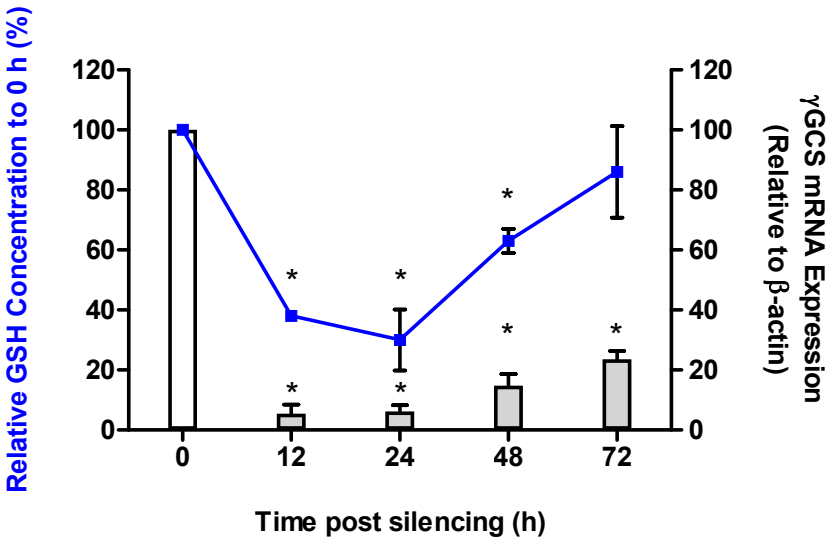

(B)

Time post silencing	nmol GSH/ mg protein
0 h	15 ± 0.00
12 h	6 ± 0.16*
24 h	4 ± 0.25*
48 h	8 ± 0.11*
72 h	12 ± 0.59

Figure 45 – Time course of γGCS mRNA expression and GSH concentration in cells transfected with siRNA against γGCS

Cells were either transfected with siRNA against γGCS or treated with scrambled non-specific siRNA control sequence over 72 h. Samples were analysed for GSH content (blue line). Data was normalised to 0 h control and expressed as a percentage of control (A) and nmol GSH/ mg protein (B). Total RNA was obtained from cells, reverse transcribed into cDNA and mRNA copy numbers of γGCS were quantified by quantitative reverse transcriptase PCR and normalised against β-actin (bars) and expressed as a percentage of control (A). The values represent the mean ± SEM from 3 independent experiments; * represents a significant difference ($p < 0.05$) from control (0 h).

4.4.2 Effect of ON-TARGETplus SMARTpool γGCS silencing in HEK 293T cells on reactive oxygen species generation

4.4.2.1 Detected using 2'-7'dichlorofluorescin (DCFH), a cell permanent indicator for reactive oxygen species

Since γGCS silencing led to a decrease in glutathione after 24 h, experiments were done to measure ROS in these cells. Reactive oxygen species generation was determined 24 h post-silencing using 20 μM DCFH. Excitation and emission were measured at 490 nm and 520 nm, respectively. Silencing γGCS caused a two-fold increase in DCF fluorescence compared to the controls (untreated and scrambled) (Figure 46).

4.4.2.2 Detected using a genetically encoded fluorescent indicator for hydrogen peroxide

Using oxidant sensitive dyes such as DCFH to monitor ROS production has been met with contention as the use of these dyes in cells is problematic concerning sensitivity, specificity and auto-oxidation (Tampo *et al.*, 2003). However, more recently a genetically encoded fluorescent indicator for intracellular hydrogen peroxide (H_2O_2) has been created to detect H_2O_2 inside living cells in real-time. The HyPer probe consists of yellow fluorescent protein (YFP) inserted into the regulatory domain of the prokaryotic H_2O_2-sensing protein, OxyR (Belousov *et al.*, 2006). To further validate and compare the observed increase in DCF fluorescence, (Figure 46, indicative of ROS generation) the HyPer probe was used in γGCS transfected cells.

To characterise the sensitivity of HyPer in HEK 293T cells, cells were transfected with the plasmid carrying HyPer using Lipofectamine transfection reagent. HyPer-transfected cells exhibiting YFP positive staining were then selected using fluorescence-activated cell sorting (FACS), as the plasmid has no antibiotic selection in mammalian cells. Transfected cells were then treated with H_2O_2 (0-160 μM) and fluorescence detected immediately. The fluorescence of HyPer was detected by flow cytometry analysis at 488 nm. The HyPer probe exhibits a basal level of fluorescence intensity (approximately 40 a.u.) (Figure 47). Concentrations as low as 10 μM H_2O_2 led to increases in HyPer fluorescence, which was saturated at approximately 60 μM. This result shows that the HyPer probe can detect H_2O_2 in HEK 293T cells.

To determine whether HyPer fluorescence following treatment with H_2O_2 was sensitive to antioxidants, HyPer-transfected cells were treated with 60 μM H_2O_2, followed by a bolus dose of NAC (1, 2 or 4 mM) immediately after the addition of H_2O_2. HyPer-transfected cells demonstrate basal fluorescence intensity, as seen in Figure 47 and the addition of 60 μM H_2O_2 increases about 2.5 fold. Treatment with NAC caused a significant decrease in HyPer fluorescence. 4 mM NAC returned the fluorescence intensity back to that of the untreated control (Figure 48).

Following the determination of HyPer sensitivity towards H_2O_2 and antioxidants, silencing experiments were performed using γGCS siRNA. Small interfering RNA was prepared, and plated into a 6 well plate. Sorted HyPer cells were then seeded on top in phenol-free, low serum media and left overnight to adhere. The fluorescence of HyPer 24 h post γGCS silencing was detected by flow cytometry analysis. HyPer-transfected cells show basal fluorescence intensity as seen in the previous two figures. The fluorescence intensity increases significantly in γGCS-silenced cells and antioxidant treatment (NAC, 4 mM) immediately prior to analysis prevents this increase (Figure 49).

Similarly to the data collected using DCFH, the results obtained using the HyPer probe show that γGCS-silenced cells have exactly a 2-fold increase in ROS generation compared to control cells.

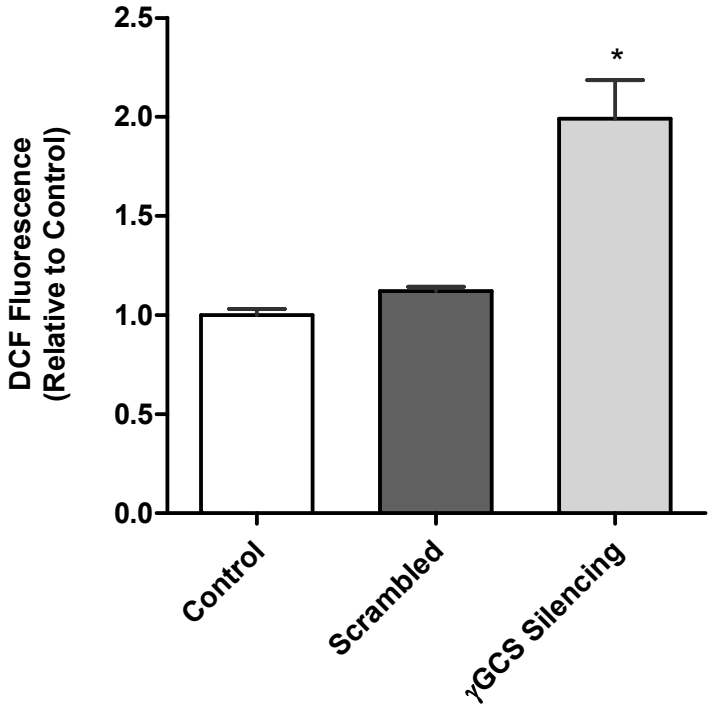

Figure 46 – Increased reactive oxygen species in cells transfected with siRNA against γGCS

Cells were either transfected with siRNA against γGCS or treated with scrambled non-specific siRNA control sequence. Samples were analysed for ROS using 20 μM DCFH. Data was normalised to control. The values represent the mean + SEM from 3 independent experiments; * represents a significant difference ($p < 0.05$) from control.

(A)

H_2O_2 (μM)	Log [H_2O_2] (μM)
0	0
5	0.69897
10	1
20	1.30103
40	1.60206
60	1.778151
80	1.90309
160	2.20412

(B)

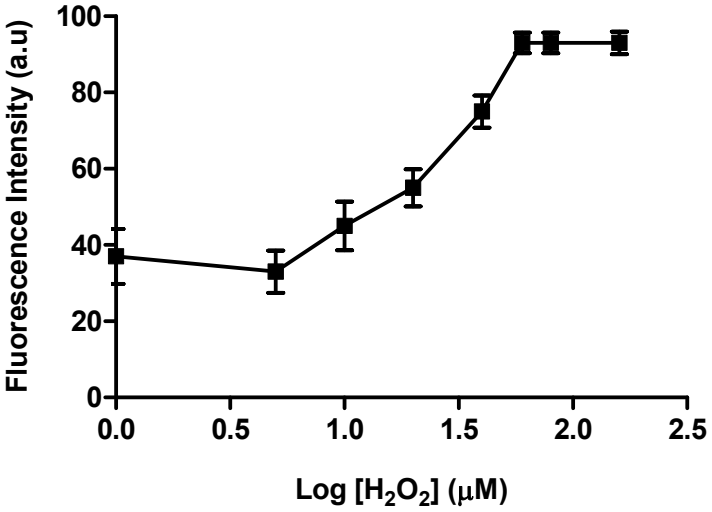

Figure 47 – Sensitivity of HyPer towards exogenously added H_2O_2

Cells were transfected with HyPer and selected using fluorescence-activated cell sorting (FACS). Cell suspensions were made, treated with 0-160 μM H_2O_2 (shown in log scale of [H_2O_2], (A)) and fluorescence analysed immediately using a Flow Cytometer. Data represent the mean ± SEM from 3 independent experiments (B).

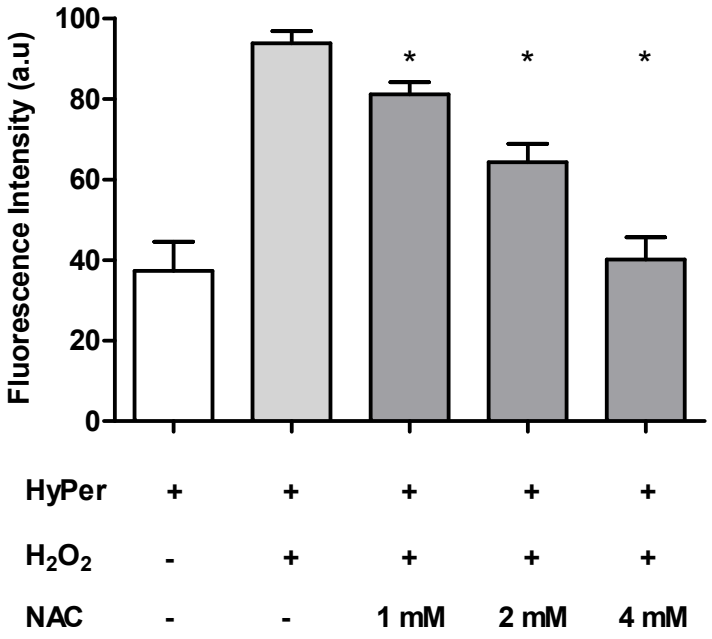

Figure 48 – Effect of NAC on H_2O_2-induced fluorescence in HEK 293T cells

Cells were transfected with HyPer and selected using fluorescence-activated cell sorting (FACS). Cell suspensions were made, and then treated with 60 μM H_2O_2 followed by an immediate bolus dose of NAC (1, 2 or 4 mM) and fluorescence analysed using a Flow Cytometer. The values represent the mean $\pm$ SEM from 3 independent experiments; * represents a significant difference ($p < 0.05$) from H_2O_2 treatment alone.

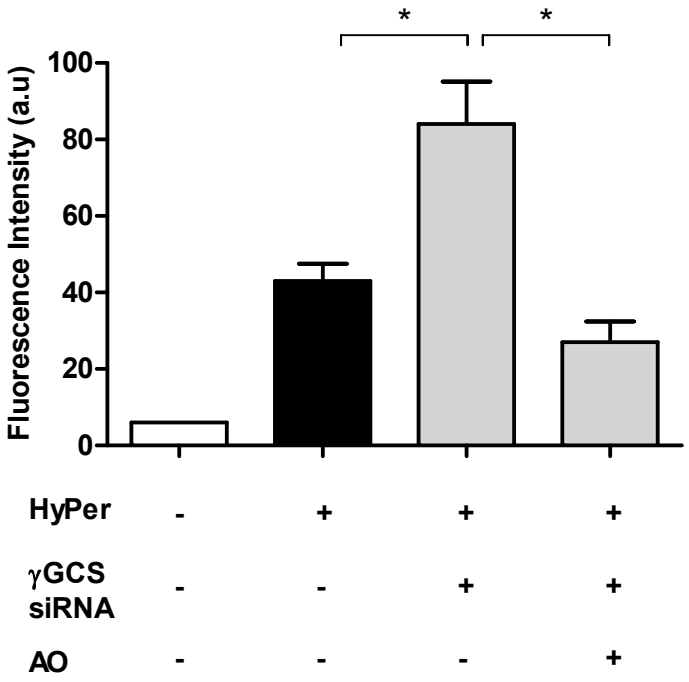

Figure 49 – HyPer fluorescence intensity in cells silenced with siRNA against γGCS

Cells were transfected with HyPer and selected using fluorescence-activated cell sorting (FACS). Cells were then silenced with siRNA against γGCS for 24 h and treated with a bolus shot of NAC (4 mM) immediately prior to analysis. Cell suspensions were made and fluorescence analysed using a CyAN Flow Cytometer (DAKO). The values represent the mean $\pm$ SEM from 3 independent experiments; * represents a significant difference ($p < 0.05$) from HyPer γGCS silenced cells.

4.4.3 Effect of γGCS silencing on HIF-1α mRNA and protein expression at 21% oxygen

Since the use of synthetic siRNA against γGCS in HEK 293T cells decreased GSH and increased ROS in agreement with the data shown using pFIV expression vector, HIF-1α mRNA and protein were determined. Silencing γGCS causes a significant increase in HIF-1α mRNA gene expression (Figure 50) and protein stabilisation (Figure 51) 24 h post-silencing.

The effect of antioxidant treatment on γGCS-silenced cells was then evaluated. Figure 52 shows cells transfected with siRNA against γGCS, stabilise HIF-1α at 21% oxygen. Treatment with antioxidants (either NAC alone or a combination of NAC and ascorbic acid) significantly prevents HIF-1α stabilisation.

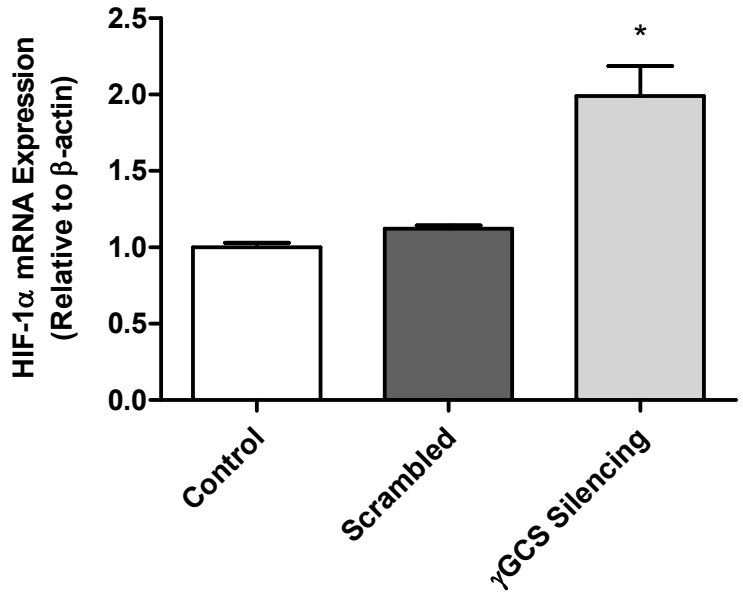

Figure 50 – HIF-1α mRNA expression in cells transfected with siRNA against γGCS

Cells were either transfected with siRNA against γGCS or treated with scrambled non-specific siRNA control sequence for 24 h. Total RNA was obtained from cells and reverse transcribed into cDNA. mRNA copy numbers of HIF-1α were quantified by quantitative reverse transcriptase PCR and normalised against β-actin and expressed relative to control. The values represent the mean $\pm$ SEM from 3 independent experiments; * represents a significant difference ($p < 0.05$) from control.

(A)

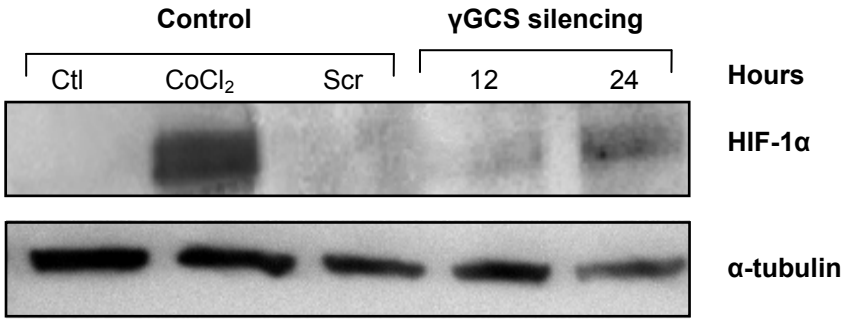

(B)

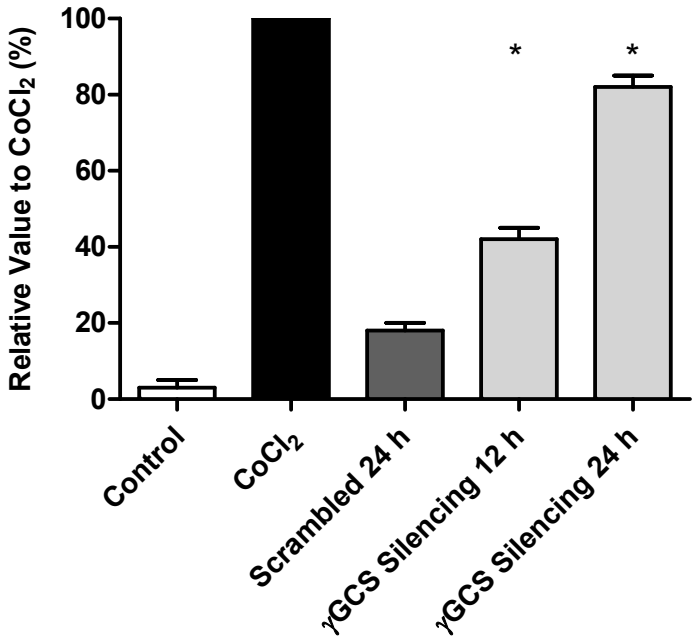

Figure 51 – HIF-1α protein stabilisation in cells transfected with siRNA against γGCS

Cells were either transfected with siRNA against γGCS or treated with scrambled non-specific siRNA (Scr). Cobalt chloride ($CoCl_2$, 160 μM) served as a positive control. Cell lysates were subject to SDS-PAGE and analysed by Western blot (A) and quantified by densitometry (B). The corresponding densitometry values were normalised with α-tubulin and results are shown as a percentage to $CoCl_2$ treated cells. The values represent the mean $\pm$ SEM from 3 independent experiments; * represents a significant difference ($p < 0.05$) from scrambled control. One representative blot is shown.

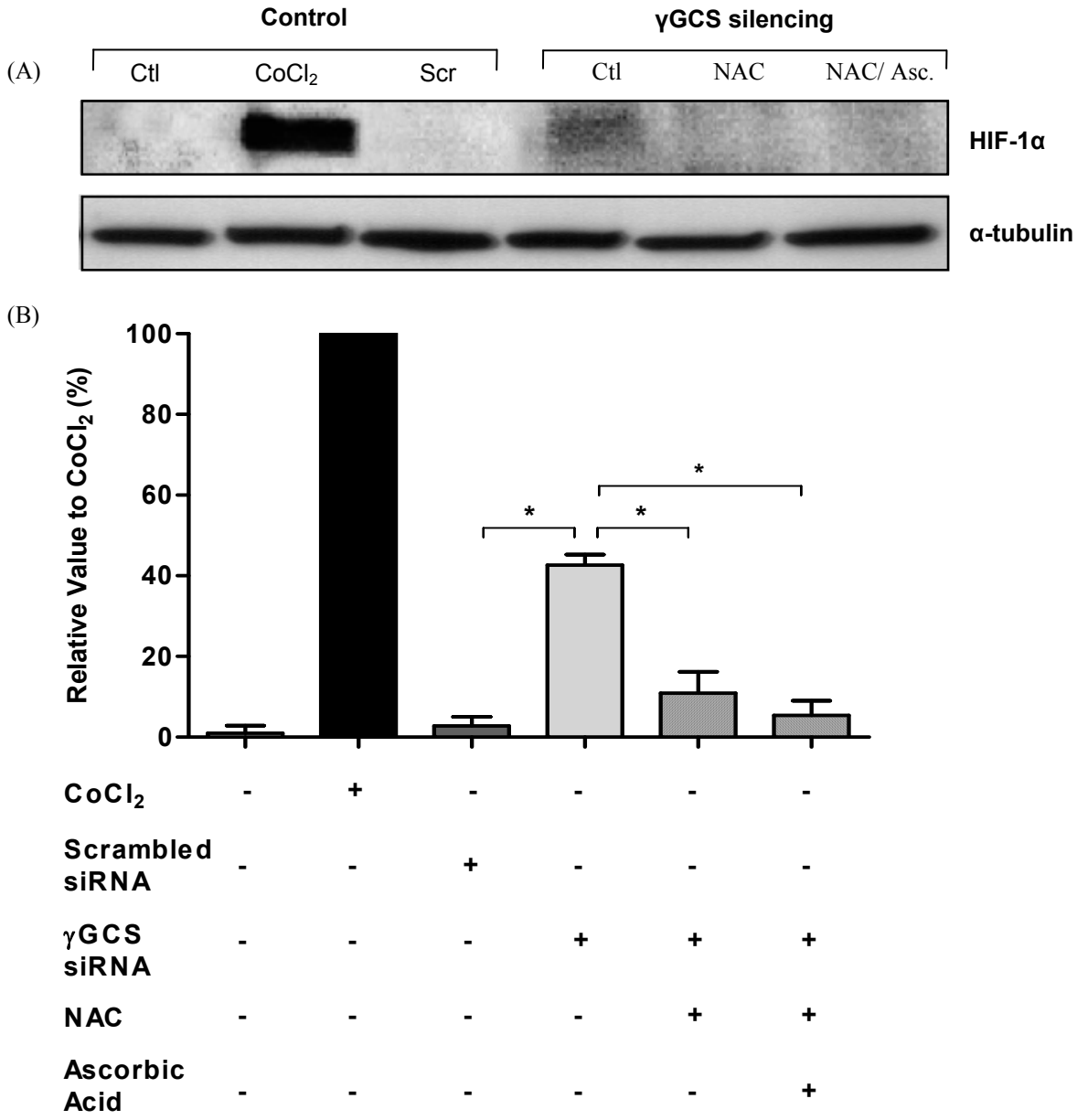

Figure 52 – Effect of antioxidants on HIF-1α stabilisation in cells transfected with siRNA against γGCS

Cells were either transfected with siRNA against γGCS or treated with scrambled non-specific siRNA (Src) for 24 h, and treated with NAC (2.5 mM) alone or NAC (2.5 mM) and ascorbic acid (1 mM) for the final 4 h. Cobalt chloride ($CoCl_2$, 160 μM) served as a positive control. Cell lysates were subject to SDS-PAGE and analysed by Western blot (A) and quantified by densitometry (B). The corresponding densitometry values were normalised with α-tubulin and results are shown as a percentage to $CoCl_2$ treated cells. The values represent the mean ± SEM from 3 independent experiments; * represents a significant difference ($p < 0.05$) from γGCS-silenced cells. One representative blot is shown.

4.4.4 Effect of γGCS silencing on other antioxidant systems and oxidant sensitive genes

Next we investigated whether knocking-down γGCS and the associated increase in cellular ROS production had consequences for the expression of antioxidant genes. The results showed a 2- to 3-fold increase in the expression of catalase, manganese superoxide dismutase (MnSOD), nuclear factor-like 2 (Nrf2) and thioredoxin (Figure 53). Since ROS production has been linked to the activation of NF-κB (Palacios-Callender *et al.*, 2004), a nuclear transcription factor, mRNA levels of NF-κB were also examined. The data show that there was a significant increase in mRNA expression in γGCS knock-down cells compared with control cells (Figure 54).

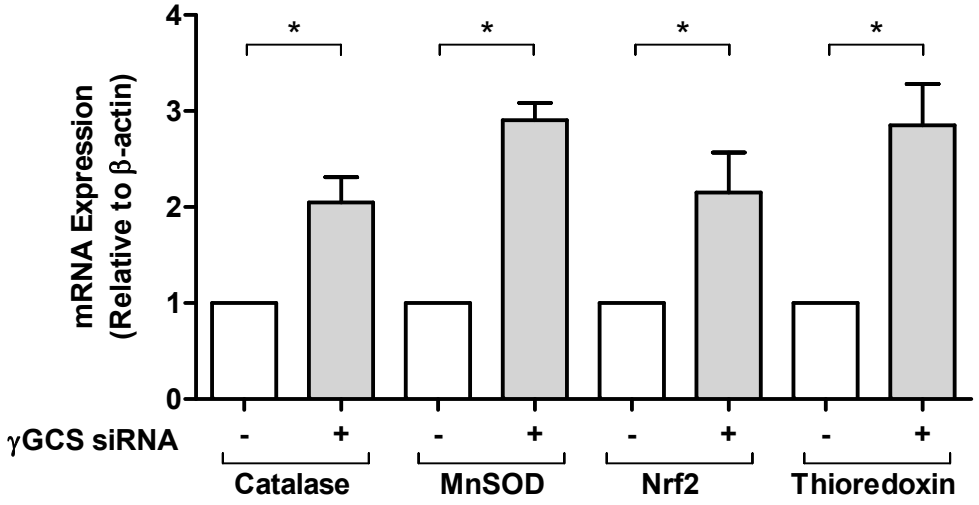

Figure 53 – Antioxidant mRNA expression in cells transfected with siRNA against γGCS

Cells were transfected with siRNA against γGCS for 24 h. Total RNA was obtained from cells, reverse transcribed into cDNA and mRNA copy numbers of catalase, manganese superoxide dismutase (MnSOD), nuclear factor-like 2 (Nrf2) and thioredoxin were quantified by quantitative reverse transcriptase PCR and normalised against β-actin and expressed relative to control (0 h un-transfected cells). The values represent the mean $\pm$ SEM from 3 independent experiments; * represents a significant difference ($p < 0.05$) from control (0 h un-transfected cells).

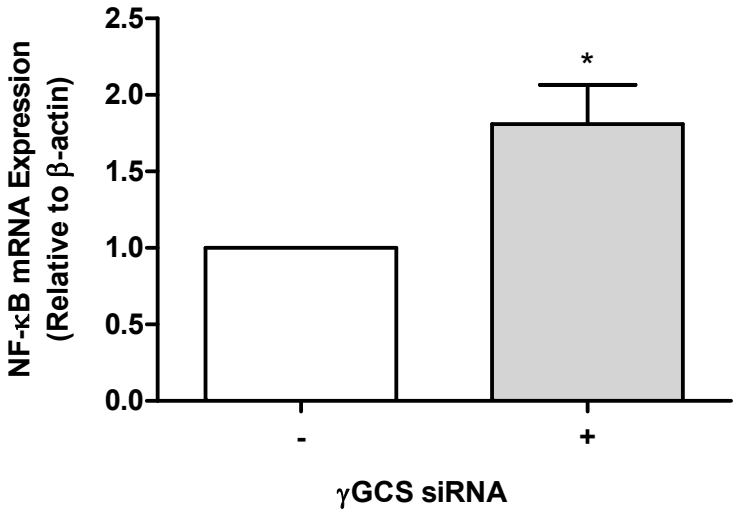

Figure 54 – NF-κB mRNA expression in cells transfected with siRNA against γGCS

Cells were transfected with siRNA against γGCS for 24 h. Total RNA was obtained from cells, reverse transcribed into cDNA and mRNA copy numbers of NF-κB were quantified by quantitative reverse transcriptase PCR and normalised against β-actin and expressed relative to control. The values represent the mean $\pm$ SEM from 3 independent experiments; * represents a significant difference ($p < 0.05$) from control.

4.5 Mechanism by which ROS stabilise HIF-1α in normoxia

A number of mediators have been described to affect the HIF system including hypoxia (Wang and Semenza, 1993), NO (Quintero *et al.*, 2006a), ROS ((Klimova and Chandel, 2008), growth factors (Fukuda *et al.*, 2002) and genetic mutations (Maxwell *et al.*, 1999). There are numerous potential mechanisms of these mediators, resulting in either the accumulation of HIF-1α or increased HIF-1 activity. These include inhibition of PHDs by Fe^{2+} chelation or activation of PI3K (Brune and Zhou, 2007), S-nitrosylation of HIF-1α (Li *et al.*, 2007), inhibition of PHDs by reducing antioxidants, or direct oxidation of catalytic Fe^{2+} (Gerald *et al.*, 2004) and NF-κB activation and HIF-1α mRNA up-regulation (Blouin *et al.*, 2004;Frede *et al.*, 2006;Jantsch *et al.*, 2008).

4.5.1 Detection of hydroxylated and ubiquitinated HIF-1α

Since γGCS silencing stabilises HIF-1α at 21% oxygen, experiments underwent to investigate the potential mechanism of this stabilisation. At 21% oxygen, PHDs normally target HIF-1α for hydroxylation, which in turn mediates ubiquitination and proteosomal degradation. To test whether the PHDs were functioning, HEK 293T cells were treated with the proteosomal inhibitor MG132 (0-10 μM, 2 h). Cell lysates were prepared, separated by SDS-PAGE and analysed by Western blot. An antibody which specifically recognises hydroxylated HIF-1α was used during immunodetection.

There is an accumulation of HIF-1α protein in MG132 treated cells, which is absent in untreated cells (Figure 55. Moreover, hydroxylated HIF-1α is detected in cells treated with 10 μM MG132 (Figure 55). Next, we investigated whether cells treated with siRNA against γGCS, which stabilise HIF-1α at 21% oxygen, have been targeted for hydroxylation by the PHDs. Figure 56 shows γGCS siRNA transfected HIF-1α have been hydroxylated.

Given that HIF-1α is hydroxylated in γGCS siRNA transfected cells, we next tested whether HIF-1α was ubiquitinated by preparing IP with anti-ubiquitin. Figure 57 shows HIF-1α ubiquitination in cells treated with γGCS siRNA, at a level similar to control.

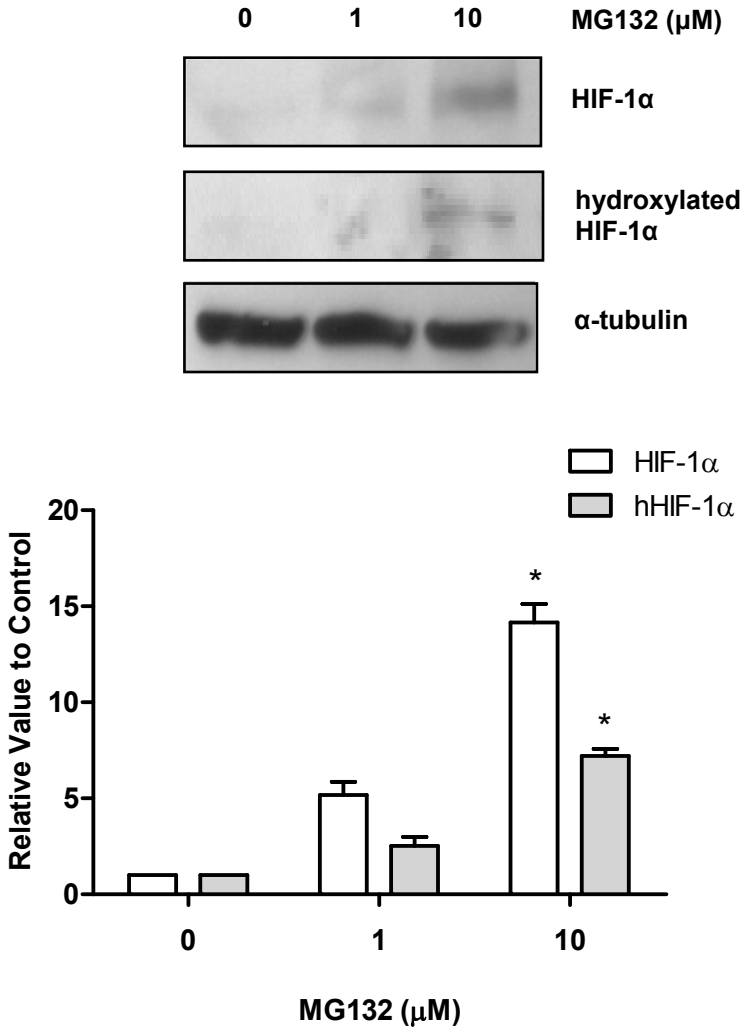

Figure 55 – HEK 293T cells treated with proteasomal inhibitor MG132

Cells were treated with MG132 (0-100 μM) for 2 h at 21% oxygen. Cell lysates were subject to SDS-PAGE and analysed by Western blot (A) and quantified by densitometry (B) HIF-1α (white bars) and hydroxylated HIF-1α (grey bars). The corresponding densitometry values were normalised with α-tubulin and results are shown relative to control. The values represent the mean ± SEM from 3 independent experiments; * represents a significant difference ($p < 0.05$) from control. One representative blot is shown.

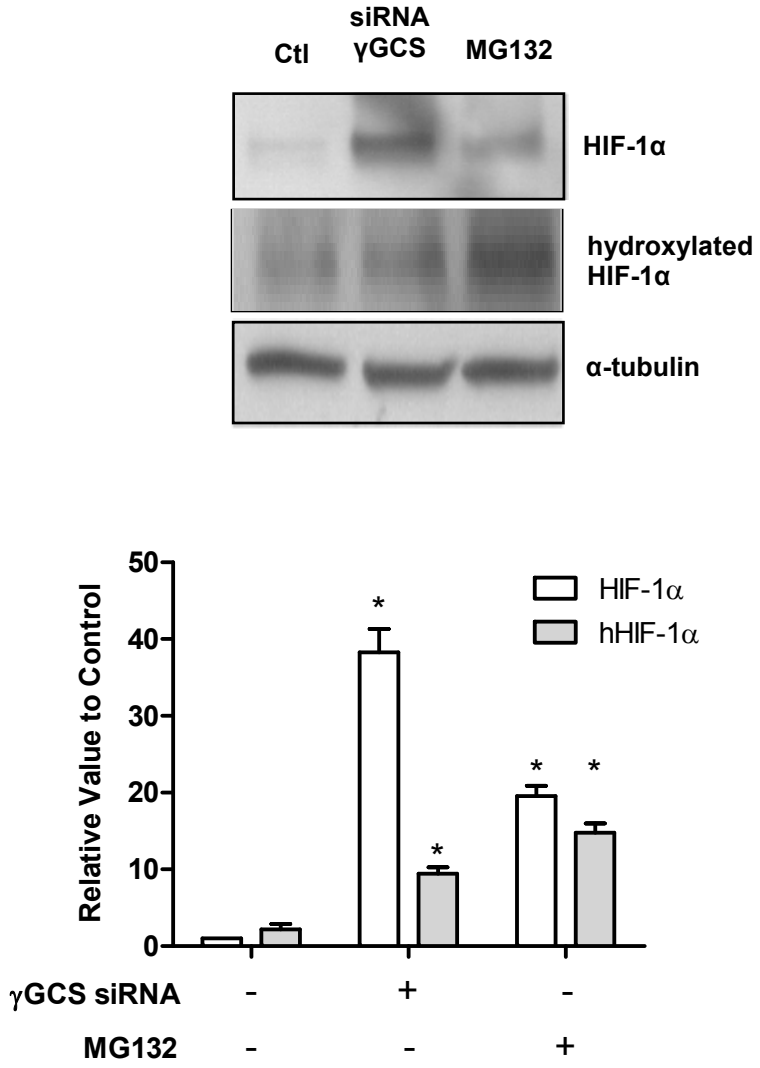

Figure 56 – Detection of hydroxylated HIF-1α in cells transfected with siRNA against γGCS

Cells were either transfected with siRNA against γGCS for 24 h or treated with MG132 (10 μM, 2 h) at 21% oxygen. Cell lysates were subject to SDS-PAGE and analysed by Western blot (A) and quantified by densitometry (B) HIF-1α (white bars) and hydroxylated HIF-1α (grey bars). The corresponding densitometry values were normalised with α-tubulin and results are shown relative to control. The values represent the mean ± SEM from 3 independent experiments; * represents a significant difference ($p < 0.05$) from control. One representative blot is shown.

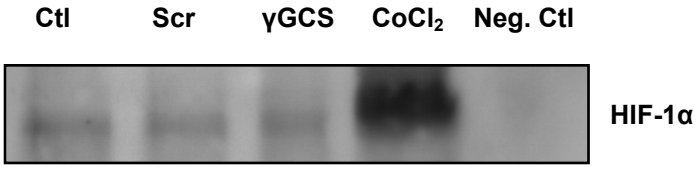

Figure 57 – HIF-1α is targeted for ubiquitination in cells transfected with siRNA against γGCS

HIF-1α protein was immunoprecipitated with an ubiquitin antibody from lysates of cells transfected with siRNA against γGCS or a non-specific control sequence (Scr) for 24 h. For controls, $CoCl_2$ was used as a positive control for HIF-1α and to verify the stringency of immunoprecipitation, experiments included samples where immunoprecipitating antibody was omitted (Neg. Ctl). The immunoprecipitated proteins were subjected to Western blotting and detected with anti-HIF-1α. One representative blot is shown from 3 independent experiments.

4.6 Summary of key results

γGlutamyl Cysteine Synthetase (γGCS), the rate limiting enzyme of GSH biosynthesis was successfully silenced in HEK 293T cells via two siRNA strategies. Silencing γGCS caused a significant decrease in cellular GSH thereby impairing the capacity of the cells to detoxify endogenously generated ROS, resulting in an increase in ROS. HIF-1α was stabilised at ambient [O_2] in γGCS-silenced cells and this effect could be prevented by treatment with antioxidants. HIF-1α appears to remain hydroxylated and ubiquitinated in γGCS siRNA transfected cells.

Chapter five:
Investigation into the origin of reactive oxygen species involved in HIF-1α stabilisation

Chapter five: Investigation into the origin of reactive oxygen species involved in HIF-1α stabilisation

5.1 Introduction

The findings presented in chapter four demonstrate ROS-induced HIF-1α stabilisation at ambient oxygen concentration. However, these data do not provide information concerning the possible origin of ROS contributing towards this normoxic stabilisation of HIF-1α. Therefore, experiments were conducted to establish the possible source of ROS involved in the stabilisation of HIF-1α in the γGCS silencing model, and to study the potential role of ROS in HIF-1α stabilisation at low [O_2].

HIF-1α stabilisation by free radicals has been previously demonstrated (Schroedl *et al.*, 2002;Wellman *et al.*, 2003;Mansfield *et al.*, 2005;Quintero *et al.*, 2006a) yet the origin of free radical required for this effect remain controversial. Originally Chandel *et* al, (1998) reported that ROS generated by the mitochondria were able to trigger binding of HIF-1α to DNA and mRNA expression of erythropoietin (EPO) and vascular endothelial growth factor (VEGF) (downstream HIF-1α targets) in human hepatoma (Hep3B) cells. However, the generation of free radicals in hypoxia and their effect of stabilising HIF-1α remain contentious.

Experiments were therefore conducted using the previously validated γGCS-silencing model to explore the hypothesis that ROS generated from the mitochondria stabilise HIF-1α. Initially, experiments were designed to characterise a genetic model in which to study the effects of HIF-1α stabilisation in cells with non-functional mitochondria (*Rho^0*) and subsequently establish the consequence on ROS production. Alternative sources of ROS-induced HIF-1α stabilisation were also investigated.

5.2 Characterisation of mutated form of DNA polymerase gamma

From the 5 isoforms (alpha, beta, gamma, delta, and epsilon) of DNA polymerase in human cells, DNA polymerase gamma (POLγ) is solely responsible for the replication of mitochondrial DNA (mtDNA). Studies by Wanrooij *et al.,* 2007 showed the effects of expressing various catalytically deficient mutants of DNA POLγ. This led to a sharp decrease in mtDNA replication and a progressive decline in mtDNA copy number (Wanrooij *et al.*, 2007). We investigated the consequence of the expression of mutated DNA POLγ on cellular ROS production and HIF-1α stabilisation.

5.2.1 Effect of DNA POLγ mutation on respiration (VO_2) and cytochrome aa_3 content

HEK 293T cells stably transfected with an inducible catalytically deficient isoform of mitochondrial DNA POLγ (D890N) were kindly provided by Johannes Spelbrink, Institute of Medical Technology and Tampere University Hospital, Tampere, Finland. The expression of this mutated isoform is under the control of an inducible promoter that can be activated by the incubation of cells with doxycycline (DC). Cells were treated with DC (0-1500 ng/ml) for 0, 5 and 10 days and placed in the respiration chamber of the visible light spectroscopy (VLS) system (experimental procedures section 2.12) to monitor oxygen consumption (VO_2) and redox changes in cytochrome aa_3 of cytochrome *c* oxidase (CcO) during cellular respiration towards anoxia.

Studies of the VO_2 showed that control cells respire at ~ 15 μM O_2/min/10^7cells. Incubation with DC led to both dose- and time-dependent decrease in VO_2. After 5 days, VO_2 dropped by ~ 50% at concentration $\geq$ 250 ng/ml. After 10 days, VO_2 was decreased by incubation with DC as low as 50 ng/ml. At concentrations > 250 ng/ml, VO_2 dropped to as little as 1 μM O_2/min/10^7cells (Figure 58, A). The corresponding changes in the redox state of aa_3 in terms of absolute concentration changes were also monitored (Figure 58, B). Incubation with DC (50-1500 ng/ml) for 5 days caused a significant reduction (> 50%) of cytochrome aa_3. Incubation with DC (50-1500 ng/ml) for 10 days caused an even greater reduction of cytochrome aa_3 to almost undetectable levels at concentrations $\geq$ 250 ng/ml. Figure 58 shows incubation with 250 ng/ml DC caused the earliest significant response in mitochondrial functionality (VO_2). Therefore all further experiments were performed using 250 ng/ml DC for 10 days.

5.2.2 Effect of DNA POLγ mutation on mtDNA content

Next, mitochondrial DNA content was determined following a 10-day time course using 250 ng/ml DC. Mitochondrial DNA was normalised to nuclear DNA and is represented in Figure 59 relative to non-induced cells. Figure 59 shows an early and steep decrease in mitochondrial DNA, with an EC50 of 8.9 hours. Mitochondrial DNA decreases by 90% after 1 day DC incubation and remains at this level throughout the time course.

5.2.3 Effect of DNA POLγ mutation on cytochrome *c* oxidase protein expression

Following the previous results demonstrating functional defects in induced D890N and the loss of mitochondrial DNA, cytochrome *c* oxidase (CcO) protein expression was determined via Western blot. Cells were incubated with 250 ng/ml DC for 3, 5 and 10 days and lysates prepared. Figure 60 shows non-induced cells to have a detectable level of CcO, which is not significantly affected after incubation with DC for 3 days. However, after 5 days incubation with DC, CcO protein concentration begins to decline, until at 10 days the protein is significantly reduced.

(A)

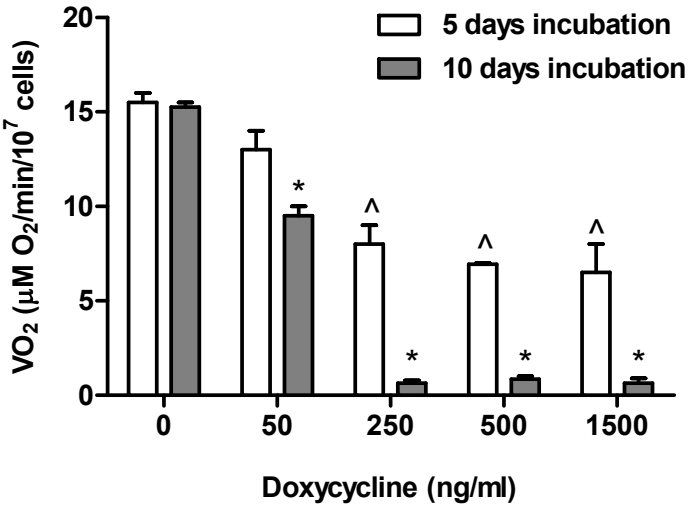

(B)

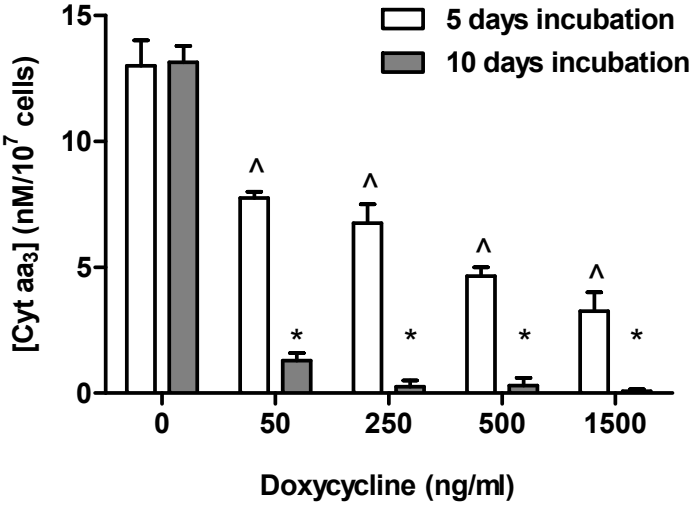

Figure 58 – Cellular respiration and cytochrome aa_3 concentration monitored by VLS in DC treated cells

D890N cells were incubated with 0-1500 ng/ml doxycycline (DC) for 5 or 10 days. Values of oxygen consumption (VO_2) (A) and changes in the redox state of cytrochromes aa_3 (B) were measured from intact cells during respiration towards anoxia using the VLS system. The values represent the mean $\pm$ SEM from 3 independent experiments; * represents a significant difference ($p < 0.05$) from untreated cells (for 10 days incubation) and ^ represents a significant difference ($p < 0.05$) from untreated cells (for 5 days incubation).

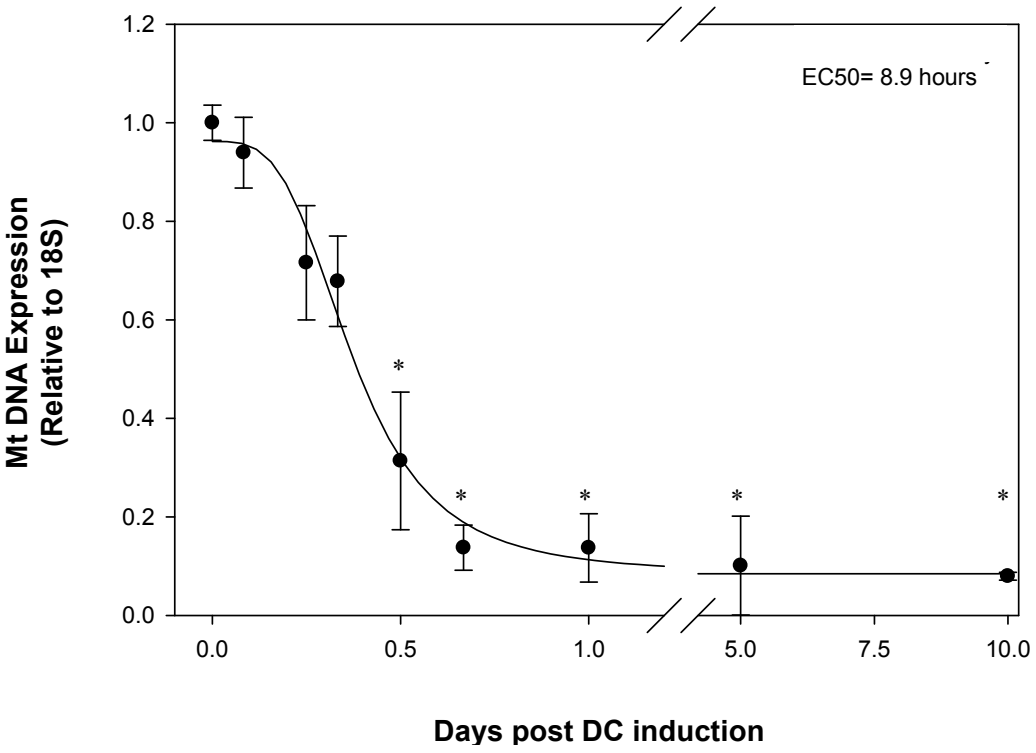

Figure 59 – Mitochondrial DNA content in induced D890N cells

MtDNA copy number was determined by real time PCR of COX1 using 18S as a nuclear standard. The data shown represents the copy numbers for cells following doxycycline (DC) induction (250 ng/ml) for up to 10 days. The values represent the mean $\pm$ SEM from 3 independent experiments; * represents a significant difference ($p < 0.05$) from untreated cells.

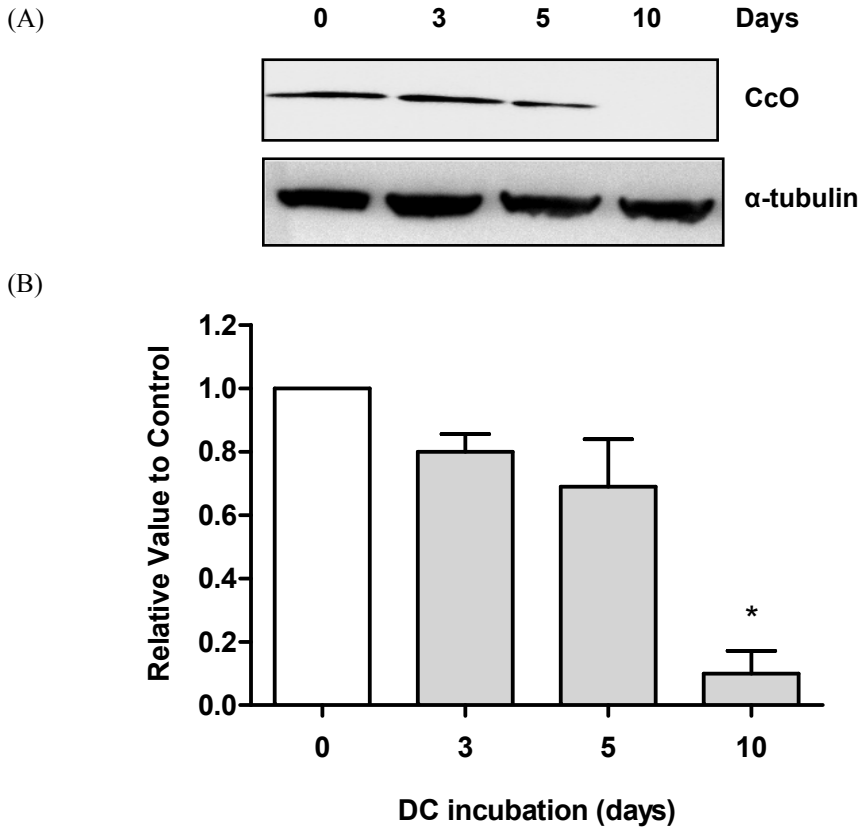

Figure 60 – Effect of DC treatment on cytochrome *c* oxidase protein expression

Cells were treated with 250 ng/ml doxycycline (DC, 0-10 days). Cell lysates were subject to SDS-PAGE and analysed by Western blot (A) and quantified by densitometry (B). The corresponding densitometry values were normalised with α-tubulin and results are shown relative to control. The values represent the mean ± SEM from 3 independent experiments; * represents a significant difference ($p < 0.05$) from control. One representative blot is shown.

5.2.4 Effect of DNA POLγ mutation on mitochondrial morphology

We next examined whether the morphology of mitochondria were affected following DC induction (250 ng/ml, 10 days). Electron microscopy images of control cells show the structure of the mitochondria, with clearly identifiable cristae space (folding of the inner membrane) (Figure 61 (A), indicated by arrows). The structure of the mitochondria is still visible in induced cells, but the cristae are no longer uniform, and in some cases have been completely lost (Figure 61 (B), indicated by arrows).

5.2.5 Mitochondrial membrane potential in induced D890N cells

Next we investigated whether the membrane potential ($\Delta\Psi_m$) was maintained in induced cells, and to see if electrons are passed through the electron transport chain. After DC induction, cells were treated with rotenone (1 μM) to inhibit Complex I of the respiratory chain; followed by treatment with p-trifluoromethoxy carbonyl cyanide phenyl hydrazone (FCCP, 25 μM), an uncoupler of mitochondrial oxidative phosphorylation, while recording $\Delta\Psi_m$ using time-lapse confocal microscopy.

Treatment with rotenone causes the $\Delta\Psi_m$ of control cells, as measured by tetramethyl rhodamine methyl ester (TMRM, 20 nM) fluorescence to be significantly reduced (Figure 62 (B); rotenone (Rot) addition). FCCP completely collapses $\Delta\Psi_m$. The $\Delta\Psi_m$ of induced D890N cells is not affected by the addition of rotenone, but collapses completely upon treatment with FCCP (Figure 62 (D)).

(A) D890N Control (B) D890N Induced

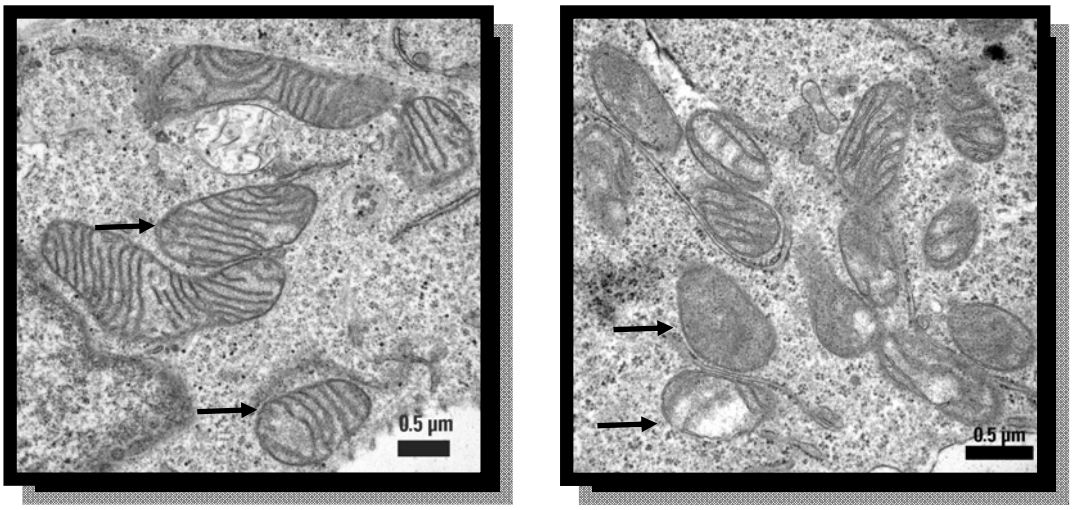

Figure 61 – Electron microscopy of D890N control and induced cells

Electron microscopy images of control (A) or induced ((B) 250 ng/ml DC, 10 days) D890N cells. Arrows depict mitochondrial structure, with cristae (A) or without cristae (B). (n = 3) One representative image for each is shown.

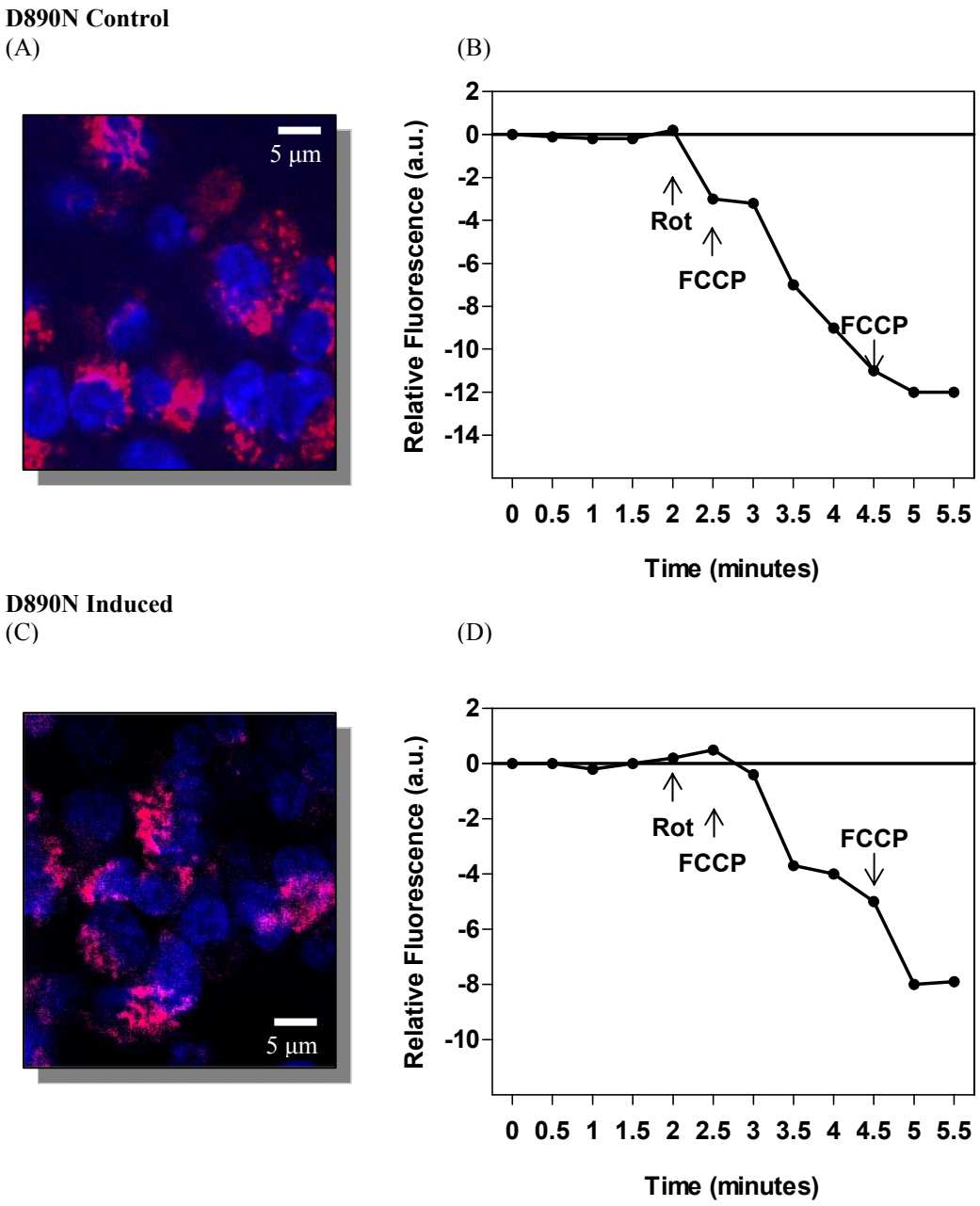

Figure 62 – Mitochondrial membrane potential in control and induced D890N cells

Control and induced (250 ng/ml DC, 10 days) D890N cells were treated with rotenone (1 µM) (Rot) followed by FCCP (25 µM), and TMRM fluorescence in whole-cells was monitored as an indicator of $\Delta\Psi_m$ (B and D). FCCP completely abolished the TMRM fluorescence in control and induced cells. The values represent the mean $\pm$ SEM from 3 independent experiments. One representative confocal image and trace of control (A) and DC induced (B) cells is shown, stained with 20 nM TMRM to indicate $\Delta\Psi$m (red) and counterstained with 2 mg/ml Hoechst 33342 to identify the nuclei (blue).

5.3 Effect of DNA POLγ mutation on HIF-1α stabilisation

Following the induction and characterisation of a *Rho*^{0} phenotype, defined as non-respiring cells with no mitochondrial DNA, experiments proceeded to investigate the implications of *Rho*^{0} cells on ROS production and HIF-1α stabilisation.

5.3.1 ROS production decreases in D890N *Rho*^{0} cells at ambient oxygen

D890N HEK 293T cells were incubated with DC (250 ng/ml) for 9 days. Induced and control cells were then seeded in a black-edged 96 well plate in phenol free media, in quadruple wells and left overnight to adhere. Small interfering RNA against γGCS was also prepared, plated into the same 96 well plate and cells (control and induced) seeded on top. Reactive oxygen species generation was determined 24 h post silencing (10 day DC incubation) using 20 μM DCFH in the absence or presence of antioxidants.

Figure 63 shows that there was a significant increase in DCF fluorescence in γGCS siRNA transfected cells compared to non-induced D890N cells. DCF fluorescence in induced D890N *Rho*^{0} cells was significantly less than non-induced cells and incubation with antioxidants had no effect. DCF fluorescence in induced D890N *Rho*^{0} cells transfected with siRNA against γGCS was also significantly less than non-induced cells and incubation with antioxidants had no effect. There was no difference observed between the DCF fluorescence of D890N *Rho*^{0} cells and D890N *Rho*^{0} cells transfected with γGCS siRNA.

5.3.2 Loss of ROS in D890N *Rho*^{0} cells at low [O_2]

D890N cells were incubated with DC (250 ng/ml) for 10 days. Cells were then incubated at ambient (21%) or low [O_2] (3%) concentration for 4 hours. Reactive oxygen species generation was determined using 20 μM DCFH and cells fixed with 70% ethanol. The fluorescence of DCF was detected by flow cytometry.

Figure 64 shows that there was a significant increase in DCF fluorescence at 3% oxygen in control D890N cells. However, this increase in DCF fluorescence was not observed in D890N *Rho*^{0} cells at 3% oxygen.

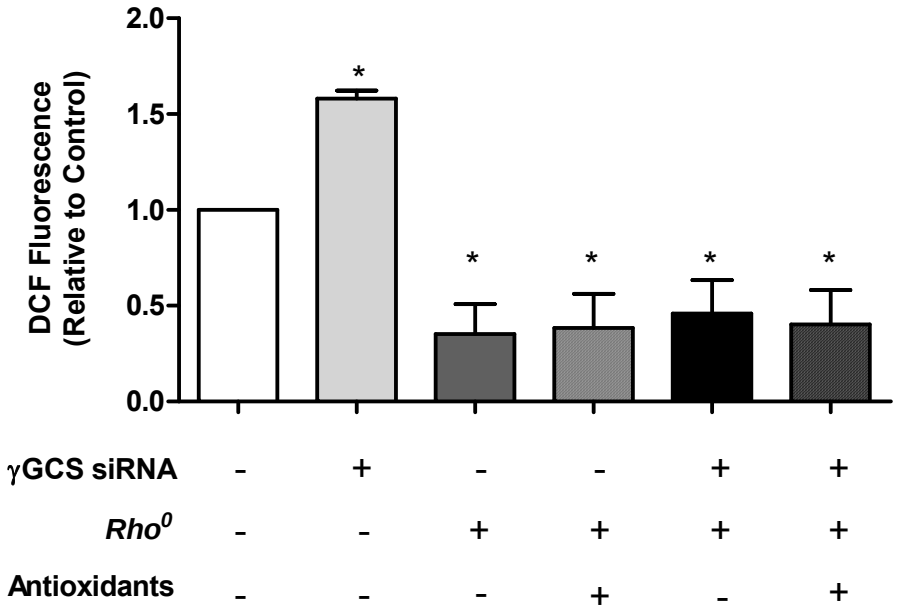

Figure 63 – Decrease in DCF fluorescence in *Rho*^{0} cells at 21% oxygen

Cells were incubated with doxycycline (250 ng/ml) for 10 days. Cells were then treated with antioxidants (NAC 2.5 mM plus ascorbic acid 1 mM) for 4 h. Samples were analysed for ROS production using 20 μM DCFH. Data was normalised to non-induced control data. The values represent the mean $\pm$ SEM from 3 independent experiments; * represents a significant difference ($p < 0.05$) from non-induced control.

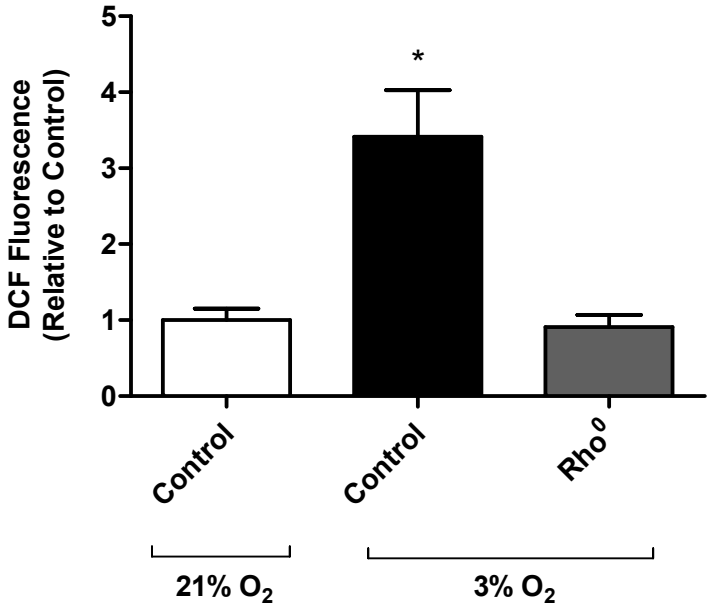

Figure 64 – Decrease in DCF fluorescence in *Rho*^{0} cells in low [O_2]

Cells were incubated with doxycycline (250 ng/ml) for 10 days. Samples were analysed for ROS production using 20 μM DCFH. Fluorescence was analysed using a flow cytometer. Data was normalised to non-induced control data. The values represent the mean $\pm$ SEM from 3 independent experiments; * represents a significant difference ($p < 0.05$) from non-induced control.

5.3.3 Inhibition of HIF-1α stabilisation in D890N *Rho^0* cells

HIF-1α protein stabilisation was determined at 21% and 3% oxygen in *Rho^0* cells (250 ng/ml, 10 days) and in *Rho^0* cells following transfection with γGCS siRNA. HIF-1α stabilisation was also determined in *Rho^0* cells at 0.5% oxygen.

Figure 65 shows a significant increase in HIF-1α stabilisation in non-induced cells transfected with γGCS siRNA at 21% oxygen. However, silencing γGCS in *Rho^o* cells at 21% oxygen does not result in HIF-1α stabilisation. At 3% oxygen, HIF-1α is stabilised, and this stabilisation is significantly increased in γGCS siRNA transfected cells. However, HIF-1α stabilisation is prevented at 3% oxygen in *Rho^o* cells. HIF-1α stabilisation is not significantly different in γGCS siRNA transfected *Rho^o* cells at 3% oxygen. HIF-1α stabilisation is not altered in *Rho^o* cells at 0.5% oxygen.

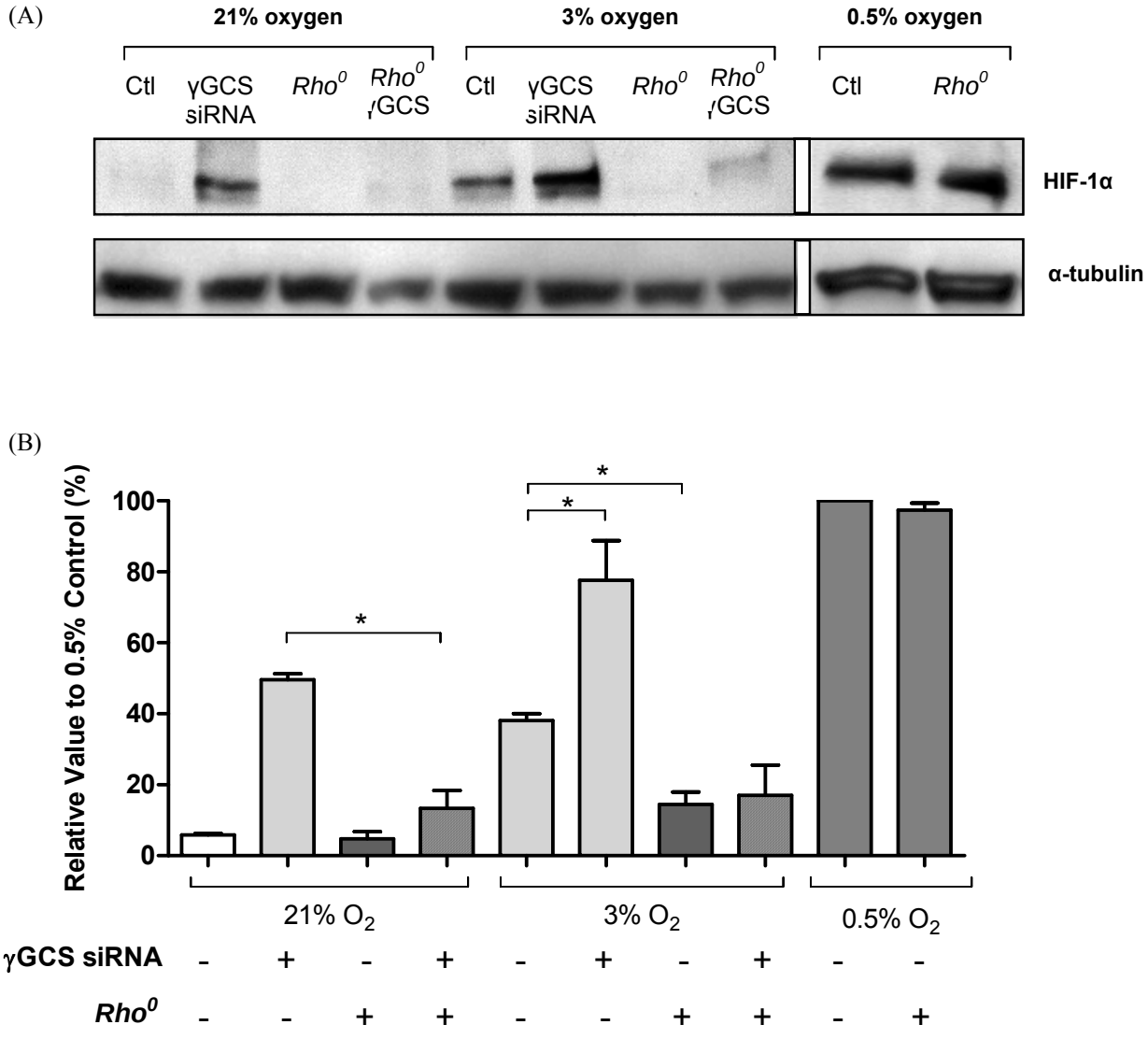

Figure 65 – HIF-1α stabilisation in *Rho*^{0} cells and its sensitivity towards γGCS silencing

Rho^0 cells were transfected with siRNA against γGCS at 21% and 3% oxygen. Cell lysates were subject to SDS-PAGE and analysed by Western blot (A) and quantified by densitometry (B). The corresponding densitometry values were normalised with α-tubulin and results are shown as a percentage of the 0.5% oxygen control. The values represent the mean ± SEM from 3 independent experiments; * represents a significant difference ($p < 0.05$). One representative blot is shown.

5.4 Role of mitochondrial ROS in HIF-1α stabilisation in human head and neck squamous carcinoma cells

5.4.1 Effect of inhibiting a mitochondrial gene and protein expression on HIF-1α stabilisation

Previous data had shown HIF-1α stabilisation in human head and neck squamous carcinoma (H157) cells at 21% oxygen, which can be prevented by incubation with antioxidants (Chapter 3, Figure 15), suggesting a role for ROS in this process. In order to establish if mitochondria were the source of ROS production, H157 cells were treated with ethidium bromide (EtBr) (0-500 ng/ml) for 7 days at 21% oxygen. Ethidium bromide was used since it is known to prevent the replication of mitochondrial DNA but not genomic DNA at low doses (Zylber *et al.*, 1969;Nass, 1970;Nass, 1972). HIF-1α and COXI (a mitochondrial encoded gene) mRNA was determined. Figure 66 (A) shows HIF-1α mRNA is reduced in a dose-dependent manner, with a significant reduction observed at 200 ng/ml. Figure 66 (B) shows COXI mRNA is significantly reduced with all EtBr concentrations tested.

Since HIF-1α mRNA was significantly reduced using 200 ng/ml EtBr, cells were then incubated with this concentration of EtBr for 0, 2, 5, 7 and 10 days at 21% oxygen. HIF-1α and COX1 mRNA were determined. Figure 67 (A and B) shows HIF-1α and COXI mRNA to be significantly reduced from as early as 2 days after incubation with EtBr and over the entire experimental period.

Figure 68 shows that HIF-1α is present at 21% oxygen in H157 cells, and incubation with EtBr results in loss of HIF-1α stabilisation in these cells. Cytochrome *c* oxidase is also detectable in these cells at 21% oxygen. Incubation with EtBr after 2 days causes complete loss of this protein, and this loss is maintained until the final collection at 10 days.

(A)

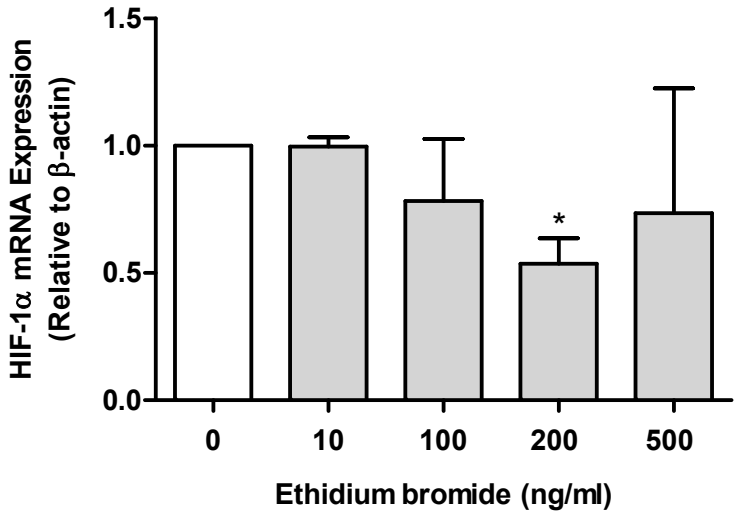

(B)

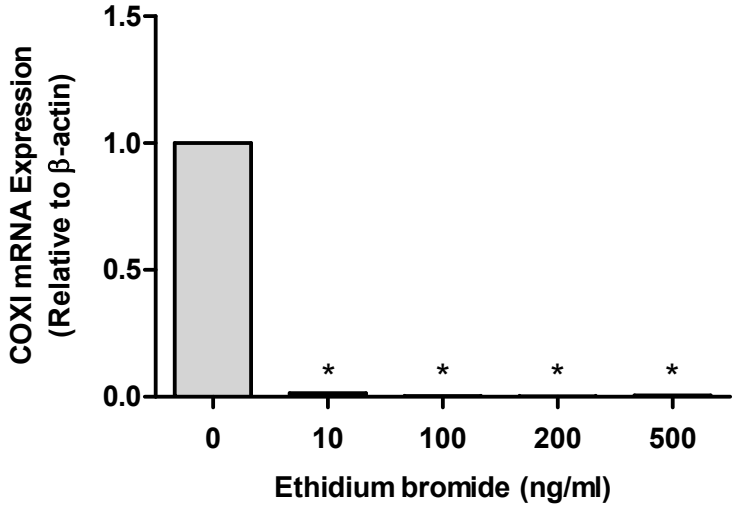

Figure 66 – Dose response of HIF-1α and COX1 mRNA following EtBr treatment

Cells were treated with ethidium bromide (0-500 ng/ml) for 7 days. Total RNA was obtained from cells, reverse transcribed into cDNA and mRNA copy numbers of HIF-1α (A) and COX1 (B) were quantified by quantitative reverse transcriptase PCR and normalised against β-actin and expressed relative to control. The values represent the mean $\pm$ SEM from 3 independent experiments; * represents a significant difference ($p < 0.05$) from control.

(A)

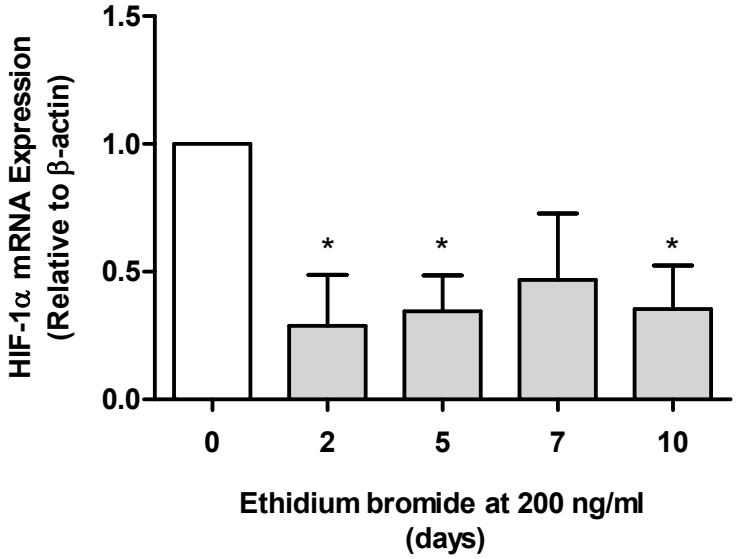

(B)

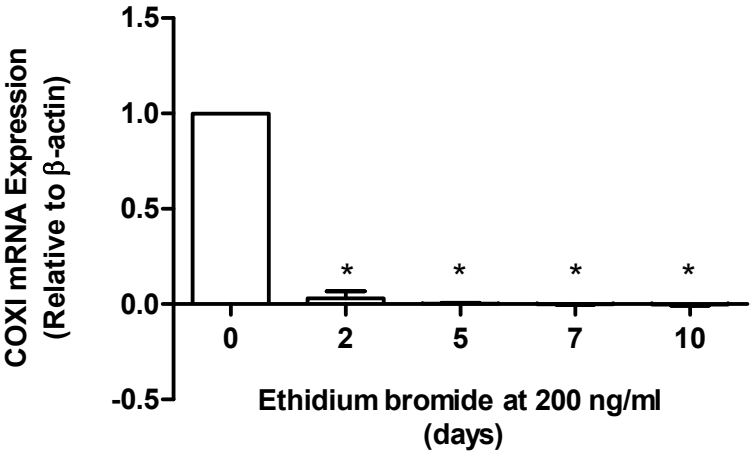

Figure 67 – Time course of HIF-1α and COX1 mRNA after 200 ng/ml EtBr

Cells were treated with 200 ng/ml ethidium bromide (EtBr) (0-10 days). Total RNA was obtained from cells, reverse transcribed into cDNA and mRNA copy numbers of HIF-1α (A) and COX1 (B) were quantified by quantitative reverse transcriptase PCR and normalised against β-actin and expressed relative to control. The values represent the mean ± SEM from 3 independent experiments; * represents a significant difference ($p < 0.05$) from control.

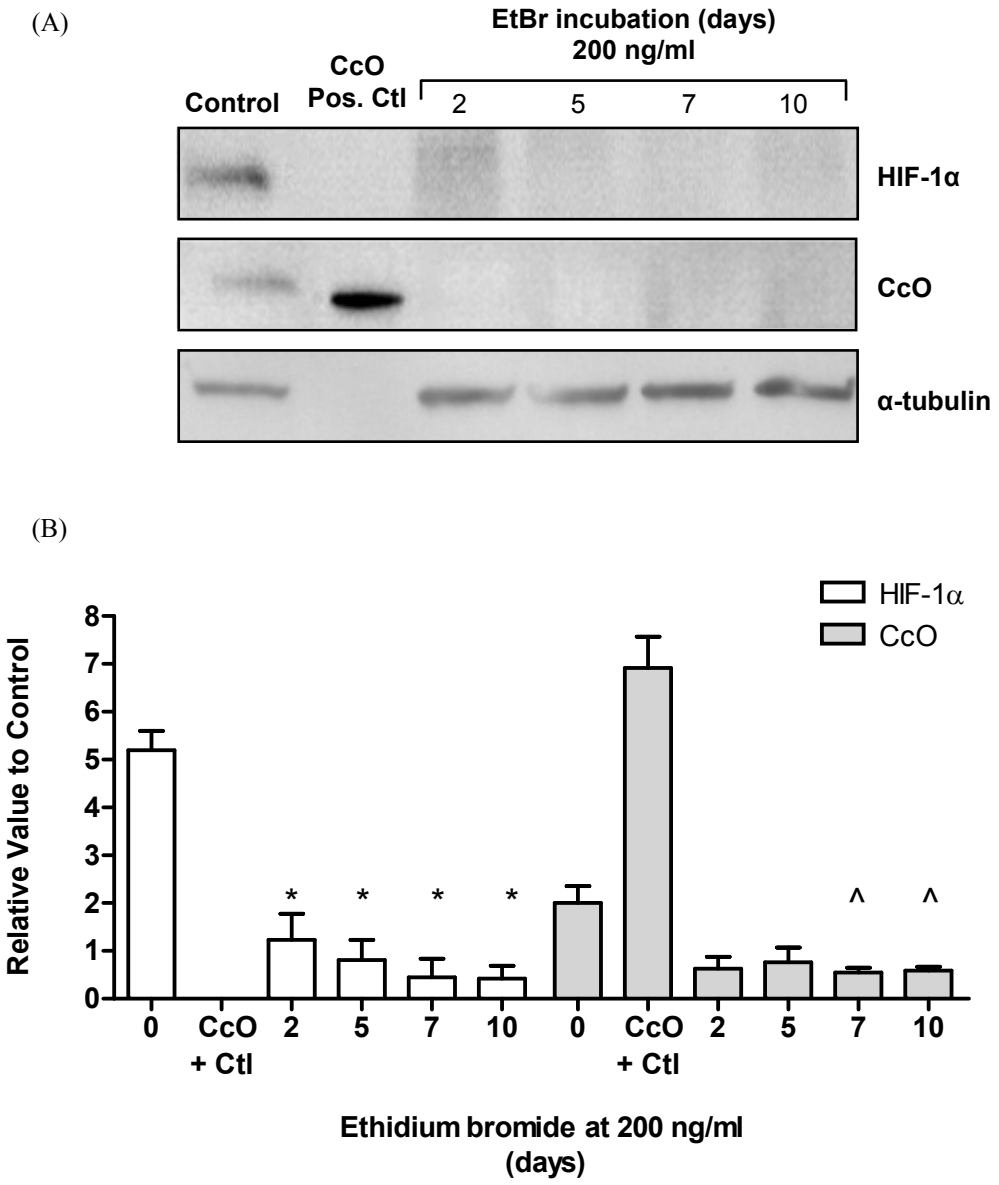

Figure 68 – Effect of Ethidium bromide on HIF-1α and CcO protein expression

Cells were treated with 200 ng/ml ethidium bromide (EtBr) for up to 10 days. Cell lysates were subject to SDS-PAGE and analysed by Western blot (A) and quantified by densitometry (B). The corresponding densitometry values were normalised with α-tubulin and results are shown relative to control. The values represent the mean ± SEM from 3 independent experiments; * represents a significant difference ($p < 0.05$) from HIF-1α control and ^ represents a significant difference ($p < 0.05$) from CcO control. One representative blot is shown.

5.4.2 Effect of ethidium bromide on respiration in H157 cells

Cells were incubated with 200 ng/ml EtBr for 10 days and placed in the respiration chamber of the VLS system to monitor VO_2 during cellular respiration to anoxia. Studies of the VO_2 showed that control cells respire at ~ 18 μM O_2/min/10^7cells. Cells treated with ethidium bromide respire at ~ 12 μM O_2/min/10^7cells (Figure 69).

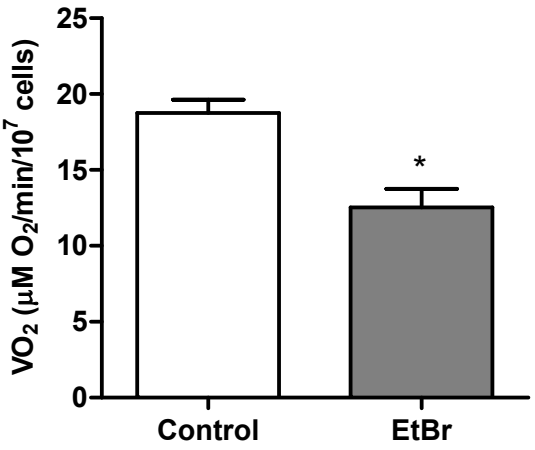

Figure 69 – Effect of Ethidium bromide on VO_2 in H157 cancerous cells

HI157 cells were incubated with 200 ng/ml ethidium bromide (EtBr) for 10 days. Values of VO_2 were measured from intact cells during respiration to anoxia using the VLS system. The values represent the mean $\pm$ SEM from 3 independent experiments; * represents a significant difference ($p < 0.05$) from control (non-treated cells).

5.4.3 Hypoxic HIF-1α stabilisation in ethidium bromide treated cells

To confirm the inhibition of HIF-1α stabilisation was not due to a direct effect of EtBr treatment, cells were placed in hypoxia (0.5%) for 7 days and treated with 200 ng/ml EtBr. Stabilisation of HIF-1α was observed in both control and EtBr treated cells at 0.5% oxygen (Figure 70).

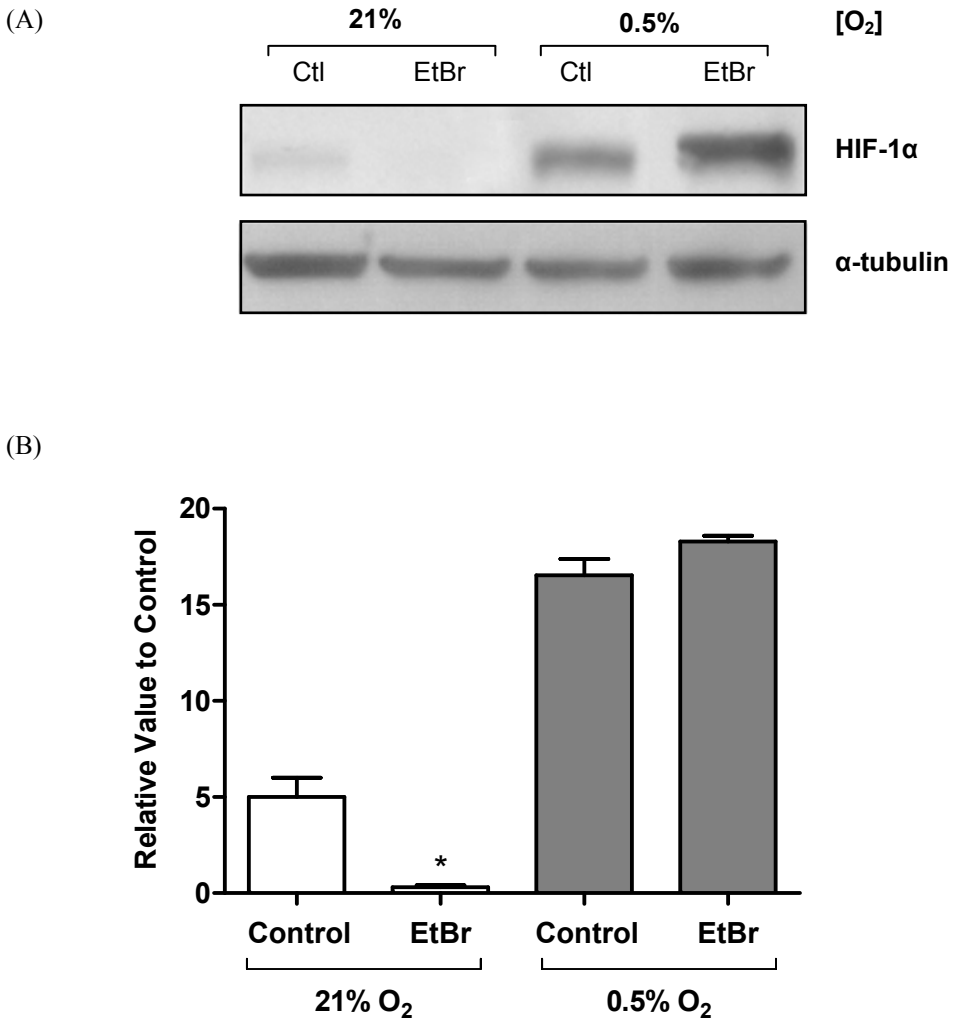

Figure 70 – Effect of Ethidium bromide on HIF-1α stabilisation in hypoxia

Cells were treated with 200 ng/ml ethidium bromide (EtBr) for 7 days. Cells were then incubated at 0.5% oxygen for 2 h. Cell lysates were subject to SDS-PAGE and analysed by Western blot (A) and quantified by densitometry (B). The corresponding densitometry values were normalised with α-tubulin and results are shown relative to control. The values represent the mean $\pm$ SEM from 3 independent experiments; * represents a significant difference ($p < 0.05$) from control. One representative blot is shown.

5.5 Alternative source of ROS induced HIF-1α stabilisation

The data above suggests HIF-1α can be stabilised by mitochondrial ROS, other ROS sources, however, may be responsible. Another major contributor to cellular ROS generation is the family of NADPH oxidases (NOX). Hypoxic up-regulation of a NOX and subsequent augmented ROS generation has been linked to HIF-1α accumulation (Goyal *et al.*, 2004).

To establish whether ROS generated from NOX stabilise HIF-1α, the expression of NOX in HEK 293T cells was evaluated. Isoforms NOX2 and NOX4 of NADPH oxidase are reportedly expressed in HEK 293T cells at an endogenous level (Anilkumar *et al.*, 2008). Therefore, NOX2 and NOX4 protein expression was determined via Western blot in cell lysates. Figure 71 shows endogenous NOX2 can be detected in cell lysates. Endogenous NOX4 was not detectable in cell lysates (data not shown).

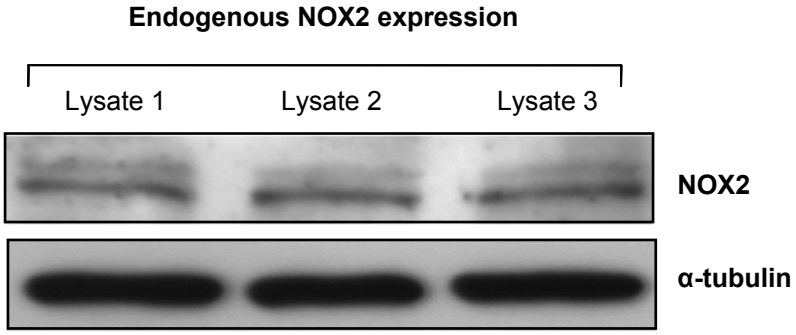

Figure 71 – Endogenous NOX2 protein expression in HEK 293T cells

HEK 293T cell lysates were subject to SDS-PAGE and analysed by Western blot for endogenous NOX2 protein expression. (n = 3).

5.5.1 NOX2 silencing in HEK 293T cells

We next set out to silence NOX2 using siRNA. Previous data (section 4.4.1) demonstrated that optimal fluorescence for siRNA conjugated to Alexa Fluor 555 was between 12 and 24 h post silencing. A similar time frame was therefore used to study the silencing of NOX2 in cells. Small interfering RNA (scrambled and NOX2) was prepared, and plated into a 6 well plate. Cells were then seeded on top in low serum, antibiotic free media.

To determine successful NOX2 silencing, NOX2 mRNA and protein was determined. In parallel, NOX1, NOX4 and NOX5 mRNA gene expression was also evaluated. Silencing NOX2 causes a time-dependent reversible decrease in NOX2 mRNA (Figure 72) and protein (Figure 74). There was also a time-dependent reversible decrease in NOX1, NOX4 and NOX5 mRNA (Figure 73). There was no difference in mRNA and protein expression in scrambled transfected cells (data not shown).

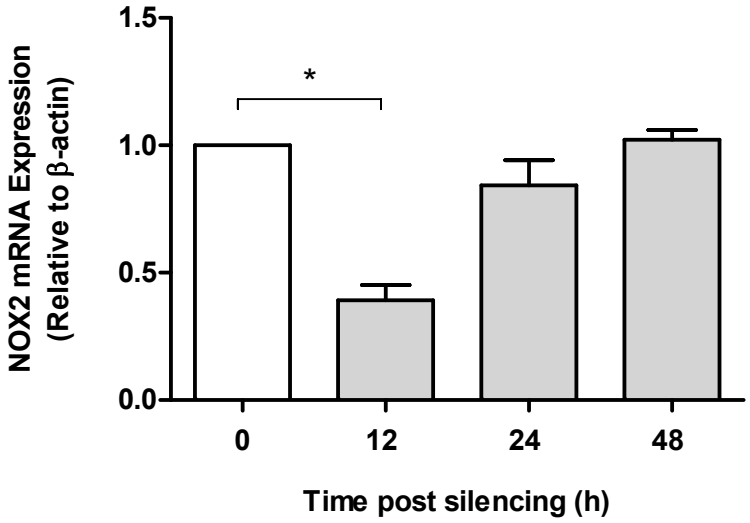

Figure 72 – NOX2 mRNA expression in NOX2 silenced cells

Cells were transfected with NOX2 siRNA at 21% oxygen for 24 h. Total RNA was obtained from cells, reverse transcribed into cDNA and mRNA copy numbers of NOX2 were quantified by quantitative reverse transcriptase PCR and normalised against β-actin and expressed relative to control. The values represent the mean $\pm$ SEM from 3 independent experiments; * represents a significant difference ($p < 0.05$) from control.

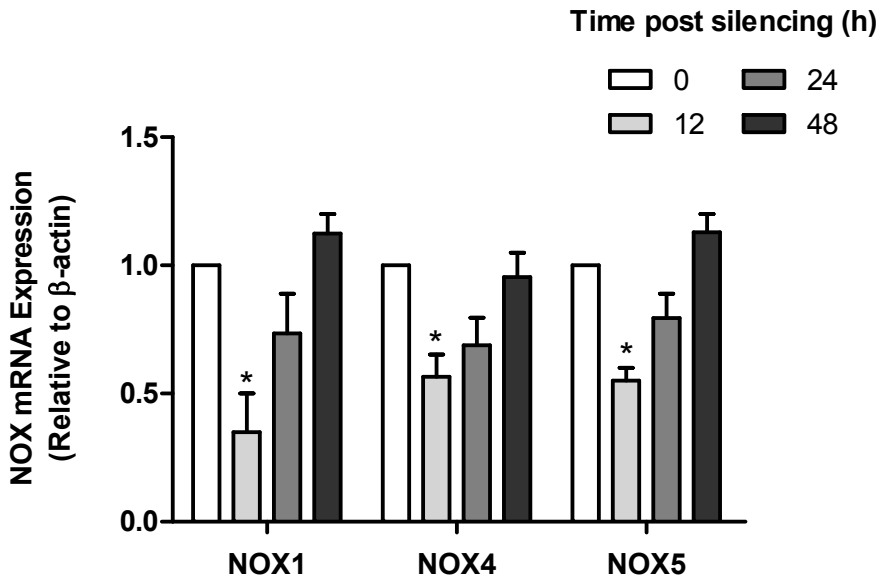

Figure 73 – NOX1, NOX4 and NOX5 mRNA expression in NOX2 silenced cells

Cells were transfected with NOX2 siRNA at 21% oxygen for 24 h. Total RNA was obtained from cells, reverse transcribed into cDNA and mRNA copy numbers of NOX1, 4 and 5 were quantified by quantitative reverse transcriptase PCR and normalised against β-actin and expressed relative to control. The values represent the mean $\pm$ SEM from 3 independent experiments; * represents a significant difference ($p < 0.05$) from control.

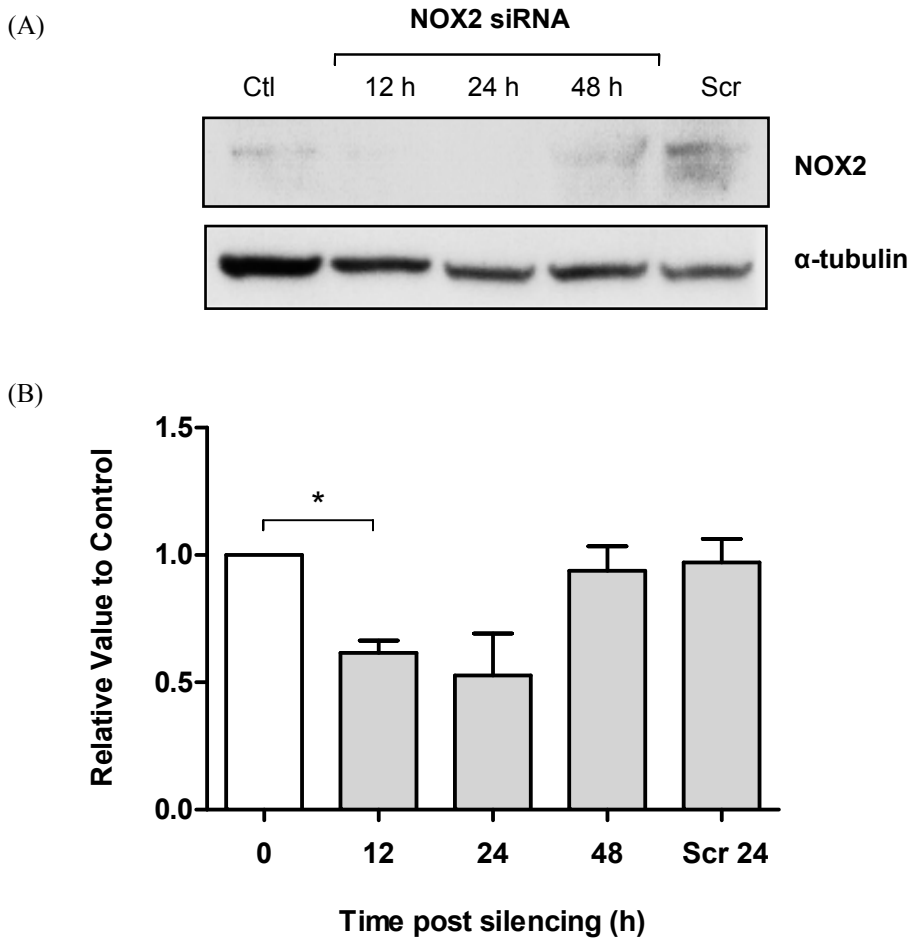

Figure 74 – NOX2 protein expression after NOX2 siRNA transfection

Cells were transfected with NOX2 siRNA at 21% oxygen (0-48 h) and a non-targeting control siRNA sequence (Scr) for 24 h. Cell lysates were subject to SDS-PAGE and analysed by Western blot (A) and quantified by densitometry (B). The corresponding densitometry values were normalised with α-tubulin and results are shown relative to control. The values represent the mean $\pm$ SEM from 3 independent experiments; * represents a significant difference ($p < 0.05$) from control.

5.5.2 Silencing NOX2 at 3% oxygen does not effect HIF-1α stabilisation

Once successful silencing of NOX2 (and other NOX isoforms) had been confirmed, experiments were performed to investigate the effect this would have on HIF-1α stabilisation at low [O_2]. To determine the effect of transfecting NOX2 siRNA in cells at 3% oxygen, NOX2 protein was determined. Figure 75 (A) and (B) shows NOX2 is silenced at 3% oxygen but there is no effect on HIF-1α stabilisation (Figure 75 (A) and (C)).

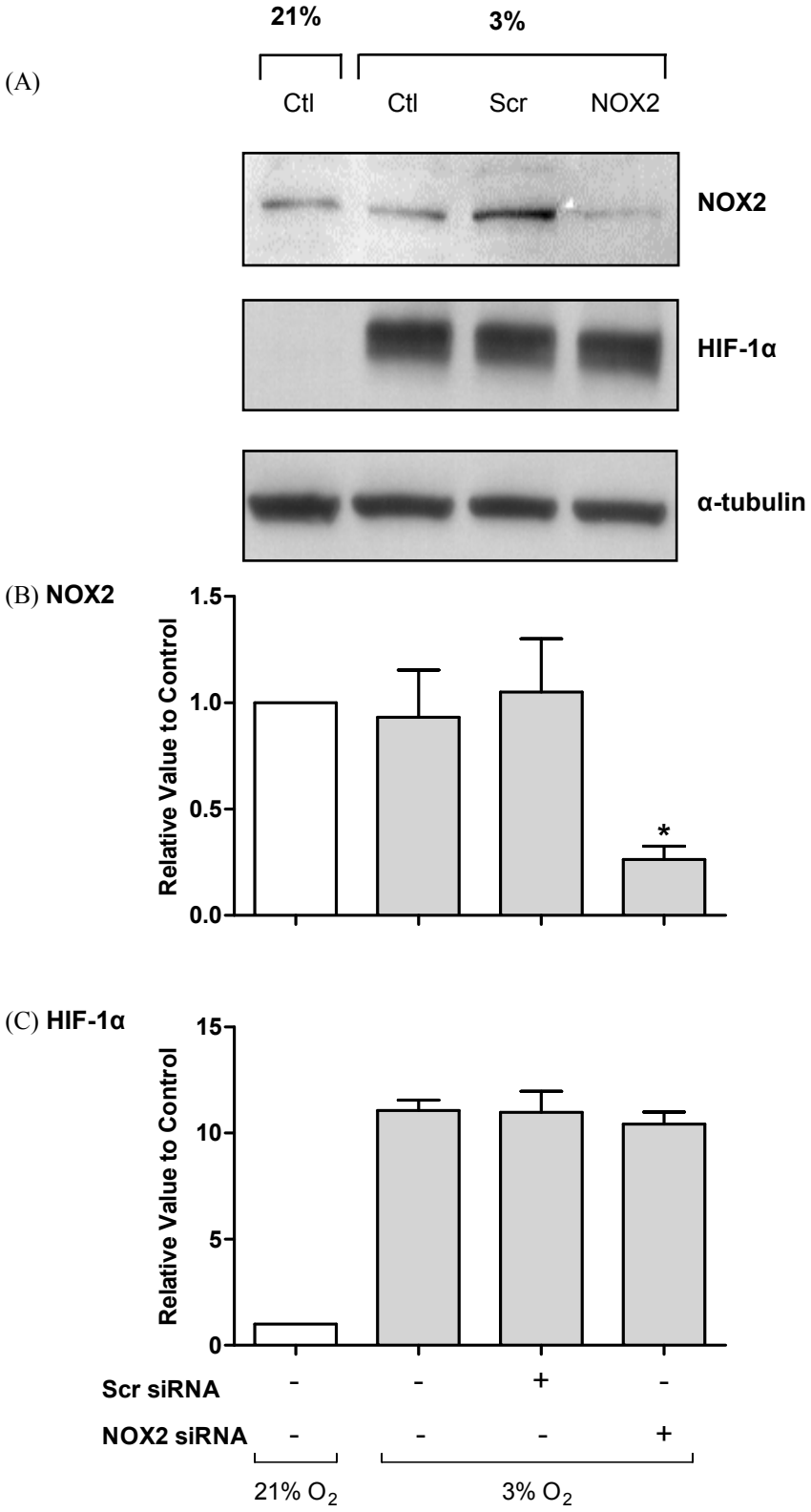

Figure 75 – HIF-1α stabilisation in cells transfected with NOX2 siRNA

Cells were transfected with NOX2 siRNA at 21% and 3% oxygen (24 h) and a non-targeting control siRNA sequence (Scr) at 3% oxygen (24 h). Cell lysates were subject to SDS-PAGE and analysed by Western blot (A) and quantified by densitometry (B) NOX2 and (C) HIF-1α. The corresponding densitometry values were normalised with α-tubulin and results are shown relative to control. The values represent the mean ± SEM from 3 independent experiments; * represents a significant difference ($p < 0.05$) from control.

5.6 Summary of key results

A *Rho*^{0} phenotype, defined as non-respiring cells with no mitochondrial DNA was successfully induced in HEK 293T cells. We were able to demonstrate that these cells produced less ROS compared to un-induced cells and cells transfected with γGCS siRNA at 21% oxygen. In addition, antioxidants had no effect. The level of ROS produced at 3% oxygen was also diminished to that of normoxic control cells. Crucially, *Rho*^{0} cells did not stabilise HIF-1α in response to treatment with γGCS siRNA or at 3% oxygen, with no effect observed at 0.5% oxygen. In another model of normoxic HIF-1α stabilisation, H157 carcinoma cells were successfully induced as *Rho*^{0} cells using ethidium bromide. In these cells, HIF-1α stabilisation was prevented at 21% oxygen, but remained stable at 0.5% oxygen. Silencing NOX2 (and the other isoforms) had no effect on HIF-1α stabilisation at 3% oxygen.

Chapter six:
Discussion and conclusion

Chapter six: Discussion and conclusion

6.1 Background and aim of current study

Hypoxia-inducible factor-1 (HIF-1) is a transcriptional activator that functions as a master regulator of the cellular response to decreases in oxygen concentration. The importance of HIF-1 in physiological processes is emphasised by the vast array of target genes that are controlled by HIF-1, including genes involved in erythropoiesis, glucose transport, glycolysis, iron transport and cell proliferation/survival. HIF-1 also plays key roles in critical aspects of tumour progression by promoting angiogenesis, cell survival, glucose metabolism and invasion. Tumour micro-environment and genetic mutations can lead to HIF-1α over-expression, and this is closely correlated with increased patient mortality in several cancer types (Semenza, 2009a).

HIF-1 is a heterodimeric protein that consists of a constitutively expressed HIF-1β subunit and a HIF-1α subunit, the expression of which is highly regulated. The α-subunit is degraded under normoxic oxygen conditions (21%) but is stabilised at low (3%), hypoxic (0.5%) and anoxic (0%) oxygen concentrations ($[O_2]$). More recently, evidence from several groups has demonstrated that HIF-1α can be regulated by oxygen-independent mechanisms, and more specifically, by the generation of reactive oxygen species (ROS) at low $[O_2]$ (Chandel *et al.*, 1998;Agani *et al.*, 2000;Chandel *et al.*, 2000a;Guzy *et al.*, 2005;Quintero *et al.*, 2006a). Stabilisation of the α-subunit by ROS has been shown to be a possible consequence of mitochondrial ROS production (Mansfield *et al.*, 2005;Brunelle *et al.*, 2005).

The aim of this study was to investigate the effect of ROS on the stabilisation of HIF-1α, both in normoxic and low $[O_2]$, and ultimately to determine the cellular source of free radicals involved in HIF-1α stabilisation.

6.2 Mechanisms of HIF-1α stabilisation

Most organisms are dependent on a continuous supply of oxygen for survival. Sensing and responding to changes in oxygen partial pressure assures that the cellular oxygen supply is tightly controlled in order to balance the risk of oxidative damage vs. oxygen deficiency (Brune and Zhou, 2007). This delicate balance is disrupted in a variety of pathological conditions including heart disease and cancer (Semenza, 2000). A decrease in oxygen availability needs to be sensed in order to provoke appropriate changes that in turn circumvent hypoxic episodes, which are potentially harmful to cells, organs or the organism. A fundamental step in oxygen sensing involves a transcription factor named HIF-1 (Wang and Semenza, 1993).

The intracellular oxygen concentration varies widely in different tissues due to the dynamic relationship between oxygen supply and demand, making hypoxia difficult to define. Many authors use the term 'hypoxia' to describe the oxygen concentration used in their study. However, little consistency exists between studies concerning the actual oxygen concentrations used, thus leading to confusing interpretation of results. For the purpose of this discussion, we have defined low [O_2] as between 3% and 1.5%, and hypoxia as below 1.5% oxygen.

HIF-1α can be stabilised through both oxygen-dependent and independent mechanisms. Indeed, a decrease in oxygen availability, as well as increases in nitric oxide (NO) and reactive oxygen species (ROS) have been described in the regulation of HIF-1α. This study has investigated the role of these different parameters in HIF-1α stabilisation.

6.2.1 Oxygen-dependent stabilisation of HIF-1α

6.2.1.1 HIF-1α stabilisation in hypoxia

HIF-1 was first detected in nuclear extracts from Hep3B cells cultured in 1% oxygen, during studies investigating the hypoxia-dependent expression of erythropoietin (EPO) (Wang and Semenza, 1993). These authors also demonstrated HIF-1 DNA binding activity decayed rapidly when hypoxic cells were exposed to increased oxygen tension. It was later described that the expression of HIF-1α, and HIF-1 transcriptional activity increased exponentially as cellular oxygen concentrations decrease (Jiang *et al.*, 1996). HIF expression is therefore most commonly associated with hypoxia. Hypoxia is a

fundamental physiological stimulus that occurs in response to tissue growth during normal development and in disease states such as anemia, haemorrhage, cardiovascular disease and cancer (Semenza, 2009b). When cells are subjected to acute hypoxia, the hydroxylation reactions, which prepare HIF-1α for proteasomal degradation, are inhibited as a result of substrate (O_2) deprivation and/or, as we have now shown, mitochondrial ROS production (section 6.5). Loss of hydroxylase activity increases HIF-1α stability and transactivation function, leading to dimerisation with HIF-1β, translocation to the nucleus, binding of HIF-1 to its recognition sequence (HRE) and increased transcription of target genes.

Initial experiments were therefore designed to test whether HIF-1α was stabilised in HEK 293T and H157 carcinoma cells following exposure to experimental normoxia (21% oxygen) through to hypoxia. As expected, oxygen deprivation results in a progressive increase in HIF-1α stabilisation, attributed to the decrease in PHD activity (Willam *et al.*, 2004), as oxygen, the key substrate required for their hydroxylation activity becomes the limiting factor.

6.2.1.2 HIF-1α stabilisation at low [O_2]

Originally, Chandel *et al.*, 1998 suggested that ROS generated at low [O_2] (1.5% oxygen) were responsible for stabilising HIF-1α, and in recent years further evidence has been produced (Sanjuan-Pla *et al.*, 2005;Mansfield *et al.*, 2005).

In support of this, our data shows that HIF-1α stabilisation at low [O_2], but not in hypoxia, is prevented by treatment with antioxidants (NAC plus ascorbate). It is worth noting that HIF-1α stabilisation is greater at 0.5% oxygen than at 3% oxygen. Therefore, the effect of antioxidants was compared when levels of HIF-1α stabilisation were similar (24 h 3% oxygen vs. 2 h 0.5% oxygen). This observation implies that in hypoxia HIF-1α stabilisation is oxygen-dependent, whereas at low [O_2] HIF-1α stabilisation is dependent on free radicals. However, the addition of ascorbate has been suggested to enhance PHD activity (hence increasing hydroxylation reactions) rather than decreasing ROS via reduction of ferric iron to ferrous iron, thereby modulating HIF-1α protein accumulation (Pan *et al.*, 2007). With this in mind, further experiments were performed using an alternative antioxidant, one that is not a co-factor for PHD activity. Glutathione (GSH) is the most abundant intracellular antioxidant. As native

GSH does not permeate the cell membrane, methylated GSH was used. Treatment of cells with methylated GSH at low [O_2] prevented HIF-1α stabilisation in a dose-dependent manner. This data provides further evidence to suggest that HIF-1α stabilisation is dependent on a free radical mechanism at low [O_2] since it can be suppressed by antioxidants NAC plus ascorbate and GSH.

We have also been able to demonstrate that H157 carcinoma cells incubated with either L-NMMA (a non-specific NOS inhibitor) or antioxidants at low [O_2] show a reduction in the stabilisation of HIF-1α. However, in hypoxia this treatment has no effect. This supports data from Quintero *et al.,* 2006 demonstrating that HIF-1α stabilisation was prevented at 3% oxygen in H157, H357 and B1CR6 oral squamous carcinoma cells by inhibition of NOS activity using L-NMMA and also by antioxidants, thus suggesting that the mechanism is dependent on a free radical reaction (Quintero *et al.*, 2006a). Exposure of these cells to hypoxia however, resulted in HIF-1α stabilisation, which was not prevented by L-NMMA or antioxidants.

From the observations made using HEK 293T and H157 carcinoma cells exposed to varying oxygen concentrations, our data suggests that at low [O_2], but not in hypoxia, a ROS-dependent mechanism of HIF-1α stabilisation exists. It has also been shown by other authors that the addition or expression of antioxidants is sufficient to reverse HIF-1α stabilisation at low [O_2] (Sanjuan-Pla *et al.*, 2005;Guzy *et al.*, 2005). However, conflicting reports have demonstrated that enzymatically-generated superoxide actually reduces HIF-1α protein levels (Wellman *et al.*, 2003) and a separate study has demonstrated that non-toxic levels of hydrogen peroxide did not result in HIF-1α stabilisation (Tuttle *et al.*, 2007). Herein, further experiments were designed to study HIF-α stabilisation by both exogenous and endogenously released ROS.

6.3 ROS-dependent stabilisation of HIF-1α in normoxia

Reactive oxygen species (ROS) have long been recognised as bona fide second messengers, having been suggested to activate a number of transcription factors, including nuclear factor kappa B (NF-κB), activator protein 1 (AP-1), specificity protein 1 (Sp1), peroxisome proliferator-activated receptors (PPARs), among others (Lavrovsky *et al.*, 2000). ROS have also been implicated in the regulation of HIF-1α stability (Chandel *et al.*, 1998)

6.3.1 Pharmacological agents

Pharmacological agents such as cobalt chloride ($CoCl_2$) have also been shown to regulate HIF-1α stability in normoxia via various mechanisms. These include increased ROS production (Chandel *et al.*, 1998) and inhibition of the interaction between HIF-1α and the VHL protein (Yuan *et al.*, 2003). We found that indeed, the addition of $CoCl_2$ stabilised HIF-1α in normoxia. In order to validate our experiments, we also used menadione, which has also been reported to release ROS (Criddle *et al.*, 2006). Our own experiments showed that menadione did release ROS and we used it to investigate whether exogenous ROS stabilised HIF-1α. Both compounds stabilised HIF-1α in a dose-dependent manner. Treatment with antioxidants prevented the observed normoxic stabilisation of HIF-1α, further validating the role of ROS. Furthermore, both compounds have a synergistic effect on HIF-1α stabilisation in hypoxia.

6.3.2 Carcinoma cells

We were able to extend these findings by looking at HIF-1α stabilisation in H157 carcinoma cells at 21% oxygen. These cells express HIF-1α and iNOS (Quintero *et al.*, 2006a) which make them ideal to investigate the role of ROS in HIF-1α stabilisation. Malignant tissue often produces free radicals (Szatrowski and Nathan, 1991;Bae *et al.*, 1997;Ha *et al.*, 2000), thus in these cells, NO might be released in an environment favouring free radical reactions leading to peroxynitrite formation. Our results show that HIF-1α was present at 21% oxygen in these cells. Treatment with antioxidants, but not L-NMMA prevented normoxic stabilisation of HIF-1α, providing additional evidence towards a ROS-induced mechanism of HIF-1α stabilisation.

6.3.3 Macrophages

It has recently been shown that bacterial infection and inflammatory sites, often characterised by low oxygen concentrations (Zinkernagel *et al.*, 2007) stabilise HIF-1α in macrophages (MΦ) in a way that is independent of oxygen concentration (Peyssonnaux *et al.*, 2005).

It is well known that MΦ produce high concentrations of nitric oxide (NO) upon activation (Stuehr and Nathan, 1989;Garedew and Moncada, 2008) and hence investigations proceeded to explore the role of NO in HIF-1α stabilisation in activated murine MΦ. Upon activation, nitrite concentrations increased suggesting an increase in iNOS activity, as this is the major source of NO in these cells (Garedew and Moncada, 2008). Nitrite accumulation was abolished in activated MΦ when co-treated with SEITU, a specific iNOS inhibitor. In these experiments, we also found that HIF-1α was stabilised after MΦ activation in a biphasic manner. The early stabilisation observed after 1.5 h was insensitive to treatment with SEITU but sensitive to antioxidants. It was not surprising that SEITU had no effect on HIF-1α stabilisation at 1.5 h post-activation since nitrite accumulation was not observed until 6 h activation. The later stabilisation, however, was dependent on the generation of NO as it could be abolished by treatment with SEITU. Treatment with antioxidants did not prevent HIF-1α stabilisation in the latter time points, initially suggesting this was entirely NO-dependent. However, in a situation where there is a lot of free radicals and NO (as in the case of activated MΦ), HIF-1α may be stabilised by possible peroxynitrite formation. Thus perhaps, in these conditions the antioxidants used were not enough to detoxify the ROS produced. Therefore, the latter stabilisation could still be ROS-dependent rather than exclusively NO-dependent.

Our data is in agreement with Peyssonnaux *et al.*, 2005. These authors show that the loss of HIF-1$\alpha^{-/-}$ in MΦ attenuates iNOS induction in response to bacterial stimulation (Peyssonnaux *et al.*, 2005). During inflammation HIF-1 is critically involved in iNOS up-regulation, while reduced NO production as seen in HIF-1$\alpha^{-/-}$ cells, impairs MΦ TNF-α production and bactericidal activity (Peyssonnaux *et al.*, 2005).

6.3.4 Genetically-induced pro-oxidant environment

With conflicting data in the literature, we wanted to tackle the issue of ROS-induced HIF-1α stabilisation in normoxia (initially) without the addition of pharmacological agents. We decided to decrease the biosynthesis of glutathione (GSH) (an important cellular antioxidant) (Krzywanski *et al.*, 2004) using an *in vitro* model previously employed by Diaz-Hernandez *et al*., 2007. These authors showed that impairment of GSH biosynthesis in primary cortical neurons induced ROS production and triggered apoptotic death (Diaz-Hernandez *et al.*, 2007). This demonstrates the importance of GSH biosynthesis in protecting cells from the harmful effects of excessive ROS production.

We used RNA interference (RNAi) to selectively knock down the catalytic subunit of γ-glutamyl cysteine synthetase (γGCS), the rate-limiting enzyme in GSH biosynthesis. Using small interfering RNA (siRNA) sequences against human γGCS, we observed a reduction in the expression of the protein higher than 80%. This correlated with a ~ 40% decrease in total cellular GSH levels. Furthermore, our own data has showed that silencing the catalytic subunit of γGCS results in a 2-fold increase in ROS production at 21% oxygen, accompanied by an increase in HIF-1α protein stabilisation. Treatment with antioxidants abolished this enhanced stabilisation of HIF-1α, further suggesting a role of ROS in the observed stabilisation of HIF-1α. Previously, it has been shown in a B cell lymphoma cell line that administration of L-buthionine sulfoximine (L-BSO); a competitive inhibitor of γGCS activity, resulted in apoptosis, which correlated with depleted GSH levels and an increase in ROS production (Armstrong *et al.*, 2002). These data further extend our findings, which demonstrate that genetic inhibition of γGCS in HEK 293T cells was sufficient to cause a decrease in GSH concentrations, as well as increases in ROS production.

We also decided to confirm these results using an alternative method to achieve γGCS silencing. We used synthetic double-stranded siRNA molecules which can be introduced into cells to suppress gene expression transiently. We silenced the catalytic subunit of γGCS, both at the mRNA and protein levels (approximately 90% and 80% reduction respectively). We confirmed the functional silencing of γGCS by analysing the cellular GSH levels and observed a marked decrease (approximately 60% decrease) when compared with control (mock-transfected) cells. We also found that as previously

observed, there was a 2-fold increase in DCF fluorescence in cells where γGCS had been silenced. Thus, we achieved two independent genetic models in which the desired phenotype was attained.

There are concerns, however, that the detection of ROS using DCFH may be unreliable due to superoxide formation during the conversion of DCFH to the fluorescent dye DCF or upon exposure to light (Rota *et al.*, 1999). In addition, DCFH and related compounds/dyes are sensitive to multiple types of ROS, including ROS and RNS species (Droge, 2002) and cannot be targeted to specific intracellular components. Thus, there are multiple shortcomings to detection and visualisation of ROS with DCFH, which may result in false positive or over amplified signals (Belousov *et al.*, 2006). Alternative methods to measure the formation of ROS and RNS include fluorometric and spectrophotometric methods, chemiluminescence and electron paramagnetic resonance (Chance *et al.*, 1979;Pou *et al.*, 1989;Tarpey and Fridovich, 2001). These methods rely on the redox properties of specific ROS and RNS, and therefore are prone to artefacts (as with DCFH) caused by species of similar reactivity or by reactive intermediates produced by the probe itself (Picker and Fridovich, 1984;Faulkner and Fridovich, 1993;Liochev and Fridovich, 1995;Liochev and Fridovich, 1998).

To address the weakness of DCFH (and other such ROS indicators) as a probe to measure ROS, we proceeded to utilise a new class of ROS sensor. To overcome the disadvantages of existing methods for detecting ROS, Belousov *et al*., 2006 developed a genetically encoded biosensor for hydrogen peroxide (H_2O_2). This sensor consists of yellow fluorescent protein (YFP) inserted into the regulatory domain of *Escherichia coli* OxyR (OxyR-RD). The indicator, named HyPer (from hydrogen peroxide) demonstrates sub-micromolar reactivity to H_2O_2, and at the same time it is insensitive to other oxidants (Belousov *et al.*, 2006). Based on these characteristics, HyPer can be used as an accurate monitor of intracellular H_2O_2 levels. Using HyPer transfected HEK 293T cells, where γGCS has been silenced, we observed that H_2O_2 levels were twice that of the control. Additionally, treatment with an antioxidant abolished this increase. These data corroborate our previous DCFH-based observations that ROS accumulation occurs in cells where γGCS is silenced. Since there was a two-fold increase in HyPer fluorescence it would strongly suggest that the vast majority of ROS produced in this silencing model is H_2O_2.

Following confirmation of increased ROS production in our γGCS-silencing model, HIF-1α stabilisation was also observed. Moreover, antioxidants reversed this normoxic stabilisation confirming our previous observations showing stabilisation of HIF-1α in normoxic conditions by ROS.

We also observed a two-fold increase in catalase and Nrf2 and a three-fold increase in manganese superoxide dismutase and thioredoxin, suggesting that when γGCS has been disrupted, cells attempt to compensate for the increase in ROS by increasing the expression of other antioxidant genes (Colombo and Moncada, 2009). ROS production has also been linked to the activation of the nuclear factor kappa B (NF-κB) (Palacios-Callender *et al.*, 2004). Our experiments show that down-regulation of γGCS caused an increase in ROS which correlated with an increase in NF-κB expression.

6.4 Mechanism of ROS-induced HIF-1α stabilisation

Our findings add to an increasing body of evidence that suggests ROS stabilise HIF-1α in both normoxia and at low [O_2]. The mechanism by which ROS stabilise HIF-1α has yet to be fully clarified. It has been proposed to occur through modifications in the PHDs, such as nitrosylation (Metzen *et al.*, 2003) or changes in the redox state of their ferrous iron (Gerald *et al.*, 2004).

The immediate regulators of HIF-1α stability are the prolyl hydroxylases (PHD), a family of oxidases involved in the post-translational modification that signals HIF-1α for degradation (Epstein *et al.*, 2001;Berra *et al.*, 2003). PHD use 2-oxoglutarate and oxygen as substrates and require ferrous iron (Fe^{2+}) as a cofactor. Chemical inhibitors that block the activity of PHD, such as iron chelators that deprive the enzyme of Fe^{2+} (desferoxamine), or which consequently competes with 2-oxoglutarate for binding at the hydroxylase (DMOG), prevent HIF-1α proline hydroxylation and cause accumulation of HIF-1α as well as activation of HIF-dependent gene expression (Ivan *et al.*, 2002).

Cells cultured under low [O_2] stabilise HIF-1α; however, recent studies, including our own, have found that such accumulation is dependent on functional mitochondria (section 6.5) (Chandel *et al.*, 2000a;Mansfield *et al.*, 2005). Questions remain concerning the signalling pathway linking mitochondrial ROS production to the inhibition of PHD activity. ROS may regulate the redox state of iron through the Fenton

reaction. Therefore, low oxygen levels may inhibit PHD activity because ROS decrease the availability of the PHD cofactor Fe^{2+} (Gerald *et al.*, 2004) rendering the enzyme inactive. It has been shown however that low-level ROS formation increased PHD activity in both normoxia and hypoxia (Callapina *et al.*, 2005).

In both our genetic models, we have observed HIF-1α stabilisation, implying an inhibition of PHD activity (since the observed stabilisation was in normoxic conditions). Exogenous hydrogen peroxide has been shown to stabilise HIF-1α at ambient oxygen concentrations (Simon, 2006;Bell *et al.*, 2007), implying ROS inhibit the hydroxylation reaction. To investigate this further, we used a proteasomal inhibitor (MG132) to detect hydroxylated HIF-1α protein at 21% oxygen. Prelimary results showed that HIF-1α was hydroxylated in our ROS-induced HIF-1α model, suggesting it had been targeted for hydroxylation and therefore the PHD were not inhibited by enhanced ROS production. We went on to show that HIF-1α appeared to be ubiquitinated and thus possibly being targeted for proteasomal degradation. How then is it that HIF-1α is stabilised in our model? Our data shows that the gene expression of HIF-1α was increased 2-fold in our ROS-induced model of HIF-1α stabilisation. This preliminary data suggests that HIF1-α is stabilised by ROS increasing its synthesis (transcription), rather than ROS inhibiting PHD activity and ultimately preventing HIF-1α degradation. Indeed, Yuan *et al.,* 2008 demonstrate that ROS generated by NADPH oxidase was required for HIF-1α accumulation by intermittent hypoxia (IH) in PC12 cells. HIF-1α levels in cells exposed to IH with cyclohexamide (an inhibitor of protein synthesis) were similar to those exposed to IH alone, suggesting that increased HIF-1α accumulation in the absence of cyclohexamide was at least in part due to new synthesis of HIF-1α protein (Yuan *et al.*, 2008).

However, to confirm this hypothesis, further studies would be required using cyclohexamide and treatment with actinomycin D (a transcription inhibitor). Also, questions remain as to which signal transduction pathways lead to HIF-1α synthesis. In the case of intermittent hypoxia (IH)- induced HIF-1α stabilisation are known to involve NADPH oxidase-dependent ROS production that, through a signalling cascade involving inostitol 1,4, 5- triphosphate (IP3), diacylglycerol (DAG), calcium-calmodulin kinase (Ca/CAMK) and protein kinase C (PKC), stimulate mTOR-dependent HIF-1α synthesis.

Furthermore, recent data demonstrates that there is no evidence for hydrogen peroxide dependent inhibition of PHD activity (Chua *et al.*, 2010). This confirms our own results that ROS do not regulate PHD activity directly.

6.5 Mitochondrial ROS-induced HIF-1α stabilisation

Studies investigating the involvement of the electron transport chain in oxygen sensing revealed that a functional mitochondrial chain was required for HIF-1α stabilisation. This observation was made during studies using electron transport chain inhibitors, since rotenone (an inhibitor of the distal end of Complex I), myxothiazol and stigmatellin (inhibitors of the upstream end of Complex III), were capable of preventing HIF-1α stabilisation at low [O_2] (Chandel *et al.*, 1998;Agani *et al.*, 2000;Guzy *et al.*, 2005). However, these studies relied heavily on the use of pharmacological agents, which may have non-specific effects on the cell. Furthermore, the role of ROS in the stabilisation of HIF-1α at low [O_2] has not been completely clarified, since data has challenged these findings (Vaux *et al.*, 2001;Srinivas *et al.*, 2001). However, our own data has demonstrated that ROS play a role in the stabilisation of HIF-1α in normoxia and at low [O_2]. Therefore, we next investigated the cellular source of ROS involved in HIF-1α stabilisation.

Mitochondria and NADPH oxidases are a major cellular source of ROS. Both mitochondrial derived ROS (Chandel *et al.*, 1998;Chandel *et al.*, 2000a;Schroedl *et al.*, 2002) and NOX derived ROS (Hirota and Semenza, 2001;Goyal *et al.*, 2004;Mekhail *et al.*, 2004) have been previously implicated in HIF-1α stabilisation. Thus we decided to investigate the role of these ROS sources in HIF-1α stabilisation.

6.5.1 Mitochondrial ROS

Mitochondria contain their own DNA (mtDNA), which encodes 13 genes that are essential for the assembly of a functional electron transport chain. Mitochondrial DNA (mtDNA) is replicated by an assembly of proteins and enzymes including DNA polymerase γ (POLγ) and its accessory protein, mitochondrial single stranded DNA binding protein (mtSSB) and mtDNA helicase (Twinkle). DNA POLγ is the only known DNA POLγ in human mitochondria and is essential for mitochondrial DNA replication. It is well established that defects in mtDNA replication lead to mitochondrial

dysfunction and disease. Wanrooij *et al.,* 2007 characterised the inducible expression of mutant POLγ in cultured human cells. The expression of the mutated form D890N (representing an amino acid change from an aspartate residue (D) to an asparagine residue (N)) was under the control of an inducible promoter activated by incubation of cells with doxycycline (DC). Over-expressed catalytically-inactive mutant POLγ out competes with the endogenous wild type POLγ for binding to mtDNA, thus preventing the cell to replicate mtDNA (Wanrooij *et al.*, 2007) and eventually producing non-functional respiratory mitochondria. HEK 293T cells stably transfected with an inducible mutated isoform of mitochondrial DNA POLγ (D890N) were kindly provided by Johannes Spelbrink, Institute of Medical Technology and Tampere University Hospital, Tampere, Finland, and were further characterised for use in our studies for use as Rho^0 cells (cells without respiratory functionality and mtDNA).

Our results show that mutating DNA POLγ over a period of 5-10 days depletes the cell of its mtDNA. DC induction also decreases the expression of cytochrome *c* oxidase, a partially mitochondrial-encoded protein. We also show that mutating DNA POLγ results in the inhibition of cellular respiration and a decrease in cytochrome aa_3 content.

It has been estimated that 1-3% of oxygen consumed by the mitochondria is converted to ROS (Boveris and Chance, 1973). The rate of ROS production is strongly linked to the mitochondrial membrane potential ($\Delta\Psi_m$), which is generated by protons in the intermembrane space. Mild uncoupling of mitochondria strongly reduces ROS production (Brand *et al.*, 2004). We observed in our Rho^0 cells that the $\Delta\Psi_m$ was not affected by the addition of rotenone, which inhibits Complex I (by preventing the transfer of electrons from Complex I to ubiquinone), suggesting the absence of electron transport along the ETC in these cells. Indeed, ROS production in DC induced Rho^0 cells were significantly less than that of non-induced cells. Knocking-down γGCS in HEK 293T cells has previously demonstrated a 2-fold increase in ROS production. However, this increased ROS production is not observed in our Rho^0 cells in which γGCS has been knocked down. Treatment with antioxidants in both cases has no further effect on ROS production. This data suggests that the vast majority of ROS produced in our Rho^0 cells is of mitochondrial origin since even when γGCS has been silenced, no increase in ROS is observed. A study utilising the mitochondrial-targeted antioxidant, Mito-Q has provided further evidence towards the role for ROS in mitochondrial signalling to the HIF pathway at low $[O_2]$ (Bell *et al.*, 2007).

ROS production at 3% oxygen was next to be examined in these cells especially since it has been well documented that low [O_2] increase ROS production (Chandel *et al.*, 1998;Vanden Hoek *et al.*, 1998;Waypa and Schumacker, 2002). Our data confirm results of Chandel *et al.*, 1998. At 3% oxygen we demonstrate a clear increase in ROS production compared to cells cultured in normoxia. This increase in ROS is absent in our *Rho*^{0} cells, suggesting that mitochondria are responsible for ROS production at low [O_2]. Elimination of ROS in both our normoxic model of HIF-1α stabilisation and at 3% oxygen, resulted in the prevention of HIF-1α stabilisation in these cells. In both however, HIF-1α was stabilised at 0.5% oxygen.

Due to the central role of HIF in the adaptive response to decreased oxygen tension, the HIF pathway has become an area of intense investigation as a therapeutic target in ischaemic disease and cancer, since hypoxia plays a significant role in disease development (Poellinger and Johnson, 2004;Semenza, 2006). In our studies we have demonstrated that HIF-1α stabilisation in human head and neck squamous carcinoma (H157) cells is dependent on ROS generation at 21% and 3% oxygen. Upon induction of a *Rho*^{0} phenotype in these cells, HIF-1α stabilisation is inhibited in normoxia but not in hypoxia. These data provide further evidence for the role of mitochondrial-derived ROS in HIF-1α stabilisation, since in the absence of functional mitochondria, ROS production decreases.

The integrity of the mitochondrial electron transport chain in HIF-1α stabilisation is confirmed in our own data and is in agreement with the work by several other groups. Initial observations by Chandel *et al.,* 1998 and Agani *et al.,* 2000 which concluded a role of the electron transport chain in HIF-1α stabilisation were made using pharmacological agents that may have had non-specific effects on cells and in turn the mitochondria. Thus these authors went on to utilise an alternative method to study the role of the electron transport chain in HIF-1α stabilisation. They too utilised cells that had been depleted of their mitochondrial DNA. First they induced mitochondria-depleted cells using ethidium bromide. Ethidium bromide interferes with DNA replication and caused a progressive decline in mtDNA. This results in a loss of electron transport in the mitochondria and was subsequently associated with an absence in HIF-1α stabilisation at low [O_2] (Chandel *et al.*, 1998;Chandel *et al.*, 2000a). More recently,

genetic approaches have been developed to investigate the requirement of functional mitochondria in hypoxic HIF-1α stabilisation.

One study knocked out cytochrome *c* (Mansfield *et al.*, 2005) which carries electrons from Complex III to Complex IV. Murine embryonic cells lacking cytochrome *c* fail to stabilise HIF-1α at low [O_2] (Mansfield *et al.*, 2005). Two further studies demonstrated that inhibiting Complex III function by knocking- down the Rieske iron-sulphur protein inhibits the ability of multiple cell lines to stabilise HIF-1α at low [O_2] (Guzy *et al.*, 2005;Brunelle *et al.*, 2005).

6.5.2 NADPH oxidase ROS

The NADPH oxidase (NOX) family of superoxide and hydrogen peroxide producing proteins have emerged as an important source of ROS in signal transduction. ROS produced by NOX proteins NOX1-5 and DUOX1 /2 play essential roles in the physiology of the brain, the immune system, the vasculature, and the digestive tract as well as in hormone synthesis (Brown and Griendling, 2009).

Early *in vitro* studies showed that NOX enzymes were less active in hypoxia than normoxia (Gabig *et al.*, 1979). However there is evidence for (He *et al.*, 2002) and against (Chang *et al.*, 2005) NOX-derived ROS in HIF-1α stabilisation. There is a report showing that stimulation of human umbilical vein cells (HUVEC) with prostacyclin stabilised HIF-1α under prolonged hypoxia, by attenuating NOX-derived ROS production due to suppressed Rac1 and $p47^{phox}$ expression (Chang *et al.*, 2005). To the contrary, other groups have not confirmed the inhibitory effect of NADPH oxidase signalling on HIF but instead report that ROS production by renal NOX4 is essential for HIF-2α expression and vascular endothelial growth actor (VEGF) or glucose transporter 1 (Glut-1) expression in renal tumour cells (Mekhail *et al.*, 2004). Furthermore, the GTPase Rac1, which stimulates NOX activity, was stimulated by hypoxia and a dominant-negative Rac1 repressed hypoxia-dependent HIF-1α accumulation (Hirota and Semenza, 2001). In A549, a human epithelial cell line, hypoxia increased NOX1 mRNA and protein expression, which was accompanied by enhanced ROS production and activation of HIF-1-dependent target gene expression (Goyal *et al.*, 2004).

Conflicting reports have been published on whether NOX-derived ROS stabilise HIF-1α, we therefore investigated the role of NOX-derived ROS in HIF-1α stabilisation in our own experiments. We found that NOX2 was expressed most abundantly, and preceded to silence NOX2 gene expression in our cells (HEK 293T). Upon silencing NOX2, it became apparent that this also resulted in the concomitant decrease of the other NOX isoforms, NOX1, 4 and 5, possibly because of sequence conservation amongst the isoforms. Exposure of the cells to a low [O_2] (3%) did not up-regulate NOX2. Furthermore, silencing NOX2 gene expression did not effect HIF-1α stabilisation at 3% oxygen. This data therefore suggests that ROS necessary to stabilise HIF-1α do not come from NOX at low [O_2]. It has been demonstrated that during hypoxia, increased mitochondrial ROS generation leads to activation of NOX1 by protein kinase C (PKC), thereby augmenting ROS production, and thus the elevation intracellular Ca^{2+} concentrations, and pulmonary artery smooth muscle cell (PASMC) shortening (Rathore *et al.*, 2008). This could imply a positive feedback pathway for ROS generation (Ward, 2008). However, since in our model there is no effect on HIF-1α stabilisation in cells where NOX2 has been silenced, this may be either a cell specific mechanism or dependent on the duration of hypoxia and/or re-oxygenation episodes, though further investigations would be required.

Taken together, our data provide evidence for participation of mitochondrial-derived ROS in HIF-1α stabilisation. In our *Rho*^{0} models (POLγ mutant in HEK and ethidium bromide treatment in H157), HIF-1α stabilisation is prevented. First in normoxia when γGCS has been silenced, secondly at 3% oxygen where HIF-1α is consistently stable and thirdly in cancerous cells that have previously demonstrated normoxic stabilisation. To support this further, we have shown that upon silencing γGCS in *Rho*^{0} cells, ROS production does not increase indicative that the main source of ROS in these cells is indeed mitochondrial. NF-κB has also been shown to be up-regulated in our normoxic model of HIF-1α stabilisation, and several studies have linked the production of mitochondrial ROS to the activation of NF-κB (Chandel *et al.*, 2000b;Pearlstein *et al.*, 2002;Palacios-Callender *et al.*, 2004).

6.6 Mitochondrial ROS production at low [O_2]

The mitochondria are considered a likely site of oxygen sensing, and it has been proposed that the electron transport chain acts as an oxygen sensor by releasing ROS in response to 'hypoxia'. The ROS released during 'hypoxia' act as signalling agents that trigger diverse responses, including the stabilisation of HIF-1α (Guzy and Schumacker, 2006).

The paradoxical generation of mitochondrial ROS at low [O_2] may exist due to the influence of oxygen concentration on the activity of cytochrome *c* oxidase (C*c*O). NO may bind and inhibit C*c*O, resulting in an increase in its K_m for oxygen and an increased reduction of electron carriers located upstream from the terminal oxidase (Cooper and Davies, 2000), favouring superoxide formation at low [O_2] (Palacios-Callender *et al.*, 2004). Thus, in normoxic oxygen conditions, the enzyme (C*c*O) is predominately in an oxidised state, it consumes oxygen and metabolises NO. At low [O_2], when the enzyme is predominately in a reduced state, oxygen and NO compete for binding to the enzyme and NO is not metabolised. Allowing for the possibility that, as oxygen concentration falls, there lies a 'window' in which the mitochondria are able to produce free radicals which is not a direct affect of low [O_2] but is instead due to the reduction of the electron transport chain via NO (Palacios-Callender *et al.*, 2004). When the enzyme is fully reduced in hypoxia, there is not enough oxygen consumed by the electron transport chain to yield the production of ROS (Figure 76).

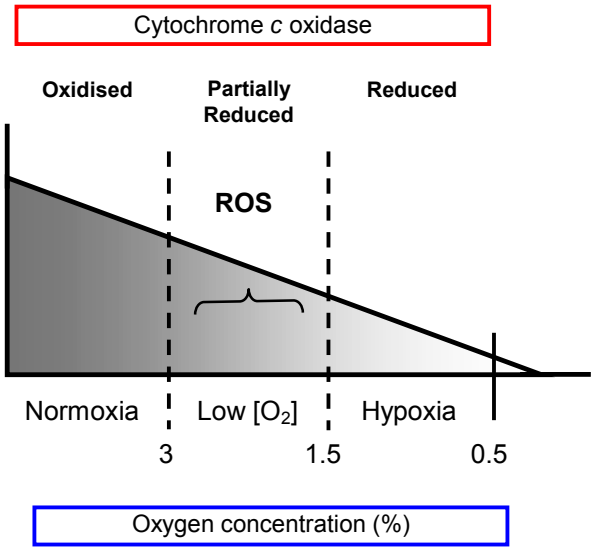

Figure 76 – A model summarising ROS production at low [O_2]

As the oxygen concentration ([O_2]) decreases from normoxia to hypoxia, the cytochrome *c* oxidase changes from an oxidised state to a reduced state. Between ~ 3% and 1.5% oxygen (low [O_2]) lies a 'window' in which the production of ROS is favoured.

6.7 Conclusion and future work

The results from the current study indicate that reactive oxygen species (ROS) stabilise HIF-1α in both normoxia (21%) and at a low [O_2] (3%). We have also provided preliminary data to suggest that ROS do not inhibit the hydroxylation or ubiquitination of HIF-1α but instead ROS enhance the synthesis of HIF-1α.

Furthermore, we have been able to demonstrate that the source of ROS involved in HIF-1α stabilisation in HEK 293T and oral squamous carcinoma cells is of mitochondrial origin. Our results also indicate that as oxygen concentrations decrease (without reaching hypoxia or anoxia), mitochondria produce more free radicals. Additionally, our work has demonstrated that two distinct mechanisms of HIF-1α stabilisation exist within the cell depending on the oxygen concentration. At low [O_2], HIF-1α stabilisation is dependent of the formation of ROS, yet in hypoxic conditions, oxygen becomes the limiting factor.

To further this study it would be of interest to clearly demonstrate the mechanism of action by which reactive oxygen species result in HIF-1α stabilisation. Prolyl hydroxylases (PHD) mediate hydroxylation and degradation of HIF-1α at 21% oxygen. PHD should be active in normoxia yet HIF-1α is stable in our γGCS knock-down model. Thus, it would be important to investigate further whether ROS affect the activity of PHD in this model. We have provided preliminary data suggesting that PHD are active and that HIF-1α is targeted for hydroxylation. However, the method used in this study does not demonstrate this clearly. In order to investigate this further, PHD activity could be measured in cells where γGCS has been silenced at 21% using a HIF-1α-pVHL binding assay. This assay is based on the knowledge that only hydroxylated HIF-1α is capable of binding pVHL, thus reflecting PHD activity.

Hypoxia plays an important role in determining disease progression in a vast array of pathologies, including vascular disease, cancer and chronic inflammation. However, as observed in this study, not just low or hypoxic oxygen conditions results in HIF-1α stabilisation. This study could provide means of therapeutic intervention in the treatment of inflammatory diseases and cancer.

Chapter seven:
References

Chapter seven: References

Abe,J.I., Takahashi,M., Ishida,M., Lee,J.D., and Berk,B.C. (1997). c-Src is required for oxidative stress-mediated activation of Big Mitogen-activated Protein Kinase 1 (BMK1). *J. Biol. Chem.,* **272,** 20389-20394.

Agani,F.H., Pichiule,P., Chavez,J.C., and LaManna,J.C. (2000). The role of mitochondria in the regulation of Hypoxia-inducible Factor 1 expression during hypoxia. *J. Biol. Chem.,* **275,** 35863-35867.

al-Bekairi,A.M., Nagi,M.N., Shoeb,H.A., and al-Sawaf,H.A. (1994). Evidence for superoxide radical production by a simple flavoprotein: glucose oxidase. *Biochem. Mol. Biol. Int.,* **34,** 233-238.

Alvarez,S., Valdez,L.B., Zaobornyj,T., and Boveris,A. (2003). Oxygen dependence of mitochondrial nitric oxide synthase activity. *Biochem. Biophys. Res. Commun.,* **305,** 771-775.

Anderson,M.T., Staal,F.J., Gitler,C., Herzenberg,L.A., and Herzenberg,L.A. (1994). Separation of oxidant-initiated and redox-regulated steps in the NF-kappa B signal transduction pathway. *Proc. Natl. Acad. Sci. U. S. A,* **91,** 11527-11531.

Anilkumar,N., Weber,R., Zhang,M., Brewer,A., and Shah,A.M. (2008). Nox4 and Nox2 NADPH Oxidases mediate distinct cellular redox signaling responses to agonist stimulation. *Arterioscler. Thromb. Vasc. Biol.,* **28,** 1347-1354.

Armstrong,J.S., Steinauer,K.K., Hornung,B., Irish,J.M., Lecane,P., Birrell,G.W., Peehl,D.M., and Knox,S.J. (2002). Role of glutathione depletion and reactive oxygen species generation in apoptotic signaling in a human B lymphoma cell line. *Cell Death Differ.,* **9,** 252-263.

Arnold,R.S., Shi,J., Murad,E., Whalen,A.M., Sun,C.Q., Polavarapu,R., Parthasarathy,S., Petros,J.A., and Lambeth,J.D. (2001). Hydrogen peroxide mediates the cell growth and transformation caused by the mitogenic oxidase Nox1. *Proc. Natl. Acad. Sci. U. S. A,* **98,** 5550-5555.

Babior,B.M., Kipnes,R.S., and Curnutte,J.T. (1973). Biological defense mechanisms. The production by leukocytes of superoxide, a potential bactericidal agent. *J. Clin. Invest.,* **52,** 741-744.

Bae,Y.S., Kang,S.W., Seo,M.S., Baines,I.C., Tekle,E., Chock,P.B., and Rhee,S.G. (1997). Epidermal growth factor (EGF)-induced generation of hydrogen peroxide. Role in EGF receptor-mediated tyrosine phosphorylation. *J. Biol. Chem.,* **272,** 217-221.

Baeuerle,P.A. and Henkel,T. (2003). Function and activation of NF-kappaB in the immune system. *Annu. Rev. Immunol.,* **12,** 141-179.

Baeuerle,P.A. and Baltimore,D. (1996). NF-kappaB: Ten years after. *Cell,* **87,** 13-20.

Balaban,R.S., Nemoto,S., and Finkel,T. (2005). Mitochondria, oxidants, and Aging. *Cell,* **120,** 483-495.

Ballatori,N., Hammond,C.L., Cunningham,J.B., Krance,S.M., and Marchan,R. (2005). Molecular mechanisms of reduced glutathione transport: role of the MRP/CFTR/ABCC and OATP/SLC21A families of membrane proteins. *Toxicol. Appl. Pharmacol.,* **204,** 238-255.

Ballinger,S.W., Patterson,C., Knight-Lozano,C.A., Burow,D.L., Conklin,C.A., Hu,Z., Reuf,J., Horaist,C., Lebovitz,R., Hunter,G.C., McIntyre,K., and Runge,M.S. (2002). Mitochondrial integrity and function in atherogenesis. *Circulation,* **106,** 544-549.

Banfi,B., Malgrange,B., Knisz,J., Steger,K., Dubois-Dauphin,M., and Krause,K.H. (2004a). NOX3, a superoxide-generating NADPH Oxidase of the inner ear. *J. Biol. Chem.,* **279,** 46065-46072.

Banfi,B., Maturana,A., Jaconi,S., Arnaudeau,S., Laforge,T., Sinha,B., Ligeti,E., Demaurex,N., and Krause,K.H. (2000). A mammalian H+ channel generated through alternative splicing of the NADPH Oxidase homolog NOH-1. *Science,* **287,** 138-142.

Banfi,B., Molnar,G., Maturana,A., Steger,K., Hegedus,B., Demaurex,N., and Krause,K.H. (2001). A Ca2+-activated NADPH Oxidase in testis, spleen, and lymph nodes. *J. Biol. Chem.,* **276,** 37594-37601.

Banfi,B., Tirone,F., Durussel,I., Knisz,J., Moskwa,P., Molnar,G., Krause,K.H., and Cox,J.A. (2004b). Mechanism of Ca2+ activation of the NADPH Oxidase 5 (NOX5). *J. Biol. Chem.,* **279,** 18583-18591.

Bardos,J.I. and Ashcroft,M. (2005). Negative and positive regulation of HIF-1: A complex network. *Biochim. Biophys. Acta. - Reviews on Cancer,* **1755,** 107-120.

Barja,G. (1999). Mitochondrial oxygen radical generation and leak: sites of production in states 4 and 3, organ specificity, and relation to aging and longevity. *J. Bioenerg. Biomembr.,* **31,** 347-366.

Barry-Lane,P.A., Patterson,C., van der,M.M., Hu,Z., Holland,S.M., Yeh,E.T., and Runge,M.S. (2001). p47phox is required for atherosclerotic lesion progression in ApoE(-/-) mice. *J. Clin. Invest.,* **108,** 1513-1522.

Bauskin,A.R., Alkalay,I., and Ben-Neriah,Y. (1991). Redox regulation of a protein tyrosine kinase in the endoplasmic reticulum. *Cell,* **66,** 685-696.

Bedard,K. and Krause,K.H. (2007). The NOX family of ROS-generating NADPH Oxidases: Physiology and pathophysiology. *Physiol. Rev.,* **87,** 245-313.

Beg,A.A., Finco,T.S., Nantermet,P.V., and Baldwin,A.S., Jr. (1993). Tumor necrosis factor and interleukin-1 lead to phosphorylation and loss of I kappa B alpha: a mechanism for NF-kappa B activation. *Mol. Cell Biol.,* **13,** 3301-3310.

Bejarano,I., Terron,M.P., Paredes,S.D., Barriga,C., Rodriguez,A.B., and Pariente,J.A. (2007). Hydrogen peroxide increases the phagocytic function of human neutrophils by calcium mobilisation. *Mol. Cell Biochem.,* **296,** 77-84.

Bell,E.L., Klimova,T.A., Eisenbart,J., Moraes,C.T., Murphy,M.P., Budinger,G.R.S., and Chandel,N.S. (2007). The Qo site of the mitochondrial complex III is required for the transduction of hypoxic signaling via reactive oxygen species production. *J. Cell Biol.,* **177,** 1029-1036.

Belousov,V.V., Fradkov,A.F., Lukyanov,K.A., Staroverov,D.B., Shakhbazov,K.S., Terskikh,A.V., and Lukyanov,S. (2006). Genetically encoded fluorescent indicator for intracellular hydrogen peroxide. *Nat. Meth.,* **3,** 281-286.

Benhar,M., Engelberg,D., and Levitzki,A. (2002). ROS, stress-activated kinases and stress signaling in cancer. *EMBO Rep.,* **3,** 420-425.

Berra,E., Benizri,E., Ginouves,A., Volmat,V., Roux,D., and Pouyssegur,J. (2003). HIF prolyl-hydroxylase 2 is the key oxygen sensor setting low steady-state levels of HIF-1alpha in normoxia. *EMBO J.,* **22,** 4082-4090.

Blouin,C.C., Page,E.L., Soucy,G.M., and Richard,D.E. (2004). Hypoxic gene activation by lipopolysaccharide in macrophages: Implication of Hypoxia-Inducible Factor 1alpha. *Blood,* **103,** 1124-1130.

Bosch-Marce,M., Okuyama,H., Wesley,J.B., Sarkar,K., Kimura,H., Liu,Y.V., Zhang,H., Strazza,M., Rey,S., Savino,L., Zhou,Y.F., McDonald,K.R., Na,Y., Vandiver,S., Rabi,A., Shaked,Y., Kerbel,R., LaVallee,T., and Semenza,G.L. (2007). Effects of aging and Hypoxia-Inducible Factor-1 activity on angiogenic cell mobilization and recovery of perfusion after limb ischemia. *Circ. Res.,* **101,** 1310-1318.

Boveris,A. and Chance,B. (1973). The mitochondrial generation of hydrogen peroxide. General properties and effect of hyperbaric oxygen. *Biochem. J.,* **134,** 707-716.

Boveris,A., Oshino,N., and Chance,B. (1972). The cellular production of hydrogen peroxide. *Biochem. J.,* **128,** 617-630.

Brahimi-Horn,M.C., Chiche,J., and Pouyssegur,J. (2007). Hypoxia signalling controls metabolic demand. *Curr. Opin. Cell Biol.,* **19,** 223-229.

Brahimi-Horn,M.C. and Pouyssegur,J. (2007). Oxygen, a source of life and stress. *FEBS Lett.,* **581,** 3582-3591.

Brand,M.D., Affourtit,C., Esteves,T.C., Green,K., Lambert,A.J., Miwa,S., Pakay,J.L., and Parker,N. (2004). Mitochondrial superoxide: production, biological effects, and activation of uncoupling proteins. *Free Radic. Biol. Med.,* **37,** 755-767.

Bredt,D.S. and Snyder,S.H. (1990). Isolation of nitric oxide synthetase, a calmodulin-requiring enzyme. *Proc. Natl. Acad. Sci. U. S. A,* **87,** 682-685.

Brown,D.I. and Griendling,K.K. (2009). Nox proteins in signal transduction. *Free Radic. Biol. Med.,* **47,** 1239-1253.

Brune,B. and Zhou,J. (2007). Nitric oxide and superoxide: Interference with hypoxic signaling. *Cardiovasc. Res.,* **75,** 275-282.

Brunelle,J.K., Bell,E.L., Quesada,N.M., Vercauteren,K., Tiranti,V., Zeviani,M., Scarpulla,R.C., and Chandel,N.S. (2005). Oxygen sensing requires mitochondrial ROS but not oxidative phosphorylation. *Cell Metab.,* **1,** 409-414.

Callapina,M., Zhou,J., Schmid,T., Kohl,R., and Brune,B. (2005). NO restores HIF-1alpha hydroxylation during hypoxia: Role of reactive oxygen species. *Free Radic. Biol. Med.,* **39,** 925-936.

Cassina,A. and Radi,R. (1996). Differential inhibitory action of Nitric Oxide and Peroxynitrite on mitochondrial electron transport. *Arch. Biochem. Biophys.,* **328,** 309-316.

Cave,A.C., Brewer,A.C., Narayanapanicker,A., Ray,R., Grieve,D.J., Walker,S., and Shah,A.M. (2006). NADPH oxidases in cardiovascular health and disease. *Antioxid. Redox. Signal.,* **8,** 691-728.

Ceradini,D.J., Kulkarni,A.R., Callaghan,M.J., Tepper,O.M., Bastidas,N., Kleinman,M.E., Capla,J.M., Galiano,R.D., Levine,J.P., and Gurtner,G.C. (2004). Progenitor cell trafficking is regulated by hypoxic gradients through HIF-1 induction of SDF-1. *Nat. Med.,* **10,** 858-864.

Chae,H.Z., Kim,H.J., Kang,S.W., and Rhee,S.G. (1999). Characterization of three isoforms of mammalian peroxiredoxin that reduce peroxides in the presence of thioredoxin. *Diabetes Res. Clin. Pract.,* **45,** 101-112.

Chance,B., Sies,H., and Boveris,A. (1979). Hydroperoxide metabolism in mammalian organs. *Physiol. Rev.,* **59,** 527-605.

Chandel,N.S., Maltepe,E., Goldwasser,E., Mathieu,C.E., Simon,M.C., and Schumacker,P.T. (1998). Mitochondrial reactive oxygen species trigger hypoxia-induced transcription. *Proc. Natl. Acad. Sci. U. S. A,* **95,** 11715-11720.

Chandel,N.S. and Budinger,G.R.S. (2007). The cellular basis for diverse responses to oxygen. *Free Radic. Biol. Med.,* **42,** 165-174.

Chandel,N.S., McClintock,D.S., Feliciano,C.E., Wood,T.M., Melendez,J.A., Rodriguez,A.M., and Schumacker,P.T. (2000a). Reactive oxygen species generated at mitochondrial Complex III stabilize Hypoxia-inducible Factor-1alpha during hypoxia. A mechanism of oxygen sensing. *J. Biol. Chem.,* **275,** 25130-25138.

Chandel,N.S., Schumacker,P.T., and Arch,R.H. (2001). Reactive oxygen species are downstream products of TRAF-mediated signal transduction. *J. Biol. Chem.,* **276,** 42728-42736.

Chandel,N.S., Trzyna,W.C., McClintock,D.S., and Schumacker,P.T. (2000b). Role of oxidants in NF-kappaB activation and TNF-alpha gene transcription induced by hypoxia and endotoxin. *J. Immunol.,* **165,** 1013-1021.

Chang,E.I., Loh,S.A., Ceradini,D.J., Chang,E.I., Lin,S., Bastidas,N., Aarabi,S., Chan,D.A., Freedman,M.L., Giaccia,A.J., and Gurtner,G.C. (2007). Age decreases endothelial progenitor cell recruitment through decreases in Hypoxia-Inducible Factor 1alpha stabilization during ischemia. *Circulation,* **116,** 2818-2829.

Chang,T.C., Huang,C.J., Tam,K., Chen,S.F., Tan,K.T., Tsai,M.S., Lin,T.N., and Shyue,S.K. (2005). Stabilization of Hypoxia-inducible Factor-1alpha by prostacyclin under prolonged hypoxia via reducing reactive oxygen species level in endothelial cells. *J. Biol. Chem.,* **280,** 36567-36574.

Chelikani,P., Fita,I., and Loewen,P.C. (2004). Diversity of structures and properties among catalases. *Cell Mol. Life Sci.,* **61,** 192-208.

Cheng,G., Cao,Z., Xu,X., Meir,E.G.V., and Lambeth,J.D. (2001). Homologs of gp91phox: cloning and tissue expression of Nox3, Nox4, and Nox5. *Gene,* **269,** 131-140.

Chiarugi,P. and Cirri,P. (2003). Redox regulation of protein tyrosine phosphatases during receptor tyrosine kinase signal transduction. *Trends Biochem. Sci.,* **28,** 509-514.

Chua,Y.L., Dufour,E., Dassa,E.P., Rustin,P., Jacobs,H.T., Taylor,C.T., and Hagen,T. (2010). Stabilization of HIF-1alpha protein in hypoxia occurs independently of mitochondrial reactive oxygen species production. *J. Biol. Chem.,* **285,** 31277-31284.

Chung,S.H., Chung,S.M., Lee,J.Y., Kim,S.R., Park,K.S., and Chung,J.H. (1999). The biological significance of non-enzymatic reaction of menadione with plasma thiols: enhancement of menadione-induced cytotoxicity to platelets by the presence of blood plasma. *FEBS Lett.,* **449,** 235-240.

Colombo,S.L. and Moncada,S. (2009). AMPKalpha1 regulates the antioxidant status of vascular endothelial cells. *Biochem. J.,* **421,** 163-169.

Commoner,B., Townsend,J., and Pake,G. (1954). Free radicals in biological materials. *Nature,* **174,** 689-691.

Cooper,C.E. and Davies,N.A. (2000). Effects of nitric oxide and peroxynitrite on the cytochrome oxidase Km for oxygen: implications for mitochondrial pathology. *Biochim. Biophys. Acta. - Bioenergetics,* **1459,** 390-396.

Cooper,C.E. and Giulivi,C. (2007). Nitric oxide regulation of mitochondrial oxygen consumption II: molecular mechanism and tissue physiology. *Am. J. Physiol. Cell Physiol.,* **292,** C1993-C2003.

Counts,D.F., Cardinale,G.J., and Udenfriend,S. (1978). Prolyl hydroxylase half reaction: peptidyl prolyl-independent decarboxylation of alpha-ketoglutarate. *Proc. Natl. Acad. Sci. U. S. A,* **75,** 2145-2149.

Crapo,J.D., Freeman,B.A., Barry,B.E., Turrens,J.F., and Young,S.L. (1983). Mechanisms of hyperoxic injury to the pulmonary microcirculation. *Physiologist,* **26,** 170-176.

Criddle,D.N., Gillies,S., Baumgartner-Wilson,H.K., Jaffar,M., Chinje,E.C., Passmore,S., Chvanov,M., Barrow,S., Gerasimenko,O.V., Tepikin,A.V., Sutton,R., and Petersen,O.H. (2006). Menadione-induced reactive oxygen species generation via redox cycling promotes apoptosis of murine pancreatic acinar cells. *J. Biol. Chem.,* **281,** 40485-40492.

de la Asuncion,J.G., Millan,A., Pla,R., Bruseghini,L., Esteras,A., Pallardo,F.V., Sastre,J., and Vina,J. (1996). Mitochondrial glutathione oxidation correlates with age-associated oxidative damage to mitochondrial DNA. *FASEB J.,* **10,** 333-338.

Devary,Y., Gottlieb,R.A., Smeal,T., and Karin,M. (1992). The mammalian ultraviolet response is triggered by activation of src tyrosine kinases. *Cell,* **71,** 1081-1091.

Diaz-Hernandez,J.I., Moncada,S., Bolanos,J.P., and Almeida,A. (2007). Poly(ADP-ribose) polymerase-1 protects neurons against apoptosis induced by oxidative stress. *Cell Death Differ.,* **14,** 1211-1221.

Dikalov,S.I., Dikalova,A.E., Bikineyeva,A.T., Schmidt,H.H.H.W., Harrison,D.G., and Griendling,K.K. (2008). Distinct roles of Nox1 and Nox4 in basal and angiotensin II-stimulated superoxide and hydrogen peroxide production. *Free Radic. Biol. Med.,* **45,** 1340-1351.

Droge,W. (2002). Free radicals in the physiological control of cell function. *Physiol. Rev.,* **82,** 47-95.

Epstein,A.C.R., Gleadle,J.M., McNeill,L.A., Hewitson,K.S., O'Rourke,J., Mole,D.R., Mukherji,M., Metzen,E., Wilson,M.I., and Dhanda,A. (2001). C. elegans EGL-9 and mammalian homologs define a family of dioxygenases that regulate HIF by prolyl hydroxylation. *Cell,* **107,** 43-54.

Epstein,F.H., Barnes,P.J., and Karin,M. (2009). Nuclear Factor-kappaB - A pivotal transcription factor in chronic inflammatory diseases. *N. Engl. J. Med.,* **336,** 1066-1071.

Erbel,P.J., Card,P.B., Karakuzu,O., Bruick,R.K., and Gardner,K.H. (2003). Structural basis for PAS domain heterodimerization in the basic helix--loop--helix-PAS transcription factor hypoxia-inducible factor. *Proc. Natl. Acad. Sci. U. S. A,* **100,** 15504-15509.

Faulkner,K. and Fridovich,I. (1993). Luminol and lucigenin as detectors for O2.-. *Free Radic. Biol. Med.,* **15,** 447-451.

Fire,A., Xu,S., Montgomery,M.K., Kostas,S.A., Driver,S.E., and Mello,C.C. (1998). Potent and specific genetic interference by double-stranded RNA in Caenorhabditis elegans. *Nature,* **391,** 806-811.

Forbes,J.M., Coughlan,M.T., and Cooper,M.E. (2008). Oxidative Stress as a Major Culprit in Kidney Disease in Diabetes. *Diabetes,* **57,** 1446-1454.

Forman,H.J., Fukuto,J.M., and Torres,M. (2004). Redox signaling: thiol chemistry defines which reactive oxygen and nitrogen species can act as second messengers. *Am. J. Physiol. Cell Physiol.,* **287,** C246-C256.

Forman,H.J. and Torres,M. (2002). Reactive Oxygen Species and Cell Signaling: Respiratory Burst in Macrophage Signaling. *Am. J. Respir. Crit. Care Med.,* **166,** 4S-8.

Forstermann,U. (2010). Nitric oxide and oxidative stress in vascular disease. *Pflugers Arch.,* **459,** 923-939.

Forstermann,U. and Kleinert,H. (1995). Nitric oxide synthase: expression and expressional control of the three isoforms. *Naunyn Schmiedebergs Arch. Pharmacol.,* **352,** 351-364.

Forsythe,J.A., Jiang,B.H., Iyer,N.V., Agani,F., Leung,S.W., Koos,R.D., and Semenza,G.L. (1996). Activation of vascular endothelial growth factor gene transcription by hypoxia-inducible factor 1. *Mol. Cell Biol.,* **16,** 4604-4613.

Frede,S., Stockmann,C., Freitag,P., and Fandrey,J. (2006). Bacterial lipopolysaccharide induces HIF-1 activation in human monocytes via p44/42 MAPK and NF-kappaB. *Biochem. J.,* **396,** 517-527.

Fridovich,I. (1995). Superoxide Radical and Superoxide Dismutases. *Annu. Rev. Biochem.,* **64,** 97-112.

Fukuda,R., Hirota,K., Fan,F., Jung,Y.D., Ellis,L.M., and Semenza,G.L. (2002). Insulin-like Growth Factor 1 Induces Hypoxia-inducible Factor 1-mediated Vascular Endothelial Growth Factor Expression, Which is Dependent on MAP Kinase and Phosphatidylinositol 3-Kinase Signaling in Colon Cancer Cells. *J. Biol. Chem.,* **277,** 38205-38211.

Fukuda,R., Zhang,H., Kim,J.W., Shimoda,L., Dang,C.V., and Semenza,G.L. (2007). HIF-1 Regulates Cytochrome Oxidase Subunits to Optimize Efficiency of Respiration in Hypoxic Cells. *Cell,* **129,** 111-122.

Fukui,T., Ishizaka,N., Rajagopalan,S., Laursen,J.B., Capers,Q., Taylor,W.R., Harrison,D.G., de Leon,H., Wilcox,J.N., and Griendling,K.K. (1997). p22phox mRNA Expression and NADPH Oxidase Activity Are Increased in Aortas From Hypertensive Rats. *Circ. Res.,* **80,** 45-51.

Gabig,T.G., Bearman,S.I., and Babior,B.M. (1979). Effects of oxygen tension and pH on the respiratory burst of human neutrophils. *Blood,* **53,** 1133-1139.

Garcia-Ruiz,C., Colell,A., Mari,M., Morales,A., and Fernandez-Checa (1997). Direct Effect of Ceramide on the Mitochondrial Electron Transport Chain Leads to Generation of Reactive Oxygen Species. *J. Biol. Chem.,* **272,** 11369-11377.

Gardner,P.R., Raineri,I.s., Epstein,L.B., and White,C.W. (1995). Superoxide Radical and Iron Modulate Aconitase Activity in Mammalian Cells. *J. Biol. Chem.,* **270,** 13399-13405.

Garedew,A., Henderson,S.O., and Moncada,S. (2010). Activated macrophages utilize glycolytic ATP to maintain mitochondrial membrane potential and prevent apoptotic cell death. *Cell Death Differ.,* **17,** 1540-1550.

Garedew,A. and Moncada,S. (2008). Mitochondrial dysfunction and HIF1alpha stabilization in inflammation. *J. Cell Sci.,* **121,** 3468-3475.

Geiszt,M.S., Kopp,J.B., Varnai,P., and Leto,T.L. (2000). Identification of Renox, an NAD(P)H oxidase in kidney. *Proc. Natl. Acad. Sci. U. S. A,* **97,** 8010-8014.

Genius,J. and Fandrey,J. (2000). Nitric oxide affects the production of reactive oxygen species in hepatoma cells: implications for the process of oxygen sensing. *Free Radic. Biol. Med.,* **29,** 515-521.

Gerald,D., Berra,E., Frapart,Y.M., Chan,D.A., Giaccia,A.J., Mansuy,D., Pouyssegur,J., Yaniv,M., and Mechta-Grigoriou,F. (2004). JunD Reduces Tumor Angiogenesis by Protecting Cells from Oxidative Stress. *Cell,* **118,** 781-794.

Gerber,H.P., Condorelli,F., Park,J., and Ferrara,N. (1997). Differential Transcriptional Regulation of the Two Vascular Endothelial Growth Factor Receptor Genes. *J. Biol. Chem.,* **272,** 23659-23667.

Ghafourifar,P. and Richter,C. (1997). Nitric oxide synthase activity in mitochondria. *FEBS Lett.,* **418,** 291-296.

Giulivi,C., Poderoso,J.J., and Boveris,A. (1998). Production of Nitric Oxide by Mitochondria. *J. Biol. Chem.,* **273,** 11038-11043.

Gopalakrishna,R. and Anderson,W.B. (1989). Ca2+- and phospholipid-independent activation of protein kinase C by selective oxidative modification of the regulatory domain. *Proc. Natl. Acad. Sci. U. S. A,* **86,** 6758-6762.

Gopalakrishna,R. and Anderson,W.B. (1991). Reversible oxidative activation and inactivation of protein kinase C by the mitogen/tumor promoter periodate. *Arch. Biochem. Biophys.,* **285,** 382-387.

Goyal,P., Weissmann,N., Grimminger,F., Hegel,C., Bader,L., Rose,F., Fink,L., Ghofrani,H.A., Schermuly,R.T., Schmidt,H.H.H.W., Seeger,W., and Hanze,J. (2004). Upregulation of NAD(P)H oxidase 1 in hypoxia activates hypoxia-inducible factor 1 via increase in reactive oxygen species. *Free Radic. Biol. Med.,* **36,** 1279-1288.

Graham,F.L., Smiley,J., Russell,W.C., and Nairn,R. (1977). Characteristics of a Human Cell Line Transformed by DNA from Human Adenovirus Type 5. *J. Gen. Virol.,* **36,** 59-72.

Griffith,O.W. and Meister,A. (1985). Origin and turnover of mitochondrial glutathione. *Proc. Natl. Acad. Sci. U. S. A,* **82,** 4668-4672.

Grimble,R.F., Jackson,A.A., Persaud,C., Wride,M.J., Delers,F., and Engler,R. (1992). Cysteine and glycine supplementation modulate the metabolic response to Tumor Necrosis Factor alpha in rats fed a low protein diet. *J. Nutr.,* **122,** 2066-2073.

Guzik,T.J., Korbut,R., and Adamek-Guzik,T. (2003). Nitric oxide and superoxide in inflammation and immune regulation. *J. Physiol. Pharmacol.,* **54,** 469-487.

Guzy,R.D., Hoyos,B., Robin,E., Chen,H., Liu,L., Mansfield,K.D., Simon,M.C., Hammerling,U., and Schumacker,P.T. (2005). Mitochondrial complex III is required for hypoxia-induced ROS production and cellular oxygen sensing. *Cell Metab.,* **1,** 401-408.

Guzy,R.D. and Schumacker,P.T. (2006). Oxygen sensing by mitochondria at complex III: the paradox of increased reactive oxygen species during hypoxia. *Exp Physiol,* **91,** 807-819.

Ha,H.C., Thiagalingam,A., Nelkin,B.D., and Casero,R.A. (2000). Reactive Oxygen Species Are Critical for the Growth and Differentiation of Medullary Thyroid Carcinoma Cells. *Clin. Cancer Res.,* **6,** 3783-3787.

Halliwell and Gutteridge (1989). Free Radicals in Biology and Medicine.Oxford: Clarendon Press, 188-207.

Han,D., Antunes,F., Canali,R., Rettori,D., and Cadenas,E. (2003). Voltage-dependent Anion Channels Control the Release of the Superoxide Anion from Mitochondria to Cytosol. *J. Biol. Chem.,* **278,** 5557-5563.

Hanahan,D. and Weinberg,R.A. (2000). The hallmarks of cancer. *Cell,* **100,** 57-70.

Harman,D. (1956). Aging: A Theory Based on Free Radical and Radiation Chemistry. *J. Gerontol.,* **11,** 298-300.

Hayes,G.R. and Lockwood,D.H. (1987). Role of insulin receptor phosphorylation in the insulinomimetic effects of hydrogen peroxide. *Proc. Natl. Acad. Sci. U. S. A,* **84,** 8115-8119.

He,L., Chen,J., Dinger,B., Sanders,K., Sundar,K., Hoidal,J., and Fidone,S. (2002). Characteristics of carotid body chemosensitivity in NADPH oxidase-deficient mice. *Am. J. Physiol. Cell Physiol.,* **282,** C27-C33.

Heinzel,B., John,M., Klatt,P., Bohme,E., and Mayer,B. (1992). Ca2+/calmodulin-dependent formation of hydrogen peroxide by brain nitric oxide synthase. *Biochem. J.,* **281 (Pt 3),** 627-630.

Hellwig-Burgel,T., Stiehl,D.P., Wagner,A.E., Metzen,E., and Jelkmann,W. (2005). Review: Hypoxia-Inducible Factor-1 (HIF-1): A Novel Transcription Factor in Immune Reactions. *J. Interferon Cytokine Res.,* **25,** 297-310.

Hinchman,C.A. and Ballatori,N. (1990). Glutathione-degrading capacities of liver and kidney in different species. *Biochem. Pharmacol.,* **40,** 1131-1135.

Hink,U., Li,H., Mollnau,H., Oelze,M., Matheis,E., Hartmann,M., Skatchkov,M., Thaiss,F., Stahl,R.A.K., Warnholtz,A., Meinertz,T., Griendling,K., Harrison,D.G., Forstermann,U., and Munzel,T. (2001). Mechanisms Underlying Endothelial Dysfunction in Diabetes Mellitus. *Circ. Res.,* **88,** e14-e22.

Hirota,K. and Semenza,G.L. (2001). Rac1 Activity Is Required for the Activation of Hypoxia-inducible Factor 1. *J. Biol. Chem.,* **276,** 21166-21172.

Hollis,V.S., Palacios-Callender,M., Springett,R.J., Delpy,D.T., and Moncada,S. (2003). Monitoring cytochrome redox changes in the mitochondria of intact cells using multi-wavelength visible light spectroscopy. *Biochim. Biophys. Acta. - Bioenergetics,* **1607,** 191-202.

Huang,R.P., Wu,J.X., Fan,Y., and Adamson,E.D. (1996). UV activates growth factor receptors via reactive oxygen intermediates. *J. Cell Biol.,* **133,** 211-220.

Ivan,M., Haberberger,T., Gervasi,D.C., Michelson,K.S., Gunzler,V., Kondo,K., Yang,H., Sorokina,I., Conaway,R.C., Conaway,J.W., and Kaelin,W.G. (2002). Biochemical purification and pharmacological inhibition of a mammalian prolyl hydroxylase acting on hypoxia-inducible factor. *Proc. Natl. Acad. Sci. U. S. A,* **99,** 13459-13464.

Jackson,M.J., Papa,S., Bolanos,J.P., Bruckdorfer,R., Carlsen,H., Elliott,R.M., Flier,J., Griffiths,H.R., Heales,S., Holst,B., Lorusso,M., Lund,E., Ïivind Moskaug,J., Moser,U., Di Paola,M., Cristina Polidori,M., Signorile,A., Stahl,W., Vina,R.J., and Astley,S.B. (2002). Antioxidants, reactive oxygen and nitrogen species, gene induction and mitochondrial function. *Mol. Aspects Med.,* **23,** 209-285.

Jantsch,J., Chakravortty,D., Turza,N., Prechtel,A.T., Buchholz,B., Gerlach,R.G., Volke,M., Glasner,J., Warnecke,C., Wiesener,M.S., Eckardt,K.U., Steinkasserer,A., Hensel,M., and Willam,C. (2008). Hypoxia and Hypoxia-Inducible Factor-1alpha modulate lipopolysaccharide-induced dendritic cell activation and function. *J. Immunol.,* **180,** 4697-4705.

Jiang,B.H., Semenza,G.L., Bauer,C., and Marti,H.H. (1996). Hypoxia-inducible factor 1 levels vary exponentially over a physiologically relevant range of O2 tension. *Am. J. Physiol. Cell Physiol.,* **271,** C1172-C1180.

Jiang,F., Roberts,S.J., Datla,S.R., and Dusting,G.J. (2006). NO Modulates NADPH Oxidase Function Via Heme Oxygenase-1 in Human Endothelial Cells. *Hypertension,* **48,** 950-957.

Kadota,S., Fantus,I.G., Deragon,G., Guyda,H.J., and Posner,B.I. (1987). Stimulation of insulin-like growth factor II receptor binding and insulin receptor kinase activity in rat adipocytes. Effects of vanadate and H2O2. *J. Biol. Chem.,* **262,** 8252-8256.

Kalinina,E.V., Chernov,N.N., and Saprin,A.N. (2008). Involvement of thio-, peroxi-, and glutaredoxins in cellular redox-dependent processes. *Biochemistry (Mosc.),* **73,** 1493-1510.

Kaneto,H., Kajimoto,Y., Miyagawa,J., Matsuoka,T., Fujitani,Y., Umayahara,Y., Hanafusa,T., Matsuzawa,Y., Yamasaki,Y., and Hori,M. (1999). Beneficial effects of antioxidants in diabetes: possible protection of pancreatic beta-cells against glucose toxicity. *Diabetes,* **48,** 2398-2406.

Kaneto,H., Katakami,N., Matsuhisa,M., and Matsuoka,T.A. (2010). Role of reactive oxygen species in the progression of type 2 diabetes and atherosclerosis. *Mediators. Inflamm.,* **2010,** 453892.

Kaneto,H., Xu,G., Song,K.H., Suzuma,K., Bonner-Weir,S., Sharma,A., and Weir,G.C. (2001). Activation of the hexosamine pathway leads to deterioration of pancreatic B-cell function through the induction of oxidative stress. *J. Biol. Chem.,* **276,** 31099-31104.

Karlsson,K. and Marklund,S.L. (1988). Extracellular superoxide dismutase in the vascular system of mammals. *Biochem. J.,* **255,** 223-228.

Karlsson,K. and Marklund,S.L. (1989). Binding of human extracellular-superoxide dismutase C to cultured cell lines and to blood cells. *Lab Invest,* **60,** 659-666.

Kelly,B.D., Hackett,S.F., Hirota,K., Oshima,Y., Cai,Z., Berg-Dixon,S., Rowan,A., Yan,Z., Campochiaro,P.A., and Semenza,G.L. (2003). Cell Type-Specific Regulation of Angiogenic Growth Factor Gene Expression and Induction of Angiogenesis in Nonischemic Tissue by a Constitutively Active Form of Hypoxia-Inducible Factor 1. *Circ. Res.,* **93,** 1074-1081.

Kerr,S., Brosnan,M.J., McIntyre,M., Reid,J.L., Dominiczak,A.F., and Hamilton,C.A. (1999). Superoxide anion production is increased in a model of genetic hypertension: Role of the endothelium. *Hypertension,* **33,** 1353-1358.

Kietzmann,T. and Gorlach,A. (2005). Reactive oxygen species in the control of hypoxia-inducible factor-mediated gene expression. *Semin. Cell Dev. Biol.,* **16,** 474-486.

Kikuchi,H., Hikage,M., Miyashita,H., and Fukumoto,M. (2000). NADPH oxidase subunit, gp91phox homologue, preferentially expressed in human colon epithelial cells. *Gene,* **254,** 237-243.

Kim,J.W., Tchernyshyov,I., Semenza,G.L., and Dang,C.V. (2006). HIF-1-mediated expression of pyruvate dehydrogenase kinase: A metabolic switch required for cellular adaptation to hypoxia. *Cell Metab.,* **3,** 177-185.

Klimova,T. and Chandel,N.S. (2008). Mitochondrial complex III regulates hypoxic activation of HIF. *Cell Death Differ.,* **15,** 660-666.

Knaapen,A.M., Borm,P.J., Albrecht,C., and Schins,R.P. (2004). Inhaled particles and lung cancer. Part A: Mechanisms. *Int. J. Cancer,* **109,** 799-809.

Knowles,R.G. and Moncada,S. (1994). Nitric oxide synthases in mammals. *Biochem. J.,* **298 (Pt 2),** 249-258.

Koivunen,P., Hirsila,M., Remes,A.M., Hassinen,I.E., Kivirikko,K.I., and Myllyharju,J. (2007). Inhibition of Hypoxia-inducible Factor (HIF) Hydroxylases by Citric Acid Cycle Intermediates. *J. Biol. Chem.,* **282,** 4524-4532.

Konishi,H., Tanaka,M., Takemura,Y., Matsuzaki,H., Ono,Y., Kikkawa,U., and Nishizuka,Y. (1997). Activation of protein kinase C by tyrosine phosphorylation in response to H2O2. *Proc. Natl. Acad. Sci. U. S. A,* **94,** 11233-11237.

Koshio,O., Akanuma,Y., and Kasuga,M. (1988). Hydrogen peroxide stimulates tyrosine phosphorylation of the insulin receptor and its tyrosine kinase activity in intact cells. *Biochem. J.,* **250,** 95-101.

Krause,K.H. (2004). Tissue distribution and putative physiological function of NOX family NADPH oxidases. *Jpn. J. Infect. Dis.,* **57,** S28-S29.

Krzywanski,D.M., Dickinson,D.A., Iles,K.E., Wigley,A.F., Franklin,C.C., Liu,R.M., Kavanagh,T.J., and Forman,H.J. (2004). Variable regulation of glutamate cysteine ligase subunit proteins affects glutathione biosynthesis in response to oxidative stress. *Arch. Biochem. Biophys.,* **423,** 116-125.

Kurata,S.I. (2000). Selective Activation of p38 MAPK Cascade and Mitotic Arrest Caused by Low Level Oxidative Stress. *J. Biol. Chem.,* **275,** 23413-23416.

Landmesser,U., Dikalov,S., Price,S.R., McCann,L., Fukai,T., Holland,S.M., Mitch,W.E., and Harrison,D.G. (2003). Oxidation of tetrahydrobiopterin leads to uncoupling of endothelial cell nitric oxide synthase in hypertension. *J. Clin. Invest.,* **111,** 1201-1209.

Landmesser,U., Cai,H., Dikalov,S., McCann,L., Hwang,J., Jo,H., Holland,S.M., and Harrison,D.G. (2002). Role of p47phox in Vascular Oxidative Stress and Hypertension Caused by Angiotensin II. *Hypertension,* **40,** 511-515.

Larsson,R. and Cerutti,P. (1989). Translocation and Enhancement of Phosphotransferase Activity of Protein Kinase C following Exposure in Mouse Epidermal Cells to Oxidants. *Cancer Res.,* **49,** 5627-5632.

Lash,L.H. (2006). Mitochondrial glutathione transport: Physiological, pathological and toxicological implications. *Chem. Biol. Interact.,* **163,** 54-67.

Laursen,J.B., Somers,M., Kurz,S., McCann,L., Warnholtz,A., Freeman,B.A., Tarpey,M., Fukai,T., and Harrison,D.G. (2001). Endothelial Regulation of Vasomotion

in ApoE-Deficient Mice : Implications for Interactions Between Peroxynitrite and Tetrahydrobiopterin. *Circulation,* **103,** 1282-1288.

Lavrovsky,Y., Chatterjee,B., Clark,R.A., and Roy,A.K. (2000). Role of redox-regulated transcription factors in inflammation, aging and age-related diseases. *Exp. Gerontol.,* **35,** 521-532.

Lenzen,S., Drinkgern,J., and Tiedge,M. (1996). Low antioxidant enzyme gene expression in pancreatic islets compared with various other mouse tissues. *Free Radic. Biol. Med.,* **20,** 463-466.

Li,C.Y., Shan,S., Huang,Q., Braun,R.D., Lanzen,J., Hu,K., Lin,P., and Dewhirst,M.W. (2000). Initial stages of tumor cell-induced angiogenesis: evaluation via skin window chambers in rodent models. *J. Natl. Cancer Inst.,* **92,** 143-147.

Li,F., Sonveaux,P., Rabbani,Z.N., Liu,S., Yan,B., Huang,Q., Vujaskovic,Z., Dewhirst,M.W., and Li,C.Y. (2007). Regulation of HIF-1alpha stability through S-Nitrosylation. *Mol. Cell,* **26,** 63-74.

Li,H. and Forstermann,U. (2000). Nitric oxide in the pathogenesis of vascular disease. *J. Pathol.,* **190,** 244-254.

Li,H., Witte,K., August,M., Brausch,I., Godtel-Armburst,U., Habermeier,A., Closs,E.I., Oelze,M., Munzel,T., and Forstermann,U. (2006). Reversal of Endothelial Nitric Oxide Synthase Uncoupling and Up-Regulation of Endothelial Nitric Oxide Synthase Expression Lowers Blood Pressure in Hypertensive Rats. *J. Am. Coll. Cardiol.,* **47,** 2536-2544.

Li,N. and Karin,M. (1999). Is NF-kappaB the sensor of oxidative stress? *FASEB J.,* **13,** 1137-1143.

Linares,E., Giorgio,S., Mortara,R.A., Santos,C.X.C., Yamada,A.T., and Augusto,O. (2001). Role of peroxynitrite in macrophage microbicidal mechanisms in vivo revealed by protein nitration and hydroxylation. *Free Radic. Biol. Med.,* **30,** 1234-1242.

Liochev,S.I. and Fridovich,I. (1995). Superoxide from Glucose Oxidase or from Nitroblue Tetrazolium? *Arch. Biochem. Biophys.,* **318,** 408-410.

Liochev,S.I. and Fridovich,I. (1998). Lucigenin as mediator of superoxide production: revisited. *Free Radic. Biol. Med.,* **25,** 926-928.

Lirk,P., Hoffmann,G., and Rieder,J. (2002). Inducible nitric oxide synthase--time for reappraisal. *Curr. Drug Targets. Inflamm. Allergy,* **1,** 89-108.

Liu,F., Liu,Y., Lui,V.C.H., Lamb,J.R., Tam,P.K.H., and Chen,Y. (2008a). Hypoxia modulates lipopolysaccharide induced TNF-alpha expression in murine macrophages. *Exp. Cell Res.,* **314,** 1327-1336.

Liu,L., Marti,G.P., Wei,X., Zhang,X., Zhang,H., Liu,Y.V., Nastai,M., Semenza,G.L., and Harmon,J.W. (2008b). Age-dependent impairment of HIF-1alpha expression in diabetic mice: Correction with electroporation-facilitated gene therapy increases wound healing, angiogenesis, and circulating angiogenic cells. *J. Cell Physiol.,* **217,** 319-327.

Liu,S.F., Adcock,I.M., Old,R.W., Barnes,P.J., and Evans,T.W. (1993). Lipopolysaccharide Treatment in Vivo Induces Widespread Tissue Expression of Inducible Nitric Oxide Synthase mRNA. *Biochem. Biophys. Res. Commun.,* **196,** 1208-1213.

Lo,Y.Y.C. and Cruz,T.F. (1995). Involvement of Reactive Oxygen Species in Cytokine and Growth Factor Induction of c-fos Expression in Chondrocytes. *J. Biol. Chem.,* **270,** 11727-11730.

Mabrouk,G.M., Jois,M., and Brosnan,J.T. (1998). Cell signalling and the hormonal stimulation of the hepatic glycine cleavage enzyme system by glucagon. *Biochem. J.,* **330 (Pt 2),** 759-763.

Makino,Y., Cao,R., Svensson,K., Bertilsson,G., Asman,M., Tanaka,H., Cao,Y., Berkenstam,A., and Poellinger,L. (2001). Inhibitory PAS domain protein is a negative regulator of hypoxia-inducible gene expression. *Nature,* **414,** 550-554.

Manna,S.K., Zhang,H.J., Yan,T., Oberley,L.W., and Aggarwal,B.B. (1998). Overexpression of Manganese Superoxide Dismutase Suppresses Tumor Necrosis Factor-induced Apoptosis and Activation of Nuclear Transcription Factor-kappa B and Activated Protein-1. *J. Biol. Chem.,* **273,** 13245-13254.

Mansfield,K.D., Guzy,R.D., Pan,Y., Young,R.M., Cash,T.P., Schumacker,P.T., and Simon,M.C. (2005). Mitochondrial dysfunction resulting from loss of cytochrome c impairs cellular oxygen sensing and hypoxic HIF-alpha activation. *Cell Metab.,* **1,** 393-399.

Marklund,S.L. (1982). Human copper-containing superoxide dismutase of high molecular weight. *Proc. Natl. Acad. Sci. U. S. A,* **79,** 7634-7638.

Marklund,S.L. (1984). Extracellular superoxide dismutase in human tissues and human cell lines. *J. Clin. Invest.,* **74,** 1398-1403.

Marklund,S.L. (1990). Expression of extracellular superoxide dismutase by human cell lines. *Biochem. J.,* **266,** 213-219.

Marklund,S.L., Holme,E., and Hellner,L. (1982). Superoxide dismutase in extracellular fluids. *Clin. Chim. Acta,* **126,** 41-51.

Masters,B.S., McMillan,K., Sheta,E.A., Nishimura,J.S., Roman,L.J., and Martasek,P. (1996). Neuronal nitric oxide synthase, a modular enzyme formed by convergent evolution: structure studies of a cysteine thiolate-liganded heme protein that hydroxylates L-arginine to produce NO. as a cellular signal [published erratum appears in FASEB J 1996 Jul;10(9):1107]. *FASEB J.,* **10,** 552-558.

Matsuno,K., Yamada,H., Iwata,K., Jin,D., Katsuyama,M., Matsuki,M., Takai,S., Yamanishi,K., Miyazaki,M., Matsubara,H., and Yabe-Nishimura,C. (2005). Nox1 Is Involved in Angiotensin II-Mediated Hypertension: A Study in Nox1-Deficient Mice. *Circulation,* **112,** 2677-2685.

Maxwell,P.H., Wiesener,M.S., Chang,G.W., Clifford,S.C., Vaux,E.C., Cockman,M.E., Wykoff,C.C., Pugh,C.W., Maher,E.R., and Ratcliffe,P.J. (1999). The tumour suppressor protein VHL targets hypoxia-inducible factors for oxygen-dependent proteolysis. *Nature,* **399,** 271-275.

McCord,J.M. and Fridovich,I. (1969a). Superoxide dismutase. An enzymic function for erythrocuprein (hemocuprein). *J. Biol. Chem.,* **244,** 6049-6055.

McCord,J.M. and Fridovich,I. (1969b). The Utility of superoxide dismutase in studying free radical reactions. I. Radicals generated by the interaction of sulfite, dimethyl sulfoxide, and oxygen. *J. Biol. Chem.,* **244,** 6056-6063.

McNally,J.S., Davis,M.E., Giddens,D.P., Saha,A., Hwang,J., Dikalov,S., Jo,H., and Harrison,D.G. (2003). Role of xanthine oxidoreductase and NAD(P)H oxidase in endothelial superoxide production in response to oscillatory shear stress. *Am J Physiol Heart Circ Physiol,* **285,** H2290-H2297.

Meister,A. (1988). Glutathione metabolism and its selective modification. *J. Biol. Chem.,* **263,** 17205-17208.

Mekhail,K., Gunaratnam,L., Bonicalzi,M.E., and Lee,S. (2004). HIF activation by pH-dependent nucleolar sequestration of VHL. *Nat. Cell Biol.,* **6,** 642-647.

Metzen,E., Zhou,J., Jelkmann,W., Fandrey,J., and Brune,B. (2003). Nitric Oxide impairs normoxic degradation of HIF-1alpha by inhibition of prolyl hydroxylases. *Mol. Biol. Cell,* **14,** 3470-3481.

Meyer,M., Schreck,R., and Baeuerle,P.A. (1993). H2O2 and antioxidants have opposite effects on activation of NF-kappa B and AP-1 in intact cells: AP-1 as secondary antioxidant-responsive factor. *EMBO J.,* **12,** 2005-2015.

Meziane-El-Hassani,R., Morand,S., Boucher,J.L., Frapart,Y.M., Apostolou,D., Agnandji,D., Gnidehou,S., Ohayon,R.e., Noel-Hudson,M., Francon,J., Lalaoui,K., Virion,A., and Dupuy,C. (2005). Dual Oxidase-2 Has an Intrinsic Ca2+-dependent H2O2-generating Activity. *J. Biol. Chem.,* **280,** 30046-30054.

Milenkovic,M., De Deken,X., Jin,L., De Felice,M., Di Lauro,R., Dumont,J.E., Corvilain,B., and Miot,F. (2007). Duox expression and related H2O2 measurement in mouse thyroid: onset in embryonic development and regulation by TSH in adult. *J. Endocrinol.,* **192,** 615-626.

Mills,G.C. (1957). Hemoglobin catabolism I. Glutathione peroxidase, an erythrocyte enzyme which protects hemoglobin from oxidative breakdown. *J. Biol. Chem.,* **229,** 189-197.

Miquel,J., Economos,A.C., Fleming,J., and Johnson,J. (1980). Mitochondrial role in cell aging. *Exp. Gerontol.,* **15,** 575-591.

Mitchell,P. (1977). A commentary on alternative hypotheses of protonic coupling in the membrane systems catalysing oxidative and photosynthetic phosphorylation. *FEBS Lett.,* **78,** 1-20.

Mollnau,H., Wendt,M., Szocs,K., Lassegue,B., Schulz,E., Oelze,M., Li,H., Bodenschatz,M., August,M., Kleschyov,A.L., Tsilimingas,N., Walter,U., Forstermann,U., Meinertz,T., Griendling,K., and Munzel,T. (2002). Effects of Angiotensin II Infusion on the Expression and Function of NAD(P)H Oxidase and Components of Nitric Oxide/cGMP Signaling. *Circ. Res.,* **90,** e58-e65.

Moncada,S. and Higgs,A. (1993). The L-arginine-nitric oxide pathway. *N. Engl. J. Med.,* **329,** 2002-2012.

Mukhopadhyay,C.K., Mazumder,B., and Fox,P.L. (2000). Role of Hypoxia-inducible Factor-1 in Transcriptional Activation of Ceruloplasmin by Iron Deficiency. *J. Biol. Chem.,* **275,** 21048-21054.

Murley,J.S., Kataoka,Y., Hallahan,D.E., Roberts,J.C., and Grdina,D.J. (2001). Activation of NF-KappaB and MnSOD gene expression by free radical scavengers in human microvascular endothelial cells. *Free Radic. Biol. Med.,* **30,** 1426-1439.

Murphy,M.P. (2009). How mitochondria produce reactive oxygen species. *Biochem. J.,* **417,** 1-13.

Nass,M.M. (1970). Abnormal DNA patterns in animal mitochondria: ethidium bromide-induced breakdown of closed circular DNA and conditions leading to oligomer accumulation. *Proc. Natl. Acad. Sci. U. S. A,* **67,** 1926-1933.

Nass,M.M. (1972). Differential effects of ethidium bromide on mitochondrial and nuclear DNA synthesis in vivo in cultured mammalian cells. *Exp. Cell Res.,* **72,** 211-222.

Newton,A.C. (1995). Protein Kinase C: Structure, Function, and Regulation. *J. Biol. Chem.,* **270,** 28495-28498.

Newton,A.C. (1997). Regulation of protein kinase C. *Curr. Opin. Cell Biol.,* **9,** 161-167.

Nishizuka,Y. (1995). Protein kinase C and lipid signaling for sustained cellular responses. *FASEB J.,* **9,** 484-496.

Noji,H. and Yoshida,M. (2001). The Rotary Machine in the Cell, ATP Synthase . *J. Biol. Chem.,* **276,** 1665-1668.

Ochoa,J.B., Udekwu,A.O., Billiar,T.R., Curran,R.D., Cerra,F.B., Simmons,R.L., and Peitzman,A.B. (1991). Nitrogen oxide levels in patients after trauma and during sepsis. *Ann. Surg.,* **214,** 621-626.

Ohara,Y., Peterson,T.E., and Harrison,D.G. (1993). Hypercholesterolemia increases endothelial superoxide anion production. *J. Clin. Invest.,* **91,** 2546-2551.

Ohashi,M., Runge,M.S., Faraci,F.M., and Heistad,D.D. (2006). MnSOD Deficiency Increases Endothelial Dysfunction in ApoE-Deficient Mice. *Arterioscler. Thromb. Vasc. Biol.,* **26,** 2331-2336.

Okado-Matsumoto,A. and Fridovich,I. (2001). Subcellular Distribution of Superoxide Dismutases (SOD) in Rat Liver. *J. Biol. Chem.,* **276,** 38388-38393.

Palacios-Callender,M., Quintero,M., Hollis,V.S., Springett,R.J., and Moncada,S. (2004). Endogenous NO regulates superoxide production at low oxygen concentrations by modifying the redox state of cytochrome c oxidase. *Proc. Natl. Acad. Sci. U. S. A,* **101,** 7630-7635.

Pallardo,F.V., Asensi,M., Garcia de la,A.J., Anton,V., Lloret,A., Sastre,J., and Vina,J. (1998). Late onset administration of oral antioxidants prevents age-related loss of motor co-ordination and brain mitochondrial DNA damage. *Free Radic. Res.,* **29,** 617-623.

Palmer,R.M., Ferrige,A.G., and Moncada,S. (1987). Nitric oxide release accounts for the biological activity of endothelium-derived relaxing factor. *Nature,* **327,** 524-526.

Pan,Y., Mansfield,K.D., Bertozzi,C.C., Rudenko,V., Chan,D.A., Giaccia,A.J., and Simon,M.C. (2007). Multiple Factors Affecting Cellular Redox Status and Energy Metabolism Modulate Hypoxia-Inducible Factor Prolyl Hydroxylase Activity In Vivo and In Vitro. *Mol. Cell Biol.,* **27,** 912-925.

Panov,A., Dikalov,S., Shalbuyeva,N., Taylor,G., Sherer,T., and Greenamyre,J.T. (2005). Rotenone Model of Parkinson Disease. *J. Biol. Chem.,* **280,** 42026-42035.

Papandreou,I., Cairns,R.A., Fontana,L., Lim,A.L., and Denko,N.C. (2006). HIF-1 mediates adaptation to hypoxia by actively downregulating mitochondrial oxygen consumption. *Cell Metab.,* **3,** 187-197.

Pearlstein,D.P., Ali,M.H., Mungai,P.T., Hynes,K.L., Gewertz,B.L., and Schumacker,P.T. (2002). Role of Mitochondrial Oxidant Generation in Endothelial Cell Responses to Hypoxia. *Arterioscler. Thromb. Vasc. Biol.,* **22,** 566-573.

Peyssonnaux,C., Zinkernagel,A.S., Schuepbach,R.A., Rankin,E., Vaulont,S., Haase,V.H., Nizet,V., and Johnson,R.S. (2007). Regulation of iron homeostasis by the hypoxia-inducible transcription factors (HIFs). *J. Clin. Invest.,* **117,** 1926-1932.

Peyssonnaux,C., Datta,V., Cramer,T., Doedens,A., Theodorakis,E.A., Gallo,R.L., Hurtado-Ziola,N., Nizet,V., and Johnson,R.S. (2005). HIF-1alpha expression regulates the bactericidal capacity of phagocytes. *J. Clin. Invest.,* **115,** 1806-1815.

Picker,S.D. and Fridovich,I. (1984). On the mechanism of production of superoxide radical by reaction mixtures containing NADH, phenazine methosulfate, and nitroblue tetrazolium. *Arch. Biochem. Biophys.,* **228,** 155-158.

Poderoso,J.J., Carreras,M.C., Lisdero,C., Riobo,N., Schopfer,F., and Boveris,A. (1996). Nitric Oxide Inhibits Electron Transfer and Increases Superoxide Radical Production in Rat Heart Mitochondria and Submitochondrial Particles. *Arch. Biochem. Biophys.,* **328,** 85-92.

Poellinger,L. and Johnson,R.S. (2004). HIF-1 and hypoxic response: the plot thickens. *Curr. Opin. Genet. Dev.,* **14,** 81-85.

Pollard,P.J., Briere,J.J., Alam,N.A., Barwell,J., Barclay,E., Wortham,N.C., Hunt,T., Mitchell,M., Olpin,S., Moat,S.J., Hargreaves,I.P., Heales,S.J., Chung,Y.L., Griffiths,J.R., Dalgleish,A., McGrath,J.A., Gleeson,M.J., Hodgson,S.V., Poulsom,R., Rustin,P., and Tomlinson,I.P.M. (2005). Accumulation of Krebs cycle intermediates and over-expression of HIF1alpha in tumours which result from germline FH and SDH mutations. *Hum. Mol. Genet.,* **14,** 2231-2239.

Pollock,J.S., Forstermann,U., Mitchell,J.A., Warner,T.D., Schmidt,H.H., Nakane,M., and Murad,F. (1991). Purification and characterization of particulate endothelium-derived relaxing factor synthase from cultured and native bovine aortic endothelial cells. *Proc. Natl. Acad. Sci. U. S. A,* **88,** 10480-10484.

Potter,D.W. and Tran,T.B. (1993). Apparent Rates of Glutathione Turnover in Rat Tissues. *Toxicol. Appl. Pharmacol.,* **120,** 186-192.

Pou,S., Hassett,D.J., Britigan,B.E., Cohen,M.S., and Rosen,G.M. (1989). Problems associated with spin trapping oxygen-centered free radicals in biological systems. *Anal. Biochem.,* **177,** 1-6.

Pou,S., Keaton,L., Surichamorn,W., and Rosen,G.M. (1999). Mechanism of Superoxide Generation by Neuronal Nitric-oxide Synthase. *J. Biol. Chem.,* **274,** 9573-9580.

Pouyssegur,J. and Mechta-Grigoriou,F. (2006). Redox regulation of the hypoxia-inducible factor. *Biol. Chem.,* **387,** 1337-1346.

Powis,G., Mustacich,D., and Coon,A. (2000). The role of the redox protein thioredoxin in cell growth and cancer. *Free Radic. Biol. Med.,* **29,** 312-322.

Pritchard,K.A., Jr., Groszek,L., Smalley,D.M., Sessa,W.C., Wu,M., Villalon,P., Wolin,M.S., and Stemerman,M.B. (1995). Native Low-Density Lipoprotein Increases Endothelial Cell Nitric Oxide Synthase Generation of Superoxide Anion. *Circ. Res.,* **77,** 510-518.

Puddu,P., Puddu,G.M., Cravero,E., Rosati,M., and Muscari,A. (2008). The molecular sources of reactive oxygen species in hypertension. *Blood Press.,* **17,** 70-77.

Quintero,M., Brennan,P.A., Thomas,G.J., and Moncada,S. (2006a). Nitric Oxide Is a Factor in the Stabilization of Hypoxia-Inducible Factor-1alpha in Cancer: Role of Free Radical Formation. *Cancer Res.,* **66,** 770-774.

Quintero,M., Colombo,S.L., Godfrey,A., and Moncada,S. (2006b). Mitochondria as signaling organelles in the vascular endothelium. *Proc. Natl. Acad. Sci. U. S. A,* **103,** 5379-5384.

Rada,B., Hably,C., Meczner,A., Timar,C., Lakatos,G., Enyedi,P., and Ligeti,E. (2008). Role of Nox2 in elimination of microorganisms. *Semin. Immunopathol.,* **30,** 237-253.

Radi,R., Cassina,A., and Hodara,R. (2002). Nitric oxide and peroxynitrite interactions with mitochondria. *Biol. Chem.,* **383,** 401-409.

Ramachandran,A., Levonen,A.L., Brookes,P.S., Ceaser,E., Shiva,S., Barone,M.C., and Darley-Usmar,V. (2002). Mitochondria, nitric oxide, and cardiovascular dysfunction. *Free Radic. Biol. Med.,* **33,** 1465-1474.

Rathore,R., Zheng,Y.M., Niu,C.F., Liu,Q.H., Korde,A., Ho,Y.S., and Wang,Y.X. (2008). Hypoxia activates NADPH oxidase to increase [ROS]i and [Ca2+]i through the mitochondrial ROS-PKC[var epsilon] signaling axis in pulmonary artery smooth muscle cells. *Free Radic. Biol. Med.,* **45,** 1223-1231.

Rhee,S.G., Kang,S.W., Jeong,W., Chang,T.S., Yang,K.S., and Woo,H.A. (2005). Intracellular messenger function of hydrogen peroxide and its regulation by peroxiredoxins. *Curr. Opin. Cell Biol.,* **17,** 183-189.

Rolfe,D.F. and Brown,G.C. (1997). Cellular energy utilization and molecular origin of standard metabolic rate in mammals. *Physiol. Rev.,* **77,** 731-758.

Rolfs,A., Kvietikova,I., Gassmann,M., and Wenger,R.H. (1997). Oxygen-regulated Transferrin Expression Is Mediated by Hypoxia-inducible Factor-1. *J. Biol. Chem.,* **272,** 20055-20062.

Rota,C., Chignell,C.F., and Mason,R.P. (1999). Evidence for free radical formation during the oxidation of 2'-7'-dichlorofluorescin to the fluorescent dye 2'-7'-dichlorofluorescein by horseradish peroxidase: Possible implications for oxidative stress measurements. *Free Radic. Biol. Med.,* **27,** 873-881.

Ryan,H.E., Lo,J., and Johnson,R.S. (1998). HIF-1alpha is required for solid tumor formation and embryonic vascularization. *EMBO J.,* **17,** 3005-3015.

Sanjuan-Pla,A., Cervera,A.M., Apostolova,N., Garcia-Bou,R., Victor,V.M., Murphy,M.P., and McCreath,K.J. (2005). A targeted antioxidant reveals the importance of mitochondrial reactive oxygen species in the hypoxic signaling of HIF-1alpha. *FEBS Lett.,* **579,** 2669-2674.

Scarpulla,R.C. (2008). Transcriptional Paradigms in Mammalian Mitochondrial Biogenesis and Function. *Physiol. Rev.,* **88,** 611-638.

Schofield,C.J. and Ratcliffe,P.J. (2004). Oxygen sensing by HIF hydroxylases. *Nat Rev Mol Cell Biol,* **5,** 343-354.

Schofield,C.J. and Ratcliffe,P.J. (2005). Signalling hypoxia by HIF hydroxylases. *Biochem. Biophys. Res. Commun.,* **338,** 617-626.

Schreck,R., Rieber,P., and Baeuerle,P.A. (1991). Reactive oxygen intermediates as apparently widely used messengers in the activation of the NF-kappa B transcription factor and HIV-1. *EMBO J.,* **10,** 2247-2258.

Schroedl,C., McClintock,D.S., Budinger,G.R.S., and Chandel,N.S. (2002). Hypoxic but not anoxic stabilization of HIF-1alpha requires mitochondrial reactive oxygen species. *Am. J. Physiol. Lung Cell Mol. Physiol.,* **283,** L922-L931.

Schumacker,P.T. (2002). Hypoxia, anoxia, and O2 sensing: the search continues. *Am. J. Physiol. Lung Cell Mol. Physiol.,* **283,** L918-L921.

Seagroves,T.N., Ryan,H.E., Lu,H., Wouters,B.G., Knapp,M., Thibault,P., Laderoute,K., and Johnson,R.S. (2001). Transcription factor HIF-1 is a necessary mediator of the pasteur effect in mammalian cells. *Mol. Cell Biol.,* **21,** 3436-3444.

Semenza,G.L. (2000). HIF-1 and human disease: one highly involved factor. *Genes Dev.,* **14,** 1983-1991.

Semenza,G.L. (2006). Development of novel therapeutic strategies that target HIF-1. *Expert. Opin. Ther. Targets.,* **10,** 267-280.

Semenza,G.L. (2003). Targeting HIF-1 for cancer therapy. *Nat Rev Cancer,* **3,** 721-732.

Semenza,G.L. (2007). Oxygen-dependent regulation of mitochondrial respiration by hypoxia-inducible factor 1. *Biochem. J.,* **405,** 1-9.

Semenza,G.L. (2009a). Regulation of cancer cell metabolism by hypoxia-inducible factor 1. *Semin. Cancer Biol.,* **19,** 12-16.

Semenza,G.L. (2009b). Regulation of Oxygen Homeostasis by Hypoxia-Inducible Factor 1. *Physiology,* **24,** 97-106.

Semenza,G.L., Jiang,B.H., Leung,S.W., Passantino,R., Concordet,J.P., Maire,P., and Giallongo,A. (1996). Hypoxia Response Elements in the Aldolase A, Enolase 1, and Lactate Dehydrogenase A Gene Promoters Contain Essential Binding Sites for Hypoxia-inducible Factor 1. *J. Biol. Chem.,* **271,** 32529-32537.

Shiose,A., Kuroda,J., Tsuruya,K., Hirai,M., Hirakata,H., Naito,S., Hattori,M., Sakaki,Y., and Sumimoto,H. (2001). A Novel Superoxide-producing NAD(P)H Oxidase in Kidney. *J. Biol. Chem.,* **276,** 1417-1423.

Simon,M.C. (2006). Mitochondrial reactive oxygen species are required for hypoxic HIF alpha stabilization. *Adv. Exp. Med. Biol,* **588,** 165-170.

Simon,M.P., Tournaire,R., and Pouyssegur,J. (2008). The angiopoietin-2 gene of endothelial cells is up-regulated in hypoxia by a HIF binding site located in its first intron and by the central factors GATA-2 and Ets-1. *J. Cell Physiol.,* **217,** 809-818.

Singh,K.K. (2006). Mitochondria damage checkpoint, aging, and cancer. *Ann. N. Y. Acad. Sci.,* **1067,** 182-190.

Soderberg,A., Sahaf,B., and Rosen,A. (2000). Thioredoxin Reductase, a Redox-active Selenoprotein, Is Secreted by Normal and Neoplastic Cells: Presence in Human Plasma. *Cancer Res.,* **60,** 2281-2289.

Sorescu,D., Weiss,D., Lassegue,B., Clempus,R.E., Szocs,K., Sorescu,G.P., Valppu,L., Quinn,M.T., Lambeth,J.D., Vega,J.D., Taylor,W.R., and Griendling,K.K. (2002). Superoxide Production and Expression of Nox Family Proteins in Human Atherosclerosis. *Circulation,* **105,** 1429-1435.

Srinivas,V., Leshchinsky,I., Sang,N., King,M.P., Minchenko,A., and Caro,J. (2001). Oxygen Sensing and HIF-1 Activation Does Not Require an Active Mitochondrial Respiratory Chain Electron-transfer Pathway. *J. Biol. Chem.,* **276,** 21995-21998.

Stocker,R. and Perrella,M.A. (2006). Heme Oxygenase-1: A Novel Drug Target for Atherosclerotic Diseases? *Circulation,* **114,** 2178-2189.

Stuehr,D.J., Cho,H.J., Kwon,N.S., Weise,M.F., and Nathan,C.F. (1991a). Purification and characterization of the cytokine-induced macrophage nitric oxide synthase: an FAD- and FMN-containing flavoprotein. *Proc. Natl. Acad. Sci. U. S. A,* **88,** 7773-7777.

Stuehr,D.J., Kwon,N.S., Nathan,C.F., Griffith,O.W., Feldman,P.L., and Wiseman,J. (1991b). N omega-hydroxy-L-arginine is an intermediate in the biosynthesis of nitric oxide from L-arginine. *J. Biol. Chem.,* **266,** 6259-6263.

Stuehr,D.J. and Nathan,C.F. (1989). Nitric oxide. A macrophage product responsible for cytostasis and respiratory inhibition in tumor target cells. *J Exp. Med.,* **169,** 1543-1555.

Stuehr,D., Pou,S., and Rosen,G.M. (2001). Oxygen Reduction by Nitric-oxide Synthases. *J. Biol. Chem.,* **276,** 14533-14536.

Suh,Y.A., Arnold,R.S., Lassegue,B., Shi,J., Xu,X., Sorescu,D., Chung,A.B., Griendling,K.K., and Lambeth,J.D. (1999). Cell transformation by the superoxide-generating oxidase Mox1. *Nature,* **401,** 79-82.

Suzuki,Y.J., Forman,H.J., and Sevanian,A. (1997). Oxidants as Stimulators of Signal Transduction. *Free Radic. Biol. Med.,* **22,** 269-285.

Szatrowski,T.P. and Nathan,C.F. (1991). Production of large amounts of hydrogen peroxide by human tumor cells. *Cancer Res.,* **51,** 794-798.

Tacchini,L., Bianchi,L., Bernelli-Zazzera,A., and Cairo,G. (1999). Transferrin Receptor Induction by Hypoxia. *J. Biol. Chem.,* **274,** 24142-24146.

Taille,C., El-Benna,J., Lanone,S., Dang,M.C., Ogier-Denis,E., Aubier,M., and Boczkowski,J. (2004). Induction of Heme Oxygenase-1 Inhibits NAD(P)H Oxidase Activity by Down-regulating Cytochrome b558 Expression via the Reduction of Heme Availability. *J. Biol. Chem.,* **279,** 28681-28688.

Tampo,Y., Kotamraju,S., Chitambar,C.R., Kalivendi,S.V., Keszler,A., Joseph,J., and Kalyanaraman,B. (2003). Oxidative Stress-Induced Iron Signaling Is Responsible for Peroxide-Dependent Oxidation of Dichlorodihydrofluorescein in Endothelial Cells: Role of Transferrin Receptor-Dependent Iron Uptake in Apoptosis. *Circ. Res.,* **92,** 56-63.

Tanudji,M., Hevi,S., and Chuck,S.L. (2003). The nonclassic secretion of thioredoxin is not sensitive to redox state. *Am. J. Physiol. Cell Physiol.,* **284,** C1272-C1279.

Tapiero,H., Mathe,G., Couvreur,P., and Tew,K.D. (2002). II. Glutamine and glutamate. *Biomed. Pharmacother.,* **56,** 446-457.

Tarpey,M.M. and Fridovich,I. (2001). Methods of Detection of Vascular Reactive Species: Nitric Oxide, Superoxide, Hydrogen Peroxide, and Peroxynitrite. *Circ. Res.,* **89,** 224-236.

Tiedge,M., Lortz,S., Drinkgern,J., and Lenzen,S. (1997). Relation between antioxidant enzyme gene expression and antioxidative defense status of insulin-producing cells. *Diabetes,* **46,** 1733-1742.

Touyz,R.M. (2004). Reactive oxygen species and angiotensin II signaling in vascular cells -- implications in cardiovascular disease. *Braz. J. Med. Biol. Res.,* **37,** 1263-1273.

Tsan,M.F., Clark,R.N., Goyert,S.M., and White,J.E. (2001). Induction of TNF-alpha and MnSOD by endotoxin: role of membrane CD14 and Toll-like receptor-4. *Am. J. Physiol. Cell Physiol.,* **280,** C1422-C1430.

Turrens,J.F., Alexandre,A., and Lehninger,A.L. (1985). Ubisemiquinone is the electron donor for superoxide formation by complex III of heart mitochondria. *Arch. Biochem. Biophys.,* **237,** 408-414.

Turrens,J.F., Freeman,B.A., Levitt,J.G., and Crapo,J.D. (1982). The effect of hyperoxia on superoxide production by lung submitochondrial particles. *Arch. Biochem. Biophys.,* **217,** 401-410.

Turrens,J.F. (2003). Mitochondrial formation of reactive oxygen species. *J. Physiol.,* **552,** 335-344.

Tuttle,S.W., Maity,A., Oprysko,P.R., Kachur,A.V., Ayene,I.S., Biaglow,J.E., and Koch,C.J. (2007). Detection of reactive oxygen species via endogenous oxidative Pentose Phosphate Cycle activity in response to oxygen concentration: Implications for the mechanism of HIF-1alpha stabilisation under moderate hypoxia. *J. Biol. Chem.,* **282,** 36790-36796.

Valko,M., Rhodes,C.J., Moncol,J., Izakovic,M., and Mazur,M. (2006). Free radicals, metals and antioxidants in oxidative stress-induced cancer. *Chem. Biol. Interact.,* **160,** 1-40.

Vanden Hoek,T.L., Becker,L.B., Shao,Z., Li,C., and Schumacker,P.T. (1998). Reactive Oxygen Species Released from Mitochondria during Brief Hypoxia Induce Preconditioning in Cardiomyocytes. *J. Biol. Chem.,* **273,** 18092-18098.

Vaquero,J., Zurita,M., Aguayo,C., and Coca,S. (2004). Relationship between apoptosis and proliferation in secondary tumors of the brain. *Neuropathology.,* **24,** 302-305.

Vaux,E.C., Metzen,E., Yeates,K.M., and Ratcliffe,P.J. (2001). Regulation of hypoxia-inducible factor is preserved in the absence of a functioning mitochondrial respiratory chain. *Blood,* **98,** 296-302.

Vijg,J. (1999). Genetics of aging: Sponsored by Cold Spring Harbor Laboratory, 2-5 April 1998. *Biochim. Biophys. Acta. - Reviews on Cancer,* **1423,** 1-12.

Wang,G.L. and Semenza,G.L. (1993). Characterization of hypoxia-inducible factor 1 and regulation of DNA binding activity by hypoxia. *J. Biol. Chem.,* **268,** 21513-21518.

Wang,X., Gjorloff-Wingren,A., Saxena,M., Pathan,N., Reed,J.C., and Mustelin,T. (2000). The tumor suppressor PTEN regulates T cell survival and antigen receptor signaling by acting as a phosphatidylinositol 3-phosphatase. *J. Immunol.,* **164,** 1934-1939.

Wang,X., Martindale,J.L., Liu,Y., and Holbrook,N.J. (1998). The cellular response to oxidative stress: influences of mitogen-activated protein kinase signalling pathways on cell survival. *Biochem. J.,* **333 (Pt 2),** 291-300.

Wanrooij,S., Goffart,S., Pohjoismaki,J.L.O., Yasukawa,T., and Spelbrink,J.N. (2007). Expression of catalytic mutants of the mtDNA helicase Twinkle and polymerase POLG causes distinct replication stalling phenotypes. *Nucl. Acids Res.,* **35,** 3238-3251.

Ward,J.P.T. (2008). Oxygen sensors in context. *Biochim. Biophys. Acta. - Bioenergetics,* **1777,** 1-14.

Warner,B.B., Stuart,L., Gebb,S., and Wispe,J.R. (1996). Redox regulation of manganese superoxide dismutase. *Am. J. Physiol. Lung Cell Mol. Physiol.,* **271,** L150-L158.

Warnholtz,A., Nickenig,G., Schulz,E., Macharzina,R., Brasen,J.H., Skatchkov,M., Heitzer,T., Stasch,J.P., Griendling,K.K., Harrison,D.G., Bohm,M., Meinertz,T., and Munzel,T. (1999). Increased NADH-Oxidase mediated superoxide production in the

early stages of atherosclerosis: Evidence for involvement of the renin-angiotensin system. *Circulation,* **99,** 2027-2033.

Waypa,G.B. and Schumacker,P.T. (2002). O2 sensing in hypoxic pulmonary vasoconstriction: the mitochondrial door re-opens. *Respir. Physiol. Neurobiol.,* **132,** 81-91.

Weisiger,R.A. and Fridovich,I. (1973). Mitochondrial superoxide simutase. Site of synthesis and intramitochondrial localization. *J. Biol. Chem.,* **248,** 4793-4796.

Wellman,T.L., Jenkins,J., Penar,P.L., Tranmer,B., Zahr,R., and Lounsbury,K.M. (2003). Nitric oxide and reactive oxygen species exert opposing effects on the stability of hypoxia inducible factor-1alpha; (HIF-1alpha;) in explants of human pial arteries. *FASEB J.,* **18,** 379-381.

Whisler,R.L., Goyette,M.A., Grants,I.S., and Newhouse,Y.G. (1995). Sublethal Levels of Oxidant Stress Stimulate Multiple Serine/Threonine Kinases and Suppress Protein Phosphatases in Jurkat T Cells. *Arch. Biochem. Biophys.,* **319,** 23-35.

White,C.R., Darley-Usmar,V., Berrington,W.R., McAdams,M., Gore,J.Z., Thompson,J.A., Parks,D.A., Tarpey,M.M., and Freeman,B.A. (1996). Circulating plasma xanthine oxidase contributes to vascular dysfunction in hypercholesterolemic rabbits. *Proc. Natl. Acad. Sci. U. S. A,* **93,** 8745-8749.

Willam,C., Nicholls,L.G., Ratcliffe,P.J., Pugh,C.W., and Maxwell,P.H. (2004). The prolyl hydroxylase enzymes that act as oxygen sensors regulating destruction of hypoxia-inducible factor alpha. *Adv. Enzyme Regul.,* **44,** 75-92.

Wittenberg,B.A. and Wittenberg,J.B. (1989). Transport of oxygen in muscle. *Annu. Rev. Physiol.,* **51,** 857-878.

Woo,H.A., Yim,S.H., Shin,D.H., Kang,D., Yu,D.Y., and Rhee,S.G. (2010). Inactivation of Peroxiredoxin I by Phosphorylation Allows Localized H2O2 Accumulation for Cell Signaling. *Cell,* **140,** 517-528.

Xia,Y., Tsai,A.L., Berka,V., and Zweier,J.L. (1998). Superoxide Generation from Endothelial Nitric-oxide Synthase. *J. Biol. Chem.,* **273,** 25804-25808.

Yamawaki,H., Haendeler,J., and Berk,B.C. (2003). Thioredoxin: A Key Regulator of Cardiovascular Homeostasis. *Circ. Res.,* **93,** 1029-1033.

Yang,H., Roberts,L.J., Shi,M.J., Zhou,L.C., Ballard,B.R., Richardson,A., and Guo,Z.M. (2004). Retardation of Atherosclerosis by Overexpression of Catalase or Both Cu/Zn-Superoxide Dismutase and Catalase in Mice Lacking Apolipoprotein E. *Circ. Res.,* **95,** 1075-1081.

Yang,S., Madyastha,P., Bingel,S., Ries,W., and Key,L. (2001). A New Superoxide-generating Oxidase in Murine Osteoclasts. *J. Biol. Chem.,* **276,** 5452-5458.

Yoon,D., Pastore,Y.D., Divoky,V., Liu,E., Mlodnicka,A.E., Rainey,K., Ponka,P., Semenza,G.L., Schumacher,A., and Prchal,J.T. (2006). Hypoxia-inducible Factor-1 Deficiency Results in Dysregulated Erythropoiesis Signaling and Iron Homeostasis in Mouse Development. *J. Biol. Chem.,* **281,** 25703-25711.

Yuan,G., Nanduri,J., Khan,S., Semenza,G.L., and Prabhakar,N.R. (2008). Induction of HIF-1alpha expression by intermittent hypoxia: involvement of NADPH oxidase, Ca2+ signaling, prolyl hydroxylases, and mTOR. *J. Cell Physiol.,* **217,** 674-685.

Yuan,Y., Hilliard,G., Ferguson,T., and Millhorn,D.E. (2003). Cobalt Inhibits the Interaction between Hypoxia-inducible Factor-alpha and von Hippel-Lindau Protein by Direct Binding to Hypoxia-inducible Factor-alpha. *J. Biol. Chem.,* **278,** 15911-15916.

Zhang,Y., Griendling,K.K., Dikalova,A., Owens,G.K., and Taylor,W.R. (2005). Vascular Hypertrophy in Angiotensin II-Induced Hypertension Is Mediated by Vascular Smooth Muscle Cell-Derived H2O2. *Hypertension,* **46,** 732-737.

Zinkernagel,A.S., Johnson,R.S., and Nizet,V. (2007). Hypoxia inducible factor (HIF) function in innate immunity and infection. *J Mol. Med.,* **85,** 1339-1346.

Zylber,E., Vesco,C., and Penman,S. (1969). Selective inhibition of the synthesis of mitochondria-associated RNA by ethidium bromide. *J Mol Biol,* **44,** 195-204.